

TECHNISCHE UNIVERSITÄT MÜNCHEN

FAKULTÄT CHEMIE

LEHRSTUHL ORGANISCHE CHEMIE II



KINETIC AND THEORETICAL STUDIES OF  
BETA-LACTONE REACTIVITY

---

AMINO-EPOXYCYCLOHEXENONES AND THEIR  
PROTEIN TARGETS IN SALMONELLA TYPHIMURIUM

DISSERTATION ZUR ERLANGUNG DES AKADEMISCHEN GRADES EINES  
DOKTORS DER NATURWISSENSCHAFTEN VON

FRANZISKA ANNA MARIA MANDL

MÜNCHEN 2016





TECHNISCHE UNIVERSITÄT MÜNCHEN

FAKULTÄT CHEMIE

LEHRSTUHL ORGANISCHE CHEMIE II

**KINETIC AND THEORETICAL STUDIES OF  
BETA-LACTONE REACTIVITY  
and  
AMINO-EPOXYCYCLOHEXENONES AND THEIR PROTEIN  
TARGETS IN SALMONELLA TYPHIMURIUM**

FRANZISKA ANNA MARIA MANDL

Vollständiger Abdruck der von der Fakultät für Chemie der Technischen Universität München  
zur Erlangung des akademischen Grades eines

**DOKTORS DER NATURWISSENSCHAFTEN**

genehmigten Dissertation.

Vorsitzender:

Prof. Dr. Michael Groll

Prüfer der Dissertation:

1. Prof. Dr. Stephan A. Sieber
2. Prof. Dr. Tobias A. M. Gulder

Die Dissertation wurde am 18.02.2016 bei der Technischen Universität München  
eingereicht und durch die Fakultät für Chemie am 22.03.2016 angenommen.









## DANKSAGUNG

An erster Stelle möchte ich mich bei Prof. Dr. Stephan Sieber für die Möglichkeit bedanken, meine Doktorarbeit an seinem Lehrstuhl angefertigt haben zu können. Besonders geschätzt habe ich die große Bandbreite an wissenschaftlichen Fragestellungen und die damit erlernten vielfältigen Themengebiete und Techniken. Ich möchte mich auch für die Begeisterung und Unterstützung, die mir bei meinen Projekten entgegengebracht wurden, bedanken.

Den Mitgliedern der Prüfungskommission danke ich für die Bemühungen bei der Bewertung dieser Arbeit. Zudem möchte ich mich ganz herzlich bei Annabelle Hoegl, Markus Lakemeyer und Mathias Hackl für das Korrekturlesen des Manuskripts bedanken.

Besonders möchte ich mich auch bei Dr. Sabine Schneider und Astrid König für die sehr angenehme Zusammenarbeit und ihre Hilfe bei der Kristallstrukturanalyse bedanken. Des Weiteren bedanke ich mich bei meinen Kooperationspartnern der LMU München und dabei besonders Iris Blank, für die freundliche Zusammenarbeit.

Ein großer Dank geht an die besten chemisch-technischen Assistentinnen, die man sich als Doktorand nur wünschen kann, Katja Bäuml und Mona Wolff. Eure tägliche Hilfe und großartige Unterstützung im Labor sind mitverantwortlich für das tolle Arbeitsklima. Euer Engagement und das Übernehmen vieler Aufgaben, die eigentlich gar nicht eure wären, sind wirklich eine große Hilfe.

Außerdem danke ich sehr herzlich meinen lieb gewonnenen Laborkollegen, die die letzten vier Jahre zu einer tollen Zeit gemacht haben. Besonders danke ich meinem Dr. Mäxchen Koch für insgesamt neun Jahre gemeinsames Studium und Promotion, die schlechten Witze, die mich (fast) immer zum Lachen gebracht haben und jeden Gin. Ich bin froh, dass ich dich getroffen hab und bin gespannt was uns in Zukunft noch so alles einfällt. Meiner unmittelbar betroffenen bayrisch-chinesischen Laborkollegen-Kombi Mathias Hackl und Weining Zhao danke ich für jede, (auch nicht)-wissenschaftliche Unterhaltung, alle hilfreichen und nicht-hilfreichen Diskussionen und die große Toleranz gegenüber meinem Redebedarf. Weiter bedanke ich mich bei Lena Kunold, Volker Kirsch, Anni Hoegl, Christian Fetzer, Jan Vomacka, Markus Lakemeyer, Wolfi Heydenreuter, Dr. Märri Dahmen, Johannes Lehmann, Matthias Stahl, Dóri Balogh, Philipp Kleiner, Dr. Megan Wright und Dr. Pavel Kielkowski. Ich danke euch für das tolle Arbeitsklima, jeden Kaffee, jeden Krapfen, jedes Bier, und jeden Sekt, für die vielen hilfreichen Diskussionen und vor allem für alle sinnlosen Unterhaltungen.

Zudem möchte ich mich auch bei den ehemaligen Kollegen und Freunden bedanken, die den „Absprung“ schon geschafft haben. Dr. Tanja Wirth, Dr. Max Pitscheider, Dr. Oli Battenberg, Dr. Georg Rudolf, Dr. Roman Kolb, Dr. Matt Nodwell und Dr. Bianca Bauer. Ich freue mich, dass wir uns alle immer noch sehen oder hören.

Den „Nachfolgern“ Thomas Gronauer und Barbara Hofbauer möchte ich außerdem viel Erfolg und Ausdauer für die nächste Zeit wünschen.

Mein letzter und größter Dank gilt meinen Eltern Marianne und Gerhard Mandl, meinem Bruder Johannes Mandl und vor allem meinem Mann Patrick Hofmann. Ich danke euch für eure Unterstützung während der Promotion und dem Studium und dass ihr immer für mich da seid. Papa, dir danke ich für jedes Fuchzgerl als Belohnung für eine geschriebene Seite, Mama für die immer zu verdünnten Weinschorlen und Hanne für jeden WhatsApp Witz zur Ablenkung. Und Schatz, dir Danke ich für deine bemerkenswerte Geduld und dafür, dass es dich (für mich) gibt.

## TABLE OF CONTENTS

TABLE OF CONTENTS .....	1
INTRODUCTORY REMARKS .....	5
ZUSAMMENFASSUNG.....	7
 I - INTRODUCTION.....	 11
1 THE EVOLVING THREAT OF ANTIBIOTIC RESISTANCE .....	13
2 RESEARCH ABSTRACT .....	16
 II – KINETIC AND THEORETICAL STUDIES OF BETA-LACTONE REACTIVITY - A QUANTITATIVE SCALE FOR BIOLOGICAL APPLICATION .....	 19
1 INTRODUCTION .....	21
2 RESULTS AND DISCUSSION .....	23
2.1 GENERAL CONSIDERATIONS.....	23
2.2 REACTIVITY OF BBL IN AQUEOUS BUFFER SOLUTIONS .....	24
2.3 REACTIVITY OF BBL TOWARDS AMINES IN AQUEOUS SOLUTIONS .....	25
2.3.1 QM/MM studies on the C1 vs C3 selectivity of amine attack on BBL .....	26
2.3.2 Kinetic studies of the reactions of BBL with amine nucleophiles.....	29
2.4 ELECTROPHILIC REACTIVITY OF <i>BETA</i> -LACTAMS .....	31
2.4.1 Reactivity of methyl-1-azetidin-2-one towards amines .....	32
2.4.2 Reactivity of penicillin G towards amines .....	33
3 CONCLUSION AND OUTLOOK .....	35
 III – AMINO-EPOXYCYCLOHEXENONES AND THEIR PROTEIN TARGETS IN <i>SALMONELLA</i> <i>TYPHIMURIUM</i> .....	 37
1 INTRODUCTION .....	39
1.1 ACTIVITY-BASED PROTEIN PROFILING .....	39
1.2 BIOACTIVE EPOXY-CYCLOHEXENONE NATURAL PRODUCTS .....	42

1.2.1	Structural diversity .....	43
1.2.2	Structure-activity related probe design .....	45
1.2.3	Previous synthetic approaches towards epoxy-cyclohexenones .....	47
<b>2</b>	<b>RESULTS AND DICUSSION .....</b>	<b>55</b>
2.1	SYNTHESES OF AMINO-EPOXYCYCLOHEXENONES .....	55
2.1.1	Synthetic strategy according to <i>Umezawa</i> .....	55
2.1.2	Synthetic strategy according to <i>Wipf</i> and <i>Taylor</i> .....	58
2.2	BIOLOGICAL ACTIVITY OF THE PROBES ON BACTERIAL CELLS .....	62
2.3	IDENTIFICATION OF PROTEIN TARGETS VIA ABPP .....	64
2.3.1	<i>In situ</i> analytical labeling .....	64
2.3.2	Gel-based target identification .....	67
2.3.3	Gel-free target identification .....	68
2.4	TARGET VALIDATION .....	69
2.4.1	Overexpression and thermal stability of SCRP-27A.....	69
2.4.2	Labeling experiments .....	71
2.4.3	Binding studies via full-length MS .....	73
2.4.4	Binding site identification .....	75
2.5	PROTEIN FUNCTIONALITY.....	79
2.5.1	Assay-based functional characterization.....	80
2.5.2	<i>Salmonella typhimurium</i> LT2- $\Delta$ yhbl knockout.....	82
2.5.3	Extended target identification and discussion .....	83
<b>3</b>	<b>CONCLUSION AND OUTLOOK .....</b>	<b>86</b>
 <b>IV – EXPERIMENTAL SECTION .....</b>		<b>89</b>
<b>1</b>	<b>CHEMISTRY.....</b>	<b>91</b>
1.1	MATERIAL AND METHODS .....	91
1.2	SYNTHETIC PROCEDURES .....	93
1.2.1	Kinetik products .....	93
1.2.2	Epoxy-cyclohexenones and precursors .....	97
<b>2</b>	<b>MICROBIOLOGY .....</b>	<b>134</b>
2.1	BACTERIAL STRAINS AND MEDIA.....	134
2.2	CULTIVATION METHODS .....	135
2.3	MIC ASSAY .....	135
<b>3</b>	<b>PROTEOMICS.....</b>	<b>137</b>

3.1	GEL-BASED PROTEIN PROFILING PROTEOMICS.....	137
3.1.1	Analytical <i>in situ</i> labeling and Click reaction .....	137
3.1.2	Preparative in situ labeling including Click reaction.....	138
3.1.3	SDS-PAGE and Coomassie staining.....	139
3.1.4	In-gel digest .....	141
3.2	GEL-FREE PROTEIN PROFILING PROTEOMICS .....	142
3.2.1	In-solution digest .....	142
3.2.2	On-column dimethyl labeling.....	142
3.3	SAMPLE PREPARATION AND STATISTICAL EVALUATION .....	143
<b>4</b>	<b>GENOMICS .....</b>	<b>145</b>
4.1	PCR FOR GATEWAY .....	145
4.2	GATEWAY CLONING .....	146
4.2.1	BP cloning reaction .....	146
4.2.2	LR cloning reaction.....	147
4.3	SITE-DIRECTED MUTAGENESIS .....	147
4.4	OVEREXPRESSION AND PURIFICATION OF RECOMBINANT PROTEINS .....	148
4.5	THERMAL SHIFT ASSAY.....	149
4.6	CRYSTALLIZATION OF <i>SALMONELLA TYPHIMURIUM</i> LT2 SCRP-27A.....	149
<b>V</b>	<b>BIBLIOGRAPHY .....</b>	<b>151</b>
<b>VI</b>	<b>ABBREVIATIONS .....</b>	<b>167</b>
<b>VII</b>	<b>APPENDICES .....</b>	<b>171</b>
<b>VIII</b>	<b>CURRICULUM VITAE .....</b>	<b>201</b>





## INTRODUCTORY REMARKS

The present doctoral dissertation was accomplished between October 2012 and February 2016 under the supervision of Prof. Dr. Stephan A. Sieber at the Chair of Organic Chemistry II of the Technische Universität München.

### PARTS OF THIS THESIS HAVE BEEN PUBLISHED IN:

Franziska A. Mandl,\* Elija N. Wiedemann,\* Iris D. Blank,\* Christian Ochsenfeld, Armin R. Ofial and Stephan A. Sieber: *Kinetic and theoretical studies of beta-lactone reactivity - a quantitative scale for biological application*, ChemPlusChem **2015**, 80 (11), 1673 - 1679.

\*contributed equally

Franziska A. Mandl, Volker Kirsch, Max F. Koch, Elena Kunold, T. Fuchs and Stephan A. Sieber: *Amino-epoxycyclohexenones and their protein targets in Salmonella typhimurium*, manuscript in preparation.

### PUBLICATIONS NOT HIGHLIGHTED IN THIS THESIS:

Georg C. Rudolf\*, Maximilian F. Koch\*, Franziska A. Mandl and Stephan A. Sieber: *Subclass-specific capture of protein-reactive natural products with customized nucleophilic probes*, Chemistry **2015**, 21 (9), 3701-3707.

\*contributed equally



## ZUSAMMENFASSUNG

Antibiotika-Resistenzen und die damit verbundene immer schwieriger werdende Behandlung von bakteriellen Infektionskrankheiten gilt als eine der größten Gesundheitsrisiken des 21. Jahrhundert. Da zudem immer weniger neue Antibiotika entdeckt und zugelassen werden, spricht die Weltgesundheitsorganisation bereits von einer post-antibiotischen Ära. Vor allem die Resistenzentwicklung bei *Gram*-negativen Bakterienstämmen ist auf Grund der geringen Anzahl an potentiellen, neuen Wirkstoffen sehr besorgniserregend. Salmonellen und die durch sie verursachte Salmonellose, die am häufigsten auftretende Lebensmittelinfektion weltweit, stehen dabei besonders im Fokus. Die Entwicklung von neuen, wirksamen Antibiotika ist also von grundlegender Bedeutung. Häufig besteht deren Wirkweise in der kovalenten Inhibition eines Proteins und beruht demnach auf der generellen Reaktivität von elektrophilen Gruppen als Teil der Antibiotika-Struktur mit zellulären Nukleophilen, wie beispielsweise die aktiven Zentren von Enzymen. Die Reaktivität zwischen elektrophilen, kleinen Molekülen und deren nukleophilen Angriffspartner stellt dabei eine Gemeinsamkeit beider Projekte dieser Arbeit dar.

In Bezug auf die Entwicklung neuer Inhibitoren wäre eine Möglichkeit zur Vorhersage von deren Reaktivität unter physiologischen Bedingungen von großem Nutzen. Als ersten Schritt zu einer solchen Reaktivitätsskala beschreibt der erste Teil der Arbeit die Reaktivität von monozyklischem *beta*-Butyrolacton gegenüber verschiedener Nukleophile im Vergleich zur Reaktivität von mono- und bizyklischen *beta*-Lactamen. Die Reaktivität von *beta*-Butyrolacton gegenüber verschiedener Amin-Nukleophile erfolgte dabei in wässrigen Pufferlösungen bei 37 °C durch die Bestimmung der Geschwindigkeitskonstanten mittel zeitaufgelöster <sup>1</sup>H-NMR Spektroskopie. Auf Grund des ambidenten Charakters der elektrophilen Grundstruktur von *beta*-Butyrolacton ist ein nukleophiler Angriff generell sowohl an C1 als auch an C3 des Vierrings möglich. Interessanterweise konnte gezeigt werden, dass die Regioselektivität des Angriffs von der Struktur des Nukleophils abhängt: Während aromatische Amin-Nukleophile den Lactonring an C1 angreifen, erfolgt die Bildungsbildung bei aliphatischen Amin-Nukleophilen an C3. Um die Ursache dieses Unterschieds bestimmen zu können, wurden quantenmechanische Berechnungen durchgeführt. Die berechneten Reaktionsbarrieren bestätigten die dabei experimentell festgestellten Unterschiede. Zudem konnte gezeigt werden, dass im Falle des C3-Angriffs der Übergangszustand der Reaktion durch ein H<sub>3</sub>O<sup>+</sup>-Molekül stabilisiert wird. Die Reaktionsbarriere des C3-Angriffs wird dabei, im Gegensatz zum nicht-stattfindenden Angriff an C1, soweit herabgesetzt, dass die Reaktion abläuft. Mittels HPLC-MS durchgeführte Produktstudien, bestätigten diese Berechnungen. Um die spätere Anwendbarkeit der Plattform auf weitere Elektrophile zu überprüfen, wurde im nächsten Schritt

die Reaktivität von mono- und bityklischen *beta*-Lactamen gegenüber den bereits verwendeten Referenz-Nukleophilen bestimmt. Die Bestimmung der Reaktionsgeschwindigkeiten erfolgte dabei erneut mittels  $^1\text{H}$  NMR Spektroskopie und auch die gewählten Reaktionsbedingungen entsprachen denen des ersten Teils des Projekts. Während das monozyklische Methyl-1-azetidin-2-on mit keinem der Referenz-Nukleophile reagierte, überstiegen die Reaktionsgeschwindigkeit des bityklischen *beta*-Lactam Antibiotikums Penicillin G sogar die des *beta*-Butyrolactons. Zusätzlich durchgeführte Produktstudien und quantenmechanische Berechnungen des Reaktionsverlaufs bestätigten die experimentell erhaltenen Geschwindigkeitskonstanten. Diese Erkenntnisse entsprechen somit genau dem Verhalten dieser Verbindungen im Proteom von Bakterien: Während bityklische *beta*-Lactame als Antibiotika Anwendung finden und somit auch *in vivo* mit den nukleophilen Resten der aktiven Zentren in Enzymen reagieren, weisen monozyklische Lactame nur sehr geringe Aktivität auf. Die entwickelte Plattform stellt somit eine gute Grundlage für die Reaktivitätsbestimmung von elektrophilen Naturstoffen dar. Zudem können durch die semiquantitative Einordnung Naturstoff-basierter Elektrophile in eine Reaktivitätsskala zukünftig Vorhersagen bezüglich der zu erwartenden Reaktivität des Naturstoffs gemacht werden, was vor allem in Bezug auf die Entwicklung neuer Wirkstoffe von immenser Bedeutung ist.

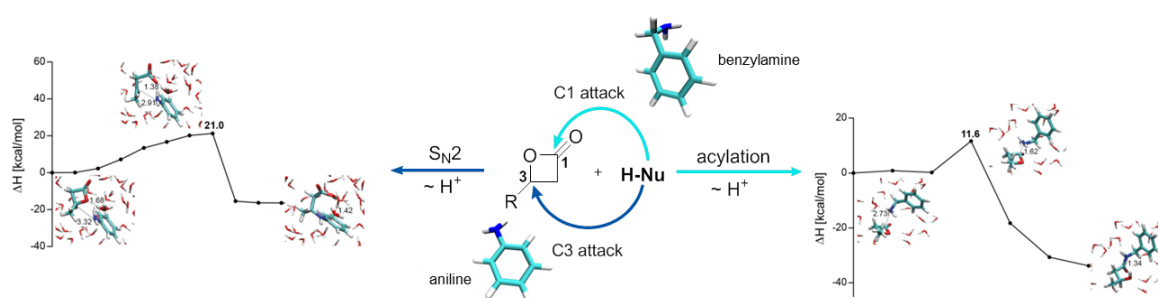


**Figure 1:** Grafische Darstellung des Projekts - Kinetic and theoretical studies of *beta*-lactone reactivity - a quantitative scale for biological application.

Der zweite Teil der Arbeit beschäftigt sich ebenfalls mit der Reaktivität eines elektrophilen Naturstoffs gegenüber Nukleophilen, allerdings in einem komplexeren Zusammenhang. Im Falle der Nukleophile handelt es sich um die aktiven Zentren von bakteriellen Enzymen, die auf Grund ihrer vielfältigen und teilweise essentiellen Funktionen sehr interessante Ziele für neue Wirkstoffforschungsansätze darstellen. Um die Identität und Funktion von Proteinen *in vivo* bestimmen zu können, eignet sich besonders die Proteomik-Technologie des aktivitäts-basierten Protein-Profiling (ABPP). Mit Hilfe dieser Methode lässt sich der Einfluss von elektrophilen, kleinen Molekülen auf ein komplexes, bakterielles Proteom aktivitätsbasiert bestimmen. Bei einem solchen Experiment reagiert eine sogenannte ABPP-Sonde auf Grund ihrer elektrophilen Reaktivität

kovalent mit dem aktiven Zentrum ihres spezifischen Zielenzyms. Dadurch werden diese Enzyme auf Basis ihrer tatsächlichen Aktivität und nicht nur auf Grund ihrer Häufigkeit charakterisiert. Vorbilder für die reaktive Einheit einer solchen Sonde sind häufig Naturstoffe, die auf Grund ihrer evolutionären Entwicklung eine große Vielfalt an Strukturen aufweisen. ABPP stellt somit eine leistungsfähige Methode dar, neue pathogen-assoziierte Enzyme zu identifizieren und bietet dadurch eine Basis für die Entwicklung neuer Wirkstoffe. Ein Beispiel für Naturstoff-basierte Elektrophile, deren bakterielle Angriffsziele und Wirkweise weitestgehend unbekannt sind, sind Amino-Epoxycyclohexenone. Dabei weist diese Stoffklasse eine große strukturelle Vielfalt mit einhergehender unterschiedlichster biologischer Aktivität auf. Das allen Mitgliedern gemeinsame, elektrophile Strukturelement ist dabei eine Kombination aus Epoxid und *Michael*-Akzeptor. In dieser Arbeit wurden daher zunächst verschiedene ABPP-Sonden synthetisiert, die zum einen alle die Amino-Epoxycyclohexenonen Kerneinheit enthalten, sich zum anderen aber durch eine große Vielfalt an Substitutionsmustern auszeichnen. Im Anschluss wurde die Bioaktivität der synthetisierten Verbindungen bezüglich pathogener Bakterienstämme mittels MIC bestimmt. Dabei zeigten besonders Moleküle mit einer Amino-Epoxybenzochinon Struktur antibakterielle Aktivität gegenüber *Gram*-positiven und *Gram*-negativen Stämmen. Zudem konnte gezeigt werden, dass Analoga dieser Sonden, in denen die elektrophile Epoxid-Einheit durch eine Doppelbindung ersetzt wurde, keine wachstumsinhibierende Wirkung in Bakterien aufweisen. Dies deutet auf eine Epoxid-abhängige antibiotische Aktivität der Sonden hin. Um nun die Angriffsziele dieser Sonden aktivitätsbasiert bestimmen zu können, wurde ein ABPP-Experiment durchgeführt. Interessanterweise zeigte sich in den *Gram*-negativen *Salmonella* Stämmen ein Epoxid- und damit Aktivitäts-abhängiges Markierungsmuster. Im nächsten Schritt wurden die markierten Zielenzyme deshalb sowohl Gel-basiert als auch mit Gel-freien Methoden identifiziert. Die statistische Auswertung der Markierungsexperimente zeigte dabei das unbekannte Sigma cross-reacting Protein 27A (SCRIP-27A) als Zielenzym der Sonde **FM233** in *Salmonella typhimurium*. Zur Validierung der Ergebnisse wurden anschließend verschiedene Gel-basierte Markierungsexperimente mit dem rekombinanten Protein durchgeführt, die durch MS-basierte Volllängemessungen des markierten Proteins bestätigt wurden. SCRIP-27A konnte dadurch eindeutig als cytosolisches Zielenzym der Sonde bestätigt werden. Mit Hilfe der erfolgreich durchgeführten Kristallstrukturanalyse und der gezielten Mutagenese konnte des Weiteren die Enzym-Bindestelle der Sonde als Cystein C135 identifiziert werden. Um die Funktionalität von SCRIP-27A bestimmen zu können wurden verschiedene Enzymaktivitätsassays durchgeführt. Dabei zeigte das Enzym eine leichte, aber dennoch eindeutige Esteraseaktivität. Zudem konnte gezeigt werden, dass nach einer vorangegangenen Inkubation mit der Sonde, keine Aktivität des Enzyms mehr feststellbar war.

Zusammenfassend konnte also auch die Inhibitor-Eigenschaft der Sonde nachgewiesen werden. Zusätzlich wurde ein SCRP-27A-Knockout Stamm von *Salmonella typhimurium* generiert, um einen eventuell bestehenden Zusammenhang zwischen der Inhibition des SCRP-27A und der antibakteriellen Eigenschaft der Sonde festzustellen. Überraschenderweise zeigte die Sonde auch im Knockout-Stamm eine wachstumshemmende Wirkung, wodurch kein direkter Zusammenhang zwischen der Proteininhibition und dem auftretenden Phänotyp nachgewiesen werden konnte. Neben SCRP-27A wurden allerdings drei weitere Enzyme als Ziel der Sonde im bakteriellen Cytosol identifiziert, welche in Kombination die antibakteriellen Eigenschaften von **FM233** erklären können: eine FMN-abhängigen Azoreduktase (azoR), Thioredoxin-1 (trxA) und Glutaredoxin 2 (grxB). Dabei zeigen mehrere Veröffentlichungen, dass die Azoreduktase azoR ebenso Chinon-reduzierende Eigenschaften aufweist und somit Bakterien in ihrer Funktion vor Thiol-basiertem Stress schützt: Chinone reduzieren durch die Reaktion mit freien Thiolen die effektive freie Thiolkonzentration in der Zelle. Zudem ist bekannt, dass die gleichzeitige Inhibition von Proteinen, die wie trxA und grxB zu den Oxidoreduktasen gehören, ein verlangsamtes Bakterienwachstum zur Folge haben kann. Darüber hinaus besitzen alle diese Enzyme ein Cystein im aktiven Zentrum, womit deren Reaktivität gegenüber der Epoxychinon Struktur offensichtlich ist. Zusammenfassend erzeugt die synthetisierte Sonde also einerseits selbst Thiol-spezifischen Stress in den Bakterien und inhibiert gleichzeitig die Enzyme, die in dieser Situation normalerweise aktiv sind. Amino-Epoxycyclohexenone stellen somit eine interessante, neue Molekülklasse für den Einsatz als antibiotisch wirksame Substanzen in Salmonellen dar.

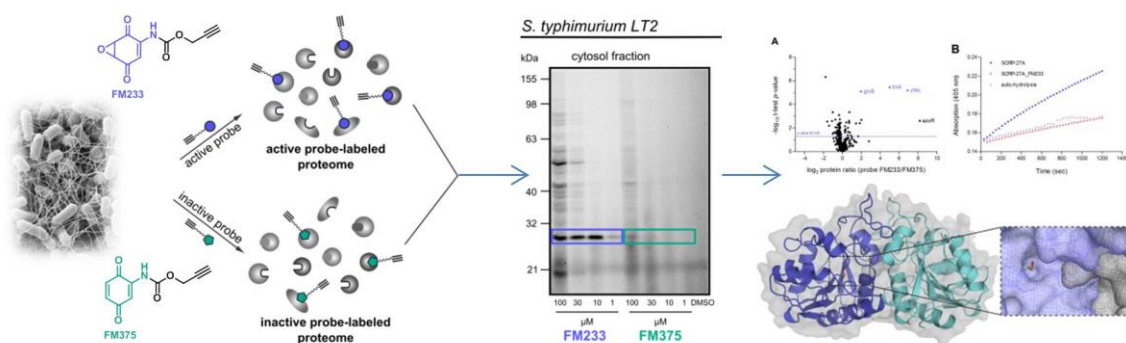


**Figure 2:** Grafische Darstellung des Projekts - Amino-epoxycyclohexenones and their protein targets in *Salmonella typhimurium*.



## I - INTRODUCTION

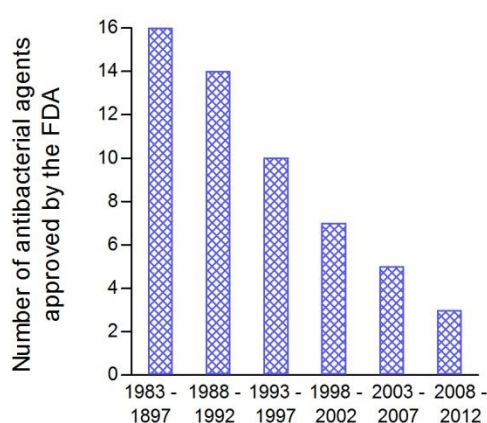




## 1 THE EVOLVING THREAT OF ANTIBIOTIC RESISTANCE

Serious infections caused by bacteria resistant to commonly used antibiotics have become a major global healthcare problem in the 21<sup>st</sup> century.<sup>[1]</sup> The importance of this issue is emphasized by the antimicrobial resistance report of the World Health Organization (WHO) published in 2014, wherein there is talk of a ‘post-antibiotic’ era in which common infections and minor injuries can be lethal.<sup>[2]</sup> Furthermore, antimicrobial resistance was a topic of discussion at the G7 summit in 2015, putting this topic on par with terrorism and climate change.<sup>[3]</sup>

However, resistance development of bacterial strains towards antibiotics is nothing new. Already in his Nobel Prize speech in 1945,<sup>[4]</sup> Alexander Fleming, who discovered penicillin in 1929,<sup>[5]</sup> warned of this issue. But indeed, the amount of time between the deployment of a novel antibiotic and the evolution of resistance towards this substance is getting shorter.<sup>[6]</sup> Besides the liberal use of antibiotics in the farming industry and the treatment of infections with broad-spectrum antibiotics, the limited number of cellular targets of bacteria addressed by the different antibiotics is a major issue leading to multidrug-resistant strains.<sup>[1]</sup> Moreover, the number of systemic antibiotics approved by the US Food and Drug Administration (FDA) since 1983 has steadily decreased as shown in figure 3.



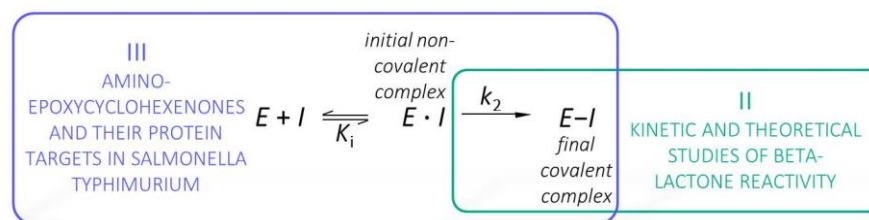
Drug/Pathogen	Resistance (%)
Methicillin/ <i>S. aureus</i>	57.1
Vancomycin/ <i>Enterococci</i>	27.5
Quinolone/ <i>P. aeruginosa</i>	32.8
Imipenem/ <i>P. aeruginosa</i>	22.3
Penicillin/ <i>S. pneumoniae</i>	11.3
3 <sup>rd</sup> -gen. Cephalosporin/ <i>E. coli</i>	6.3
3 <sup>rd</sup> -gen. Cephalosporin/ <i>P. aeruginosa</i>	30.2
3 <sup>rd</sup> -gen. Cephalosporin/ <i>Enterobacter ssp.</i>	32.2

**Figure 3:** Left - New systemic antibacterial agents approved by the FDA per 5-year period, through 2012, modified from;<sup>[7]</sup> Right - Percent of drug resistance in hospital-acquired infections in the US in 2002.<sup>[8]</sup>

Resistance among *Gram*-negative bacteria is especially concerning, as there are only a very limited number of antimicrobial agents towards these in late-stage development. Additionally, the spread of multidrug-resistant *Gram*-negative bacteria is increasing.<sup>[9]</sup> Among them, infections caused by resistant non-typhoidal *Salmonella* serotypes are of particular concern as salmonellosis is one of the most common and widely distributed foodborne diseases worldwide, with estimated 1.4 million cases each year in the United States alone.<sup>[10]</sup> *Salmonella typhimurium* and *Salmonella*

*enteritidis* are the two most common serotypes of salmonellosis, transmitted from host animals such as cattle, pig, poultry and sheep, to humans.<sup>[11]</sup> Although, most *Salmonella* infections are contained and cause acute gastrointestinal illness in humans, severe infections that spread to the bloodstream or meningeal lining of the brain have been reported.<sup>[9]</sup> Therefore, the development of resistance to key antibiotics such as fluoroquinolones, often caused by the presence of extended-spectrum  $\beta$ -lactamase (ESBL), are of particular concern in these serotypes.<sup>[11]</sup> ESBL's are enzymes capable of hydrolyzing an extended-spectrum of antibiotics (compared to  $\beta$ -lactamases) such as the penicillins, first-, second-, and third-generation cephalosporins and aztreonam. Therefore, antibiotic options for the treatment of ESBL-producing organisms are extremely limited.<sup>[12,13]</sup> While person-to-person transmission is not of major concern in developed countries and antibiotic therapy is often not required, in developing countries like India, south-east Asia or Africa, infections caused by these strains are associated with a high incidence of invasive illness, which often result in septicemia and consequently high mortality.<sup>[11]</sup>

Because of the discussed reasons, there is a high demand for new antibiotics with diverse core structures that are capable of targeting different or even unknown bacterial enzymes, ideally with novel modes of action. Natural products represent a rich source of structurally diverse bioactive and unique compounds, which have inspired new scaffolds for drugs. The vast majority of natural products isolated and elucidated to date have a molecular weight of greater than 1000, making their characterization and synthesis reasonable.<sup>[14]</sup> Structure-activity studies combined with total synthesis may help to identify simplified bioactive fragments of the parent structure. The high complexity of natural products makes the selection of appropriate drug candidates difficult. Since several drugs exert their antibacterial effects by reacting with the active-sites of their bacterial target enzymes, ranking the reactivities of the electrophilic core units towards their nucleophilic counterpart could provide important insights into drug binding mechanisms and can help in selecting appropriate binders. As electrophilic small molecules represent putative covalent drug candidates, characterizing the covalent mechanism of action *in vitro* as well as *in vivo* is important. In general, covalent inhibition occurs in (at least) two steps, as shown in scheme 1.



**Scheme 1:** Mechanism occurring during covalent inhibition: first, the inhibitor (*I*) binds non-covalently to the target enzyme (*E*) and the resulting initial complex subsequently undergoes the final covalent bond formation (modified from <sup>[15]</sup>).

The compound must first bind non-covalently to the target protein, placing its moderately reactive electrophilic core unit close to a specific nucleophilic residue on the protein. The resulting initial non-covalent complex (*E·I*) then undergoes specific covalent bond formation, resulting in the inhibited complex (*E-I*). Especially important for natural-product-based drug development is the selectivity of electrophilic small molecules towards its protein targets, characterized by the initial binding step ( $K_i$ ) and the subsequent chemical step ( $k_2$ ). For high selectivity, the non-covalent affinity ( $K_i$ ) of the inhibitor must be high enough to ensure that the compound binds selectively to the desired target and achieves a residence time sufficient for a covalent reaction. Similarly, the reaction rate of the bound inhibitor ( $k_2$ ) must be high enough to give a high probability that the reaction will take place within the life time of the non-covalent complex. As highly electrophilic core units must be avoided due to poor specificity, this reaction rate must be achieved primarily by optimal positioning of the electrophile relative to the nucleophile on the target protein. Thus, achieving good selectivity requires optimization of both,  $K_i$  and  $k_2$ .<sup>[15,16]</sup>

The research objectives in this work comprise two individual projects that are thematically linked by the binding of covalent electrophilic small molecules to nucleophilic target. The first chapter covers the general reactivity of electrophiles towards standard nucleophiles '*in vitro*', comparable to the last step of covalent complex binding shown in scheme 1. The second part comprises the target identification of an electrophilic small molecule in the bacterial proteome and therefore represents the complete covalent mechanism of action *in vivo*. A more precise overview of the research objectives to both projects is described in the next section.

## 2 RESEARCH ABSTRACT

### I) KINETIC AND THEORETICAL STUDIES OF BETA-LACTONE REACTIVITY - A QUANTITATIVE SCALE FOR BIOLOGICAL APPLICATION

The electrophilic reactivity of natural products towards their nucleophilic counterpart in the active-sites of enzymes is of great interest with regard to drug development. Prominent examples of interesting core units are *beta*-lactams and *beta*-lactones, which specifically acylate serine residues in diverse peptidases. Although these scaffolds appear similar, their bioactivities and corresponding protein targets vary. In order to quantify these differences in bioactivity, the kinetics of the reactions of *beta*-butyrolactone with a set of reference amine nucleophiles in buffered aqueous solution at 37 °C were analyzed via time-resolved <sup>1</sup>H-NMR spectroscopy. First the stability of *beta*-butyrolactone in different buffer systems was determined via <sup>1</sup>H-NMR spectroscopy and product formation was further validated by HPLC-MS measurements. Because of the ambident character of *beta*-lactones, generally, two different products depending on the position of the nucleophilic attack can occur. Therefore, the regioselectivity of the attack was studied by HPLC-MS and NMR measurements of the resulting products. Differences in the ratio of C1 versus C3 attack dependent on the nucleophile were further elucidated by QM/MM calculations. Next, the reaction rates of mono- and bicyclic *beta*-lactams with the reference nucleophiles were determined via time-resolved <sup>1</sup>H-NMR spectroscopy and compared to those determined for *beta*-butyrolactone. To confirm the obtained results, theoretical QM/MM calculations were performed.

### II) AMINO-EPOXYCYCLOHEXENONES AND THEIR PROTEIN TARGETS IN *SALMONELLA TYPHIMURIUM*

The reactivity of electrophilic core units towards nucleophiles and the resulting effects caused by this inhibition plays a major role also in the second part of this thesis. In summary, the protein targets of natural product derived electrophiles were determined in the pathogenic bacterium *Salmonella typhimurium*. Therefore, amino-epoxycyclohexenones, containing an electrophilic core unit comprising of an epoxide moiety and a *Michael*-acceptor system, were chosen due to their known antibacterial activity and unknown cellular targets. First, a probe library of molecules based on this scaffold was synthesized, containing different substitution patterns and various modifications. The probes were then evaluated for their antibacterial properties in a panel of bacteria. Next, the protein targets of bioactive probe **FM233** were determined by gel-based and gel-free activity-based protein profiling (ABPP) and LC-MS/MS methods. These results were compared to the protein targets of an unreactive analog of the probe (**FM375**) and revealed the uncharacterized sigma cross-reacting protein 27A (SCR-27A) as target enzyme of amino-epoxycyclohexenones in *Salmonella typhimurium* LT2. SCR-27A was validated as a target enzyme

by conducting gel-based binding studies with the recombinant protein and could be confirmed by LC-MS/MS measurements. Further research objectives comprised the identification of the SCRP-27A binding site via mutation and the generation of a crystal-structure of the protein. In addition, different enzyme assays and a knockout study were performed to give insight into the functionality of the unknown protein with regard to the bioactivity of the probe in *Salmonella typhimurium*.



## II – KINETIC AND THEORETICAL STUDIES OF BETA-LACTONE REACTIVITY - A QUANTITATIVE SCALE FOR BIOLOGICAL APPLICATION

The following chapters are based upon: Franziska A. Mandl,\* Elija N. Wiedemann,\* Iris D. Blank,\* Christian Ochsenfeld, Armin R. Ofial and Stephan A. Sieber: *Kinetic and theoretical studies of beta-lactone reactivity - a quantitative scale for biological application*, ChemPlusChem **2015**, 80 (11), 1673 – 1679 (\*contributed equally). F.M.: synthesis, product studies, mass spectrometry; E.W.: kinetic measurements; I.B.: QM/MM calculations.





## 1 INTRODUCTION

In natural products diverse electrophilic moieties can be found, designed to covalently react with nucleophiles like amino acid residues and thereby inhibit cellular proteins.<sup>[17-19]</sup> Evolution has fine-tuned these reactive scaffolds to address a huge variety of cellular nucleophiles, like for example the active-site of enzymes. These tailored scaffolds include *beta*-lactams, *beta*-lactones, epoxides and *Michael*-acceptors, which vary in their reactivity and therefore in selectivity towards amino-, thio-, and hydroxyl-substituted amino acids (figure 4).

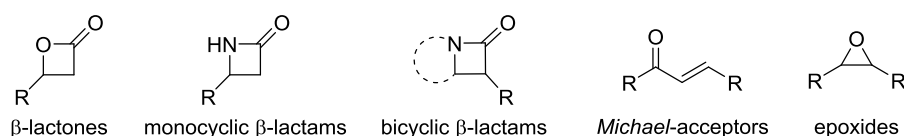


**Figure 4:** Common electrophilic motifs in natural products.

The well-known natural compound class of *beta*-lactams contains some of the most potent antibiotics like penicillins and cephalosporins. These bioactive molecules exert their cellular activity by reacting with the active-site serine in penicillin-binding-proteins (PBPs) and thereby inhibit cell wall biosynthesis and thus bacterial viability.<sup>[20]</sup> Interestingly, the electrophilic lactam moiety in these natural compounds has to be activated to react with PBP's as monocyclic *beta*-lactams lack pronounced protein reactivity.<sup>[21]</sup> Penicillins and cephalosporins, for example, contain bicyclic *beta*-lactams and in aztreonam, the lactam activation is generated by sulfonylation of the amino group (figure 5).<sup>[22,23]</sup>

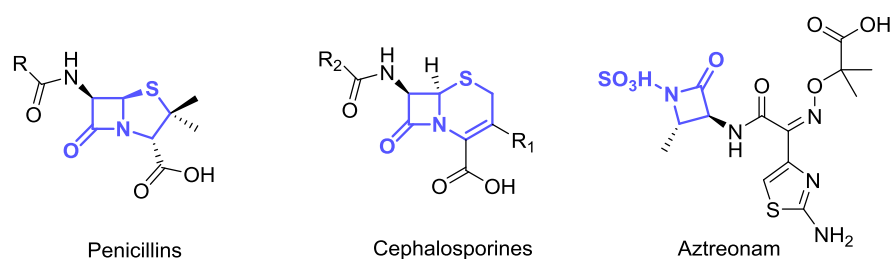
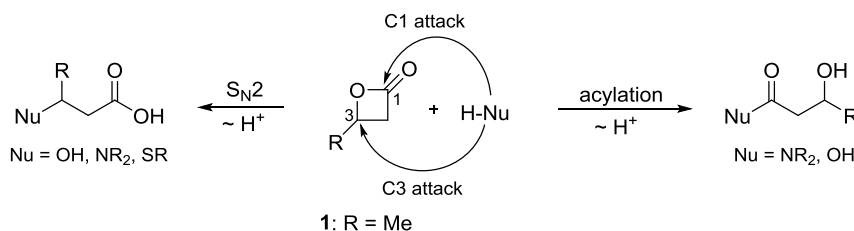


**Figure 5:** Molecular structure of activated *beta*-lactams: Penicillins, Cephalosporins and Aztreonam. The electrophilic core structure is shown in blue.

This indicates that already minor structural changes strongly affect the reactivity and thereby consequently the bioactivity of the compounds. In contrast, *beta*-lactones do not require activation in order to react with serine and cysteine residues, suggesting that monocyclic lactones and lactams show significantly different electrophilicities under physiological conditions.<sup>[24]</sup> Previous ring-opening studies with 3-alkylated *beta*-lactones revealed S-nucleophiles to require activation by deprotonation for an efficient C3 attack, a mixed  $S_N2$  reaction (attack at C3) and acylation (attack at C1) with amines, and pH-dependent C1 or C3 attack in hydrolysis reactions (scheme 2).<sup>[25,26]</sup>



**Scheme 2:** Possible *beta*-lactone ring-opening pathways of different nucleophiles.

As there are no reliable reactivity and selectivity profiles under physiological conditions, the identification of nucleophiles that distinguish between C1 vs. C3 attack, as well as an explanation for the selectivity towards these two sites, has not been described. In order to mimic biological systems accurately, the reactions have to be performed in aqueous media and with different nucleophiles that imitate the reactivity of active-sites in enzymes. The only published data veering toward these demands was the evaluation of the alkylating potential of lactones as per their reaction rates with 4-(*p*-nitrobenzyl)pyridine in water/dioxane mixtures.<sup>[27]</sup> Additionally important for the determination of natural product electrophilicities is the selection of suitable nucleophiles and a reliable description of their reaction by suitable kinetic equations. Previously, the reactivities of structurally diverse carbocations and neutral electrophiles were characterized with a set of reference nucleophiles and the corresponding second-order rate constants were evaluated according to the linear free energy relationship  $\log k(20\text{ }^\circ\text{C}) = s_N(N + E)$ .<sup>[28-31]</sup> Therein the electrophile-independent parameter *N* is a measure of the nucleophilicity of a dissolved reactant, the term *s<sub>N</sub>* provides information about its sensitivity towards changes in the electrophilicity of reaction partners and the electrophilicity *E* is a nucleophile-independent reactivity parameter. As the same *E* value is assigned to the reactivity of reference electrophiles (benzhydrylium ions and quinone methides) in different solvents, all solvent effects on reactivity are considered in the nucleophilicity parameters *N* and *s<sub>N</sub>*. To determine reactivities of lactones and lactams under physiological conditions towards nucleophiles, first of all, the reactions of *beta*-butyrolactone (BBL, **1**) with a set of standard amino-substituted nucleophiles with known *N* and *s<sub>N</sub>* parameters<sup>[31]</sup> (figure 6) were investigated as a model system to further determine its electrophilic reactivity as well as the regioselectivity of the nucleophilic attack with experimental and theoretical methods.

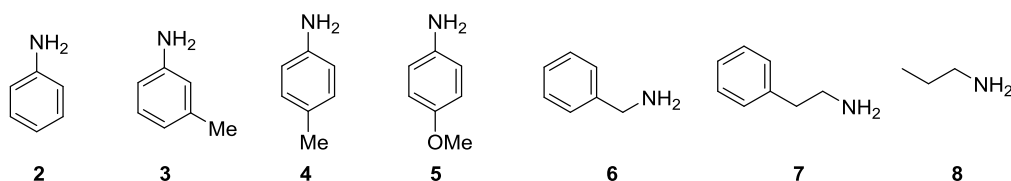
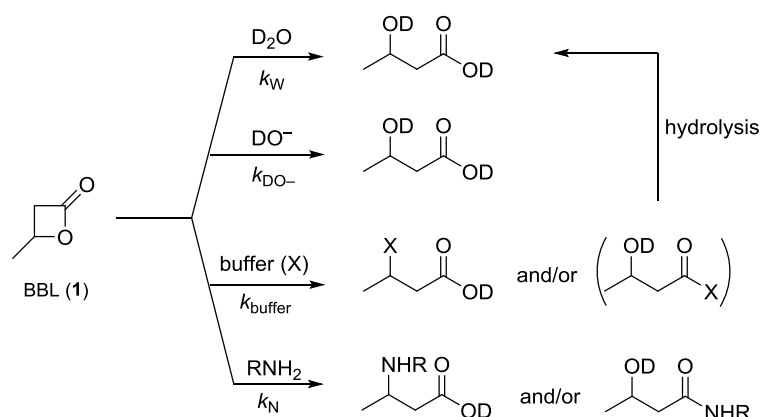


**Figure 6:** Standard amino-substituted nucleophiles used in this work: Aniline (**2**), *m*-Toluidine (**3**), *p*-Toluidine (**4**), *p*-Anisidine (**5**), Benzylamine (**6**), 2-Phenylethylamine (**7**), *n*-Propylamine (**8**).

## 2 RESULTS AND DISCUSSION

### 2.1 GENERAL CONSIDERATIONS

To obtain a comprehensive picture of BBL reactivity under physiological conditions, the reactions and with that the rate constants of **1** with the mentioned primary amines (figure 6) were performed in buffered aqueous solution at 37 °C and a constant pH. The conversion of **1** was thereby monitored by time-resolved  $^1\text{H}$  NMR spectroscopy. Under these conditions, four different nucleophiles are generally capable of reacting with BBL: water, hydroxide ions, the conjugate bases X of the respective buffer system and the selected nucleophile (scheme 3).



**Scheme 3:** Reactions of BBL (**1**) with amines in buffered aqueous solution.

Hence, to determine the rate law for the decay of the BBL concentration (equation 1) all four possible reaction channels had to be taken into consideration:

$$-d[\text{BBL}]/dt = (k_W + k_{\text{DO}^-}[\text{DO}^-] + k_{\text{buffer}}[\text{buffer}] + k_{\text{N}}[\text{amine}]) \cdot [\text{BBL}] \quad (1)$$

Previous kinetic studies on the pH-dependency of BBL hydrolysis showed that the non-catalyzed reaction of BBL with water follows a first-order rate law with a first-order rate constant  $k_W$ . Attack by hydroxide ions ( $\text{OH}^-$ ) is only relevant at  $\text{pH} > 9$ , while acid catalysis accelerates the hydrolysis only in the region of  $\text{pH} < 1$ .<sup>[32,33]</sup> Blackburn and Dodds pointed out that in buffered solutions, the reaction of pyridines and imidazoles with *beta*-propiolactone could be described by equation 2a.<sup>[34]</sup> Significant increases in the rate of the BBL hydrolysis were only observed in the presence of highly concentrated buffers ( $> 1.5 \text{ mol L}^{-1}$ ).<sup>[33]</sup> Based on the extensive work done by Gresham *et al.* on the ring opening of *beta*-propiolactone by acetate or anions of inorganic acids,<sup>[35,36]</sup> the previously mentioned possible reactions of the nucleophilic conjugate bases of the buffers ( $k_{\text{buffer}}[\text{buffer}]$ ) had to be additionally included in the calculations, leading to the extended equation 2b.<sup>[37]</sup>

$$k = k_W + k_{\text{DO}^-}[\text{DO}^-] + k_{\text{N}}[\text{amine}] \quad (2a)$$

$$k_2 = k_W + k_{\text{DO}^-}[\text{DO}^-] + k_{\text{N}}[\text{amine}] + k_{\text{buffer}}[\text{buffer}] \quad (2b)$$

$$k_1 = k_W + k_{\text{DO}^-}[\text{DO}^-] + k_{\text{buffer}}[\text{buffer}] \quad (3)$$

Due to the high initial concentration of water, the constant value of  $[\text{DO}^-]$  in buffered solution and the only partial consumption of the buffer and the amine, the concentrations of all four relevant nucleophiles did not change significantly during the kinetic experiments. Consumption of BBL was therefore expected to follow the exponential function  $[\text{BBL}]_t = [\text{BBL}]_0 e^{-kt}$ , in which  $k$  corresponds to either  $k_1$  for BBL hydrolysis in case of buffered aqueous solutions without any further amine nucleophile (equation 3), or  $k_2$  for BBL reactions in buffered aqueous solutions of amines (2b).

## 2.2 REACTIVITY OF BBL IN AQUEOUS BUFFER SOLUTIONS

One of the most important aspects in this study was to perform the kinetic measurements of BBL in aqueous solution to imitate the physiological conditions as close as possible. Thereof, different buffer systems with neutral to basic pH values between 4.75 and 8.1 (table 1) were tested for compatibility. Ideally, BBL is stable in the buffer system meaning slow hydrolysis reaction rates resulting in long half-life times and the amount of generated buffer-adduct should stay as low as possible. To select the best system, the rate of BBL consumption was initially determined in a 9:1 mixture of buffer solution in  $\text{D}_2\text{O}:\text{d}_6\text{-DMSO}$  (due to solubility) in the absence of any standard amine nucleophiles using time-resolved  $^1\text{H}$  NMR spectroscopy. To evaluate the different buffers, the non-buffered hydrolysis of BBL was measured as control. In each case, the consumption of BBL followed a mono-exponential decay and produced a mixture of 3-hydroxybutyric acid (3-HBA, hydrolysis) and the respective buffer adducts. Least squares fitting with the function  $[\text{BBL}]_t = [\text{BBL}]_0 e^{-k_1 t}$  yielded the first-order rate constants  $k_1$  as defined by equation 3, reflecting the reactivity of BBL towards the solvent at a constant pH for a 0.10 M buffer system (exemplary shown for BBL in trimethylamine (TEA) in figure 7).

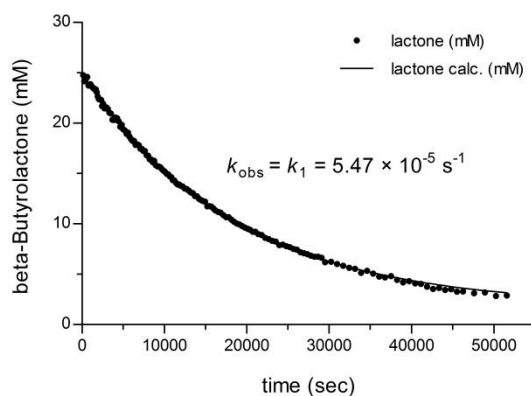
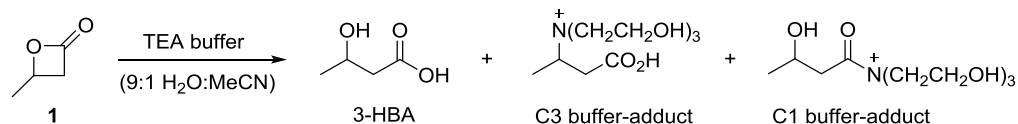


**Figure 7:** Exemplary decay of the concentration of BBL in TEA-buffered reaction mixture. The black line shows a mono-exponential fit of the data.

The attack of BBL by any of the nucleophilic buffer components (exemplarily shown for TEA buffer in scheme 4) was recorded by  $^1\text{H}$  NMR spectroscopy throughout the kinetic experiments (right column of table 1) and independently confirmed by LC-HRMS analysis.



**Scheme 4:** Reaction products of BBL in TEA buffered aqueous solution.

The rate constants of the consumption of BBL in the different buffer systems changed only within a factor of < 1.25 (entries 2–5) compared to the non-buffered BBL hydrolysis (entry 1). The half-life time of BBL decreased only from 4 h to 3 h in case of the phosphate and the TRIS buffer. As entries 1 - 5 in table 1 additionally illustrate that BBL reacted with all buffered aqueous solutions at comparable rates, aqueous TEA buffer was chosen for all further kinetic investigations of BBL reactions with primary amines. This is beneficial because the tertiary amine TEA provides a constant pH of 7.75 which is, among the tested buffers, the most similar pH to physiological conditions in living cells (entry 4).

**Table 1:** Rate constants of BBL consumption in buffered and non-buffered  $\text{D}_2\text{O}$ : $\text{d}_6$ -DMSO 9:1 (v/v) mixtures at 37 °C ([BBL] $_0$  = 25 mm, TEA = triethanolamine, TRIS = tris(hydroxymethyl)aminomethane, 3-HBA = 3-hydroxybutyric acid).

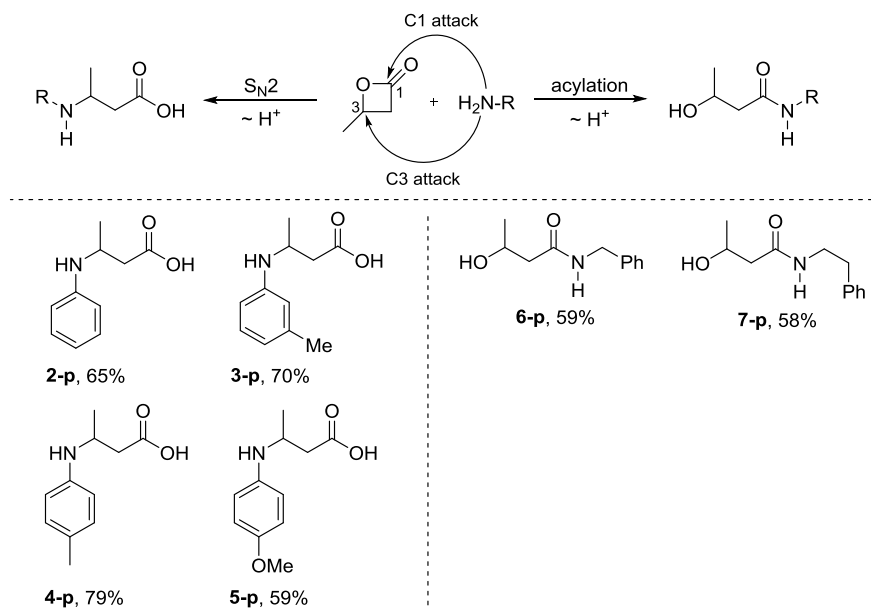
Entry	Buffer	pH	$k_1$ [s $^{-1}$ ]	$t_{1/2}$ [h]	3-HBA/Buffer adduct
1	without buffer		$4.73 \times 10^{-5}$ <sup>[a]</sup>	4.1	100/–
2	acetate	4.75	$4.14 \times 10^{-5}$	4.7	96/4
3	$\text{Na}_2\text{HPO}_4/\text{NaH}_2\text{PO}_4$	7	$5.85 \times 10^{-5}$	3.3	86/14
4	TEA	7.75	$5.47 \times 10^{-5}$	3.5	83/17 $\rightarrow$ 88/12 <sup>[b]</sup>
5	TRIS	8.1	$5.79 \times 10^{-5}$	3.3	79/21

[a] Comparison with data from<sup>[38]</sup>: with  $\Delta H^\ddagger = 87.6$  kJ/mol and  $\Delta S^\ddagger = -77.9$  J/(mol·K), the second-order rate constant for the hydrolysis of BBL is calculated to be  $k(37^\circ\text{C}) = 1.1 \times 10^{-6} \text{ M}^{-1} \text{ s}^{-1}$ . Multiplying  $k(37^\circ\text{C})$  with  $[\text{D}_2\text{O}]$  for the  $\text{D}_2\text{O}$ : $\text{d}_6$ -DMSO 9:1 mixture in our experiment gives a first-order rate constant for the BBL hydrolysis of  $k_w(37^\circ\text{C}) = 5.5 \times 10^{-5} \text{ s}^{-1}$ , in sufficient agreement with the rate constant determined under our conditions. [b] The ratio 3-HBA/buffer adduct increased during the course of the reaction (14 h) probably because of a subsequent hydrolysis of the quaternary ammonium salt formed by C3 attack of TEA on BBL (scheme 3).

### 2.3 REACTIVITY OF BBL TOWARDS AMINES IN AQUEOUS SOLUTIONS

As already depicted in the introduction, the following amines should then serve as model nucleophiles to study the reaction products of BBL in aqueous solutions: aniline (2), *m*-toluidine (3), *p*-toluidine (4), *p*-anisidine (5), benzylamine (6) and 2-phenylethylamine (7) (figure 6). We first studied the formed products of the reaction of BBL and the standard amine nucleophiles.

Interestingly, these product studies revealed that the amine structure directly influences the preferred site of attack at BBL. Aromatic amines opened the lactone ring via a  $S_N2$  attack at the C3 position of BBL (O-alkyl fission), yielding *beta*-amino acid products, whereas primary aliphatic amines underwent acylation via reaction at the C1 site of BBL (O-acyl fission), forming 3-hydroxy amides (scheme 5).



**Scheme 5:** Products (**2-p** - **7-p**) of the reactions of BBL with amines **2** - **7** in  $H_2O:MeCN$  9:1 (v/v) (yields refer to isolated products).

### 2.3.1 QM/MM STUDIES ON THE C1 VS C3 SELECTIVITY OF AMINE ATTACK ON BBL

To explain the unexpected preference for either C1 or C3 attack of aliphatic and aromatic amines on BBL, theoretical studies using a combined quantum mechanics/molecular mechanics (QM/MM) approach with linear-scaling quantum-chemical methods (QM) was performed (see ref.<sup>[39]</sup> and references therein).<sup>[40,41]</sup> The composition of the calculated systems is exemplarily illustrated for the reaction of BBL with aniline in figure 8.

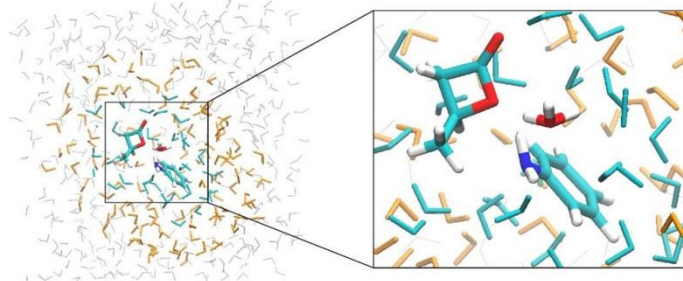


**Figure 8:** Illustration of the calculated systems using the QM/MM approach, as exemplified for the reaction of BBL with aniline. The reactants (depicted in atomic color) are part of the QM region (cyan; 156 atoms) in which chemical reactions can be described. The remaining part is described by MM (Molecular Mechanics), in which the region depicted in orange will be optimized (including the QM region; overall 681 atoms) and the grey region will be held fixed (2235 atoms in total).

In this reaction,  $\text{H}_3\text{O}^+$  stabilizes the transition state of the nucleophilic attack of aniline at the C3 position of BBL and thereby lowers the activation barrier by 28 kcal/mol to 21 kcal/mol (table 2). Specifically,  $\text{H}_3\text{O}^+$  approaches the lactone ring oxygen to a minimum distance of 1.38 Å, forming a strong hydrogen bond and thus facilitating a lactone ring opening. In a subsequent step, aniline forms a covalent bond with C3 and simultaneously protonates the lactone oxygen to form a stable product (-17 kcal/mol compared to the initial state) (figure 9). Contrastingly, in the case of the C1 attack on BBL,  $\text{H}_3\text{O}^+$  protonates the lactone ring oxygen instead of aniline, leaving aniline protonated when forming the product. This product, however, is not stable (+13 kcal/mol compared to the initial state) and immediately regenerates the starting material.

**Table 2:** Calculated reaction barriers (enthalpies) of the reaction of BBL with aniline and benzylamine in water and in water including  $\text{H}_3\text{O}^+$ .

Attack position lactone	Aniline		Benzylamine	
	C1	C3	C1	C3
In water including $\text{H}_3\text{O}^+$ (kcal/mol)	21*	21	0	78
In water (kcal/mol)	53	49	12	37

\* product not stable

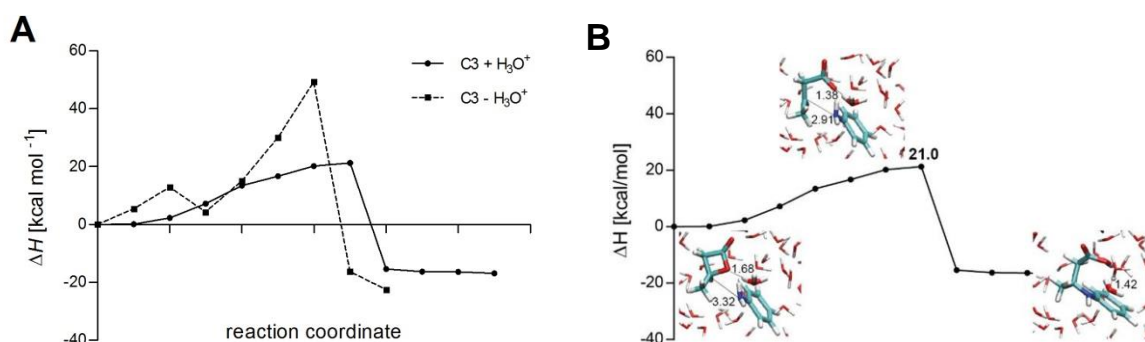


**Figure 9:** Calculated reaction profiles of the C3 attack of aniline on BBL with (black) and without (black dashed)  $\text{H}_3\text{O}^+$  (left) with structures out of the QM/MM simulation for the starting material, transition and product state (right).

Due to the explained dependence on  $\text{H}_2\text{O}/\text{H}_3\text{O}^+$ , the reaction did also experimentally not occur in non-aqueous solvents such as acetonitrile and DMSO, emphasizing the good correlation between QM/MM calculation and the performed experiments (figure 10).

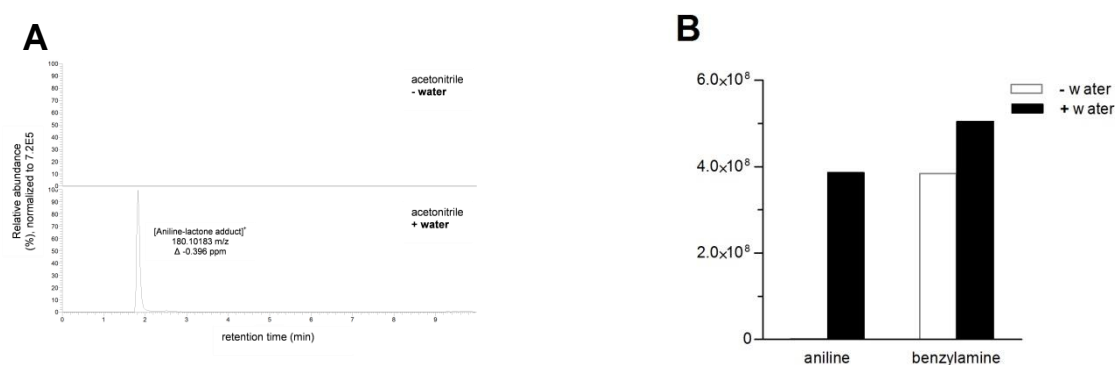


**Figure 10:** Mass range [180.10101 m/z – 180.10281] of full-scan [50-600 m/z] reversed-phase HPLC-ESI-HRMS (positive polarity) traces of the conversion of BBL with aniline after the addition of water compared to the reaction in acetonitrile (A) and relative comparison of corresponding peak areas (traces of benzylamine not shown) of formed products of the reactions of BBL with aniline and benzylamine with (black) and without (white) water in acetonitrile (B).

On the other hand, nucleophilic attack of benzylamine at C1 does not require  $\text{H}_3\text{O}^+$  stabilization. Calculations demonstrate that an attack at C1 and protonation of the lactone ring by the amine is favored (activation barrier of 12 kcal/mol) over the attack at C3 (activation barrier of 37 kcal/mol; table 2). In the transition state, the C1 atom is in a tetrahedral configuration and the lactone ring remains intact. Subsequently, proton transfer from benzylamine to the ring oxygen induces lactone opening. If  $\text{H}_3\text{O}^+$  is considered in these simulations, the reaction also occurs via the same tetrahedral transition state, but  $\text{H}_3\text{O}^+$  protonates the ring oxygen instead. Finally, the positively charged nitrogen transfers a proton to a nearby water molecule (figure 11).

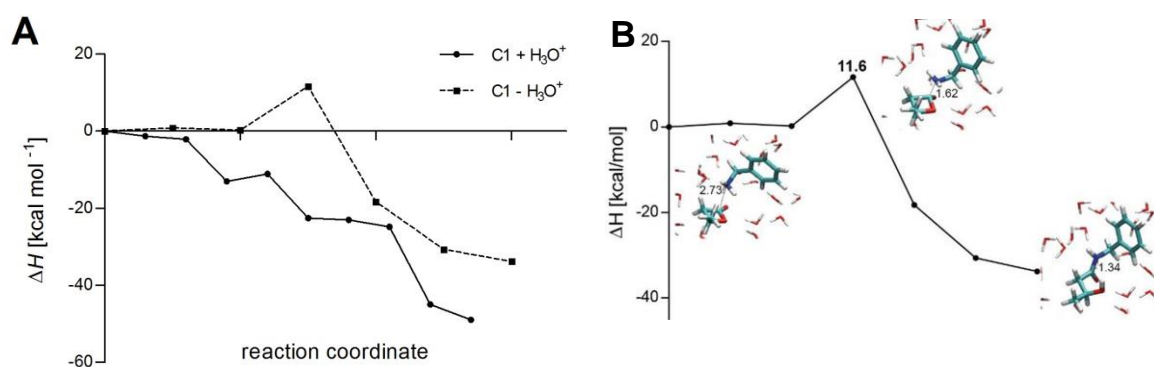


**Figure 11:** Calculated reaction profiles of the C1 attack of benzylamine on BBL with (black) and without (black dashed)  $\text{H}_3\text{O}^+$  (A) with structures from the QM/MM simulation for the starting material, transition state and product (right). Accounting for  $\text{H}_3\text{O}^+$  in the calculated system leads to barrier-free attack at C1, however, minor product formation is also possible in the absence of  $\text{H}_3\text{O}^+$  (B).

The computational data is again in line with experimental measurements of the rate constants for the reaction of benzylamine and BBL in the presence ( $5.8 \times 10^{-3} \text{ M}^{-1} \text{ s}^{-1}$ ) and in the absence of water ( $2.5 \times 10^{-4} \text{ M}^{-1} \text{ s}^{-1}$ ). These values demonstrate that C1 attack indeed takes place, even in absence of  $\text{H}_3\text{O}^+$  and  $\text{H}_2\text{O}$  (figure 10).



Since almost all naturally occurring *beta*-lactones exhibit bulky substituents at the C3 position, the biologically relevant ring-opening reaction in enzyme active-sites is likely at the C1 position. This is supported by co-crystal structures of the thioesterase domain of human fatty acid synthase inhibited by Orlistat<sup>[42]</sup> as well as kinetic studies that show rapid hydrolysis of the ester intermediate of lactone-bound enzyme.<sup>[43]</sup>

### 2.3.2 KINETIC STUDIES OF THE REACTIONS OF BBL WITH AMINE NUCLEOPHILES

To determine the electrophilic reactivity of BBL, kinetic studies were performed by following the turnover of BBL during the reaction with the same set of standard nucleophiles already used for the product studies. The reactions were again performed in aqueous TEA-buffered solutions and recorded via <sup>1</sup>H NMR spectroscopy (table 3). In order to fully solubilize these molecules, a small amount of DMSO (10 vol-%) was necessary as a co-solvent. Again, the consumption of BBL followed a mono-exponential function,  $[BBL]_t = [BBL]_0 e^{-k_2 t}$ , from which  $k_2$  was derived. The rate constants of the reaction of BBL with respective nucleophile  $k_N$  can then be calculated by rearranging equation 4 (explanation see section 2.1) to equation 5, in which  $k_1$  is the first-order rate constant of the background reactions of BBL in TEA-buffered 9:1 D<sub>2</sub>O:d<sub>6</sub>-DMSO solvent mixture (table 2, entry 4),  $k_2$  is experimentally determined and  $[amine]_{eff}$  is the effective concentration of free amines, which is calculated according to *Henderson Hasselbalch* (equation 6,<sup>[44]</sup>  $pK_{aH+}$  (25 °C) values see table 3) at pH 7.75.

$$k_2 = k_1 + k_N[amine]_{eff} \quad (4)$$

$$k_N = (k_2 - k_1)/[amine]_{eff} \quad (5)$$

$$pH = pK_a + \log \frac{[amine]_{eff}}{[amine]_0} \quad (6)$$

**Table 3:** Second-order rate constants of the reactions of amines with BBL in 0.10 M TEA-buffered aqueous solutions ( $[BBL]_0 = 25$  mM, pH 7.75 in D<sub>2</sub>O:d<sub>6</sub>-DMSO 9:1 (v/v), at 37 °C, <sup>1</sup>H NMR spectroscopy).

Nucleophile	pK <sub>a</sub> <sup>[d]</sup>	N <sup>[a]</sup>	s <sub>N</sub> <sup>[a]</sup>	k <sub>N</sub> [M <sup>-1</sup> s <sup>-1</sup> ]	k <sub>rel</sub>
Aniline ( <b>2</b> )	4.60	12.99	0.73	7.9 (±0.5) × 10 <sup>-4</sup> [b]	1
<i>m</i> -Toluidine ( <b>3</b> )	4.87	n.d.	n.d.	9.9 × 10 <sup>-4</sup>	1.25
<i>p</i> -Toluidine ( <b>4</b> )	5.08	13	0.79	1.4 × 10 <sup>-3</sup>	1.77
<i>p</i> -Anisidine ( <b>5</b> )	5.36	14.28	0.68	1.6 × 10 <sup>-3</sup>	2.03
Benzylamine ( <b>6</b> )	9.36	13.44	0.55	5.8 × 10 <sup>-3</sup> [c]	7.34
2-Phenylethylamine ( <b>7</b> )	9.89	13.40	0.57	1.1 × 10 <sup>-2</sup> [c]	13.9

[a] Reactivity parameters  $N$  and  $s_N$  of amines in water<sup>[45]</sup> [b] Average  $k_N$  of four kinetic runs at variable aniline concentration, the same value for  $k_N$  is obtained from the slope of the linear correlation of  $k_2$  vs  $[aniline]_0$  (table 4) [c] Rate constants of lower accuracy, an error of ±15% is assumed [d] see ref. <sup>[46-50]</sup>

To evaluate the experimentally obtained data the second-order rate constant  $k_N$  for the reaction of BBL with aniline was additionally determined at four different aniline concentrations (table 4).

**Table 4:** Rate constants for the reactions of BBL with aniline at 37 °C at pH 7.75 in D<sub>2</sub>O:d<sub>6</sub>-DMSO 9:1 (v/v) at variable aniline concentrations.

[Aniline] <sub>0</sub> (M)	$k_{\text{obs}}$ (s <sup>-1</sup> )	$k_N$ (M <sup>-1</sup> s <sup>-1</sup> )
$5.0 \times 10^{-2}$	$9.72 \times 10^{-5}$	$8.50 \times 10^{-4}$
$7.4 \times 10^{-2}$	$1.07 \times 10^{-4}$	$7.07 \times 10^{-4}$
$1.0 \times 10^{-1}$	$1.37 \times 10^{-4}$	$8.23 \times 10^{-4}$
$3.0 \times 10^{-1}$	$2.91 \times 10^{-4}$	$7.88 \times 10^{-4}$
Averaged $k_N$		<b><math>7.92 \times 10^{-4}</math></b>
Standard deviation		$0.54 \times 10^{-4}$

The linear dependence of the first-order rate constant  $k_2$  on the aniline concentration (figure 12) is in line with the rate laws shown in equations 2a, b and 4. Moreover, the averaged  $k_N$  is in excellent agreement with the  $k_N$  derived from the slope of the linear correlation of  $k_{\text{obs}}$  with [aniline]<sub>0</sub>. Additionally, the intercept on the ordinate ( $5.49 \times 10^{-5} \text{ s}^{-1}$ ) matches perfectly the first-order rate constant  $k_1$  (equation 3) for the background reaction in TEA-buffered solution (table 1:  $k_1 = 5.47 \times 10^{-5} \text{ s}^{-1}$ ), which demonstrates that the background reaction is not significantly affected by the presence of the amine.

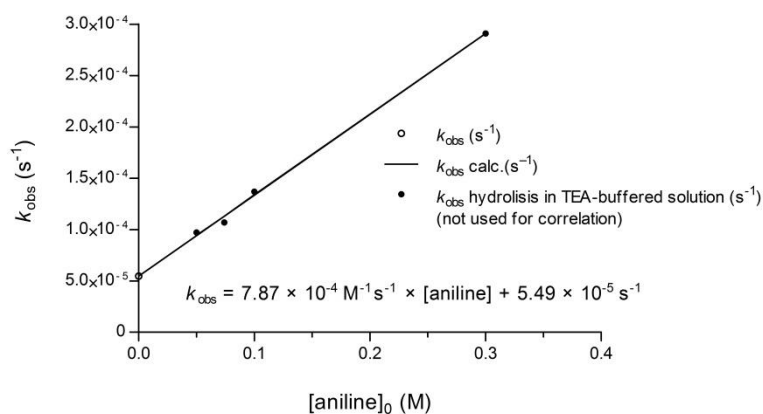


**Figure 12:** Linear dependence of the first-order rate constant  $k_2$  ( $= k_{\text{obs}}$ ) for the reaction of BBL with aniline (2) on the aniline concentration ( $k_{\text{obs}}$  for [aniline]<sub>0</sub> = 0 corresponds to BBL hydrolysis in TEA-buffered solution; not considered for the depicted linear correlation).

The consistency of the determined  $k_N$  values is finally demonstrated by a *Hammett* analysis of the data for anilines, which shows a good correlation of the rate constants  $k_N$  with the  $\sigma_p^-$  (and  $\sigma_m$ ) values of the substituents at the anilines **2 - 5** (figure 13).<sup>[51]</sup>

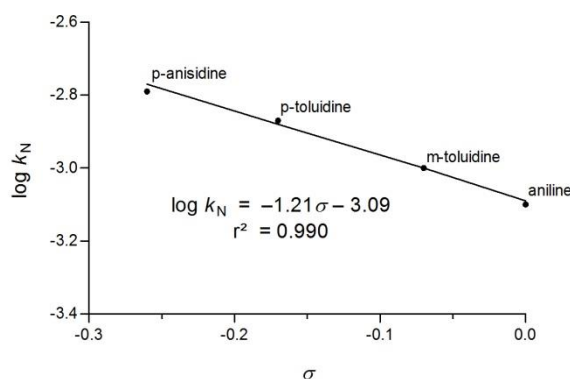


**Figure 13:** Hammett plot of the reaction of BBL with anilines at 37 °C and pH 7.75 in D<sub>2</sub>O:d<sub>6</sub>-DMSO 9:1 (v/v).

The amines **2** - **7** employed in this study cover a relatively small range in nucleophilicity in water ( $12.99 < N < 14.28$ ), which corresponds to a reactivity difference of only a factor of 20 towards a certain electrophile. As anilines attack at C3 of BBL while aliphatic amines attack at C1 position, rate constants for nucleophilic attack at BBL are additionally influenced to a certain extent by anomeric effects.<sup>[52]</sup> Mayr's reference electrophiles have been assigned the same value of  $E$  in different solvents. It can be expected, however, that the use of solvent-independent  $E$  parameters is not possible for all electrophiles: if products with highly localized charges will be formed during nucleophilic attack, solvent-dependent  $E$  parameters will be needed.<sup>[53]</sup> In this work, the rate constant of the reaction of BBL with benzylamine (**6**) decreases by a factor of 23 when changing from aqueous solution to DMSO solution, though an increase of the rate constants by about one order of magnitude ( $N:s_N$  for benzylamine in DMSO = 15.28:0.65) is expected when assuming the same electrophilic reactivity of BBL in both solvents.<sup>[31]</sup> As a consequence, it is not possible to generally determine a reliable  $E$  parameter for C1 or C3 attack on BBL. Hence, the discussion of *beta*-lactam reactivity in the following paragraph has been based on relative rate constants towards the amine nucleophiles.

## 2.4 ELECTROPHILIC REACTIVITY OF *BETA*-LACTAMS

As already mentioned in the introduction *beta*-lactams are potent antibiotics with pronounced protein reactivity as long as they are activated by for example, sulfonylation in case of aztreonam or as bicyclic compounds like penicillin. In contrast, monocyclic *beta*-lactams only exhibit limited reactivity with enzyme active-sites.<sup>[21]</sup> To further extend the previously described performed kinetic and QM/MM studies on the reactivity of *beta*-lactones in aqueous solution, exactly this interesting physiological observation of *beta*-lactams was applied. The reactions were again performed in aqueous TEA-buffered solutions and recorded via <sup>1</sup>H NMR spectroscopy.

4-Methyl-1-azetidin-2-one (**9**)<sup>[54]</sup> was used as model for monocyclic *beta*-lactams, the very well-known antibiotic penicillin G (**10**) served as bicyclic *beta*-lactam electrophile.

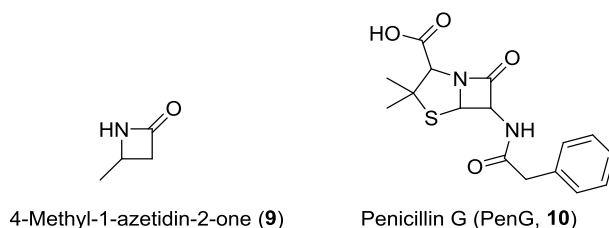


**Figure 14:** Molecular structures of monocyclic lactam 4-Methyl-1-azetidin-2-one (**9**) (left) and bicyclic Penicillin G (**10**) (right).

#### 2.4.1 REACTIVITY OF METHYL-1-AZETIDIN-2-ONE TOWARDS AMINES

The physiological observation of unreactive monocyclic *beta*-lactams was in line with our experimental and theoretical studies which revealed no turnover of 4-methyl-1-azetidin-2-one (**9**) with any of the amino-nucleophiles (figure 15).

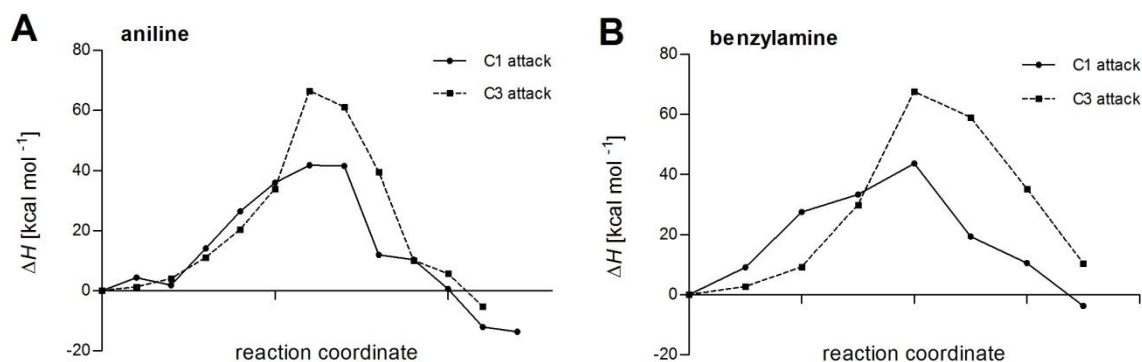


**Figure 15:** Calculated reaction profiles of aniline (A) and benzylamine (B) with 4-methyl-1-azetidin-2-one (**9**) in water. The attack at C1 is shown as black line and the attack at C3 as black-dashed line.

As can be seen in table 5, irrespective to the exact position of the nucleophilic attack, an insuperable activation barrier of 40 - 70 kcal/mol was calculated.

**Table 5:** Calculated reaction barriers (enthalpies) of the reaction of 4-methyl-1-azetidin-2-one (**9**) with aniline and benzylamine in water.

	Aniline		Benzylamine	
Attack position lactam	C1	C3	C1	C3
In water (kcal/mol)	42	67	44	68

## 2.4.2 REACTIVITY OF PENICILLIN G TOWARDS AMINES

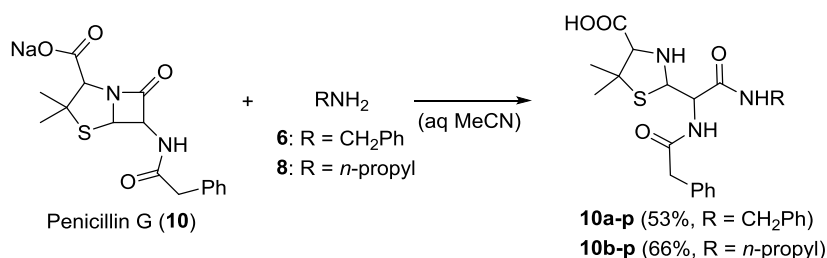
Contrastingly, penicillin G, the activated bicyclic *beta*-lactam, reacted with *n*-propylamine, benzylamine and 2-phenylethylamine at significantly higher rates ranging from  $8 \times 10^{-2} \text{ M}^{-1}\text{s}^{-1}$  to  $4 \times 10^{-1} \text{ M}^{-1}\text{s}^{-1}$  (table 6). These rates even exceeded those observed for monocyclic lactones, confirming again the compliance of the generated data with real physiological behavior. The reactions were again performed in aqueous TEA-buffered solutions and recorded via  $^1\text{H}$  NMR spectroscopy. The consumption of penicillin G (**PenG**) followed a mono-exponential function,  $[\text{PenG}]_t = [\text{PenG}]_0 e^{-k_2 t}$ , from which  $k_2$  was derived in analogy to equation 5.

**Table 6:** Second-order rate constants of the reactions of amines with penicillin G in 0.10 M TEA-buffered aqueous solutions ( $[\text{PenG}]_0 = 25 \text{ mM}$ , pH 7.75 in  $\text{D}_2\text{O}:\text{d}_6\text{-DMSO}$  9:1 (v/v), at 37 °C,  $^1\text{H}$  NMR spectroscopy).

Nucleophile	$\text{pK}_a$	$N^{[a]}$	$s_N^{[a]}$	$k_N [\text{M}^{-1} \text{s}^{-1}]$
Benzylamine ( <b>6</b> )	9.36	13.44	0.55	$8.1 \times 10^{-2}$
2-Phenylethylamine ( <b>7</b> )	9.89	13.40	0.57	$8.6 \times 10^{-2}$
<i>n</i> -Propylamine ( <b>8</b> )	10.68	13.33	0.56	$4.5 \times 10^{-1}$

[a] Reactivity parameters  $N$  and  $s_N$  (as defined in equation 1) of amines in water, from ref.<sup>[45]</sup>

The acylation products **10a** and **10b** of the reactions of penicillin G with benzylamine (**6**) and propylamine (**8**) were additionally isolated and characterized by NMR spectroscopy and HRMS to confirm the C1 attack of the nucleophile on the lactam (scheme 6).



**Scheme 6:** Products of the reactions of sodium penicillin G with amines **6** and **8** in  $\text{H}_2\text{O}:\text{MeCN}$  9:1 (v/v) (yields refer to isolated products, only one diastereomer is shown).

Additionally to the product studies, QM/MM calculation could further show the correlation of calculated energy barriers and experimentally determined rate constants as can be seen in table 7 and figure 16.

**Table 7:** Calculated reaction barriers (enthalpies) of the reaction of penicillin G with *n*-propylamine and benzylamine in water.

	<i>n</i> -Propylamine		Benzylamine	
Attack position penicillin G	C1	C3	C1	C3
In water (kcal/mol)	11	65	21	52

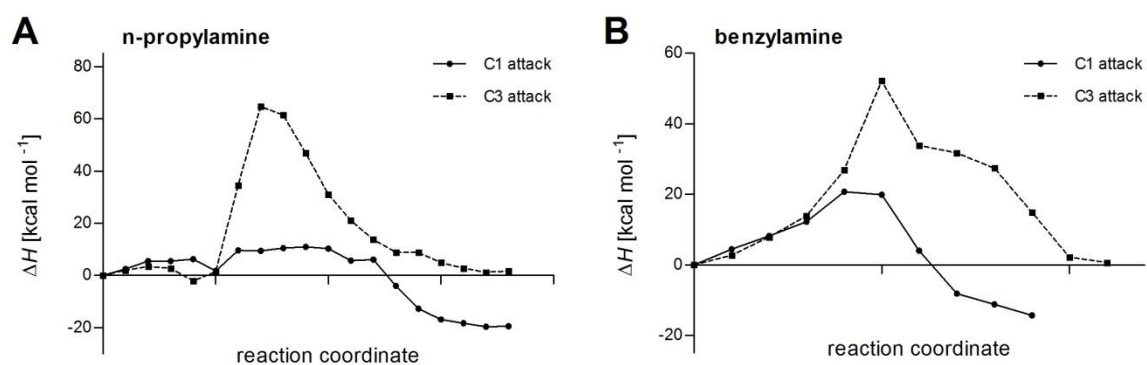


**Figure 16:** Calculated reaction profiles of *n*-propylamine (A) and benzylamine (B) with penicillin G. The attack at C1 is shown in black and the attack at C3 in black dashed. A: The first barrier represents the reorientation of *n*-propylamine during the approach towards penicillin G (**10**). The second barrier represents the nucleophilic attack at C1 and C3 respectively.

### 3 CONCLUSION AND OUTLOOK

Natural products exhibit diverse electrophilic motifs that have been customized by evolution to irreversibly bind the active-sites of enzymes. These tailored scaffolds vary in their general electrophilic reactivity resulting in different selectivities towards nucleophilic amino acids. The corresponding biological activities are as diverse as the natural compounds themselves and range from anti-cancer to antibiotic properties. Recent drug discovery efforts have focused on natural product inspired covalent inhibitors, however, a quantitative scale to describe, parameterize and ideally predict their reactivity under physiological conditions is currently lacking. One famous example of such bioactive natural compounds are *beta*-lactam antibiotics, containing penicillin being the first discovered substance inhibiting the growth of bacteria. In order to mimic the biological systems as much as possible the reactions should be performed in aqueous media with different nucleophiles imitating the active-sites in enzymes.

To establish a reliable test system under physiological conditions, the electrophilic reactivity of *beta*-lactones was compared to the reactivity of mono- and bicyclic *beta*-lactams in aqueous TEA-buffered solution. At first, the reactions of the monocyclic *beta*-lactone *beta*-butyrolactone (BBL) with a set of amino-substituted nucleophiles containing aromatic anilines and primary aliphatic amines were monitored by time-resolved  $^1\text{H}$  NMR spectroscopy. The determined rates constants were then evaluated according to the linear free energy relationship  $\log k(20\text{ }^\circ\text{C}) = s_{\text{N}}(N + E)$ . Nucleophilicity parameters  $s_{\text{N}}$  and  $N$  have been previously obtained for a variety of compound classes, providing a prognostic value for chemical reactions.<sup>[28-31]</sup>

Additionally performed product studies revealed a different regioselectivity of the attack on the lactone ring, dependent on the nucleophile: whereas aromatic amines opened the lactone on C3 position, an attack of aliphatic amines occurred at C1 position of BBL. To explain this unexpected preference, QM/MM calculations using linear-scaling QM methods were performed. Strikingly, these calculations revealed that  $\text{H}_3\text{O}^+$  molecules are crucial for catalysis due to their stabilizing effects on the transition state of aniline attack at the C3 position of the lactone. While the energy path for this reaction is significantly lower compared to a C1 attack, benzylamine prefers C1 (with or without  $\text{H}_3\text{O}^+$  catalysis) due to an insuperable C3 energy barrier. All these calculations were supported by experimental data which confirmed the influence of water for the corresponding reaction rates.

The value of this platform was then demonstrated in a second part in the direct comparison of *beta*-butyrolactone, 4-methyl-1-azetidin-2-one and penicillin G reactivity. Therefore, the

reactivities of the monocyclic *beta*-lactam 4-methyl-1-azetidin-2-one and the bicyclic *beta*-lactam penicillin G towards the same set of nucleophiles were kinetically determined and again further validated by QM/MM methods: whereas 4-methyl-1-azetidin-2-one showed no turn-over with any of the applied amino-nucleophiles, the reaction rates of penicillin G even exceeded those observed for mono-cyclic lactone BBL. This data confirmed the compliance of the observed reaction rates with real physiological behavior as bicyclic *beta*-lactams and *beta*-lactones are generally reactive with protein active-sites while monocyclic *beta*-lactams only exhibit limited reactivity with enzyme active-sites.

With this proof of principle study, the scope of application can easily be expanded to other biologically-relevant electrophilic scaffolds like *Michael*-acceptors and epoxides leading to a quantitative reactivity scale and thus, allow predictions for electrophilic modifications in biological systems.



III – AMINO-EPOXYCYCLOHEXENONES AND  
THEIR PROTEIN TARGETS IN SALMONELLA  
TYPHIMURIUM



## 1 INTRODUCTION

### 1.1 ACTIVITY-BASED PROTEIN PROFILING

As described in the general introduction, the interaction between small, electrophilic molecules and cellular nucleophiles is responsible for various important fundamental functions found in organisms. The general reactivity of electrophilic core units towards nucleophiles has been described for *beta*-lactones and *beta*-lactams in the previous project. In these studies, the interaction of a small molecule containing an electrophilic core unit and a standard nucleophile imitates small molecule-protein interactions found in biological systems. Due to the high complexity of proteins, the investigation of these interactions is challenging. However, due to their diverse biological functions proteins are the predominant drug targets for modern medicine.<sup>[55,56]</sup>

There are a number of proteomic methods available for the study of protein structure and abundance, the interaction of proteins, or the whole set of proteins found in one organism.<sup>[57-59]</sup> Nevertheless, techniques for bacterial proteome annotation including post-translational chemical modification, signal peptides or the intrinsic functions of specific proteins are still in their infancy. Strikingly, the abundance of a protein is not necessarily related to its activity and thereby its physiological role.<sup>[60-63]</sup> Therefore, an activity-based proteomic strategy is required to incorporate this important missing aspect.

Based on previous work by Powers and Walkers,<sup>[64,65]</sup> a new powerful technology named activity-based protein profiling (ABPP) was established by Cravatt<sup>[63,66-69]</sup> and Bogoy.<sup>[70-73]</sup> This multidisciplinary approach enables the identification and functional characterization of enzymes or enzyme families in complex biological systems.<sup>[74,75]</sup> Moreover, ABPP can be used to evaluate the influence of small molecules on a bacterial proteome *in vivo*, and therefore gives access to a new target-identification strategy for the treatment of diseases.<sup>[61]</sup> The basic concept of ABPP involves treatment of a protein sample with an active small molecule containing a reporter tag (figure 17). This ABPP probe selectively reacts with a nucleophilic group within the respective target protein and can subsequently be analyzed, by SDS-PAGE or via high-resolution mass spectrometry.

ABPP probes consist of three main elements: 1) a reactive binding group, which is mostly a moderate electrophilic moiety that can covalently react with a nucleophilic active-site of the target enzyme, 2) a so-called spacer that links the electrophilic core unit to the reporter tag and may additionally serve as a binding motif for the non-covalent affinity interaction between protein and

probe and, 3) a reporter tag, that enables the visualization (fluorescence dye) or enrichment (biotin tag) of the labeled proteins.

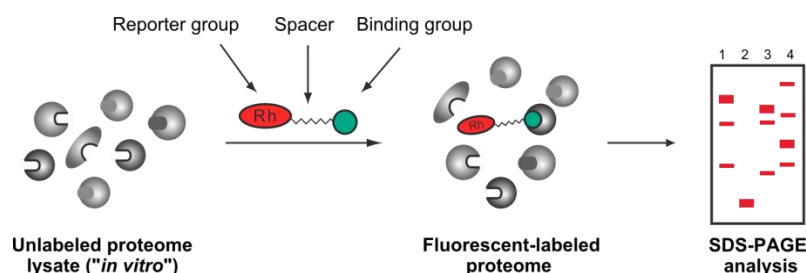


**Figure 17:** Basic concept of an *in vitro* activity-based protein profiling (ABPP) approach with fluorophore-equipped ABPP probe.<sup>[76]</sup>

Since the main advantage of ABPP is the activity-related tagging of enzymes in living systems, using tag-free or smaller tags for *in vivo* applications is of interest. The relatively bulky reporter group can therefore be replaced by a terminal alkyne (or azide), which enables the attachment of the reporter group after cell lysis using bio-orthogonal, copper-mediated 1,3-dipolar cycloaddition (Click-chemistry).<sup>[66,68,77-80]</sup> The much smaller terminal alkyne not only improves the cell-permeability of the ABPP probe, but also allows the ABPP probe to structurally resemble its natural product more closely. The basic procedure of a tag-free ABPP experiment is shown in figure 18.<sup>[68]</sup> Living bacterial cells are incubated with the cell-permeable, alkyne-tagged ABPP probe (labeling). Afterwards the cells are lysed, labeled proteins are tagged to the azide-containing reporter group by click-chemistry (tagging). The fluorescently-labeled proteins are then separated via SDS-PAGE and visualized by fluorescence-scanning (reporting).

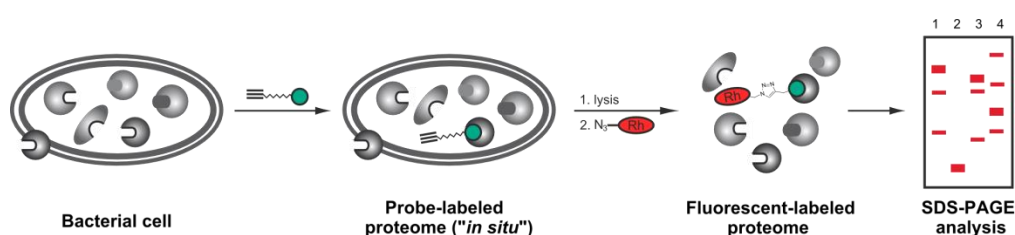


**Figure 18:** Basic concept of tag-free, *in situ*, activity-based protein profiling using an alkyne-tag containing ABPP probe.

Especially with regards to the previously discussed resistance development of antibiotics, the detection of new virulence and pathogenicity-related proteins is of major interest. One application for *in vivo* ABPP is the comparison of the labeling pattern of ABPP probes between pathogenic and non-pathogenic bacterial strains. This so-called comparative target discovery is still one of the most popular applications of this strategy and enables the visualization of possible pathogenicity-associated target proteins of an ABPP probe.<sup>[63]</sup> Since SDS-PAGE analysis of the different

fluorescently-labeled proteins only gives information about the size of the enzymes, the workflow has to be extended by an enrichment step to identify the potential targets via high-resolution mass spectrometry (HRMS). In contrast to the analytical *in vivo* approach shown in figure 18, the labeled proteins are bound to an affinity enrichment tag like biotin azide using click-chemistry, thereby enabling selective enrichment using avidin-covered beads. After separating the enriched and labeled proteins via SDS-PAGE and visualization via fluorescent scanning the specific bands of interest are isolated. After digesting the proteins directly on the beads they are subjected to MS-analysis (figure 19).

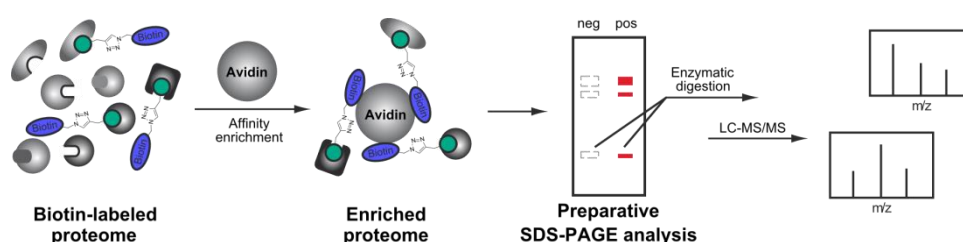


**Figure 19:** Basic concept of preparative activity-based protein profiling by using avidin-biotin affinity purification to isolate protein amounts sufficient for subsequent LC-MS/MS analysis.

A gel-free approach, which completely avoids the SDS-PAGE separation of the proteins, enables the detection of probe-labeled proteins within the complex proteomic mixture by using stable isotope labeling of amino acids, also known as Dimethyl labeling. Instead of isolating the distinct bands of a gel, the enriched and labeled proteins are digested directly in solution after the enrichment step. Without any additional separation, the digested peptides are directly subjected to MS analysis by using stable isotope dimethyl labeling to gain comparative and quantitative information about the labeled proteins. The advantage of the gel-free proteomic analysis is a more comprehensive and quantitative overview of the target proteins.<sup>[81-83]</sup>

Using enrichment step and identification of labeled proteins by MS, a second major application of ABPP becomes apparent: the target discovery of bioactive natural products.<sup>[75]</sup> Resistance development of pathogenic bacterial strains towards known antibiotics is accelerating and new drug targets as well as potent drugs are highly sought after. As previously mentioned, naturally derived compounds are often the most potent antibiotics. However, the protein targets of these interesting compounds are quite often unknown and therefore not accessible for further drug development. By revealing their protein targets and elucidating their inhibitory mechanism, one can obtain more insight into the mode of action of certain natural products and therefore enable further target-directed inhibitor development by fine-tuning their structures. Moreover, natural products have a decisive advantage in acting as an ABPP probe over synthetic compounds, as a

result of their evolutionary development. Due to their fine-tuned reactivity, they often show excellent selectivity and high affinity towards specific proteins.

In combination with the comparative target identification, ABPP is a very potent method to investigate new antibiotics. By comparing the labeled proteins in multi-resistant pathogenic bacterial strains of a bioactive, natural product-derived ABPP probe to an unreactive analog, new target proteins and therefore new drugs could be developed. In this case a bioactivity-related labeling pattern would indicate a potential new target enzyme as shown in figure 20.

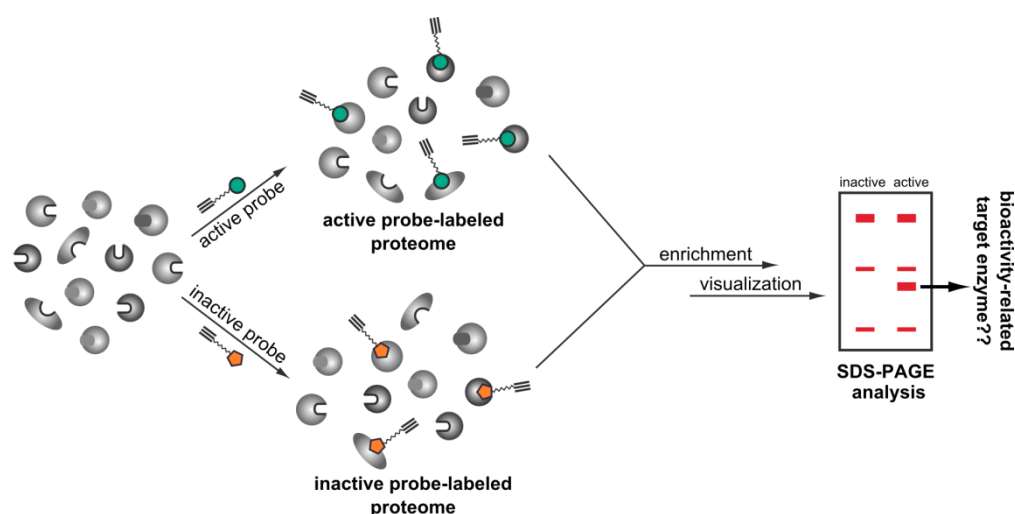


**Figure 20:** Basic concept of bioactivity-related target enzyme identification via ABPP: comparison of the labeling pattern effected by bioactive and inactive activity-based probes.

## 1.2 BIOACTIVE EPOXY-CYCLOHEXENONE NATURAL PRODUCTS

As previously mentioned in the introduction, diverse electrophilic moieties capable of reacting specifically with the active-sites of enzymes and thereby inhibiting cellular proteins can be found among natural products.<sup>[17-19]</sup> These naturally-derived, bioactive compounds are therefore attractive as potential drugs. A very interesting class of natural products that exhibits various degrees of bioactivity are epoxy-cyclohexenones\*, which are produced by microorganisms largely isolated from fungus but also from various plants and animals.<sup>[84]</sup> This compound class consists of a great number of members, ranging from very simple and small structures to highly complex, substituted molecules. Some of these compounds show good antibacterial activity among several pathogenic strains.<sup>[85-87]</sup> Since no bacterial target enzymes or mode of action of this compound class are known so far, epoxy-cyclohexenones are ideal examples for an ABPP approach, especially with regard to the resistance development of antibiotics.

\* In this thesis, the term epoxy-cyclohexenone is used specifically to refer to compounds containing the 7-oxabicyclo[4.1.0]hept-3-en-2-one structural moiety.

## 1.2.1 STRUCTURAL DIVERSITY

The common motif of substances belonging to the class of epoxy-cyclohexenones consists of two electrophilic moieties including an epoxide and a *Michael*-acceptor, which are combined in a six-membered carbon ring with a wide range of structural and stereochemical diversity. Structures that show an additional hydroxyl-group substitution in *para*-position to the carbonyl function are more precisely named epoxy-hydroxycyclohexenones and some examples are shown in figure 21.

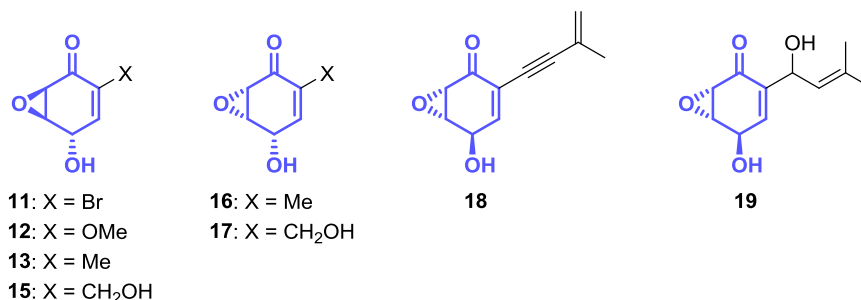


**Figure 21:** Examples of structurally simple members of the epoxy-hydroxycyclohexenone family, the core unit is highlighted in blue. Bromoxone (**11**),<sup>[88]</sup> Chaloxone (**12**),<sup>[89]</sup> Epiepoformin (**13**),<sup>[90]</sup> Epiepoxydon (**15**),<sup>[91]</sup> Epoformin (**16**)<sup>[90]</sup>, Epoxydon (**17**),<sup>[92]</sup> Harveynone (**18**),<sup>[93]</sup> Panepoxydon (**19**).<sup>[92]</sup>

Despite their simple structure, all of these molecules show a variety of biological activities. While bromoxone (**11**), panepoxydon (**19**) and harveynone (**18**) show antitumor activity, epoformin (**16**) and epiepoformin (**13**) additionally possess antibacterial properties. Moreover the compounds epoxydon (**17**) and epiepoxydon (**15**) are phytotoxic.<sup>[84,94]</sup>

These examples commonly have a substitution in *ortho*-position to the carbonyl group, but more complex structures with various other functional decorations as well as cyclic substitution pattern can be found (figure 22). Among them, isopanepoxydon (**20**), cycloepoxydon (**21**) and epoxyquinol A (**22**) are known inhibitors of the I $\kappa$ B Kinase  $\beta$ , resulting in anti-inflammatory activity.<sup>[84]</sup> The natural compound myrothecol A (**23**) possesses cytotoxic and antibacterial properties, as with other members of the quinone sesquiterpene family.<sup>[95]</sup> Interestingly, epoxyquinol A (**22**) also exhibits anti-angiogenic activity, making it interesting in targeted antitumor therapy.<sup>[96]</sup>

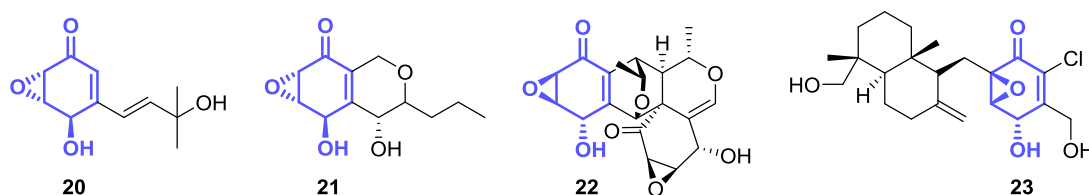


**Figure 22:** Examples of more structurally complex members of the epoxy-hydroxycyclohexenone family, the core unit is highlighted in blue. Isopanepoxydon (**20**),<sup>[97]</sup> Cycloepoxydon (**21**),<sup>[98]</sup> Epoxyquinol A (**22**)<sup>[96]</sup> and Myrothecol A (**23**).<sup>[95]</sup>

All examples illustrated so far contain an epoxy-hydroxycyclohexenone core unit with variable stereochemical arrangements (compare figures 21 and 22). Compounds containing an epoxy-benzoquinone structure as shown in figure 23 are also included into the family. Among them, especially panepoxydione (**25**) and the farnesyltransferase inhibitor UCF76 B (**27**) are notable because of the antitumor activity of these compounds.<sup>[99,100]</sup>

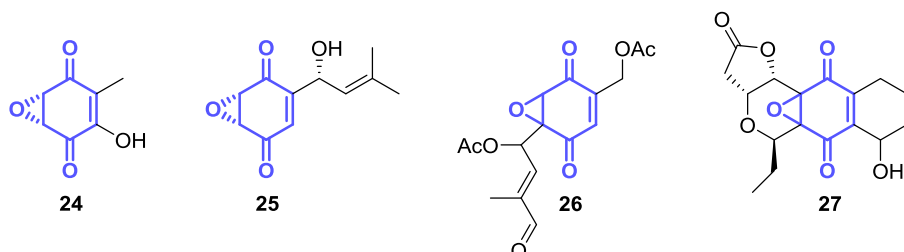


**Figure 23:** Examples of members of the epoxy-benzoquinone family, the core unit is highlighted in blue. Tereic acid (**24**),<sup>[92]</sup> Panepoxydion (**25**),<sup>[100]</sup> Flagranone C (**26**)<sup>[101]</sup> and UCF76 B (**27**).<sup>[99]</sup>

Another structural subgroup of epoxy-cyclohexenones shows additional amino- or amide-substitution on the ring system, and is called amino-epoxycyclohexenones. Some compounds, ranging from relatively simple to quite complex structures, are shown in figure 24. While compounds MM1420 (**28**) and LL-C10037 $\alpha$  (**29**) contain an additional hydroxyl-substitution on the six-membered ring, structures KT 8110 (**30**) and the natural compound epoxyquinomycin C (**31**) are amino-epoxybenzoquinones. LL-C10037 $\alpha$  (**29**) is an antitumor agent and KT8110 (**30**) and epoxyquinomycin C (**31**) exhibit anti-inflammatory activity.<sup>[102]</sup> Additionally, all of these compounds inhibit the growth of bacteria.<sup>[84]</sup>

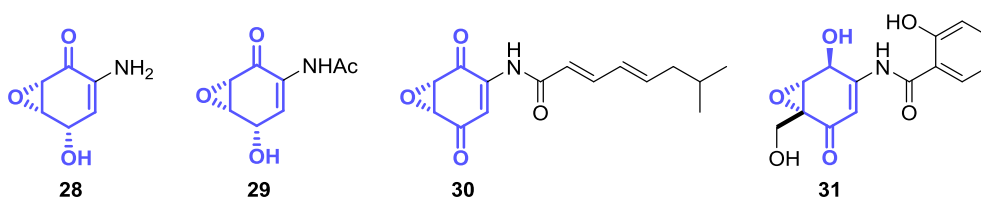


**Figure 24:** Examples of amino-epoxycyclohexenones and amino-epoxybenzoquinones, the core unit is highlighted in blue. MM 14201 (**28**),<sup>[103]</sup> LL-C10037 $\alpha$  (**29**),<sup>[104]</sup> KT 8110 (**30**)<sup>[104]</sup> and Epoxyquinomycin C (**31**).<sup>[102]</sup>

Furthermore, the most prominent and also structurally most complex representatives of amino-substituted epoxy-cyclohexenones are the so-called manumycins. Already in 1963, *Zähner* and coworkers isolated a yet unknown compound out of a *Streptomyces* strain.<sup>[105]</sup> Almost ten years later, *Schröder* and *Zeeck* established the structural elucidation and named the compound manumycin A (**32**).<sup>[106]</sup> To date, many more compounds belong to this class of natural products, which can be subdivided into two structurally different subgroups (figure 25).



Members belonging to type I manumycins show the same amino-epoxycyclohexenone core unit as described before. This core structure is also named the *m*-C<sub>7</sub>N unit because the upper and lower side chains are in *meta*-position to each other on the cyclic carbon ring. In type II manumycins, the epoxide is replaced by a hydroxyethylen moiety.<sup>[85]</sup> Researchers became interested in this compound class because of the inhibitory effects of manumycins on various enzymes, most prominently Ras-farnesyltransferase. In combination with relatively low *in vivo* toxicity, this makes manumycins potential antitumor agents.<sup>[107,108]</sup>

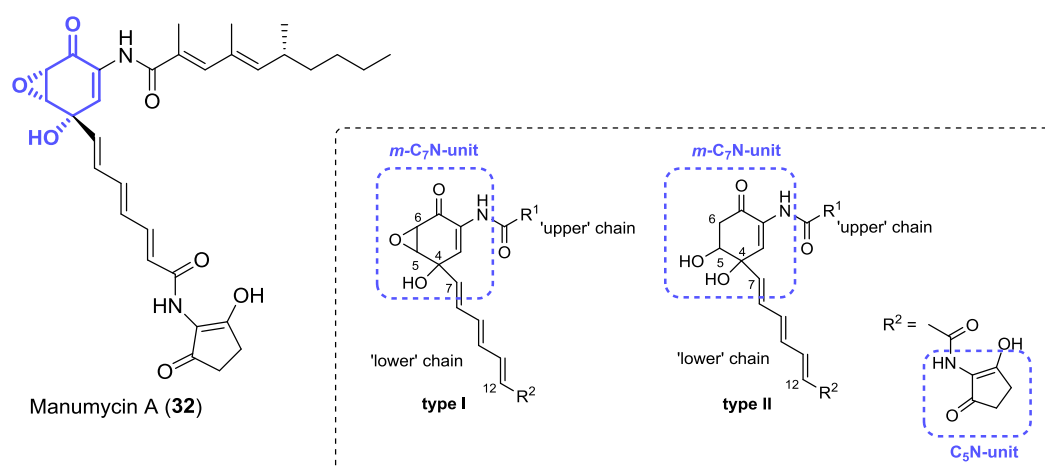


**Figure 25:** The manumycin family of antibiotics: shown is the most famous member, Manumycin A (32), and structural differences among the different subgroups.

Interestingly, members belonging to type I manumycins are known to inhibit the growth of *Gram*-positive bacteria, whereas type II members do not show any antibacterial activity.<sup>[87]</sup> With regard to the described antibacterial properties of the substances reviewed, the following section summarizes interesting structure-activity relationships, which provide a basis for synthetic efforts described herein.

### 1.2.2 STRUCTURE-ACTIVITY RELATED PROBE DESIGN

Epoxy-cyclohexenones represent a suitable class of natural products for ABPP. To select the best potential ABPP probe structures, the following section highlights interesting structure-activity relationships concerning the antibacterial activity of these substances. First, and most importantly, various studies concerning the bioactivity of epoxy-cyclohexenones have shown that the epoxide moiety is essential for antibacterial activity.<sup>[84,109,110]</sup> This is made apparent when looking at the bioactivity of the manumycin family. While compounds belonging to type I subgroup show antibacterial activity in the low  $\mu$ M range against a number of *Gram*-positive strains, no growth inhibition can be observed for type II manumycins.<sup>[87]</sup> Consistently, the natural quinone

sesquiterpenes named myrothecols (figure 22 and 26) show antibacterial activity as long as their core unit contains an epoxide moiety. In contrast, myrothecol F (**33**), which only has a *Michael*-acceptor unit as electrophilic core, and hymenopsin B (**34**), a compound that contains two epoxide moieties, both do not show any antibacterial activity.<sup>[95]</sup> This leads to the conclusion that only the combination of epoxide and *Michael*-acceptor results in growth inhibition of bacteria. Interestingly, almost all of the named compounds still exhibit their cytotoxic properties, even without any epoxide moiety.

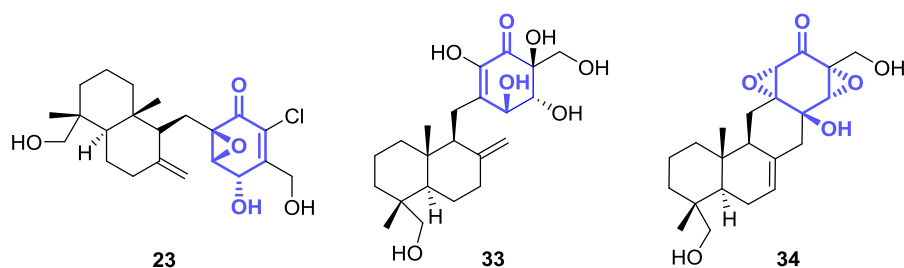


**Figure 26:** Structural differences among the natural compound class of Myrothecols. While Myrothecol A (**23**) inhibits the growth of some *Gram*-positive bacterial strains, Myrothecol F (**33**) and Hymenopsin B (**34**) do not show antibacterial properties.<sup>[95]</sup>

Secondly, the substituents of epoxy-cyclohexenones, in addition to the electrophilic core unit, are important for further probe design. Among the manumycin family, two complex sidechains are attached to the six-membered ring, resulting in very structurally diverse members. Interestingly, the C<sub>5</sub>N-unit that is present in the lower sidechain of most manumycins does not influence antibacterial activity. As an example, nisamycin (**36**), which does not have the C<sub>5</sub>N-unit, is about six times more active against *Gram*-positive bacteria than the corresponding analog alisamycin (**35**) with respect to its minimal inhibitory concentration (MIC) (figure 27).<sup>[86]</sup> Moreover, the benzoquinone analog of manumycin A UCF1-C (**37**), inhibits the growth of bacteria, despite completely lacking a lower sidechain.<sup>[84,111]</sup>

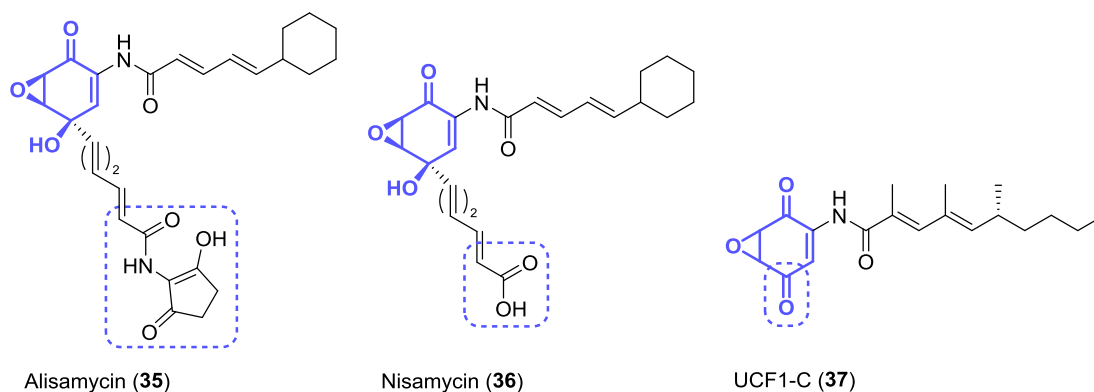


**Figure 27:** Bioactive manumycin-type compounds with structural differences in the 'lower sidechain'. While Alisamycin (35) contains the C<sub>5</sub>N-unit, this moiety is replaced by a carboxylic acid in Nisamycin (36)<sup>[112]</sup> and by an additional carbonyl group in UCF1-C (37).<sup>[111]</sup>

To summarize, substances that contain one of the substitution patterns of amino-epoxycyclohexenones shown in figure 28 have antibacterial properties and are therefore promising new ABPP probes. In compounds based on the structure of epoxyquinomycin or DHMEQ (standing for dehydroxymethylepoxyquinomycin, a synthetic epoxyquinomycin analog),<sup>[113]</sup> the amide-containing sidechain is located in *meta*-position to the carbonyl function. In contrast, the manumycin- structure has a sidechain in *ortho*-position to the carbonyl moiety. Molecules containing the epoxy-benzoquinone pattern showed interesting antibiotic properties as well.

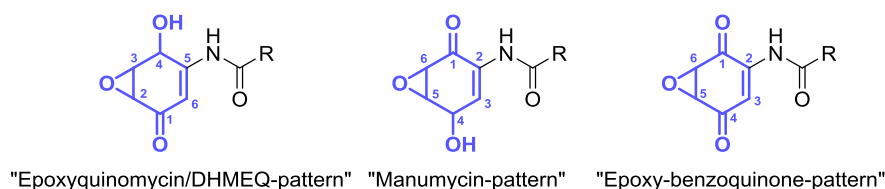


**Figure 28:** General substitution patterns of amino-epoxycyclohexenones with antibacterial activity.

As a result of the highly functionalized and complex nature of these compounds and their intriguing biological activity, they are of great interest as potent lead-compounds from a medicinal chemistry perspective. Because of this biological relevance, a number of groups developed different strategies to synthesize epoxy-cyclohexenones. Their efforts are summarized in the next section.

### 1.2.3 PREVIOUS SYNTHETIC APPROACHES TOWARDS EPOXY-CYCLOHEXENONES

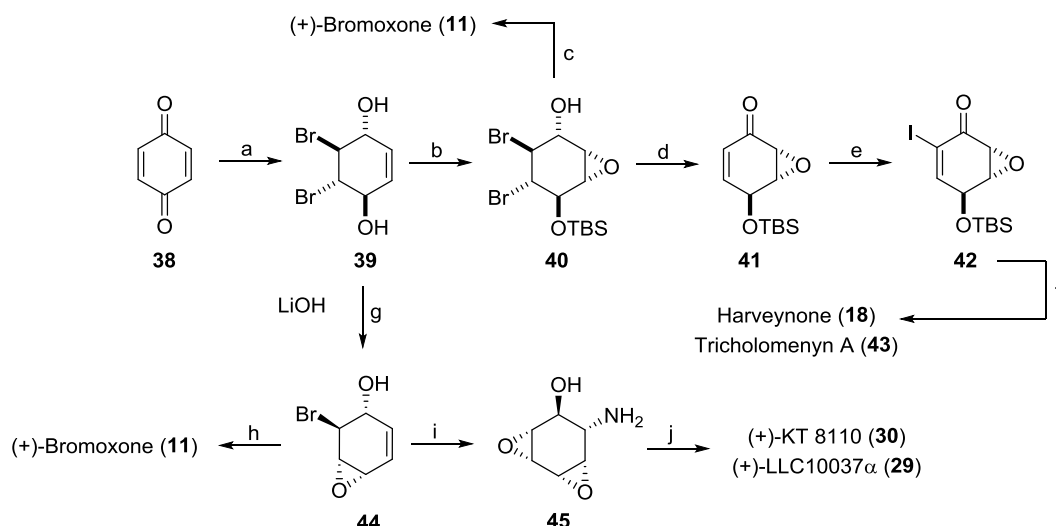
The isolation and characterization of manumycin A (32) in 1973<sup>[106]</sup> as well as the metabolites panepoxydon (19) and isoepoxydon (46)<sup>[92]</sup> only a few years later, initiated synthetic work towards this natural compound class. Besides very few exceptions, almost all approaches towards epoxy-cyclohexenones can be categorized into two different fundamental strategies:

first, by oxidation of functionalized aromatic precursors or, second, via stereoselective *Diels-Alder* reactions. In other approaches explored by *Altenbach* and *Johnson*, the cyclohexane core was derived from *para*-benzoquinone, as summarized in scheme 7.

#### 1.2.3.1 Approaches deriving epoxy-cyclohexenones from *p*-benzoquinone

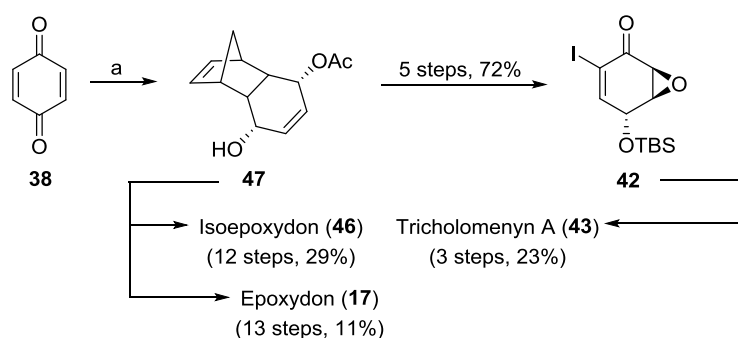
In 1978, *Altenbach* synthesized the highly functionalized di-bromine diol **39** by treating *p*-benzoquinone with one equivalent of bromine, followed by reduction with sodium borohydride.<sup>[114]</sup> This strategy was then used by *Fex* in 1981 to successfully synthesize the natural product chalozone (**12**) (scheme 7).<sup>[89]</sup> Based on these structures, *Johnson* and *Miller* subsequently optimized the strategy by including an enzymatic reaction to generate diol **39** in excellent enantioselectivity. Allylic epoxidation (b), followed by tandem *Collins* oxidation/ $\beta$ -elimination and a final desilylation step (c) afforded (+)-bromoxone (**11**) in good yields.<sup>[88]</sup> As bromoxone proved to be unreactive for organometallic coupling, *Johnson* modified the synthesis by reducing the TBS-protected epoxy-diol **40** with zinc (d). The resulted allylic alcohol was oxidized by PCC to epoxy-benzoquinone **41** and subsequent installation of vinyl-iodide (e) gave access to epoxy-iodoenone **42**. This compound proved to be an excellent substrate for *Sonogashira*-coupling (f), which was used by *Johnson* to complete the enantioselective synthesis of (+)-harveynone (**18**) and (+)-tricholomenyn (**43**) in 1997.<sup>[93]</sup>

*Altenbach* further improved upon this synthetic strategy in 2000 by treating diol **39** with LiOH (g) to afford mono-epoxide **44**. Further treatment with *m*CPBA and *Dess-Martin* periodinane afforded (+)-bromoxone (**11**) (h). More importantly, this allowed the synthesis of enantiopure compounds (+)-KT 8110 (**30**) and (+)-LLC10037 $\alpha$  (**29**). Nucleophilic opening of the epoxide moiety of **44** with sodium azide was followed by epoxidation using trifluoroacetic acid/H<sub>2</sub>O<sub>2</sub>, subsequent intramolecular S<sub>N</sub>2 reaction and reduction of the azide (i) gave diepoxy aminoinositol **45** as key fragment. Introduction of an *N*-acetyl moiety, followed by *Dess-Martin* periodinane-mediated oxidation/ $\beta$ -elimination afforded (+)-LLC10037 $\alpha$  (**29**). Diketone (+)-KT 8110 (**30**) could be obtained by acid chloride coupling of aliphatic side chains of manumycin-type compounds and a final PDC oxidation (j).<sup>[104]</sup>



**Scheme 7:** Synthesis of epoxy-cyclohexenones using *p*-benzoquinone as a starting material described by Altenbach,<sup>[104,114]</sup> Fex,<sup>[89]</sup> Johnson and Miller.<sup>[88,93]</sup> a) 1.  $\text{Br}_2$ , 2.  $\text{NaBH}_4$ , 64%; b) 1. TBSCl, 2. trifluoroacetic acid, 34%; c) 1.  $\text{CrO}_3$ , 2.  $\text{H}_2\text{SiF}_6/\text{MeCN}$ , 66%; d) 1.  $\text{Zn}$ , 2. PCC, 66%; e)  $\text{I}_2$ , pyridine/ $\text{CCl}_4$ , 77%; f) 1.  $\text{PdCl}_2(\text{PPh}_3)_2$ ,  $\text{CuI}$ ,  $\text{Pr}_2\text{NH}$ , 2.  $\text{H}_2\text{SiF}_6$  Harveynone (**18**): 42%, Tricholomenyn A (**43**): 40%; g)  $\text{LiOH}$ , 90%; h) 1. *m*CPBA, 2. Dess-Martin periodinane, 52%; i) 1.  $\text{NaN}_3$ , 2. trifluoroacetic acid, 3.  $\text{KOH}$ , 4.  $\text{H}_2$ ,  $\text{Pd/C}$ ; 65%; j) (+)-LLC10037 $\alpha$  (**29**): 1.  $\text{Ac}_2\text{O}$ , 2. Dess-Martin periodinane, 52% (+)-KT 8110 (**30**): 1. acid chloride coupling, 2. PDC, 47%.

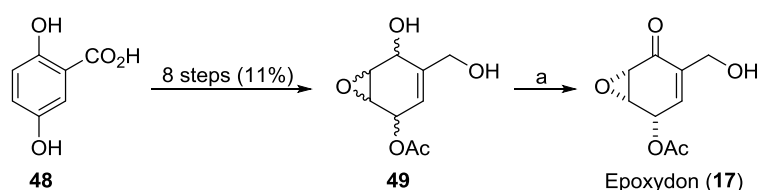
Another synthetic strategy that uses *p*-benzoquinone (**38**) as a starting material for the synthesis of isoepoxydon (**46**), epoxydon (**17**) and tricholomenyn A (**43**) was introduced by Ogasawara in the late 90's.<sup>[115,116]</sup> Therefore, *p*-benzoquinone (**38**) is first reacted with cyclopentadiene in a *Diels-Alder* cycloaddition (a), followed by stereoselective DIBAL reduction and enzyme-catalyzed acetylation to afford mono-acetate **42** as a key fragment. This strategy is noteworthy, as it remains one of the most efficient in terms of overall yield, and is therefore shown in scheme 8.



**Scheme 8:** Synthetic route of Ogasawara towards Isoepoxydon (**46**), Epoxydon (**17**) and Tricholomenyn A (**43**) via *Diels-Alder* reaction with *p*-benzoquinone:<sup>[115,116]</sup> a) 1. cyclopentadiene,  $\Delta$ , 2. DIBAL, 3. vinyl acetate, lipase PS, 2 weeks, 87%.

### 1.2.3.2 Approaches deriving epoxy-cyclohexenones through the oxidation of functionalized aromatic precursors

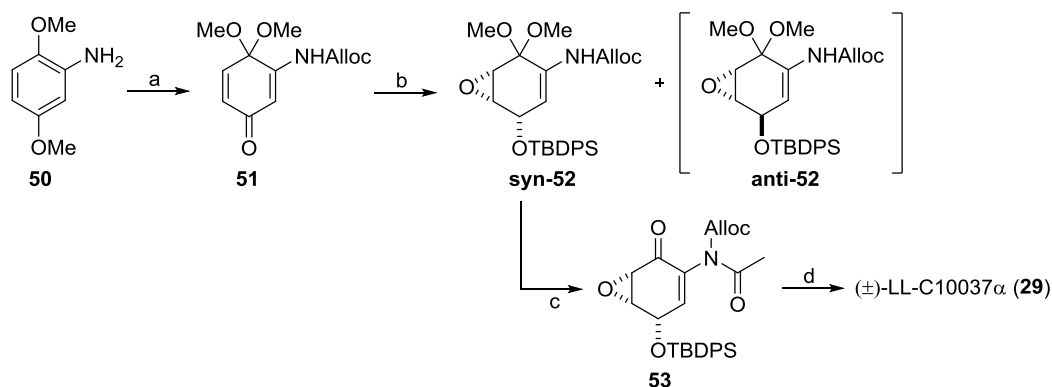
The most commonly used strategy to synthesize epoxy-cyclohexenones makes use of functionalized aromatic precursors. In 1972, *Sakamura* converted gentisyl alcohol (**48**) to a stereorandom mixture of epoxy-diol **49** in eight steps. Selective protection of the primary alcohol with triphenylmethyl chloride, followed by allylic oxidation and complete deprotection (a), resulted in the first synthesis of epoxydon (**17**) in very good overall yields (scheme 9).<sup>[117]</sup>



**Scheme 9:** Synthesis of Epoxydon (**17**) by *Sakamura*.<sup>[117]</sup> a) 1. triphenylmethyl chloride, 2.  $\text{MnO}_2$ , 3. *p*TSA, 88%.

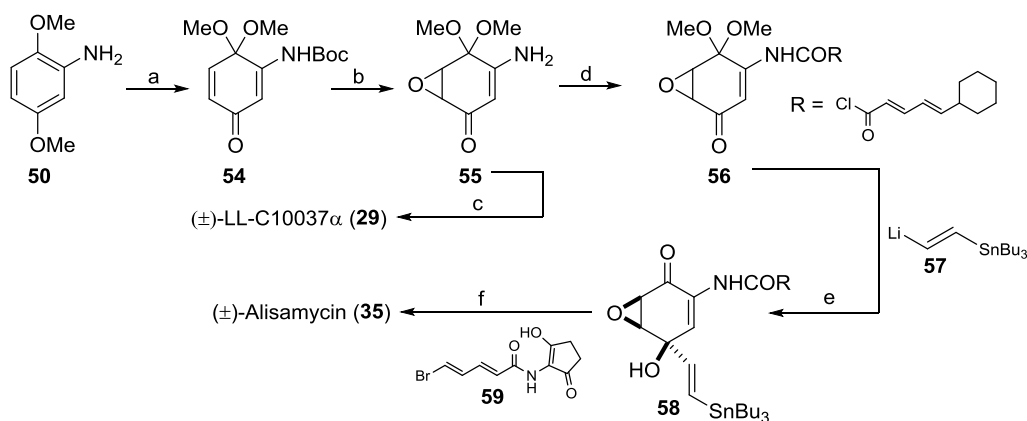
In contrast, more modern approaches made use of mild and selective phenolic oxidations, involving masked monoketals of *p*-benzoquinone as key intermediates. These molecules are usually generated by treating aromatic precursors with hypervalent iodine reagents such as  $\text{PhI}(\text{OAc})_2$  or  $\text{PhI}(\text{OPiv})_2$ .

In the mid 90's, the groups of *Wipf* and *Taylor* were the leading synthetic chemists with regard to manumycin-related natural compounds. In 1994, for example, *Wipf* accomplished the first synthesis of racemic ( $\pm$ )-LLC10037 $\alpha$  (**29**) using the above-mentioned dearomatization method (scheme 10). After protection of the amine group of 2,5-dimethoxyaniline (**50**), the compound was oxidized to monoketal **51** (a) and epoxidized using basic hydrogen peroxide, followed by reduction of the carbonyl moiety. After the silylation of the allylic alcohol (b), the acetal of the major isomer, *syn*-epoxy ether **52**, was removed and the resulting epoxyenone **53** was further subjected to *N*-acetylation with acetic anhydride (c). Palladium-catalyzed deallylation of **53** and a final deprotection of the TBDPS-protecting group led to product **29** in good overall yield (d).<sup>[118]</sup> In 1999, a similar strategy was used by this group for the preparation of racemic ( $\pm$ )-nisamycin (**36**), a type 1 manumycin (figure 25),<sup>[112]</sup> which also afforded access to related manumycin-type epoxyquinols.<sup>[119]</sup> As depicted in section 1.2.2, the lower sidechain of this natural product family proved not to be important for the antibacterial activity of these compounds. This is why the different strategies to generate epoxy-cyclohexenones discussed in this work focus on the synthesis of the *mC*<sub>7</sub>N-core unit.



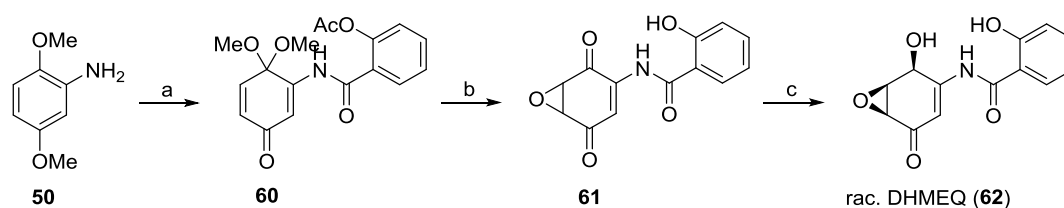
**Scheme 10:** Synthesis of the antitumor antibiotic LLC10037 $\alpha$  (**29**) by *Wipf et al.*:<sup>[118]</sup> a) 1. Alloc-Cl 2. PhI(OAc)<sub>2</sub>, 59%; b) 1. H<sub>2</sub>O<sub>2</sub>/K<sub>2</sub>CO<sub>3</sub>, 2. NaBH<sub>4</sub>, 3. TBDPS-Cl, 55%; c) 1. TsOH, PPTs, 2. Ac<sub>2</sub>O, 52%; d) 1. PdCl<sub>2</sub>(PPh<sub>3</sub>)<sub>2</sub>, 2. HF in H<sub>2</sub>O/MeCN, 47%.

In 1996, three years before the synthesis of racemic nisamycin (**36**) was published by *Wipf*,<sup>[112]</sup> *Taylor* demonstrated the first total synthesis of racemic alisamycin (**35**), the first manumycin-type natural compound synthesized (compare figure 27).<sup>[120]</sup> Even though the early steps are quite similar to those employed by *Wipf*, the strategy (scheme 11) gives access to key-fragment **55**, which was also used for the synthesis of the probes in this work. *Taylor* also used 2,5-dimethoxyaniline (**50**) as a starting material, which was *N*-protected by *tert*-butoxycarbonyl in the first step. Oxidation by PhI(OAc)<sub>2</sub> (a), followed by epoxidation and deprotection of the Boc-group with boron trifluoride diethyl etherate, gave key epoxy-amine **55** in very good yields over only four steps (b). This enabled the synthesis of racemic (±)-LLC10037 $\alpha$  (**29**) in only three further steps, with an overall yield of 31% (c).<sup>[121]</sup> The upper sidechain of alisamycin was then installed onto amine **55** by acid chloride coupling (d). The introduction of the lower sidechain was achieved by stereoselective addition of tributyl(vinyl)stannane **57** (e), followed by a *Stille*-coupling of the resultant vinyl stannane **58** with vinyl bromide **59** (f).



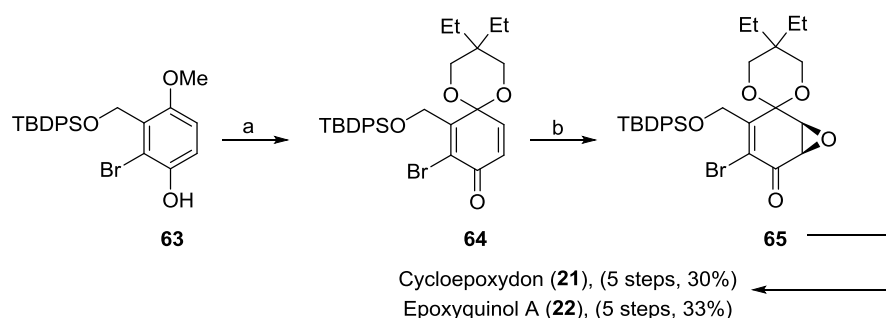
**Scheme 11:** Synthesis of racemic LL-C10037 $\alpha$  (**29**)<sup>[121]</sup> and Alisamycin (**35**)<sup>[120]</sup> by *Taylor et al.*: a) 1. Boc<sub>2</sub>O, PhI(OAc)<sub>2</sub>, 81%; b) 1. H<sub>2</sub>O<sub>2</sub>/K<sub>2</sub>CO<sub>3</sub>, 2. BF<sub>3</sub>·OEt<sub>2</sub>, 41%; c) 1. Ac<sub>2</sub>O, 2. NaBH<sub>4</sub>, 3. TsOH 42%; d) RCOCl, LiO<sup>t</sup>Bu, 73%; e) 1. **57**, 2. Montmorillonite K10, 46%; f) **59**, PdCl<sub>2</sub>(PPh<sub>3</sub>)<sub>2</sub>, 64%.

Subsequently, *Taylor* demonstrated that the enantioselective epoxidation of enone **54** is feasible using *Wynberg's* chiral phase-transfer catalysis.<sup>[122]</sup> In turn, this allowed the first enantioselective synthesis of (-)-alisamycin (**60**) and (+)-manumycin A (**32**) in 1998.<sup>[122-124]</sup> Especially the total synthesis of manumycin A, the first isolated manumycin compound, made an important contribution to its stereochemical assignment. *Taylor* could confirm the *syn*-hydroxy epoxide arrangement postulated previously by *Foss et al.*<sup>[125]</sup> and with that revised the originally wrongly assigned absolute configuration of manumycin A, which was published by *Zeeck* already in 1973.<sup>[106]</sup> In 2000, the group of *Umezawa* adapted the synthetic efforts of *Taylor* and *Wipf* to synthesize the epoxyquinomycin-based NF- $\kappa$ B inhibitor DHMEQ (**62**), as previously mentioned in section 1.2.1. Coupling of acetylsalicyloyl chloride to 2,5-dimethoxyaniline (**50**), followed by phenolix oxidation (a) and subsequent epoxidation of monoketal **60** and deprotection gave epoxybenzoquinone **61** (b). Interestingly, the reduction with NaBH(OAc)<sub>3</sub> occurred regioselectively in *ortho*-position to the amide moiety, leading to DHMEQ (**62**) in only five steps (c).<sup>[113]</sup>



**Scheme 12:** Synthesis of racemic DHMEQ (**62**) by *Umezawa et al.*<sup>[113]</sup> a) 1. acetylsalicyloyl chloride, 2. PhI(OAc)<sub>2</sub>, 50%, b) 1. H<sub>2</sub>O<sub>2</sub>/NaOH, 2. *p*-TsOH, 43%; c) NaBH(OAc)<sub>3</sub>, 86%.

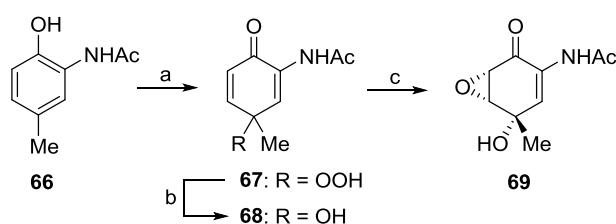
Besides the groups of *Wipf* and *Taylor*, the *Porco*-group is also worth mentioning with regard to synthetic strategies towards epoxy-cyclohexenones. The major contribution of *Porco* is the preparation of epoxyquinol A (**22**)<sup>[96]</sup> and cycloepoxydon (**21**)<sup>[126]</sup> via tartrate-mediated nucleophilic epoxidation to introduce the stereocenters (scheme 13). Phenolic oxidation of starting material **63** (a) followed by the new epoxidation protocol (b) allowed the synthesis of epoxyquinone monoketal **65** as key intermediate for the synthesis of the two mentioned compounds.



**Scheme 13:** Synthesis of Cycloepoxydon (**21**)<sup>[126]</sup> and Epoxyquinol A (**22**)<sup>[96]</sup> by *Porco et al.*: a) 1. PhI(OAc)<sub>2</sub>, 2. 2,2-diethyl-1,3-propanediol, PPTS, 75%; b) *L*-DIPT, NaHMDS, 97% (96% ee).



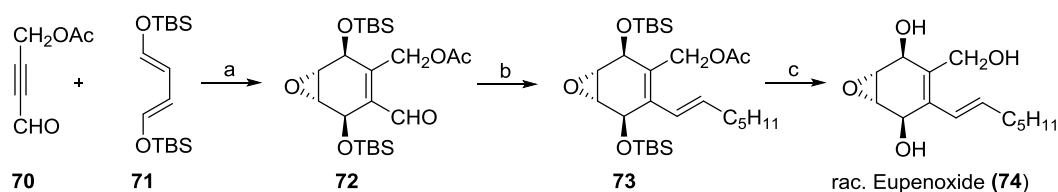
In summary, the presented synthetic approaches were all based on aromatic precursors for the synthesis of epoxy-cyclohexenones use hypervalent iodine reagents for phenolic oxidation to gain masked monoketals of *p*-benzoquinone as important intermediates. In addition it should be noted that *Kilic et al.* reported an alternative method shown in scheme 14.<sup>[127]</sup> They synthesized an LL-C10037 $\alpha$  (**29**) analog by photooxygenation of aminophenol **66** in the presence of TPP as photosensitizer (a). A subsequent reduction of the resulting hydroperoxide **67** (b) and *Weitz-Scheffer* epoxidation (c) diastereoselectively gave analog **69** in only three steps. Moreover, in 1980, *Taylor* as well as *Swenton* published the synthesis of *p*-benzoquinone-monoketals by anodic oxidation of methylated *p*-hydroxyphenols (not shown).<sup>[128,129]</sup>



**Scheme 14:** Synthesis of LL-C10037 $\alpha$  analog **69** by *Kilic et al.*:<sup>[127]</sup> a) O<sub>2</sub>, TPP, 62%; b) Me<sub>2</sub>S, Ti(O-<sup>*i*</sup>Pr)<sub>4</sub>, 83%; c) <sup>*t*</sup>BuOOH, 78%.

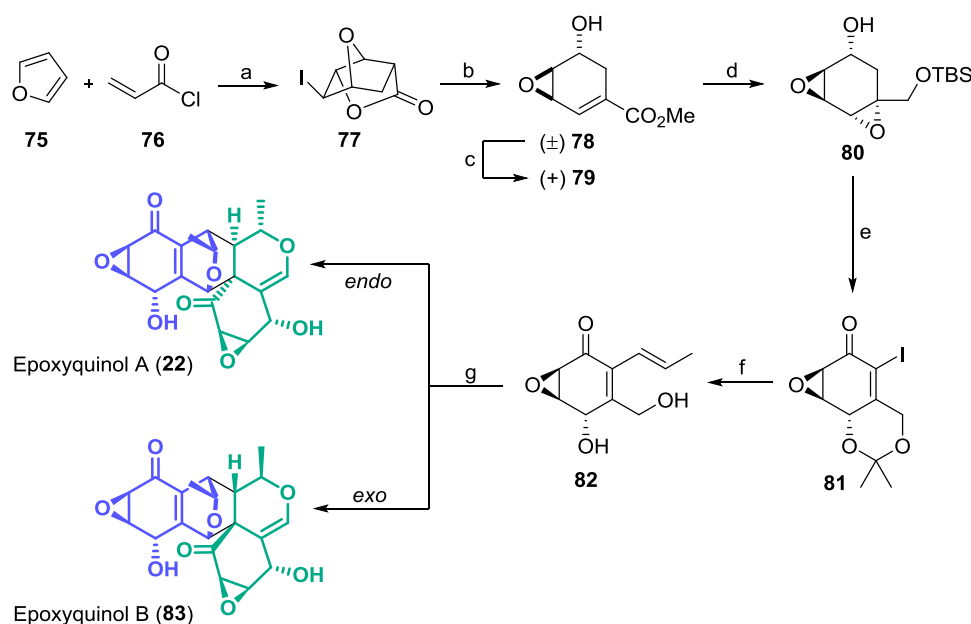
### 1.2.3.3 Approaches deriving epoxy-cyclohexenones from *Diels-Alder* reactions

Besides the strategy to synthesize epoxy-cyclohexenones by oxidative dearomatization, *Diels-Alder* reactions are popular ways to synthesize cyclohexenes. In 1984, *Rickards et al.* reported a stereoselective synthesis of the antifungal agent eupenoxide (**74**) shown in scheme 15.<sup>[130]</sup> The first step herein is a thermal *Diels-Alder* reaction of propynyl aldehyde **70** and TBS-protected butadiene **71**, which proceeded over 4 days and efficiently led to the *endo*-product **72**. Subsequent epoxidation with *m*CPBA led to cyclohexenecarbaldehyde **72** in 20% yield (a). The following *Wittig*-reaction with *n*-hexylidetriphenylphosphorane yielded the undesired *Z*-olefin, which was therefore subsequently irradiated with light in the presence of an idione catalyst to afford the more thermodynamically stable *E*-olefin **73** (b). Deacetylation with methanolic ammonia and subsequent desilylation afforded racemic eupenoxide (**74**) in only six steps (c).



**Scheme 15:** Synthesis of Eupenoxide (**74**) by *Rickards et al.*:<sup>[130]</sup> a) 1.  $\Delta$ , 2. *m*CPBA, 20%; b) 1. Ph<sub>3</sub>PC<sub>6</sub>H<sub>12</sub>, 2. *h* $\nu$ , 50%; c) 1. NH<sub>3</sub>/MeOH, 2. TBAF, 78%.

More complex structures such as the angiogenesis inhibitors epoxyquinols A (**22**) and B (**83**), which are pentaketide dimers, can be synthesized using *Diels-Alder* reactions. In 2002 for example, *Hayashi* reported the first synthesis of these molecules via biomimetic tandem  $6\pi$ -electrocyclic ring closure/*Diels-Alder* dimerization of key intermediate **82** (scheme 16).<sup>[131,132]</sup> The route begins with a base-catalyzed *Diels-Alder* reaction of furan (**75**) with acryloyl chloride (**76**) and subsequent iodolactonization to the cyclic intermediate **77** (a). After conversion of **77** by tandem lactone-hydrolysis/epoxide formation, an LDA-mediated  $\beta$ -elimination furnished allylic epoxide **78** (b). Kinetic resolution of ( $\pm$ )-**78** using lipase (c) and further hydroxyl-directed homo-allylic epoxidation, reduction and TBS-protection resulted in *bis*-epoxide **80** (d). *Altenbach*-inspired oxidation/ $\beta$ -epoxide elimination followed by iodination (e) and *Suzuki* cross-coupling and deprotection (f) gave key intermediate **82**. After oxidation with  $\text{MnO}_2$ , dimerization of the key fragment via  $6\pi$ -electrocyclisation gave epoxyquinol A (**22**) and its *exo*-analogue epoxyquinol B (**83**) (g).



**Scheme 16:** Synthesis of Epoxyquinols A (**22**) and B (**83**) by *Hayashi et al.*:<sup>[131,132]</sup> a) 1. RT, 2. NaOH, 3.  $\text{I}_2$ , 42%; b) 1. KOH then MeI, 2. LDA, 89%; c) *Pseudomonas stutzeri* lipase, Meito TL 49%; d) 1.  $\text{VO}(\text{acac})_2$ , TBHP, 2.  $\text{NaBH}_4$ , 3. TBDPSCI, 78%; e) 1. DMP, 2. Silica gel, 3. Amberlyst 15, 4.  $\text{I}_2$ ,  $\text{PhI}(\text{OCOCF}_3)_2$ , BHT, pyridine, 67%; f) 1. (*E*)-propenylborate,  $\text{Pd}(\text{II})$ , 2. Amberlyst 15, 65%; g)  $\text{MnO}_2 \rightarrow 6\pi$ -electrocyclization, 25 - 40%.

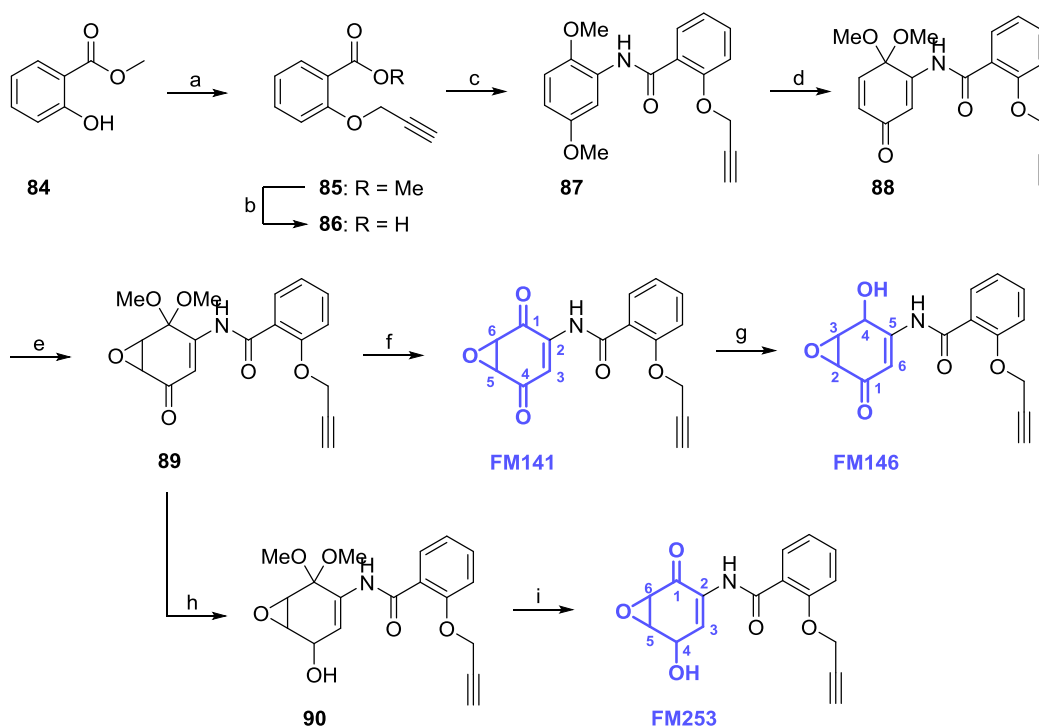
To date, no amino-substituted epoxy-cyclohexenones have been synthesized via *Diels-Alder* reaction. The strategies presented in section 1.2.3.2 for deriving the epoxy-cyclohexenone unit via phenolic oxidation of aromatic precursors like 2,5-dimethoxyaniline are of major importance. This method gives access to molecules with diverse substitution patterns and different functionalities and was therefore used for the synthesis of a probe library, as presented in the next section.

## 2 RESULTS AND DISCUSSION

### 2.1 SYNTHESIS OF AMINO-EPOXYCYCLOHEXENONES

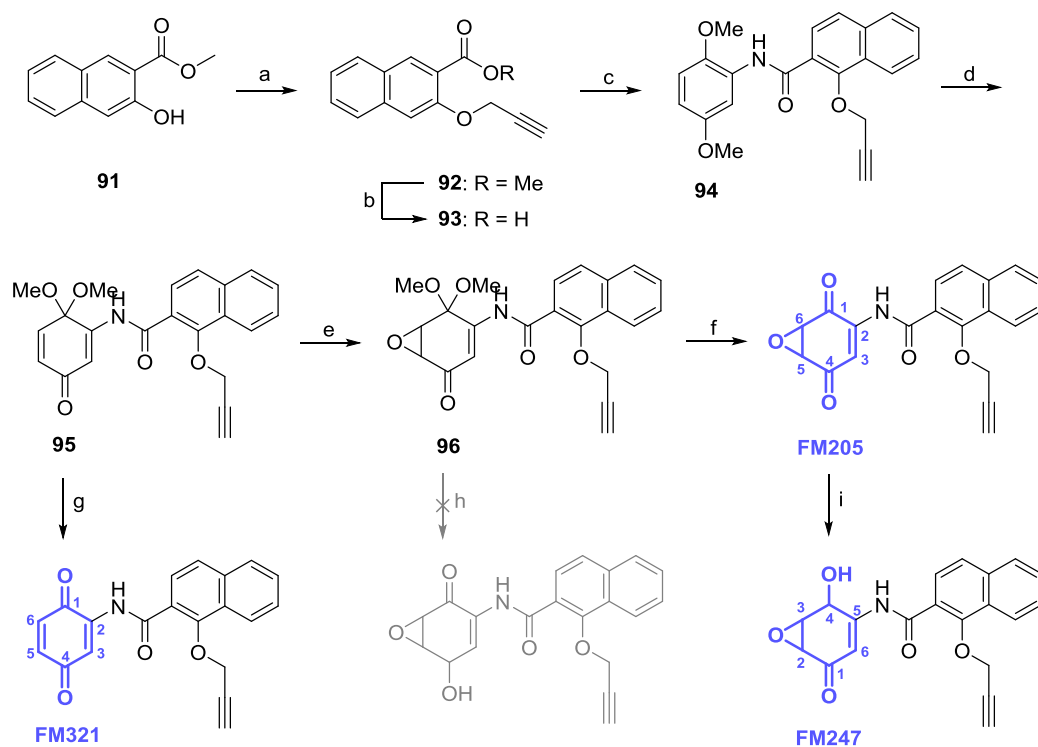
#### 2.1.1 SYNTHETIC STRATEGY ACCORDING TO UMEZAWA

As previously described in the introduction, in 2000 *Umezawa et al.* synthesized a novel NF- $\kappa$ B inhibitor named DHMEQ, which was based on the structure of epoxyquinomycin antibiotics that had previously been isolated from *Amycolatopsis* bacteria.<sup>[113,133]</sup> The synthetic route can easily be adapted to include an alkyne handle for an ABPP approach. In general, the early insertion of an alkyne handle is advantageous because synthetic intermediates can then also be used as ABPP probes. Moreover, alkyne-tagged benzoquinones can easily be generated within this route. As partially protected quinones (**88**) serve as the starting material, only one more deprotection step is required. Those benzoquinones are identical to the products of the epoxy-benzoquinone ABPP probes, except the missing epoxide, and are therefore very important reference substances for phenotype structure-activity studies and labeling experiments.



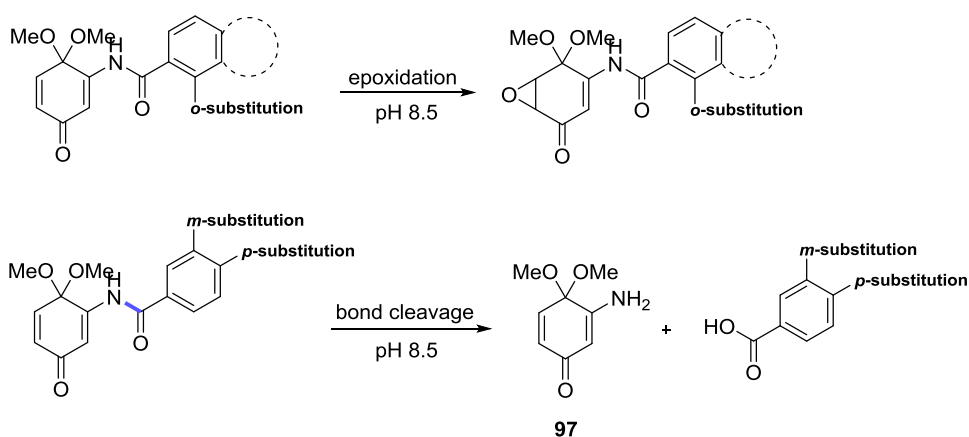
**Scheme 17:** Adapted synthetic route to generate amino-epoxycyclohexenone probes according to *Umezawa et al.*:<sup>[113]</sup> a) propargyl bromide,  $K_2CO_3$ , acetone, 60 °C, 24 h, 96%; b) KOH, EtOH, RT, 4 h, 94%; c) 1. thionyl chloride, DMAP (cat.), 75 °C, 4 h, 2. **50**, pyridine, THF, 0 °C  $\rightarrow$  RT, 6 h, 93%; d) 1. iodobenzene diacetate, MeOH, 0 °C  $\rightarrow$  RT, 4 h, 2. aqueous citric acid solution, RT, 30 min, 59%; e)  $H_2O_2$ ,  $K_2CO_3$ , THF, RT, 12 h, 14%; f)  $BF_3 \cdot OEt_3$ ,  $CH_2Cl_2$ , -20 °C  $\rightarrow$  RT, 14 h, 93%; g)  $NaBH(OAc)_3$ , MeOH, 0 °C  $\rightarrow$  RT, 2 h, 41%; h)  $LiBHET_3$ , THF, -78 °C  $\rightarrow$  RT, 3 h; i) Montmorillonite K10,  $CH_2Cl_2$ , RT, 16 h, 66% over two steps.

First, an alkyne-tagged DHMEQ-analog was synthesized (scheme 17): the propargylic alkyne tag was introduced by a substitution reaction to methyl-2-hydroxybenzoate (**84**) (a). Deprotection of the ester and subsequent acid chloride formation in thionyl chloride (b) allowed the coupling to 2,5-dimethoxyaniline (**50**), forming an amide bond (c). Treatment of **87** with the hypervalent iodine reagent iodobenzene diacetate followed by selective hydrolysis of the vinylogous amide dimethylacetal group in aqueous citric acid solution gave the partially protected quinone **88** (d). For epoxidation, aqueous  $\text{H}_2\text{O}_2$  and  $\text{K}_2\text{CO}_3$  were added to keep a constant pH of 8.5, which was crucial for successful product formation (e). Deacetalization of the carbonyl group in **89** with  $\text{BF}_3\cdot\text{OEt}_3$  (f) generated epoxy-benzoquinone **FM142** which was then regioselectively converted to compound **FM146** with  $\text{NaBH}(\text{OAc})_3$  (g), fortunately without reducing the amide bond at the same time. As mentioned previously, this synthetic route gives access to structurally related ABBP probes showing the manumycin-type substitution pattern, meaning the amide bond is in *ortho*-position to the carbonyl group. Therefore, the acetal protected epoxy-benzoquinone **89** was first reduced with  $\text{LiBHET}_3$  ("Superhydride") (h), followed by deprotection of the acetal with Montmorillonite K10<sup>[134]</sup> to generate compound **FM253** in 66% yield (i).



**Scheme 18:** Synthetic route to epoxy-aminocyclohexenones according to Umezawa *et al.*<sup>[113]</sup> a) propargyl bromide,  $\text{K}_2\text{CO}_3$ , acetone,  $60^\circ\text{C}$ , 24 h, 91%; b) KOH, EtOH, RT, 4 h, 94%; c) 1. thionyl chloride, DMAP (cat.),  $75^\circ\text{C}$ , 3 h, 2. **50**, pyridine, THF,  $0^\circ\text{C} \rightarrow \text{RT}$ , 16 h, 72%; d) iodobenzene dipivalinate, MeOH,  $0^\circ\text{C} \rightarrow \text{RT}$ , 6 h, 69%; e)  $\text{H}_2\text{O}_2$ ,  $\text{K}_2\text{CO}_3$ , THF, RT, 16 h, 14%; f)  $\text{BF}_3\cdot\text{OEt}_3$ ,  $\text{CH}_2\text{Cl}_2$ ,  $-20^\circ\text{C} \rightarrow \text{RT}$ , 14 h, 68%; g) Montmorillonite K10,  $\text{CH}_2\text{Cl}_2$ , RT, 16 h, 46%; h) 1.  $\text{LiBHET}_3$ , THF,  $-78^\circ\text{C} \rightarrow \text{RT}$ , 3 h, no conversion, 2. Montmorillonite K10,  $\text{CH}_2\text{Cl}_2$ , RT, 16 h; i)  $\text{NaBH}(\text{OAc})_3$ , MeOH,  $0^\circ\text{C} \rightarrow \text{RT}$ , 16 h, 50%.

In order to achieve more structural diversity in the probes, the synthetic strategy was further extended to other aromatic acid chlorides. The synthetic route described in scheme 17 was analogously applied to methyl-3-hydroxy-2-naphthoate (**91**) as starting material, as shown in detail in scheme 18. After insertion of the propargyl moiety (a), the free acid was again coupled to 2,5-dimethoxyaniline (**50**) via acid chloride formation (b and c). The resulting aromatic system **94** was oxidized using the hypervalent iodine reagent iodobenzene dipivalinate, which resulted in even higher yields of the acetal protected quinone **95** compared to the previous method (d). The direct deprotection of this acetal moiety by Montmorillonite K10 gave benzoquinone **FM321** in good yields (g). As this substance lacks the epoxide and only the *Michael*-acceptor system can serve as the electrophilic core structure, it is useful for structure-activity relationship studies as previously mentioned. While the reduction of epoxide **96** by  $\text{LiBHET}_3$  showed no conversion (h), all other steps (f and i) proceeded in good yields, resulting in an additional set of ABPP probes (**FM205**, **FM247**).

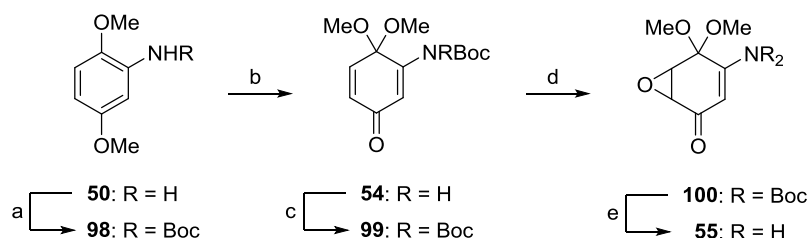


**Scheme 19:** Product formation under the conditions of the epoxidation reaction depending on the substitution pattern of the aromatic acid side chain.

To determine the influence of the substitution pattern of the compounds on the activity of the substances, we attempted to incorporate *meta*- and *para*-substituted aromatic acid chlorides using the above synthetic strategy. Interestingly, the reaction of the resulting quinones with aqueous, basic hydrogen peroxide solution did not result in epoxidized products. The basic conditions of this reaction rather led to a cleavage of the amide bond resulting in free amine **97** and the corresponding acid chloride, shown in scheme 19. In order to avoid this bond cleavage, the pH of the reaction solution was decreased from 8.5 to 7.0. However, no turn over could be detected anymore. To further extend the probe library to *meta*- and *para*-substituted aromatic or aliphatic side chains a new strategy was necessary.

## 2.1.2 SYNTHETIC STRATEGY ACCORDING TO WIPF AND TAYLOR

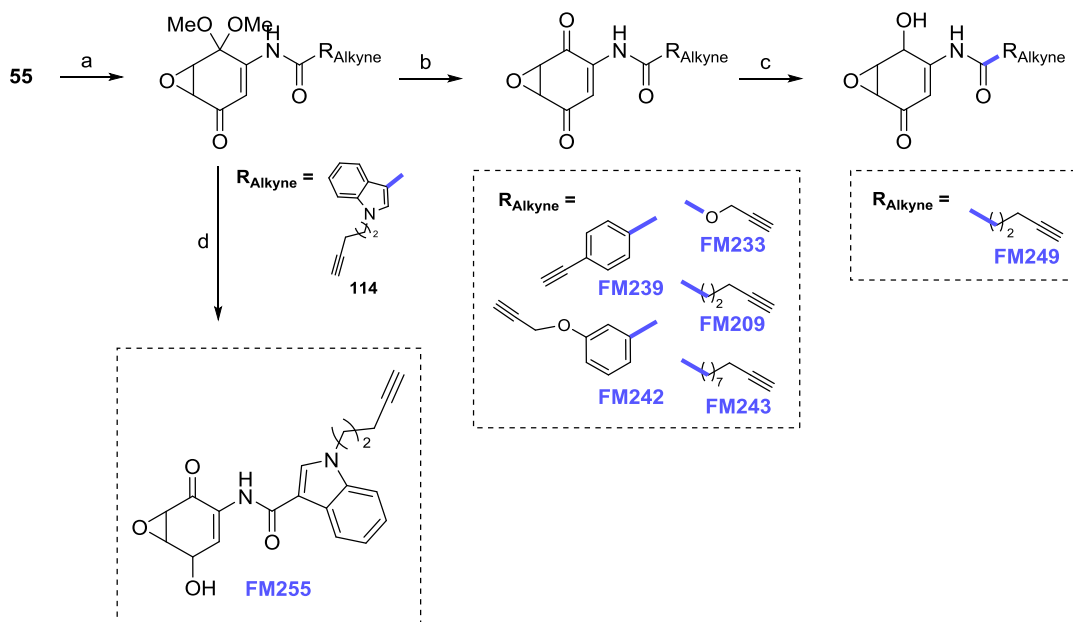
In light of the amide bond cleavage at basic pH values described in the previous chapter, a new synthetic strategy was required. As an alkyne tag (introduced by coupling the alkyne-tagged acid via amide bond formation) is essential for ABPP experiments, the logical consequence was to introduce the epoxide before coupling the amine to the alkyne-containing side chain. This led to the synthesis of the key epoxide fragment **55** as described by *Wipf* and *Taylor*<sup>[118,121]</sup> (scheme 11) and later adapted by *Umezawa*.<sup>[135]</sup> As in the previous synthetic route, 2,5-dimethoxyaniline (**50**) was used as starting material. First, the amino group was protected utilizing *tert*-butoxycarbonyl (a) followed by an oxidative dearomatization of the molecule using iodobenzene dipivalinate (b), thereby generating the partially acetal protected quinone **54**. A second Boc-protection of the NHBoc-moiety (c) generally resulted in higher yields in the following epoxidation reaction, performed using aqueous hydrogen peroxide solution (d). In the last step, both Boc-protecting groups were removed by treating Boc-protected epoxide **100** with trifluoroacetic acid solution in CH<sub>2</sub>Cl<sub>2</sub>, leaving the methyl acetal protecting group intact (e). Using this synthesis, the important key fragment **55** containing an epoxide *Michael*-acceptor system and bearing a free amino group could be synthesized over five steps with an overall yield of 29% (scheme 20).



**Scheme 20:** Synthesis of key epoxide-fragment **55** according to *Wipf* and *Taylor*.<sup>[118,121]</sup> a) Boc<sub>2</sub>O, THF, 70 °C, 16 h, 99%; b) iodobenzene dipivalinate, MeOH, 0 °C → RT, 16 h, 84%; c) Boc<sub>2</sub>O, THF, 70 °C, 16 h, 68%; d) H<sub>2</sub>O<sub>2</sub>, NaOH, THF, RT, 16 h, 53%; e) trifluoroacetic acid, CH<sub>2</sub>Cl<sub>2</sub>, RT, 2 h, 96%.

Next, the different aromatic/heteroaromatic and aliphatic acid chlorides were synthesized and coupled to the key fragment. As depicted in scheme 21 *meta*- and *para*-substituted aromatic systems, one heteroaromatic indolic compound and three aliphatic acid chlorides differing in length were chosen (for a precise description of the synthesis of the acid chlorides see experimental part). Because of this high structural variability among the side chains, it is possible to study the influence of the moieties on the bioactivity of the compounds. In the next steps the acetal of the partially protected quinones was deprotected. In the case of the hexynoic side chain, the reduction to compound **FM249** was possible, leading to an epoxy-hydroxycyclohexenone structure. In the case of the indolic moiety, the deprotection of the acetal (step b in scheme 21) led

to an additional methylation of the amide nitrogen. Therefore compound **114** was first reduced and then deprotected by Montmorillonite K10 (d) resulting in manumycin-like substituted compound **FM255**, as described in section 2.1.1.



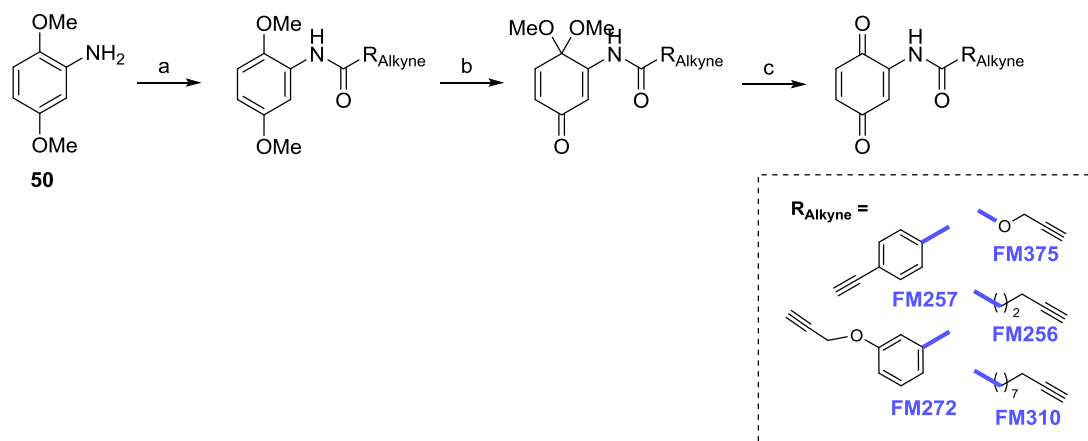
**Scheme 21:** Synthesis of epoxy-benzoquinone- and epoxy-hydroxycyclohexenone-ABBP probes: a) 1. respective carboxylic acid, oxalyl chloride, DMAP (cat.), CH<sub>2</sub>Cl<sub>2</sub>, 0 °C, 1 - 2 h, 2. **55**, generated acid chloride, lithium *tert*-butoxide, THF, -10 °C → RT, 4 - 16 h; b) BF<sub>3</sub>·OEt<sub>2</sub>, CH<sub>2</sub>Cl<sub>2</sub>, -20 °C → RT, 14 h; c) NaBH(OAc)<sub>3</sub>, MeOH, 0 °C → RT, 2 h, 53%; d) 1. LiBHET<sub>3</sub>, THF, -78 °C → RT, 3 h, 2. Montmorillonite K10, CH<sub>2</sub>Cl<sub>2</sub>, RT, 16 h, 70% over two steps.

To evaluate the influence of the epoxide on the bioactivity of the compounds, benzoquinone-analogs lacking this functional moiety were synthesized (scheme 22). In analogy to the synthetic route previously described, these molecules were synthesized, by first coupling the corresponding acid or acid chloride to 2,5-dimethoxyaniline (**50**) (a). The following table presents the different conditions of this amide bond formation, as they had to be adjusted for each of the acid or acid chlorides.

**Table 8:** Conditions for the coupling of acids (top) or acid chlorides (bottom) to 2,5-dimethoxyaniline (**50**) .

Compound	Coupling conditions	Yield
Hexynoic acid ( <b>102</b> )	DIC, (DCM), RT, 16 h	78%
4-Ethynylbenzoic acid ( <b>103</b> )	DIPEA, HOBT, pyBOP, (DMF), RT, 16 h	65%
Undecynoic acid ( <b>104</b> )	EDC, DMAP, (CH <sub>2</sub> Cl <sub>2</sub> ), RT, 16 h	78%
Indole-3-carboxylic acid ( <b>105</b> )	SOCl <sub>2</sub> , pyridine (THF), 16 h, 75 °C → 0 °C → RT	57%
3-(Prop-2-yn-1-yloxy)benzoic acid ( <b>106</b> )	SOCl <sub>2</sub> , DMF, pyridine (THF), 75 °C → 0 °C → RT, 6 h	98%
Prop-2-yn-1-yl carbonochloride ( <b>107</b> )	NEt <sub>3</sub> , DMF, (CH <sub>2</sub> Cl <sub>2</sub> ), 0 °C → RT, 16 h	64%

Second, the aromatic system was oxidized using iodobenzene dipivalinate, resulting in partially protected quinones (b). The direct deprotection of this acetal moiety by Montmorillonite K10 led then to the desired benzoquinones in good yields (c).



**Scheme 22:** Synthetic route leading to benzoquinone-analogs of the epoxide containing probes: a) for coupling conditions see table 8; b) 1. iodobenzene dipivalinate, MeOH, 0 °C  $\rightarrow$  RT, 3 h - 16 h, 2. aqueous citric acid solution, RT, 30 min, 75% - 94% over two steps; c) Montmorillonite K10, CH<sub>2</sub>Cl<sub>2</sub>, RT, 16 h, 25% - 84%.

To conclude, a very diverse probe library containing at least one example of each substitution pattern referred to in the introduction was successfully synthesized. Even though some of the reduction reactions did not result in the desired epoxy-hydroxycyclohexenones, a diverse set of epoxy-benzoquinones consisting of eight different side chains was established. Moreover, for six of these molecules the benzoquinone analog lacking the epoxide was additionally synthesized, which now gives access to structure-bioactivity evaluation of the compounds concerning their antibacterial potency (figure 29).



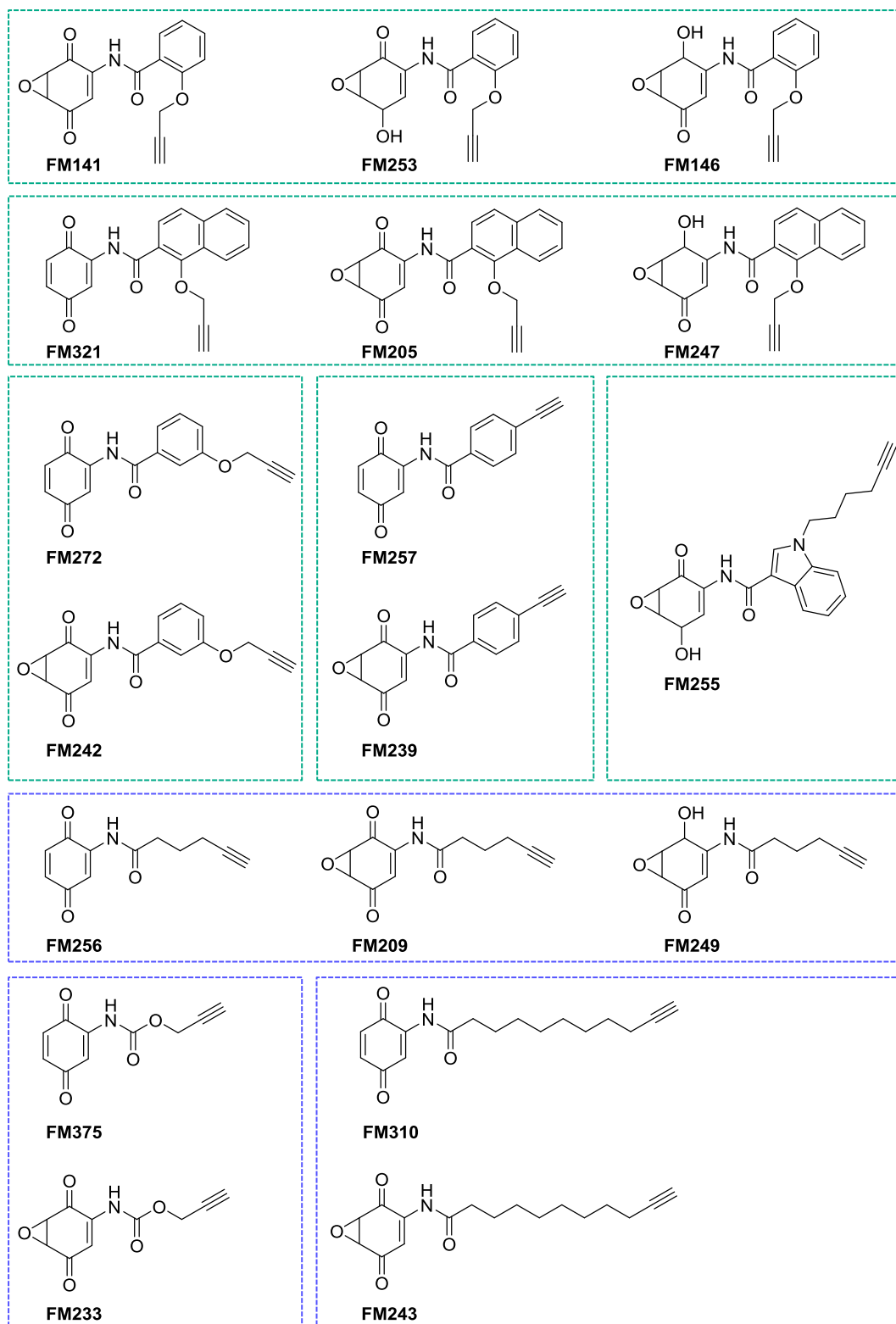


**Figure 29:** Structures of all synthesized amino-(epoxy)cyclohexenones grouped according to structural similarities of the alkyne-containing side chains. Molecules containing aromatic side chains are framed in turquoise, molecules with aliphatic side chains are framed in blue.

## 2.2 BIOLOGICAL ACTIVITY OF THE PROBES ON BACTERIAL CELLS

Amino-epoxycyclohexenones are known to show a variety of biological activities as described in detail in section 1.2.<sup>[84]</sup> Beside the interesting fact that members of this compound class inhibit human enzymes such as Ras-farnesyltransferase<sup>[111]</sup> and interleukine-1 $\beta$ -converting enzyme<sup>[136]</sup> or I $\kappa$ B kinase  $\beta$ <sup>[137,138]</sup> and therefore show antitumor and anti-inflammatory effects, some of the compounds also inhibit bacterial cell growth.<sup>[84,85]</sup> Summarizing, several studies, the epoxide moiety seems to be especially important for this antibacterial activity, whereas compounds lacking the epoxide still exhibit their cytotoxic effects.<sup>[84,95,109,110]</sup> Consequently, the synthesized probe library was tested for antibacterial activity. To find the lowest concentration of potential antibiotics by which the growth of bacteria is inhibited a minimal inhibitory concentration assay (MIC assay) is performed (table 9). Therefore, all synthesized probes of the compound library shown in figure 29 were screened for their MIC values in various non-pathogenic and pathogenic bacterial strains. Moreover, the acetale-protected epoxy-benzoquinones were included to study the influence of the carbonyl group and with that the importance of the electrophilic benzoquinone core unit.

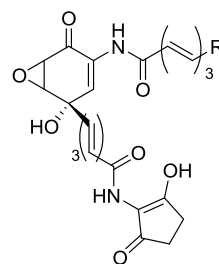
**Table 9:** Determined MIC values of ABBP probes in non-pathogenic and pathogenic bacteria.

Substitution pattern: Compound	MIC [ $\mu$ M]											
	Manumycin		DHMEQ			Epoxy-Benzoquinone						
	253	255	146	247	247	141	205	209	233	239	242	243
<i>Gram-positive bacterial strains</i>												
<i>B. subtilis</i> 168	100	100	>100	100	100	100	30	100	>100	100	100	30
<i>B. licheniformis</i> ATCC14580	100	30	>100	100	100	30	30	>100	>100	100	100	10
<i>L. welshimeri</i> SLCC 5334	30	30	100	100	100	30	30	100	100	100	100	100
<i>L. monocytogenes</i> EGD-e	100	100	>300	>300	>300	30	30	>100	100	100	100	30
<i>S. aureus</i> NCTC 8325	100	<b>30</b>	>100	100	100	<b>30</b>	<b>10</b>	100	>100	100	100	<b>10</b>
<i>S. aureus</i> Mu50	100	<b>30</b>	>100	100	100	<b>100</b>	<b>30</b>	100	100	>100	>100	<b>30</b>
<i>S. aureus</i> USA300	100	<b>30</b>	>100	100	100	<b>30</b>	<b>30</b>	100	100	>100	100	<b>30</b>
<i>E. faecalis</i> V583	>100	100	>300	>300	>300	100	100	>100	>100	>100	>100	100
<i>Gram-negative bacterial strains</i>												
<i>E. coli</i> K12	>300	>300	>300	>300	>300	>300	>300	>300	100	100	>300	>300
<i>B. thailandensis</i> E264	>300	>300	>300	>300	>300	>100	>300	>100	>100	100	100	>300
<i>B. cenocepacia</i> J2315	>300	>300	>300	>300	>300	>100	>300	>100	>100	>100	>100	>100
<i>S. typhimurium</i> TA100	>300	>300	>300	>300	>300	>100	>300	100	<b>30</b>	<b>30</b>	100	100
<i>S. typhimurium</i> LT2	>300	>300	>300	>300	>300	>300	>300	100	<b>30</b>	100	100	100
<i>S. enteritidis</i>	n.d	n.d	n.d	n.d	n.d	n.d	n.d	n.d	<b>30</b>	100	n.d	n.d
<i>P. putida</i> KT2440	>300	>300	>300	>300	>300	>300	>300	>100	>100	>100	>100	>300
<i>P. aeruginosa</i> PAO1	>300	>300	>300	>300	>300	>300	>300	>300	>100	>300	>100	>300

Interestingly, all substances containing the acetal protecting group did not inhibit the growth of any bacterial strains tested up to a concentration of 300  $\mu\text{M}$ . Most of these compounds did not show a reduction in growth at 1000  $\mu\text{M}$  concentration, which reflects the limit of solubility for the majority of the probes. In accordance with the literature, compounds with the manumycin-substitution pattern (**FM253** and **FM255**) showed an antibacterial effect in *Gram*-positive and not in *Gram*-negative strains;<sup>[85,139]</sup> in these strains cell growth was inhibited at concentrations of about 100 - 30  $\mu\text{M}$ . Interestingly, for substances bearing the DHMEQ-substitution pattern, MIC values were generally a bit higher than for those showing the manumycin-pattern. Nevertheless, the best inhibitory effects were determined for the epoxy-benzoquinones. Growth was inhibited in low  $\mu\text{M}$  concentration, even in multi-resistant *Staphylococcus aureus* strains, and moreover, two probes (**FM233** and **FM239**) inhibited the growth of *Gram*-negative *Salmonella typhimurium* and *Salmonella enteritidis* strains. Importantly, the corresponding epoxide-lacking benzoquinone analogs of these antibacterial substances did not show an inhibition of the strains tested up to a concentration of 300  $\mu\text{M}$ .

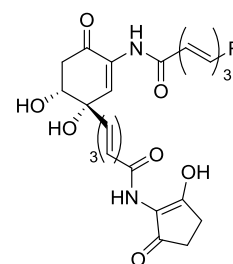
**Table 10:** Determined MIC values of the natural compounds AsuA1, AsuB1 and AsuA3, structure shown on the right.

Strain	MIC [ $\mu\text{M}$ ]		
	AsuA1	AsuB1	AsuA3
<i>S. typhimurium</i> LT2	-	-	-
<i>P. aeruginosa</i> PAO1	-	-	-
<i>S. aureus</i> NCTC 8325	3-10	100	3-10
<i>S. aureus</i> USA300	3-10	100	3-10



**AsuA1:** R = cyclohexyl

**AsuA3:** R = *sec*-butyl/*iso*-butyl



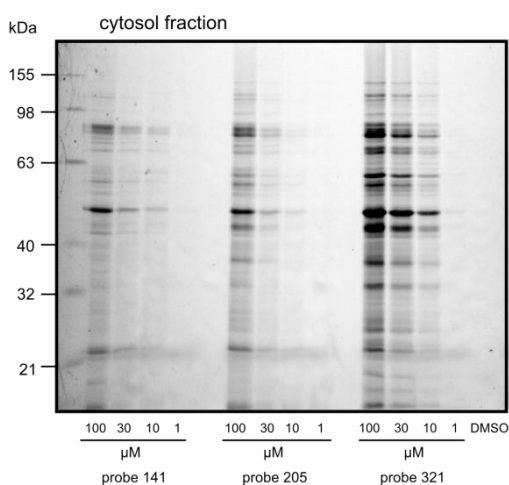
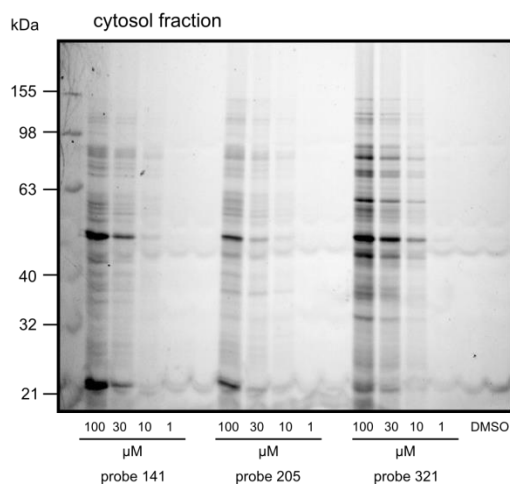
**AsuB1:** R = cyclohexyl

These results were compared to the MIC values of the natural compound asukamycin, which showed inhibitory effects in low  $\mu\text{M}$  range for **AsuA1** and **AsuA3** in the *Gram*-positive strains tested (see table 10).<sup>[139]</sup> As expected, amino-cyclohexenone **AsuB1** was about ten times less active than the corresponding epoxide-analog. All three substances did not show any growth inhibition in *Gram*-negative bacteria, highlighting the good inhibitory effects of the synthesized epoxy-benzoquinone probes in *Salmonella typhimurium*.

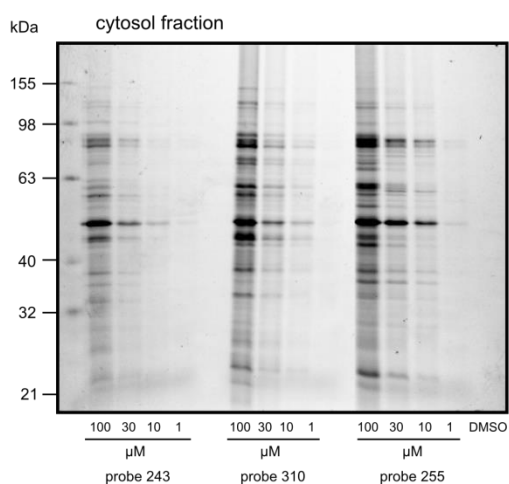
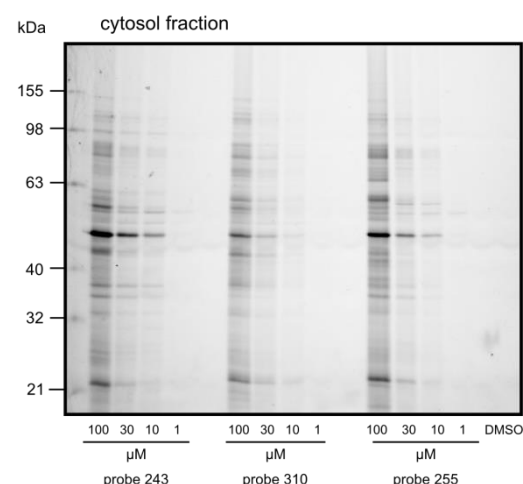
## 2.3 IDENTIFICATION OF PROTEIN TARGETS VIA ABPP

### 2.3.1 *IN SITU* ANALYTICAL LABELING

As depicted in the previous chapter, the synthesized epoxy-benzoquinone probe library (figure 29) showed interesting antibacterial bioactivity in various pathogenic strains. Especially the growth inhibition in multi-resistant *Staphylococcus aureus* and Gram-negative *Salmonella* strains is promising with regard to the recent resistance development of antibiotics.<sup>[1]</sup> While target proteins of amino-epoxycyclohexenones have been identified and studied in humans, no bacterial enzyme targets, mode of action or binding mechanism of these compounds are known so far.<sup>[111,136,137]</sup> To investigate the cellular activity especially towards the bacterial strains mentioned, an analytical *in situ* ABPP experiment was first performed (see section 6.1.1). Therefore, the bacterial cells were incubated with various concentrations of the alkyne-tagged probes, clicked to a fluorescent dye and lysed. The treated proteome was then separated by SDS-PAGE and any probe-labeled enzymes were visualized by fluorescent scanning. Using this method, important information about the cell permeability of the probes as well as their target specificity can be obtained. In all three *Staphylococcus* strains, discrete bands were observed which differed in intensity depending on the compound concentration and demonstrated the cell-permeability of the probes. Figures 30 and 31 show the labeled proteome of the cytosolic fraction of *Staphylococcus aureus* NCTC 8325 and *Staphylococcus aureus* USA300. The labeling pattern which corresponds to the related proteome of the strains, were similar in all three strains tested. Generally, the different decorations of the epoxy-probes, besides the electrophilic core structure, did not appear to have a significant influence on target specificity, which is in accordance with the similar MIC values of the different probes. For example, compounds **FM141** and **FM243** show nearly identical labeling in both strains, although compound **FM141** has quite a small aromatic side chain and compound **FM243** a relatively long aliphatic substitution. Comparing the epoxy-benzoquinone probes to their unreactive benzoquinone analogs, both probe-types showed a high binding affinity for a 50 kDa protein, whereas probes lacking the epoxide also labeled a protein with a slightly lower molecular weight. These results are not in agreement with the observed bioactivity of the compounds, as one would expect an epoxy probe-specific protein target responsible for the antibacterial effect that is not targeted by the unreactive benzoquinones. To conclude, there was no obvious correlation between the labeling pattern and the bioactivity of the different structures in *Staphylococcus aureus* strains bringing into focus the labeling results of the Gram-negative *Salmonella* strains.

**A - *S. aureus* NCTC 8325****B - *S. aureus* USA300**

**Figure 30:** Concentration-dependent *in situ* labeling of probes **FM141**, **FM205** and **FM321** of soluble proteins in *Staphylococcus aureus* NCTC 8325 (A) and *Staphylococcus aureus* USA300 (B).

**A - *S. aureus* NCTC 8325****B - *S. aureus* USA300**

**Figure 31:** Concentration-dependent *in situ* labeling of probes **FM243**, **FM310** and **FM255** of soluble proteins in *Staphylococcus aureus* NCTC 8325 (A) and *Staphylococcus aureus* USA300 (B).

Therefore, the different *Salmonella* strains were incubated with probes that showed an MIC of 100  $\mu$ M or lower. The resulting labeling pattern of the epoxy-benzoquinones was compared to the unreactive benzoquinone analogs, as shown in figure 32. Interestingly, this time a strong correlation between the determined antibacterial activity of the epoxide-containing probes and the labeling pattern in comparison to the non-active compounds could be observed. While epoxy-benzoquinone probe **FM233** and **FM239** clearly labeled a protein with a mass of about 28 kDa in *Salmonella typhimurium* LT2 and *Salmonella typhimurium* TA100, respectively, clearly, no such labeling was observed for the unreactive analogs **FM375** and **FM257**. Since the rest of the labeled proteome was comparable for both probe types, this strongly indicates an epoxide-, and with that bioactivity-related labeling pattern.

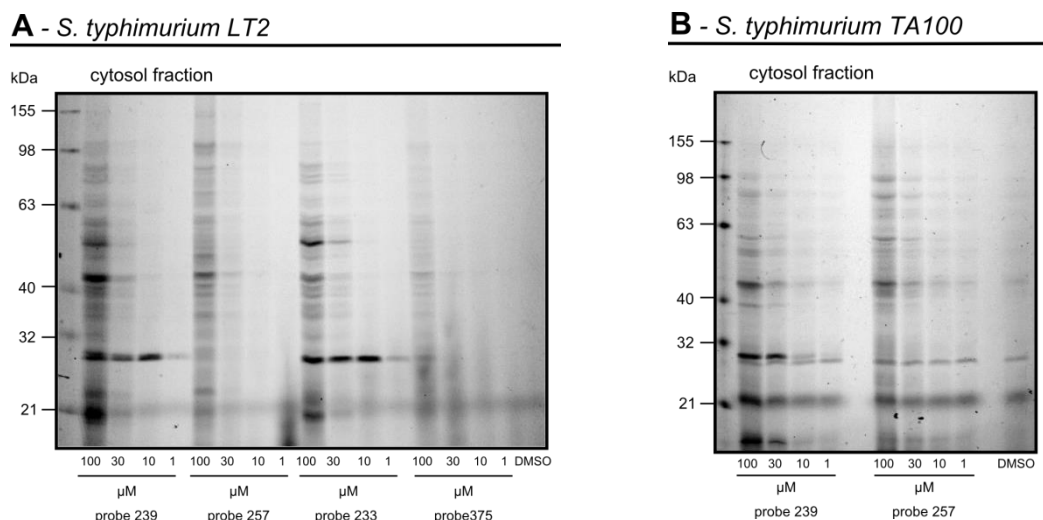


**Figure 32:** Concentration-dependent *in situ* labeling of probes **FM239**, **FM257**, **FM233** and **FM375** of soluble proteins in *Salmonella typhimurium* LT2 (A) and concentration-dependent *in situ* labeling of probes **FM239** and **FM257** in *Salmonella typhimurium* TA100 (B).

Further support for this bioactivity-labeling pattern correlation can be seen in figure 33. Compound **FM233** shows hardly any labeled proteins in the proteome of *Staphylococcus aureus* or *Enterococcus faecalis* and the MIC in these strains is at least three times higher compared to that of *Salmonella* strains.

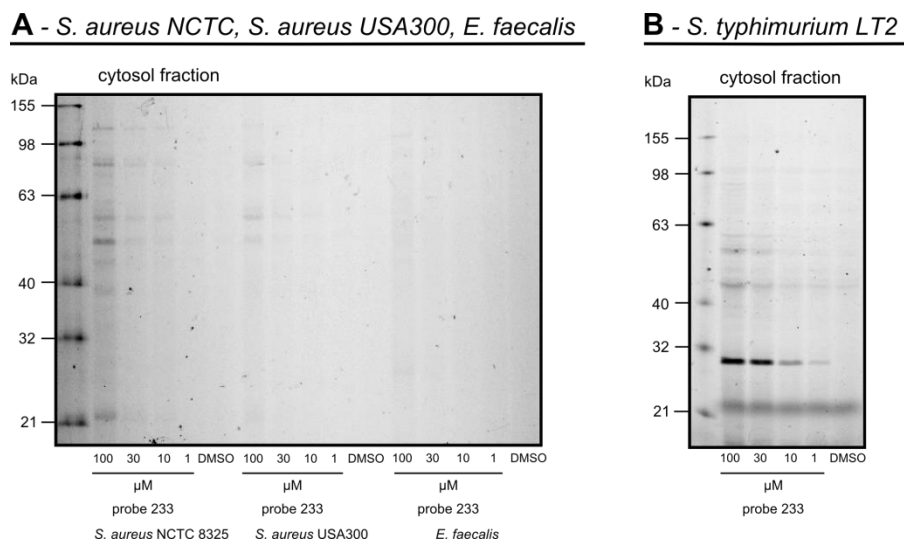


**Figure 33:** Concentration-dependent *in situ* labeling of probe **FM233** of soluble proteins in *S. aureus* NCTC 8325, *S. aureus* USA300 and *E. faecalis* (A) in comparison to *S. typhimurium* LT2 (B).

In summary, probe **FM233** showed a very clear epoxide- and activity-related labeling pattern down to a concentration of 10  $\mu\text{M}$  in comparison to the non-epoxide analog **FM375**. To identify the strongly-labeled protein with a mass of approximately 28 kDa as well as and any other potential protein targets of the probes, a gel-based target analysis in *Salmonella typhimurium* LT2 was initially performed.

## 2.3.2 GEL-BASED TARGET IDENTIFICATION

To identify labeled proteins, a trifunctional linker, containing a rhodamine fluorophore, biotin and an aliphatic azide moiety (see section IV, 3.1.2), was used to enrich the labeled proteins on avidin beads. After separating the proteome via preparative SDS-PAGE, the protein bands were visualized by fluorescent scan, isolated and digested with trypsin. The obtained peptides were then analyzed via HPLC-MS/MS using MaxQuant software and the corresponding proteins were identified with Andromeda as a search engine.

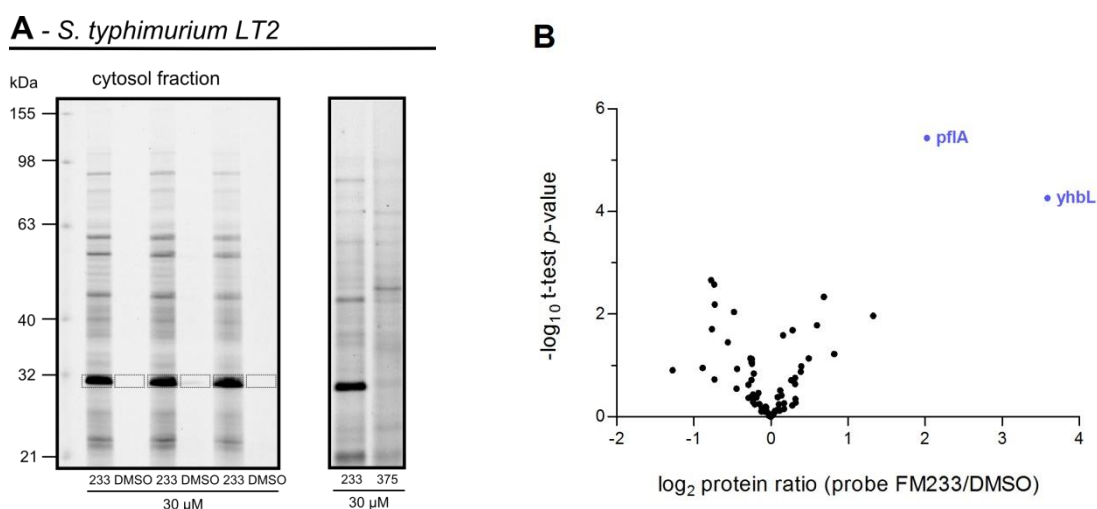


**Figure 34:** Fluorescent SDS-PAGE analysis of *in situ* preparative labeled *Salmonella typhimurium* LT2 with 30  $\mu$ M of probe **FM233** in comparison to the DMSO control, cytosol fraction. Areas, which were cut out for in-gel digest are marked as frames (A, left). Comparison of the enriched proteins labeled with reactive probe **FM233** and unreactive probe **FM375** (A, right). Gel-based LC-MS/MS identification of yhbL and pflA as target proteins of **FM233**: The volcano plot shows the statistical significance of proteins (student's t-test p-value), that were identified from the gel band (25 - 30 kDa, A). Ratios were calculated from intensities of proteins in the band (**FM233**-treated *S. typhimurium* LT2 proteome) and corresponding gel area with DMSO-treated proteome. Blue dots represent proteins that were significant at an FDR of 0.01 (Benjamini-Hochberg).

As shown in figure 34A (left), the only protein that appeared significantly enriched on avidin beads corresponded to the previously described epoxide-dependent band with a mass around 28 - 30 kDa, and was therefore selected for analysis. As expected, there was no visible band enriched at this height when labeling the *Salmonella* proteome with the inactive benzoquinone probe **FM375** (see figure 34A, right), suggesting that this protein is not the target enzyme of this probe. Two proteins were identified as statistically significant target enzymes of probe **FM233**, shown as blue dots in the volcano-plot in figure 34B. The abbreviation pflA corresponds to pyruvate formate-lyase-activating enzyme, a 31.3 kDa monomeric protein which is involved in the anaerobic glucose metabolism pathway.<sup>[140]</sup> Under anaerobic conditions, it is necessary to activate the enzyme pyruvate formate lyase (PFL), which then catalyzes the conversion of pyruvate and coenzyme-A into formate and acetyl CoA. Thereby, PflA possesses lyase and oxidoreductase activity<sup>[141]</sup> and

utilizes a [4Fe-4S] cluster and adenosylmethionine to generate a putative adenosyl radical which activates PFL for catalysis.<sup>[142]</sup> The second identified enzyme is the so-called sigma cross-reacting protein 27A (SCRP-27A, yhbL), an uncharacterized protein with unknown functionality and a mass of 22.9 kDa.<sup>[143]</sup> According to *Ueshima et al.* this protein cross-reacts with an antibody prepared against a peptide of the RNA polymerase sigma-70 region 2, and was therefore originally named sigma cross-reacting protein.<sup>[144]</sup> In 1998 *Hemmi et al.* identified SCR-27A in a mutant screen designed to recognize genes affecting lycopene formation in *Escherichia coli* and therefore re-named it to elbB, standing for enhancing lycopene biosynthesis.<sup>[145]</sup> Even though, the two proteins show a marked difference in their molecular weight, they were both statistically significant hits from the gel-based analysis. To take into account the whole set of labeled proteins and to corroborate the results of the gel-based analysis, gel-free target identification was next performed.

### 2.3.3 GEL-FREE TARGET IDENTIFICATION

To quantify labeled proteins in bacterial samples treated with the reactive epoxy-benzoquinone probe **FM233** in comparison to its unreactive analog **FM375**, triplex stable isotope dimethyl labeling was used for gel-free target identification method. Therefore, *Salmonella typhimurium* LT2 cells were incubated with either one of the two probes, or DMSO as a control. After lysis, the labeled proteins were clicked to a biotin-azide linker, enriched on avidin-beads and digested in solution (see section IV, 3.2.1). The peptides derived from individually-treated samples (**FM233**, **FM375** or DMSO) were then labeled on column with isotopomeric dimethyl labels, mixed and simultaneously analyzed by LC-MS (see section IV, 3.2).<sup>[82]</sup> By comparing the labeled proteins of the active probe **FM233** to the DMSO-treated control, six enzymes could be revealed as putative targets (figure 35A). The comparison of the labeled proteins of the active probe **FM233** to the proteins labeled by its unreactive analog **FM375** revealed four enriched enzymes, respectively (figure 35B). In analogy to the gel-based approach described in the previous section, SCR-27A was identified as a highly enriched target of **FM233**, which could not be identified using the inactive analog **FM375**. Combining the results of the gel-based and the gel-free target analysis, SCR-27A was the only protein relevant in both approaches. For a discussion of the other enriched proteins please see section 2.5.3.



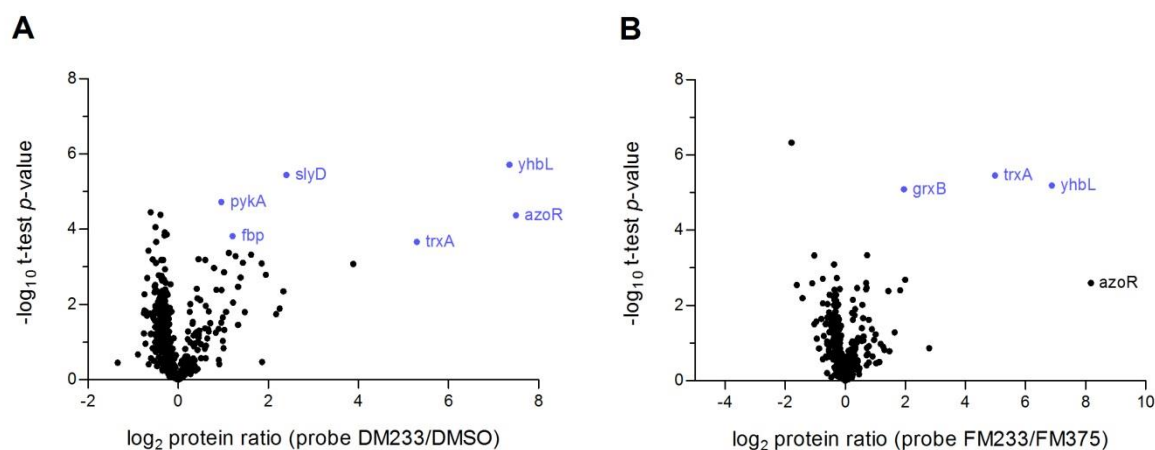


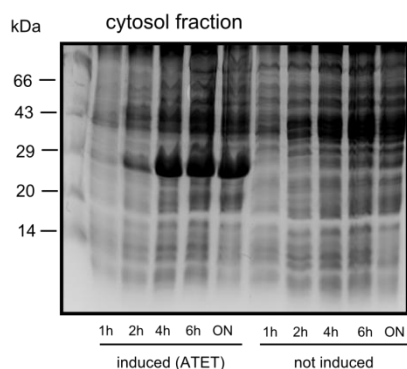
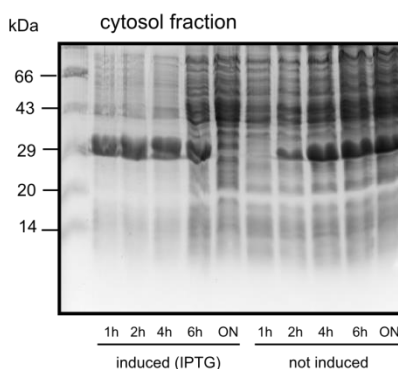
**Figure 35:** Quantitative cytosolic proteome enrichment analysis of **FM233**-treated *Salmonella typhimurium* LT2 bacterial cells compared to DMSO (A) and **FM375** (B) treated control after click reaction with biotin azide, pull-down using avidin beads and dimethyl labeling. The volcano plot shows the statistical significance of enrichment levels (student's t-test p-value) as a function of average protein ratios from nine biological replicates in probe-treated vs. control cells. Blue dots represent proteins that were significantly enriched at an FDR of 0.01 (Benjamini-Hochberg).

In order to independently confirm these results and to validate this uncharacterized protein as a cytosolic target enzyme of probe **FM233**, we decided to overexpress and purify recombinant SCRP-27A in order to directly label the protein with the probe.

## 2.4 TARGET VALIDATION

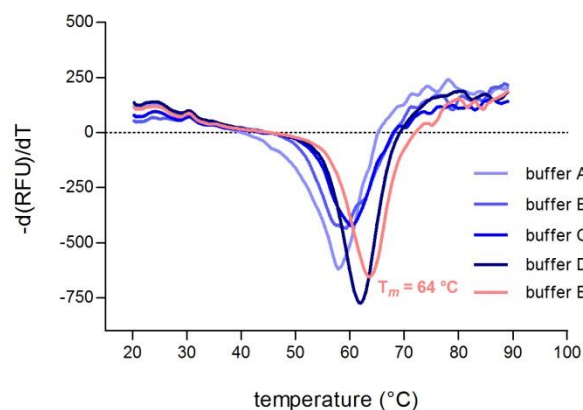
### 2.4.1 OVEREXPRESSION AND THERMAL STABILITY OF SCRP-27A

As protein SCRP-27A has not been overexpressed so far, the gene sequence of the enzyme was cloned into the two different expression vectors pET300 and pDest007. In the pDest007 vector, the construct has an N-terminal Strep-tag, while the pET300 vector contains an N-terminal His-tag. After transforming the constructs into chemically competent *E. coli* BL21(DE3) cells, the overexpression of the recombinant protein was induced by the addition of ATET or IPTG, for each vector respectively. As shown in figure 36, the test-overexpression revealed a strong protein band for both constructs after an incubation time of about 4 h. For the pDest007 vector, the non-induced cells did not produce the protein; however, for the pET300 vector, protein was non-specifically overexpressed in non-induced cells. Subsequently, the cells were lysed and the cytosolic fraction containing the protein was purified via His- or Strep-column on an ÄKTA system, followed by an additional SEC purification step for both constructs. As a result, SCRP-27A could be obtained in very good amounts and high purity with both purification methods.

**A - *E. coli* BL21-SCRP-27A\_pDest007****B - *E. coli* BL21-SCRP-27A\_pET300**

**Figure 36:** Coomassie-stained gels of the cytosol fraction of the test-overexpression showed a high production level of protein SCR-27A for both expression vectors after 4 h in *E. coli* BL21 cells. The IPTG-induced pET300 vector system (B) showed leaking expression.

Next, the thermal stability of the uncharacterized recombinant protein in different buffers was tested by thermal shift assay. Therefore, the protein was incubated with the dye SYPRO Orange and the fluorescence signal was measured with gradually increasing temperature. The midpoint value of the resulting stability curves represents the melting temperature  $T_m$  of the protein, reflecting its stability in the different buffers.<sup>[146,147]</sup> These measurements indicate that SCR-27A is in its folded state upon the purification (figure 37).



Name	Composition			
	HEPES	NaCl	EDTA	DTT
buffer A	20 mM	100 mM	-	-
buffer B	20 mM	50 mM	0.1 mM	0.1 mM
buffer C	20 mM	150 mM	0.1 mM	0.1 mM
buffer D	20 mM	300 mM	0.1 mM	0.1 mM
buffer E	20 mM	500 mM	0.1 mM	0.1 mM

**Figure 37:** Determined melting temperatures of SCR-27A in different HEPES buffers containing increasing salt concentrations via thermal shift assay with SYPRO Orange. The exact composition of the buffers is given in the table on the right.

As shown in figure 37, SCR-27A proved to be quite stable with melting temperatures around 60 °C. Although there is not much difference in the melting points among the buffers, it is evident that the stability of the protein increases with the concentration of NaCl in the buffer. Therefore, buffer E was chosen as storage- and SEC-purification-buffer for SCR-27A.

## 2.4.2 LABELING EXPERIMENTS

To validate SCRP-27A as the cytosolic target protein of probe **FM233**, the results of the MS analysis (see chapter 2.3.2 and 2.3.3) were confirmed by various labeling experiments. First, purified recombinant SCRP-27A was labeled with different amounts of **FM233** and heat-denatured SCRP-27A (=  $\Delta T$ ) served as control. In the presence of one equivalent of probe **FM233**, a distinct band could be detected by fluorescence scanning of the SDS gel, which further increased with increasing probe concentration. The heat control, performed with 10 equivalents of **FM233**, showed a strongly reduced signal intensity suggesting that the probe requires an intact and folded protein for interaction (figure 38A). The Coomassie-stained gel shown in figure 38B additionally confirmed an equal loading amount of protein in all samples.

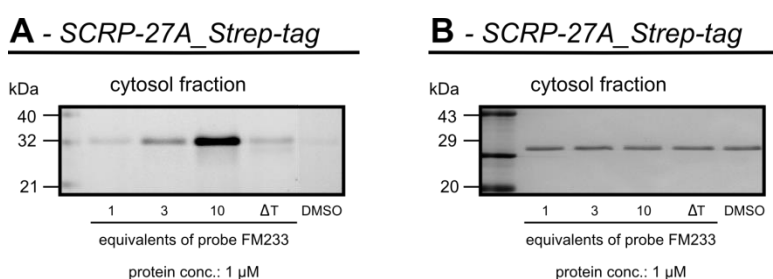


**Figure 38:** Recombinant SCRP-27A is labeled in a concentration-dependent manner by probe **FM233**. Heat denaturation (=  $\Delta T$ ) of the protein prior to labeling resulted in a strong reduction of signal intensity (A). The Coomassie-stained gel confirmed equal protein amounts in all samples (B).

Second, the induced *E. coli* BL21 expression strain was labeled with different concentrations of probe **FM233** revealing a high specificity of the probe towards SCRP-27A (figure 39).

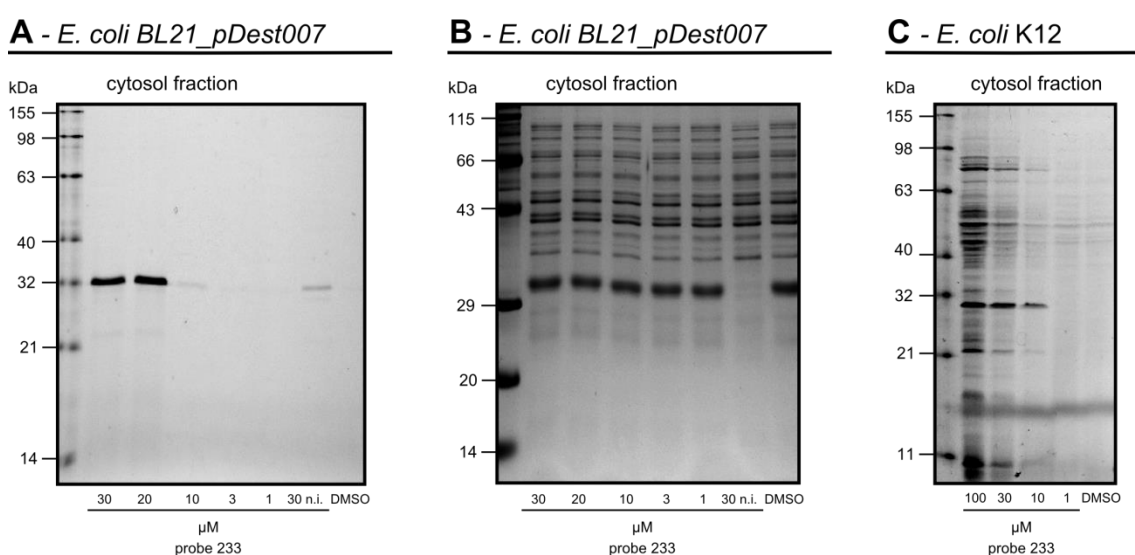


**Figure 39:** Concentration dependent labeling of induced *E. coli* BL21 with probe **FM233**: the not-induced control showed almost no labeling (A). Coomassie staining of A proved equal protein concentration among the probes (B). SCRP-27A was also labeled in *E. coli* K12 wild-type down to a concentration of 10  $\mu M$  (C).

Whereas in the Coomassie gel (B) the whole proteome of the induced *E. coli* expression strain is stained, only one distinct band in the fluorescence gel is visible. As shown in C, probe **FM233** also labeled wild-type *E. coli* K12 down to a concentration of 10  $\mu$ M, explaining the light band in the not-induced control in gel A.

These findings are in accordance with the literature as SCRP-27A is known to be part of both proteomes. The sequence identity of SCRP in *E. coli* K12 and *S. typhimurium* LT2 is 89% (see figure 40, determined by NCBI blast).<sup>[148]</sup> Remarkably, probe **FM233** is, besides probe **FM239**, the only probe of the library tested for bioactivity against bacteria which inhibits the growth of this *E. coli* strain in a concentration of 100  $\mu$ M. All other compounds did not show any growth inhibition up to a concentration of 300  $\mu$ M (compare section 2.2).

1	MKKIGV <b>V</b> LSGCGVYD <b>G</b> TEIHEAVLTLLAI <b>A</b> RSQAQAVCFAPDK <b>PQ</b> ADVINHLTGEAM <b>A</b> ET	60
1	MKKIGV <b>I</b> LSGCGVYD <b>G</b> SEIHEAVLTLLAI <b>S</b> RSQAQAVCFAPDK <b>Q</b> QVDINHLTGEAM <b>T</b> ET	60
61	RNVLIEAARITRG <b>D</b> IRPL <b>SQAQ</b> PEELDALIVPGGFGAAKNLSNFAS <b>Q</b> GSECR <b>VDS</b> SDVVAL	120
61	RNVLIEAARITRG <b>E</b> IRPL <b>AQADAA</b> EELDALIVPGGFGAAKNLSNFAS <b>L</b> GSECT <b>VD</b> RELKAL	120
121	AKAMH <b>Q</b> SGKPLGF <b>I</b> CIAPAMLPKIFDFPLRLTIGTDIDTAEVLEEMGAEHVPCPVDDIVV	180
121	A <b>Q</b> AMH <b>Q</b> AGKPLGF <b>M</b> CIAPAMLPKIFDFPLRLTIGTDIDTAEVLEEMGAEHVPCPVDDIVV	180
181	DEDNK <b>V</b> VTTPAYMLA <b>Q</b> DIA <b>Q</b> AASGIDKLVSRLVLAE	217
181	DEDNK <b>I</b> VTTPAYMLA <b>N</b> IA <b>E</b> AASGIDKLVSRLVLAE	217
	SCR-27A	<i>S. typhimurium</i> LT2
	elbB	<i>E. coli</i> K12

**Figure 40:** Sequence alignment of *Salmonella typhimurium* LT2 SCRP-27A (top line) and *Escherichia coli* K12 elbB (lower line). Differences in the protein sequence are marked in red.

Furthermore, the induced *E. coli*\_pDest007 expression strain was labeled with the inactive benzoquinone analog of probe **FM233** in different concentration. In accordance with the gel-based and gel-free target identification analysis described in section 2.3, probe **FM375** labeled SCRP-27A very weakly compared to the active probe **FM233** (figure 41).

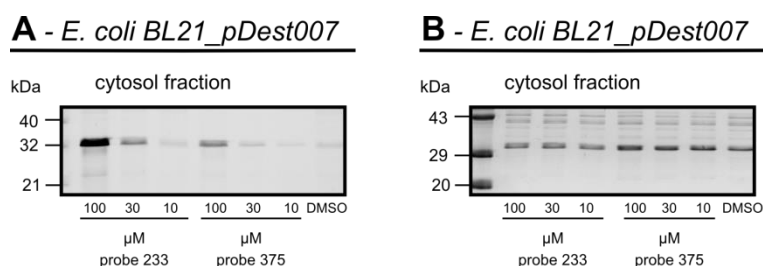


**Figure 41:** Concentration-dependent labeling of induced *E. coli* BL21 with probe **FM233** in comparison to probe **FM375** proved a much weaker binding of **FM375** to SCRP-27A (A). Coomassie staining proved equal protein concentration among the probes (B).

## 2.4.3 BINDING STUDIES VIA FULL-LENGTH MS

To further validate the binding of **FM233** to recombinant SCRP-27A, full-length MS-analysis was performed. Therefore, the purified enzyme was incubated with the probe and the resulting protein mass was determined via HR-ESI-MS. Interestingly, the incubation of SCRP-27A with an excess (3-7 equivalents) of probe **FM233** for ten minutes at room temperature in storage buffer E (pH 7.0) resulted in different protein species: in addition to a one- and two-time probe-modified protein, further mass peaks with a shift of 137 Da were observed over time (figure 42).

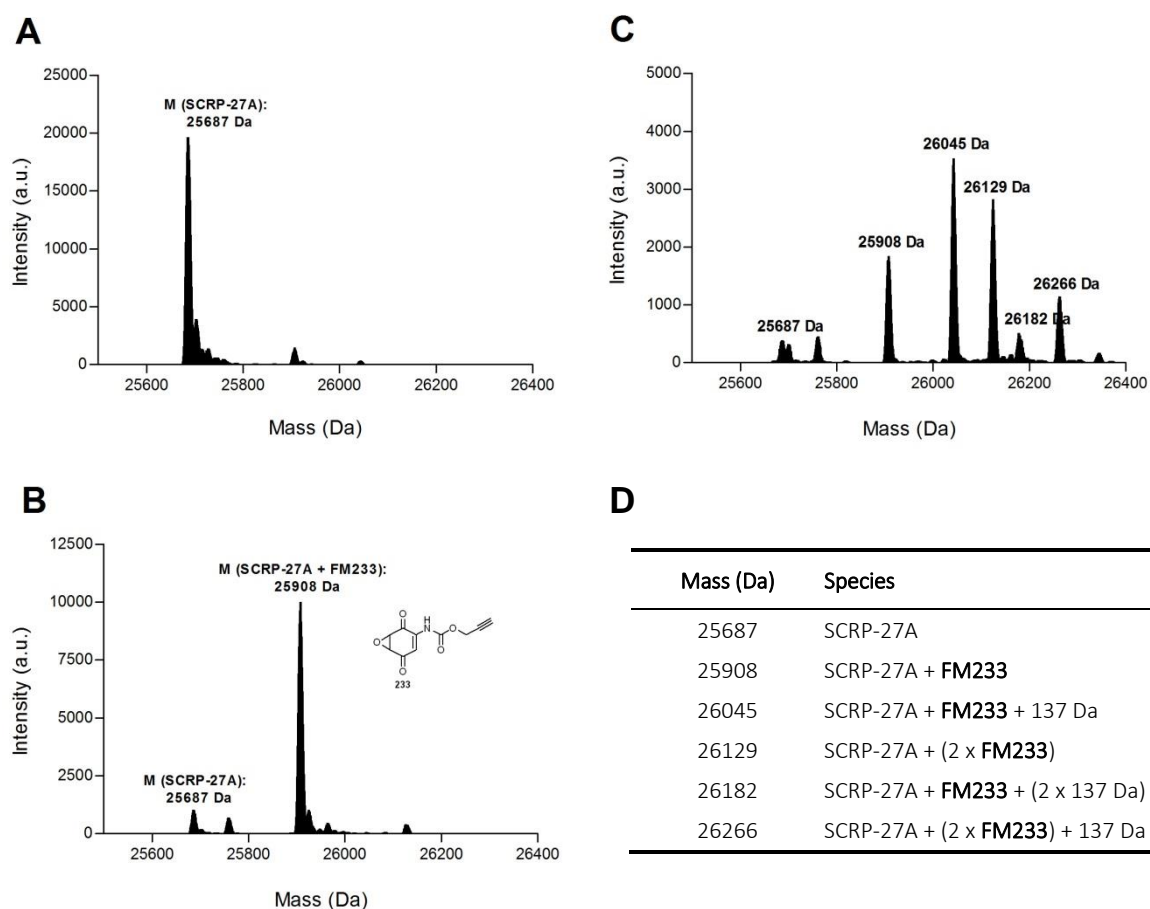


**Figure 42:** Full-length MS measurements of intact proteins. SCRP-27A without inhibitor (A) and labeled with inhibitor **FM233** after 5 minutes (B) and 50 minutes (C). The different protein species are given in table (D).

The additional mass shift can be explained by cleavage of the carbamate moiety of the probe at pH 7.0, resulting in a very reactive electrophilic molecule (figure 43B), which is then additionally bound by the enzyme. Importantly, this fragment only reacted with SCRP-27A after one equivalent of **FM233** was bound, and the first molecule bound to SCRP-27A was not cleaved as with the unbound compound in the buffer. In contrast, incubation of the enzyme with the probe in buffers with more acidic pH (6.5 - 5.5) did not result in complete binding, illustrating the strong correlation between reactivity and stability of the probe.

This is in accordance with stability measurements of compounds **FM233** and **FM375** performed by HPLC-analysis in water and PBS buffer (figure 43A). While the inactive probe **FM375** was stable over two hours in both solvents, probe **FM233** immediately decomposed in PBS and after 2 hours in water, only 50% of the probe were still intact.

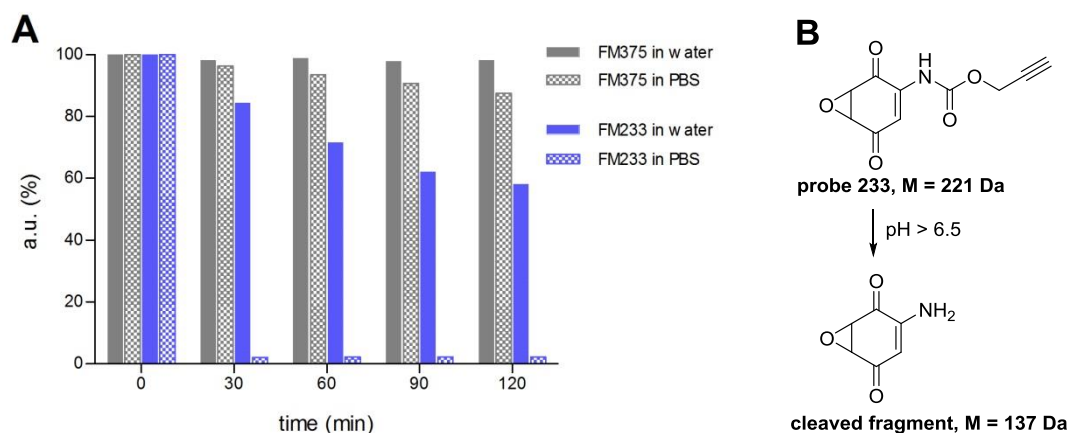


**Figure 43:** Stability of probes **FM233** and **FM375** in water and PBS over two hours. The initial amount of respective probe was set to 100%. (A). Incubation of probe **FM233** under neutral to slightly basic conditions led to a cleavage of the carbamate moiety (B).

To test the stability of the one-time modified protein-probe complex, SCR-P-27A was incubated with 3 equivalents of compound **FM233** in storage buffer (pH 7.0) for 10 minutes. Excess **FM233** was then removed from the protein solution via desalting columns and the protein mass was again measured via HR-ESI-MS. As illustrated in figure 44, besides a small amount of the protein species modified by **FM233** and the cleaved fragment, the main peak corresponds to SCR-P-27A to which one probe molecule is attached. This protein-probe complex was stable over ten hours, confirming the labeling results described in the previous chapter.

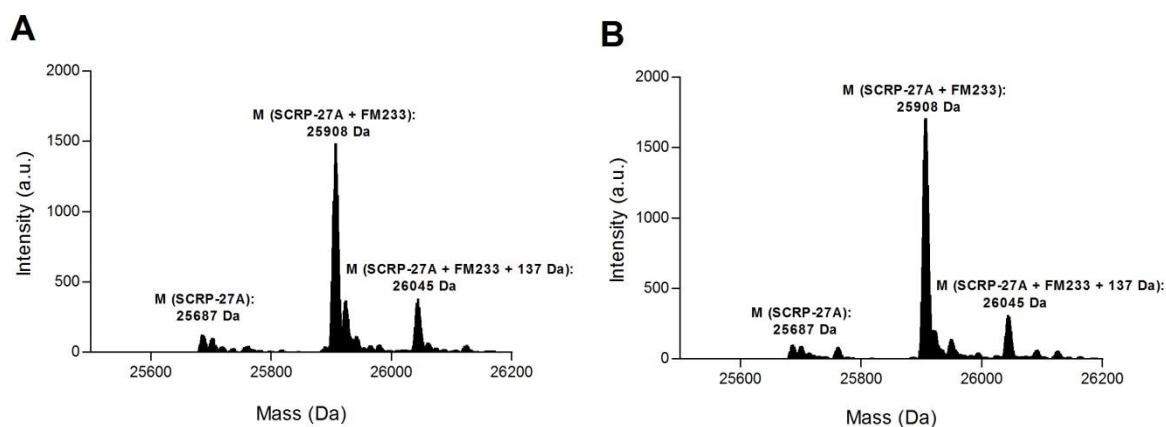


**Figure 44:** Full-length MS measurements of intact proteins: excess of **FM233** was removed after 10 minutes incubation at room temperature via Micro Bio-Spin chromatography columns. The SCR-P-27A-probe complex was measured after 5 minutes (A) and 10 hours (B).

#### 2.4.4 BINDING SITE IDENTIFICATION

In the previous section, SCRP-27A was determined to be the cytosolic protein target of inhibitor **FM233**. While labeling experiments and MS-binding studies clearly showed the stable binding of the probe to the protein, the amino acid residue reacting with the electrophilic probe was yet to be identified. To determine the binding site of **FM233**, the crystal structure of *Salmonella typhimurium* LT2 was solved. Furthermore, the binding site was validated by labeling and MS-binding studies using site-directed mutants of SCRP-27A.

##### 2.4.4.1 Crystal structure of *Salmonella typhimurium* LT2 SCRP-27A

In the course of a bacterial structural genomics project initiated by the Structural GenomiX inc. organization, several crystal structures of novel bacterial proteins were solved. The selected proteins were classified as potential anti-infective drug targets that were “either essential for bacterial growth or highly conserved among various species.”<sup>[149]</sup> In 2005 *Harris et al.* published a paper documenting the newly solved crystal structures which included *Escherichia coli* elbB, a protein with 89% sequence identity to SCRP-27A (see figure 40).<sup>[148,149]</sup> The crystal structure was solved at 1.65 Å (PDB-code: 1VHQ) and revealed a cyclic homo-dimeric symmetry (C2 point group) of the protein.<sup>[149]</sup> ElbB and SCRP-27A belong to the same superfamily, called DJ-1/Pfpl. This family contains proteins with sequence and fold similarities, which are not known to have functional commonalities and are largely uncharacterized.<sup>[150,151]</sup> As the crystal structure of *Salmonella typhimurium* LT2 SCRP-27A has not been reported so far, it was solved with a resolution of 1.9 Å via X-ray diffraction crystallography, in order to gain further information as to the binding site.

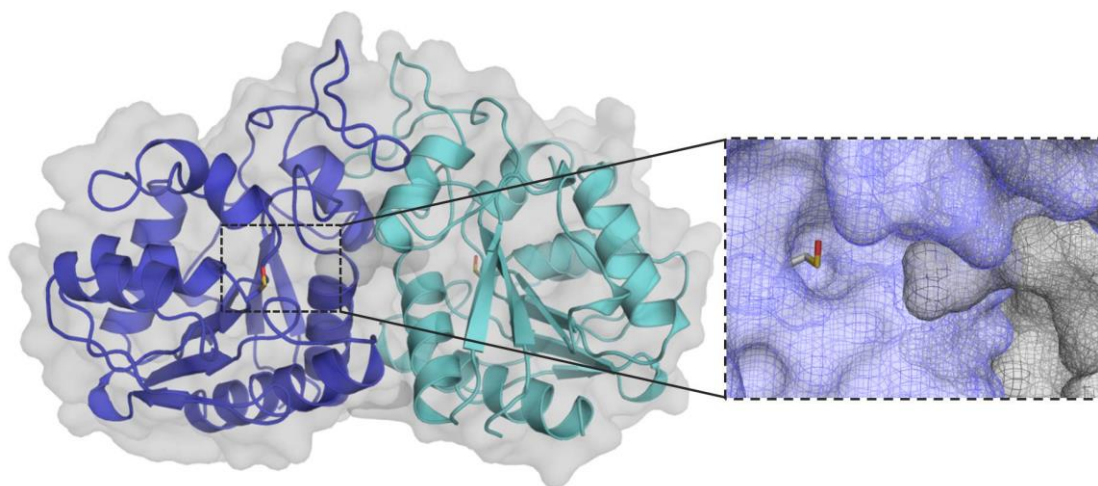


**Figure 45:** Crystal structure of *Salmonella typhimurium* SCRP-27A with a resolution of 1.9 Å reveals a dimeric conformation. On the right is shown the zoomed surface view of the predicted active-site cysteine C135 which is oxidized under the applied crystallization conditions (see section IV, 4.6).



#### 2.4.4.2 Binding site verification via site-directed mutagenesis

As mentioned in the previous chapter, *Ondrechen et al.* published information about a predicted active-site cysteine C138 of *E. coli* elbB in 2007, referring to the highly conserved cysteine C100 of Protease I, a member of the DJ-1 superfamily of proteins.<sup>[150]</sup> In accordance, the multiple-sequence alignment of various members of this family, done by *Vanderleyden et al.* in 2005, revealed a conserved cysteine residue at this position just as well.<sup>[151]</sup> With regard to the protein sequence used for the recombinant overexpression (see section IV, 4.1 and figure 40) this residue refers to C135 in case of *Salmonella* SCRP-27A. To verify the predicted active-site of SCRP-27A, a point mutation was introduced by site-directed mutagenesis. Cysteine 135 was therefore exchanged to an alanine residue, the closest structural analog that does not contain a nucleophilic thiol group. Primers containing the codon change to alanine at the desired position were designed and amplified by PCR with the SCRP\_pET300 plasmid as a template, and subsequently transformed into chemical competent *E. coli* BL21 cells. The overexpression of recombinant SCRP-27A\_C135A was induced by the addition of IPTG. As shown in figure 46A, the test-overexpression revealed a strong protein band after an induction time of about 1 h. The protein was purified via His-column followed by SEC purification, after which SCRP-27A\_C135A could be obtained in high amounts and purity.

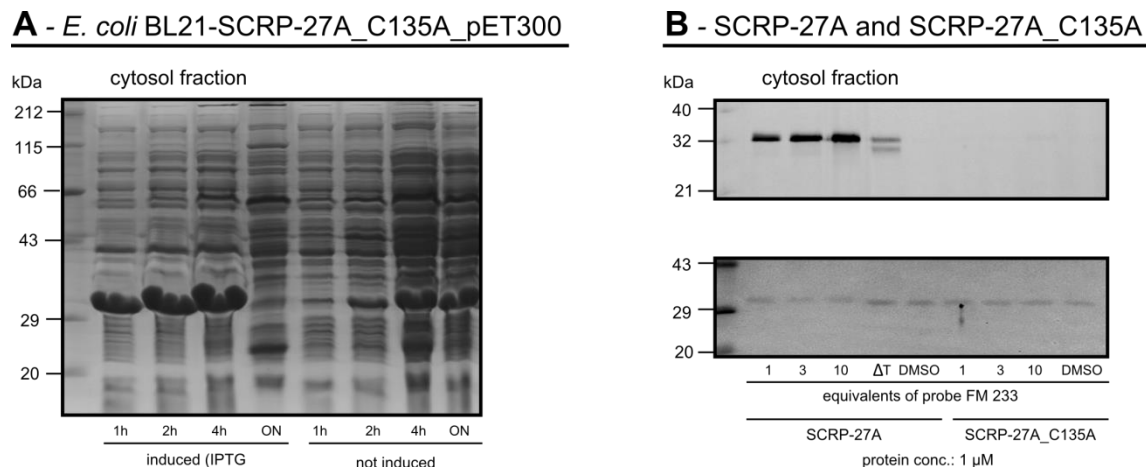


**Figure 46:** Coomassie-stained gel of the cytosol fraction of the test-overexpression showed a high production level of protein SCRP-27A for the IPTG-induced pET300 expression vector after 1 h in *E. coli* BL21 cells (A). Recombinant SCRP-27A\_C135A is in contrast to SCRP-27A not labeled by probe **FM233** (B, top). The Coomassie-stained gel confirmed equal protein amounts in all samples (B, bottom).

First, recombinant SCRP-27A\_C135A mutant was directly compared to the labeling of SCRP-27A wild-type. While recombinant SCRP-27A was clearly labeled by probe **FM233** down to a concentration of 1  $\mu$ M, point-mutated SCRP-27A\_C135A showed no labeling at any probe concentration (figure 46B, top). Thus, cysteine 135 could clearly be assigned as the binding site for probe **FM233**.



To evaluate the binding of probe **FM233** in the *E. coli* BL21 mutant strain, induced cells were labeled with different concentrations of probe **FM233** and directly compared to labeling in the wild-type expression strain. As depicted in figure 47, SCRP-27A is labeled in a concentration-dependent manner in wild-type *E. coli* expression strain, as previously shown. In contrast, no labeling was observed for the mutated SCRP-27A expression strain, again confirming the determined binding site.

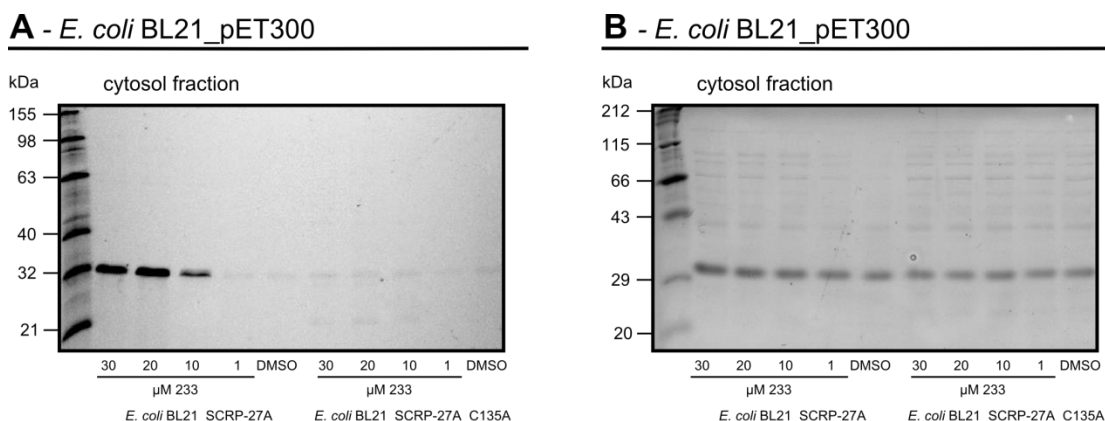


**Figure 47:** Comparison of the concentration-dependent labeling of induced *E. coli* BL21\_SCRP-27A and the expression strain of the point mutation *E. coli* BL21\_SCRP-27A\_C135A with probe **FM233**. Whereas a strong labeling was observed in the case of the wild-type expression strain, no labeling could be seen with the point mutated expression strain (A). Coomassie staining of A proved equal protein concentration among the probes.

In analogy to section 2.4.3, the labeling results of inhibitor and recombinant SCRP-27A\_C135A were evaluated via full-length MS-analysis. Therefore, SCRP-27A\_C135A was incubated with 3 equivalents of probe **FM233** for ten minutes at room temperature in storage buffer E (pH 7.0) without removing the excess of probe as done for the wild-type protein. The resulting protein mass was then determined via HR-ESI-MS. In accordance with the previous labeling results, the mutated protein did not bind the probe over a period of ten hours (compare figure 48, A and B). Interestingly, the previously observed adduct of cleaved probe **FM233** (mass of 137 Da) was not observed in the case of the mutated protein, although the same buffer was used. This further confirms the hypothesis, that adduct binding is only possible in the presence of a probe-bound enzyme. One explanation could be a destabilization of the protein by the first binding of inhibitor.

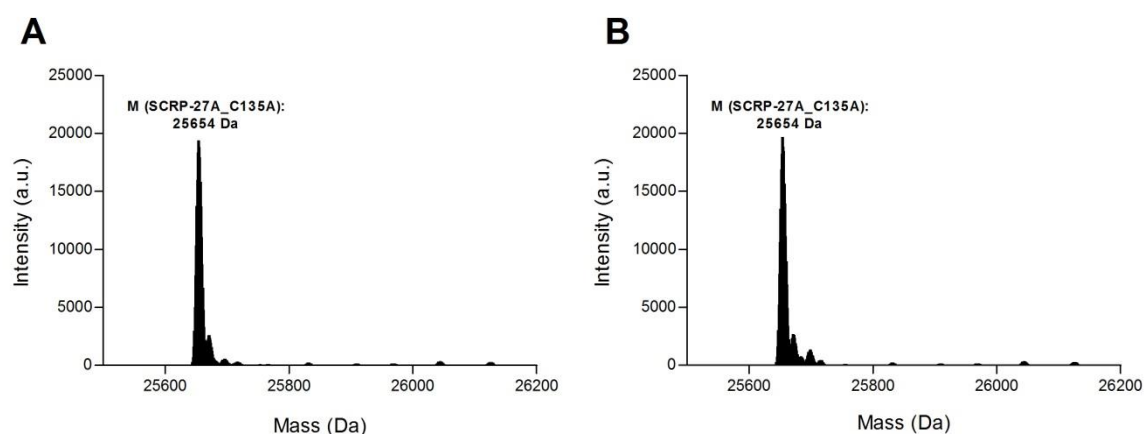


**Figure 48:** Full-length MS measurements of intact proteins. SCRP-27A\_C135A labeled with inhibitor **FM233** after 10 minutes (A) and 10 hours (B). Binding of inhibitor to the protein was not observed over the monitored time.

To verify this hypothesis, thermal shift assays using the recombinant protein in the presence of **FM233** were performed. Therefore, the proteins SCRP-27A and SCRP-27A\_C135A were incubated with several equivalents of inhibitor **FM233** and the corresponding fluorescence signals were measured with gradually increasing temperature. Whereas two equivalents of probe **FM233** clearly affected the thermal stability and folding of SCRP-27A (figure 49A), the probe had only very little influence on the mutated protein (figure 49B).

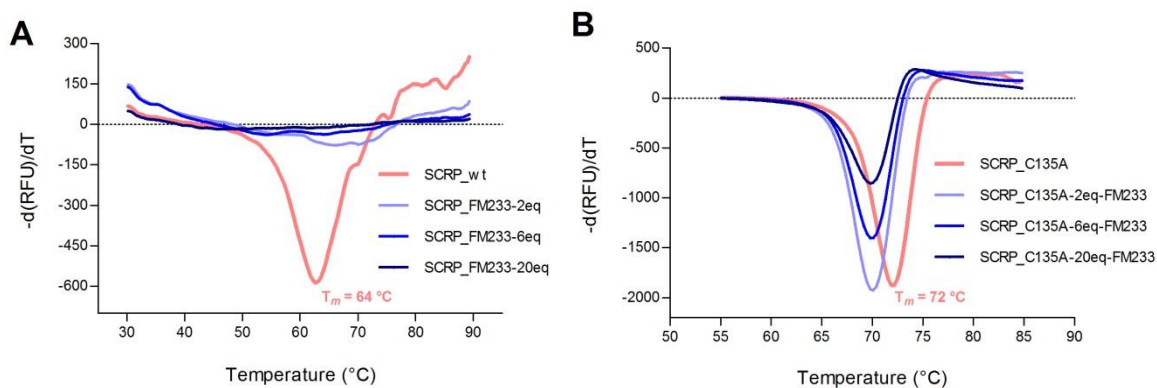


**Figure 49:** Determined melting temperatures of SCRP-27A (A) and SCRP-27A\_C135A (B) with different inhibitor concentrations via thermal shift assay with SYPRO Orange.

The performed labeling experiments, as well as full-length MS measurements and thermal shift assays of the two proteins with the probe, absolutely confirmed cysteine 135 as binding site of probe **FM233**. As SCRP-27A is an uncharacterized protein, an experimental determination that would identify the binding site of probe **FM233** to also be the active-site could not be performed. Nevertheless, the gained experimental evidence concerning the binding site together with the predicted conserved active-site cysteines of the proteins belonging to the DJ-1 superfamily, make this assumption very likely.<sup>[150]</sup>

## 2.5 PROTEIN FUNCTIONALITY

SCRP-27A is an uncharacterized protein that was first identified in 1992 by *Ishihama et al.*<sup>[144]</sup> They attempted to characterize yet unidentified  $\sigma$ -subunits in *E. coli* by preparing an antiserum against a tetradecameric peptide present in region 2.2 of sigma factors 70 and 32 of the RNA polymerase. It was found that their synthetic peptide cross-reacted with more than 10 different proteins, which were therefore named sigma cross-reacting proteins (SCRPs). The number 27 refers to the respective molecular weight of the protein found by purification and sequencing.<sup>[144]</sup> A second group additionally identified SCR-27A in a mutant screen, which was designed to identify genes affecting the lycopene formation in *E. coli* in 1998. Therefore, this group renamed SCR-27A to elb2, for enhanced lycopene biosynthesis.<sup>[145]</sup>

As referred to in the previous section, *Vanderleyden et al.* revealed a homology of SCR-27A to several enzymes belonging to the DJ-1/ThiJ/Pfpl superfamily.<sup>[152]</sup> The family members share a domain (ThiJ domain) which is structurally related to type I glutamine amidotransferases, consisting of a conserved Cys-His-Glu triad.<sup>[153]</sup> In contrast to the biological role of the GAT domain, the function of this ThiJ domain is not yet known. Besides the fact that this protein family contains many hypothetical proteins, such as SCR-27A, those members with known functionality have various activities,<sup>[154]</sup> making the functional characterization based on similarity very challenging. For instance, human DJ-1 is involved in several cellular functions,<sup>[155]</sup> has been linked to Parkinson's disease,<sup>[156]</sup> and is believed to be a cysteine protease.<sup>[150,152]</sup> Moreover, the intracellular protease 1 (gene Pfpl) of *Pyrococcus horikoshii* not only belongs to the DJ-1 family of proteins, but is also a cysteine protease with a characteristic catalytic triad (C100, H101, E474) in its active-site.<sup>[157]</sup> This active-site cysteine is conserved among various proteins of the family, as previously depicted in section 2.4.4.2. For human DJ-1 and several other family members, this conserved cysteine is located in a nucleophilic elbow-like motif,<sup>[154]</sup> which was first identified in  $\alpha/\beta$  hydrolases.<sup>[158]</sup> Additionally, SCR-27A is known to be colocalized to mtgA, a monofunctional peptidoglycan glycosyltransferase catalyzing the glycan chain elongation of the bacterial cell wall.<sup>[159,160]</sup>

In summary, the expanding DJ-1- superfamily contains various proteins over all three kingdoms of life with high functional diversity including many hypothetical proteins with unknown function. To get insight into the function of SCR-27A, various assays were performed, referring to the presumed or known facts about this protein class.

### 2.5.1 ASSAY-BASED FUNCTIONAL CHARACTERIZATION

A variety of assays were conducted to probe the function of SCR-27A based on the presumed or known facts about the DJ-1 protein class. Referring to the peptidase activity of some members, peptidase activity was tested using an AMC-peptide-based assay, however, no activity of SCR-27A was observed. Because of the colocalization of SCR-27A with mtgA, peptidoglycan hydrolase activity was tested using zymography<sup>[161-163]</sup> and a glutamine amidotransferase activity was assayed by monitoring the reaction of UTP to CTP using HPLC measurements.<sup>[164-166]</sup> However, the enzyme did also not show any activity in these assays. Additionally, two different esterase assays were performed. First, cyclic ester cleavage and with that phosphodiesterase functionality of SCR-27A was tested by monitoring the cleavage of cAMP or cGMP to AMP or GMP by HPLC. Second, the cleavage of *p*-nitrophenylacetate (pNPA) as an aromatic ester substrate was determined by absorption measurements as shown in figure 50. While nearly all performed assays showed no SCR-27A activity, the cleavage of the pNPA ester revealed a potential functional role of the enzyme. In this assay the enzyme-catalyzed hydrolysis reaction of pNPA to acetic acid and *p*-nitrophenol (pNP) is photometrically determined at 410 nm.<sup>[167,168]</sup>

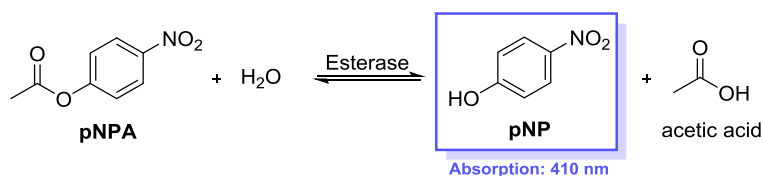


**Figure 50:** Schematic presentation of the hydrolysis reaction of pNPA to pNP followed photometrically in the esterase assay.

Due to the instability of pNPA in aqueous solution,<sup>[168]</sup> a blank, representing the auto-hydrolysis of the substrate in the buffer system without enzyme, was used as a control. As the active-site cysteine in DJ-1 is known to be easily oxidized to cysteine-sulfinic acid and is no longer able to act as a nucleophile in this state,<sup>[169]</sup> DTT was added as reducing agent in the buffer system. The esterase BS3 of *Bacillus stearothermophilus*, served as a positive control enzyme.<sup>[170]</sup> Depending on the enzyme, the following concentrations and conditions were used.

**Table 11:** Concentrations and conditions in the esterase assay depending on the used enzyme.

	Esterase BS3	SCR-27A
buffer	SCR-27A storage buffer	SCR-27A storage buffer
enzyme concentration	1 $\mu$ M	1 $\mu$ M
substrate concentration	100 $\mu$ M	1000 $\mu$ M
<b>FM233</b> concentration	3 $\mu$ M	3 $\mu$ M
<b>FM233</b> incubation time	20 minutes	20 minutes
monitored time	90 seconds	20 minutes

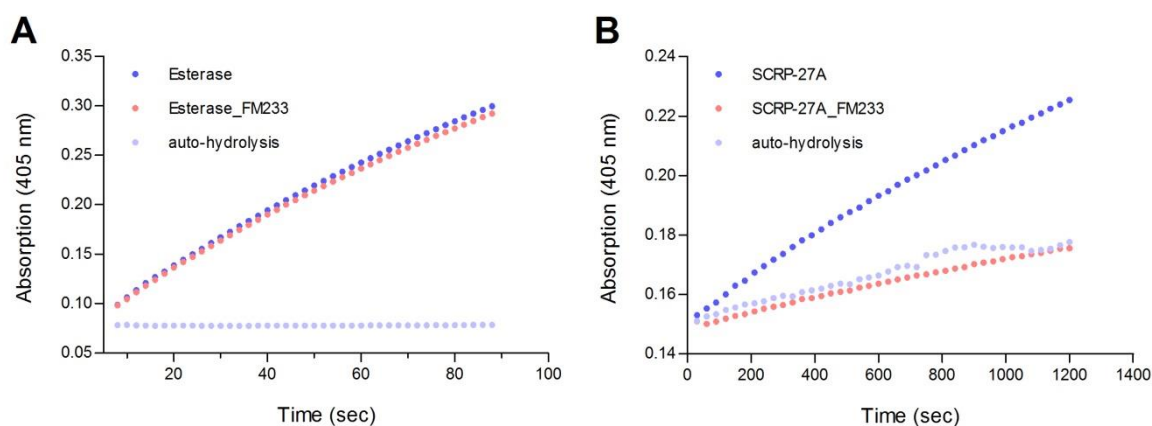


**Figure 51:** Observed absorption for pNP in the esterase assay. The reaction catalyzed by the recombinant esterase BS3 (A) in comparison to the reaction catalyzed by SCR-27A (B).

As depicted in figure 51, the BS3 esterase showed distinct conversion of pNPA. As expected the enzyme-catalyzed reaction (dark blue, figure 51A) showed much faster conversion of pNPA compared to the auto-hydrolysis of the substrate (light blue) over the monitored time. As for SCR-27A, the difference between catalyzed and non-catalyzed reaction is still visible, although less distinct (figure 51B). Furthermore, it was necessary to increase substrate concentration from 100  $\mu$ M to 1000  $\mu$ M and extend the measuring time to observe the activity of SCR-27A. This may be a result of substrate incompatibility, or distinct substrate preferences of SCR-27A. Nevertheless, SCR-27A showed a clear esterase activity distinguishable from the auto-hydrolysis reaction. Moreover, by pre-incubating SCR-27A with three equivalents of probe **FM233**, the esterase activity was reduced to the level of the non-catalyzed reaction (red). This suggests that cysteine 135 is the active-site of SCR-27A. As a control, **FM233** was tested against BS3 esterase and did not influence its activity, proving the selectivity of the probe. To conclude, the experimental evidence concerning the binding-site, together with gained experimental data concerning an esterase activity, strongly indicate an inhibitory effect of probe **FM233** on SCR-27A.

In summary, the cellular function of SCR-27A could not be fully determined, although the performed esterase assay gave a first clue as to the general hydrolase/peptidase/esterase activity of DJ-1 proteins. As previously discussed, most of the members of this protein class have more than one functional activity, making the characterization of a distinct cellular role of such a protein a challenging goal.

### 2.5.2 *SALMONELLA TYPHIMURIUM* LT2- $\Delta$ YHBL KNOCKOUT

To gain further insight into the role of SCRP-27A, a  $\Delta$ yhbL knockout of *Salmonella typhimurium* LT2 was generated via phage transduction (done by Prof. Thilo M. Fuchs, TU München, Lehrstuhl für Mikrobielle Ökologie).

To verify the absence of the yhbL gene in the knockout strain and to further prove the selectivity of the probe, an ABPP labeling experiment was performed. Therefore, *Salmonella typhimurium* LT2\_wt and *Salmonella typhimurium* LT2\_ $\Delta$ yhbL were incubated with different concentrations of probe **FM233** and the resulting labeling pattern was compared. As expected, a distinct band at a height of 30 kDa showed the labeled SCRP-27A protein in case of the wild-type strain. In contrast, this labeled protein band was not observed in the  $\Delta$ yhbL strain, thereby confirming the knockout and highlighting the selectivity of the probe (figure 52).

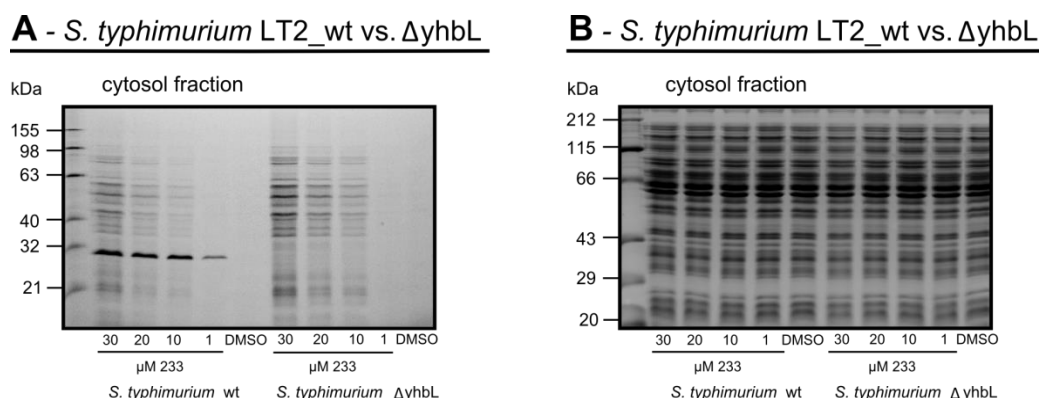


**Figure 52:** Concentration-dependent labeling of *Salmonella typhimurium* LT2\_wt and *Salmonella typhimurium*  $\Delta$ yhbL with probe **FM233**. Whereas **FM233** strongly labeled SCRP-27A, no distinct labeling could be observed in the knockout strain (A). Coomassie staining proved equal protein concentration among the probes (B).

Next, the influence of probe **FM233** on the bacterial growth in the knockout strain was tested via MIC assay. Unexpectedly, the MIC of probe **FM233** only increased to a concentration of 40-50  $\mu$ M in the knockout compared to 30  $\mu$ M in the wild-type strain. This led to the conclusions that SCRP-27A is not essential and that there is likely no direct correlation between SCRP-inhibition and the resulting phenotype.

Since all previous experiments focused on cytosolic target proteins of probe **FM233**, the next step was to analyze further targets of both probes (active and inactive) in the membrane fraction, which could explain the growth inhibition in bacteria.

## 2.5.3 EXTENDED TARGET IDENTIFICATION AND DISCUSSION

As described in section 2.3, the target identification of probes **FM233** and **FM375** were performed via gel-based and gel-free methods. Next, a concentration-dependent analytical labeling of the membrane fraction of *Salmonella typhimurium* LT2 was conducted. As shown in figure 53A, and in contrast to the cytosolic labeling results (compare figure 35), both probes revealed only very weak labeling and no distinct differences in the labeling pattern. Moreover, no labeled proteins were enriched on avidin beads, as depicted in the preparative labeling experiment shown in figure 53B.

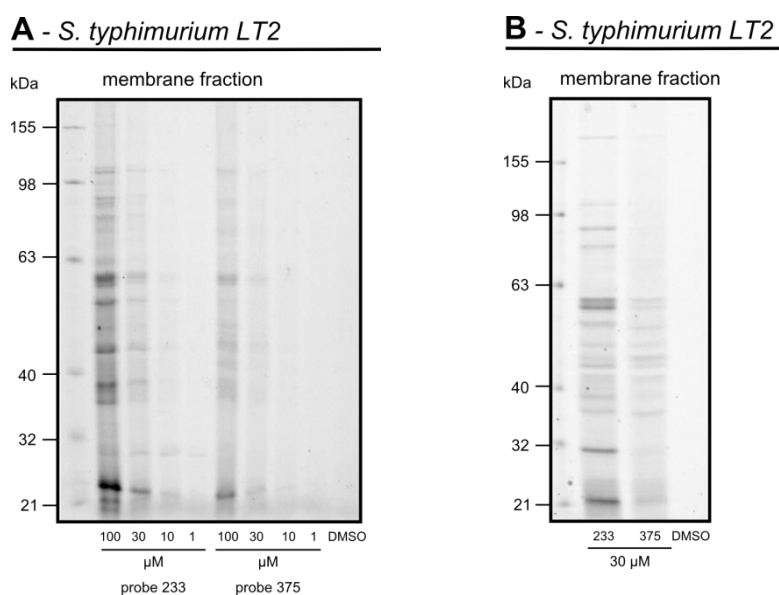


**Figure 53:** Fluorescent SDS-PAGE analysis of *in situ* labeled *Salmonella typhimurium* LT2 membrane fraction with 30 μM of probe **FM233** or **FM375** in comparison to the DMSO control (A). Comparison of the enriched proteins labeled with reactive probe **FM233** and unreactive probe **FM375** (B).

To confirm these observations, gel-free target identification of the active probe **FM233** in comparison to the unreactive analog **FM375** was performed via stable isotope dimethyl labeling in the membrane fraction. In contrast to the results of the target identification in the cytosol, no enzymes were significantly enriched in the membrane fraction (figure 54).

The only protein that was, highly enriched (significance threshold set at a *p*-value below 0.05) in comparison to the DMSO control (A) as well as to the inactive compound **FM375** (B) was azoR, a FMN-dependent NADH-azoreductase. This enzyme was also strongly enriched in the cytosol fraction (figure 35) and its general function is believed to be the reductive cleavage of azo-bonds in aromatic azo-compounds to corresponding amines. In 2009, Wang *et al.* stated that this known azo-reductase activity is not the primary role of these enzymes.<sup>[171]</sup> Moreover, they showed that azoR is a quinone reductase, and thereby capable providing resistance to thiol-specific stress

caused by quinone electrophiles. Electrophilic quinones form S-adducts with cellular thiols, such as reduced glutathione (GSH), thereby depleting their cellular concentration causing this thiol-specific stress.<sup>[171]</sup> As the molecular structure of probes **FM233** and **FM375** contain electrophilic quinone core structures, it may be possible that they cause thiol-specific stress in *Salmonella*. Previous experiments in our group have shown,<sup>[172]</sup> that epoxy-benzoquinones selectively react with thiols and current work revealed that probe **FM233** reacts with an amino acid thiol nucleophile - the active-site cysteine C135 of SCR-27A. As an outlook it would be interesting to prove whether probe **FM233** inhibits azoR, since *Wang et al.* have shown that the quinone reductase activity of azoR is essential for normal growth in *E. coli* strains.<sup>[171]</sup> By inhibiting this enzyme, the cells would become re-sensitized to thiol-specific stress. This could then possibly explain the growth inhibition of probe **FM233** in *Salmonella* as well.

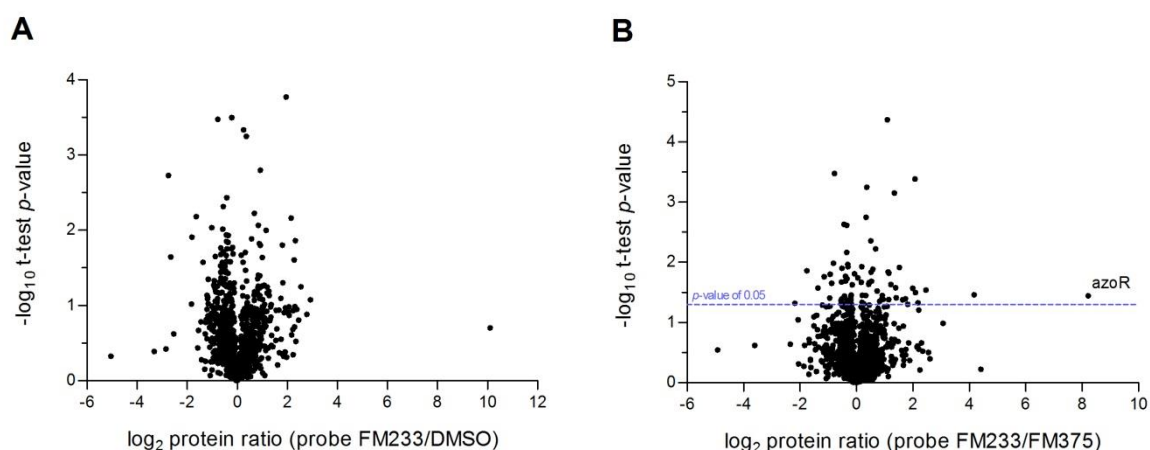


**Figure 54:** Quantitative proteome enrichment analysis of the membrane fraction of **FM233**-treated *Salmonella typhimurium* LT2 bacterial cells compared to DMSO (A) and **FM375** (B) treated control after click reaction with biotin azide, pull-down using avidin beads and dimethyl labeling. The volcano plot shows the statistical significance of enrichment levels (student's t-test  $p$ -value) as a function of average protein ratios from three biological replicates in probe-treated vs. control cells. No proteins were significant at an FDR of neither 0.01 nor 0.05 (Benjamini-Hochberg).

In accordance with this hypothesis, the functions of the two other statistically significant cytosolic target proteins of probe **FM233** are related to this quinone reductase activity. As already referred to in section 2.3.3 (figure 35B) and repetitively shown below (figure 55), enzymes thioredoxin-1 and glutaredoxin 2 were both highly enriched compared to the non-active probe **FM375**, in addition to the already identified cytosolic target protein SCR-27A.



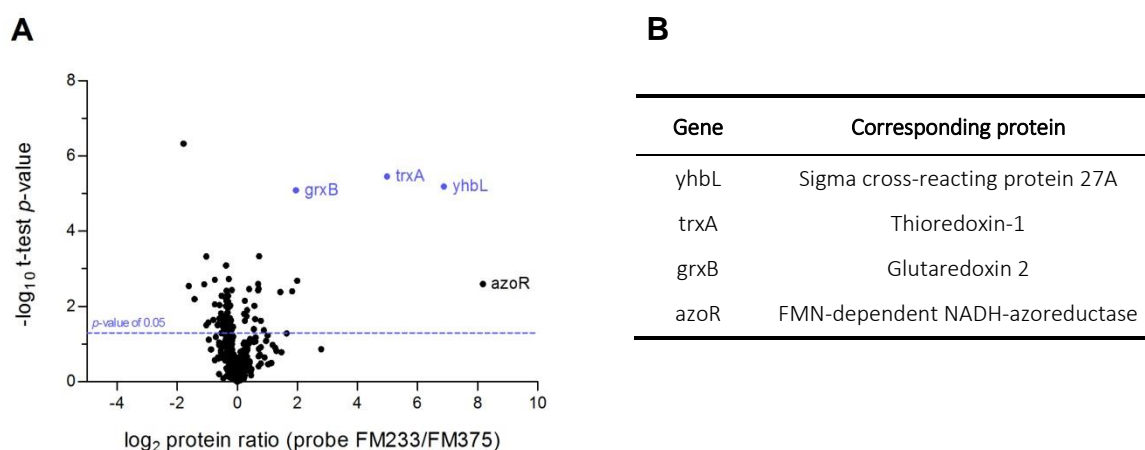


**Figure 55:** Quantitative cytosolic proteome enrichment analysis of **FM233**-treated *Salmonella typhimurium* LT2 bacterial cells compared to **FM375** (A). Blue dots represent proteins that were significantly enriched at an FDR of 0.01 (Benjamini-Hochberg). The blue line reflects a  $p$ -value of 0.05, the standard minimum level of significance. The corresponding protein names are given in table B.

Thioredoxin-1 and glutaredoxin 2 are oxidoreductases that are part of the thioredoxin and glutaredoxin systems in bacteria.<sup>[173]</sup> This so-called thioredoxin superfamily consists of thioredoxin itself, a thioredoxin reductase, glutathione, glutathione reductase and different glutaredoxins.<sup>[174]</sup> These enzymes participate in oxidation and reduction reactions using the redox chemistry of cysteine residues.<sup>[173]</sup> Additionally, thioredoxin-1 is involved in defense against oxidative stress by reducing hydrogen peroxide and by reactivating proteins that were damaged by this oxidative stress. Therefore, thioredoxin-1 has been classified to be an essential protein in *B. subtilis*.<sup>[175]</sup> Moreover, it is known, that *E. coli* missing three members of this thioredoxin superfamily - thioredoxin-1 and -2 and glutaredoxin 1 - is unable to grow. *Beckwith et al.* explained this phenotype to be a result of the inactivation of ribonucleotide reductase, the only essential interacting partner of these three proteins, and as a result the inability of the bacteria to produce deoxyribonucleotides.<sup>[173]</sup> The catalytic active-sites of both, thioredoxin-1 and glutaredoxin 2, contain a characteristic Cys-X-X-Cys motif, which is reactive towards electrophilic quinone moieties. Interestingly, *Rhen et al.* have revealed that thioredoxin-1 strongly contributes to virulence in mouse infection models by observing a significant decrease in intracellular replication of a *trxA* mutant compared to the wild-type.<sup>[176]</sup> They verified their results by showing that thioredoxin-1 is needed for the activity of the *Salmonella* pathogenicity island SPI2, a genetic region that clusters virulence-associated genes, which encodes for a secretion system called separate type III secretion system (T3SS). These systems enable the injection of effector proteins from the pathogenic bacteria into the host cell and thereby facilitate infection. T3SS can be found in several other *Gram*-negative bacteria, emphasizing the potential of an inhibitor of thioredoxin-1.<sup>[177]</sup>

### 3 CONCLUSION AND OUTLOOK

Molecules bearing an amino-epoxycyclohexenone core structure ranging from very simple small molecules like bromoxone or LL-C10037 $\alpha$  to quite complex natural compounds like manumycins show versatile bioactivity. The latter have attracted the attention of researchers because of their capacity to inhibit eukaryotic enzymes like the Ras-farnesyltransferase. Therefore, these molecules are potent anti-inflammatory and anti-cancer agents that show low *in vivo* toxicity and are thus potential anti-tumor candidates. An additional property, which has not been focused on so far is their potent anti-bacterial activity *Gram*-positive and -negative strains. Thus, this work focused on the determination of the enzyme targets of these compounds in bacteria.

First, a probe library was synthesized, which covered the most prominent representatives of this interesting compound class with regard to their different substitution patterns. The electrophilic core of compounds with known antibacterial properties always consists of a combined epoxide-*Michael*-acceptor system. To directly study the influence of these moieties on the activity, probe analogs lacking the epoxide (benzoquinones) were synthesized. In a next step the bioactivity of the probes was tested using a growth inhibition assay in several *Gram*-positive and *Gram*-negative pathogenic bacterial strains. Especially the epoxy-benzoquinone structures turned out to be potent anti-bacterial agents and some of them were even capable of inhibiting the growth of *Gram*-negative *Salmonella* strains in a low  $\mu\text{M}$  range. In accordance with the literature, the epoxide moiety turned out to be essential for this growth inhibition.

Next, the protein targets of the probes were detected by activity-based protein profiling (ABPP) and visualized by SDS-PAGE. The target enzymes of the bioactive probes were then compared to their unreactive analogs, revealing an epoxide- and with that activity-based labeling pattern in the case of probe **FM233** in *Salmonella typhimurium* strains. The identification of the labeled proteins was performed by gel-based preparative ABPP experiments and further verified by stable isotope dimethyl labeling. Interestingly, only one uncharacterized protein named SCRP-27A, a member of the so-called DJ-1/Pfpl superfamily, was identified as target enzyme by both strategies and was therefore further validated. After overexpression and purification of the recombinant protein, it could be confirmed to be a cytosolic target enzyme of probe **FM233** using different labeling experiments and additional binding studies via HR-ESI-MS.

To obtain further insights into the function of the protein, the crystal structure of the protein was solved via X-ray crystallography, which revealed a cysteine residue as a potential active-site. This

cysteine could be identified as the binding site of probe **FM233** by site-directed mutagenesis, which was again validated by labeling experiments and HR-MS binding studies. Determining the function of this protein turned out to be challenging because of the generally wide-spread functions of members of this protein class. Nevertheless, a slight esterase activity could be detected for SCRP-27A and this activity was inhibited by probe **FM233**. Surprisingly, probe **FM233** turned out to show almost the same growth inhibitory effect on a  $\Delta$ yhbl knockout strain as on the wild-type. With that, a direct link between the observed phenotype and the inhibition of SCRP-27A can be excluded. Hence, additional putative protein targets found by dimethyl labeling and the protein targets identified in the membrane fraction were reviewed. Strikingly, two proteins belonging to the thioredoxin family, thioredoxin-1 (trxA) and glutaredoxin 2 (grxB), were additionally labeled by probe **FM233**. Together with an azoreductase (azoR), which is known to reduce quinones these combination of labeled enzymes could explain the growth inhibitory effect of probe **FM233** on *Salmonella typhimurium*. Therefore, the next steps would be to overexpress the potential target enzymes and to check their inhibition by probe **FM233**.

Besides the covalent protein targets considered in this work, reversibly-binding protein targets as well as non-protein targets may also contribute to the bioactivity of these compounds. This could be determined by synthesizing a photo-probe bearing a photo-labile crosslinking moiety and identifying its targets. Another possible explanation for the bioactivity of probe **FM233** in *Salmonella* could be an aggregation of SCRP-27A induced by the inhibition by probe **FM233**, which leads to the observed growth inhibition. This theory was verified by performing analytical gel filtration chromatography and CD measurements of the inhibited enzyme, which proved, that SCRP-27A remains folded during binding of probe **FM233**. In order to explore non-protein targets responsible for the bioactivity of probe **FM233** and to further elucidate the function of SCRP-27A, changes in metabolite levels could be determined via untargeted metabolite profiling in wild-type *Salmonella typhimurium* in comparison to the  $\Delta$ yhbl knockout strain.

Finally, the synthesized probe library enables further studies concerning the reactivity of epoxy-aminocyclohexenones in various pathogenic bacteria, such as the methicillin-resistant *Staphylococcus aureus* strains.





## IV – EXPERIMENTAL SECTION



## 1 CHEMISTRY

### 1.1 MATERIAL AND METHODS

All chemical reagents and solvents were purchased in reagent grade or higher purity from the commercial sources Alfa-Aesar, AppliChem, Acros Organics, Fluka/Sigma-Aldrich, TCI Europe or Merck and used without further purification. All reactions sensitive to air and moisture were carried out in flame-dried glassware under an inert atmosphere of nitrogen. Solvents removed under reduced pressure were evaporated at 40 °C. The yields of the substances refer to purified, dried and spectroscopically pure compounds unless otherwise reported.

Flash column chromatography was performed on silica gel by Merck (Geduran Si 60, 40-63 µm), elution solvents were distilled prior to use and in case of solvent mixtures, ratios are given at the synthetic procedures for each product. Analytical thin-layer chromatography was carried out on aluminium-baked TLC Silica gel 60 F254 plates (Merck) and components were visualized by UV detection at 254 nm or stained via aqueous  $\text{KMnO}_4/\text{K}_2\text{CO}_3$  or aqueous cerium molybdate (Hanessian's stain), respectively.

Reversed-phase HPLC analysis was performed on a Waters 2695 separation module equipped with a Waters XBridge C18 column (3.5 µm, 4.6 x 100 mm, flow rate = 1.2 mL/min) and a Waters 2996 PDA detector. Preparative RP-HPLC was accomplished with a Waters 2545 quaternary gradient module, equipped with a Waters XBridge C18 column (5.0 µm, 30 x 150 mm, flow rate = 50 mL/min) and an YMC Triart C18 column (3.5 µm, 10 x 250 mm, flow rate = 10 mL/min). Detection and fractionation was done on a Waters 2998 PDA detector and a Waters Fraction Collector III. Solvents used as mobile phase for elution were a gradient mixture of 0.1% (v/v) TFA in water (buffer A, HPLC-grade) and 0.1% (v/v) TFA in acetonitrile (buffer B, HPLC-grade).

$^1\text{H}$  NMR and  $^{13}\text{C}$  NMR spectra were recorded on a Bruker Avance 360, Avance 500 or Avance III 500 spectrometer with  $\text{CDCl}_3$ ,  $d^6$ -DMSO and  $d^6$ -acetone as solvents. Chemical shifts ( $\delta$ -values) were referenced to the residual proton or carbon signal of the deuterated solvent and are reported in parts per million (ppm). Coupling constants ( $J$ ) are reported in Hertz (Hz) and the following abbreviations are used for the description of the multiplicity of the signals: s = singlet, d = doublet, dd = doublet of doublets, ddd = doublet of doublet of doublets, t = triplet, q = quartet, m = multiplet. The exact spectrometer frequency, the temperature and the solvent of the measurements are reported on each spectrum in the appendix.

Reversed-phase HPLC-ESI-HR-MS or HPLC-APCI-HR-MS analysis was performed on a Thermo Finnigan LTQ FT-ICR equipped with a Dionex Ultimate 3000 separation module eluting on a Waters XBridge C18 column (3.5  $\mu$ m, 4.6 x 100 mm, flow rate = 1.1 ml/min). The column temperature was maintained at 30 °C. The mobile phase for elution consisted of a gradient mixture of 0.1% (v/v) formic acid in water (buffer A, HPLC-MS grade) and 0.1% (v/v) formic acid in acetonitrile:water 90:10 (buffer B, HPLC-MS grade).

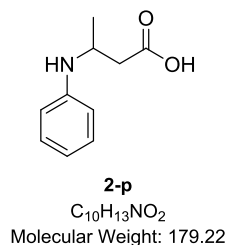
Synthesized small molecule probes used in biological experiments were dissolved in anhydrous DMSO to get a final stock concentration of 100 mM. In dilution series with a dilution factor of 3 the following working stock concentrations were obtained: 30 mM, 10 mM, 3 mM, 1 mM, 0.3 mM, 0.1 mM, 0.03 mM and 0.01 mM.



## 1.2 SYNTHETIC PROCEDURES

### 1.2.1 KINETIK PRODUCTS

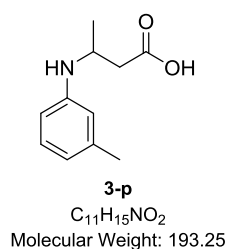
#### 3-(Phenylamino)butanoic acid (**2-p**)



To a solution of aniline (**2**) (93.1 mg, 1.00 mmol, 1.00 eq) in a 9:1-mixture of  $H_2O$  and MeCN (30 mL) was added *beta*-butyrolactone (BBL) (81.5  $\mu$ L, 1.0 mmol, 1.00 eq). The reaction mixture was stirred until HPLC-ESI-HRMS analysis showed no further increase in product formation. The solvent was evaporated under reduced pressure. Purification by reversed-phase HPLC yielded **2-p** (116 mg, 0.65 mmol, 65%) as pale yellow oil. The obtained NMR data is in accordance with previously published results.<sup>[178]</sup>

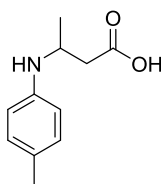
**$^1H$  NMR** (360 MHz, DMSO):  $\delta$  [ppm] = 7.26 - 7.21 (m, 2 H), 6.89 - 6.83 (m, 3 H), 3.88 - 3.75 (m, 1 H), 2.58 (dd,  $J$  = 15.6, 5.4 Hz, 1 H), 2.35 (dd,  $J$  = 15.6, 7.7 Hz, 1 H), 1.19 (d,  $J$  = 6.4 Hz, 3 H);  **$^{13}C$  NMR** (90.6 MHz, DMSO):  $\delta$  [ppm] = 172.3, 143.2, 129.4, 120.5, 116.4, 48.4, 39.7, 18.9; **HRMS (ESI)**: calcd. for  $C_{10}H_{14}NO_2$   $[M+H]^+$ : 180.1019; found: 180.1018.

#### 3-(*m*-Tolylamino)butanoic acid (**3-p**)



To a solution of *m*-toluidine (**3**) (107 mg, 1.00 mmol, 1.00 eq) in a 9:1-mixture of  $H_2O$  and MeCN (30 mL) was added BBL (81.5  $\mu$ L, 1.00 mmol, 1.00 eq). The reaction mixture was stirred until HPLC-ESI-HRMS analysis showed no further increase in product formation. The solvent was evaporated under reduced pressure. Purification by reversed-phase HPLC yielded **3-p** (135 mg, 0.70 mmol, 70%) as pale yellow solid.

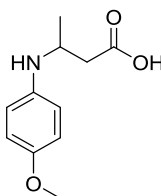
**$^1H$  NMR** (500 MHz, DMSO):  $\delta$  [ppm] = 7.16 (t,  $J$  = 7.7 Hz, 1 H), 6.86 - 6.63 (m, 3 H), 3.86 - 3.76 (m, 1 H), 2.59 (dd,  $J$  = 15.7, 5.3 Hz, 1 H), 2.37 (dd,  $J$  = 15.7, 7.8 Hz, 1 H), 2.26 (s, 3 H), 1.19 (d,  $J$  = 6.4 Hz, 3 H);  **$^{13}C$  NMR** (90.6 MHz, DMSO):  $\delta$  [ppm] = 172.1, 142.1, 138.7, 129.2, 122.2, 117.7, 114.4, 49.0, 39.4, 21.1, 18.6; **HRMS (ESI)**: calcd. for  $C_{11}H_{16}NO_2$   $[M+H]^+$ : 194.1176; found: 194.1175.

**3-(*p*-Tolylamino)butanoic acid (4-p)**

**4-p**  
 $C_{11}H_{15}NO_2$   
Molecular Weight: 193.25

To a solution of *p*-toluidine (**4**) (107 mg, 1.00 mmol, 1.00 eq) in a 9:1-mixture of  $H_2O$  and MeCN (30 mL) was added BBL (81.5  $\mu$ L, 1.00 mmol, 1.00 eq). The reaction mixture was stirred until HPLC-ESI-HRMS analysis showed no further increase in product formation. The solvent was evaporated under reduced pressure and purification by reversed-phase HPLC yielded **4-p** (153 mg, 0.79 mmol, 79%) as orange oil.

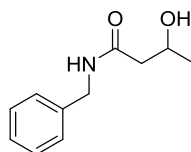
$^1H$  NMR (500 MHz, DMSO):  $\delta$  [ppm] = 7.18 (d,  $J$  = 8.1 Hz, 2 H), 7.05 (d,  $J$  = 8.1 Hz, 2 H), 3.92–3.64 (m, 1 H), 2.63 (dd,  $J$  = 16.0, 5.1 Hz, 1 H), 2.43 (dd,  $J$  = 16.0, 8.0 Hz, 1 H), 2.26 (s, 3 H), 1.21 (d,  $J$  = 6.5 Hz, 3 H);  $^{13}C$  NMR (90.6 MHz, DMSO):  $\delta$  [ppm] = 172.0, 136.6, 134.3, 130.3, 120.1, 51.7, 38.5, 20.6, 17.9; HRMS (ESI): calcd. for  $C_{11}H_{16}NO_2$   $[M+H]^+$ : 194.1176; found: 194.1175.

**3-((4-Methoxyphenyl)amino)butanoic acid (5-p)**

**5-p**  
 $C_{11}H_{15}NO_3$   
Molecular Weight: 209.25

To a solution of 4-methoxyaniline (**5**) (123 mg, 1.00 mmol, 1.00 eq) in a 9:1-mixture of  $H_2O$  and MeCN (30 mL) was added BBL (81.5  $\mu$ L, 1.00 mmol, 1.00 eq). The reaction mixture was stirred until HPLC-ESI-HRMS analysis showed no further increase in product formation. The solvent was evaporated under reduced pressure. Purification by reversed-phase HPLC yielded **5-p** (123 mg, 0.59 mmol, 59%) as colorless oil.

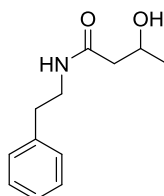
$^1H$  NMR (360 MHz, DMSO):  $\delta$  [ppm] = 7.26 (d,  $J$  = 8.8 Hz, 2 H), 7.01 (d,  $J$  = 8.9 Hz, 2 H), 3.84 - 3.77 (m,  $J$  = 13.1, 6.4 Hz, 1 H), 3.75 (s, 3 H), 2.66 (dd,  $J$  = 16.3, 4.9 Hz, 1H), 2.50 - 2.42 (m, 1 H), 1.23 (d,  $J$  = 6.5 Hz, 3 H);  $^{13}C$  NMR (90.6 MHz, DMSO):  $\delta$  [ppm] = 171.5, 157.8, 129.9, 122.9, 115.1, 55.5, 53.1, 37.8, 17.2; HRMS (ESI): calcd. for  $C_{11}H_{16}NO_3$   $[M+H]^+$ : 210.1125; found: 210.1124.

***N*-Benzyl-3-hydroxybutanamide (6-p)**

**6-p**  
 $C_{11}H_{15}NO_2$   
Molecular Weight: 193.25

To a solution of benzylamine (**6**) (109  $\mu$ L, 1.00 mmol, 1.00 eq) in a 9:1-mixture of  $H_2O$  and MeCN (30 mL) was added BBL (81.5  $\mu$ L, 1.00 mmol, 1.00). The reaction mixture was stirred until HPLC-ESI-HRMS analysis showed no further increase in product formation. The solvent was evaporated under reduced pressure. Purification by reversed-phase HPLC yielded **6-p** (114 mg, 0.59 mmol, 59%) as white powder. The obtained NMR data is in accordance with previously published results.<sup>[179]</sup>

**$^1H$  NMR** (500 MHz, DMSO):  $\delta$  [ppm] = 8.32 (t,  $J$  = 5.6 Hz, 1 H), 7.35 - 7.21 (m, 5 H), 4.70 (d,  $J$  = 2.3 Hz, 1 H), 4.29 (d,  $J$  = 6.0 Hz, 2 H), 4.04 (d,  $J$  = 5.4 Hz, 1 H), 2.31 (dd,  $J$  = 13.8, 7.3 Hz, 1 H), 2.21 (dd,  $J$  = 13.8, 5.8 Hz, 1 H), 1.10 (d,  $J$  = 6.2 Hz, 3 H);  **$^{13}C$  NMR** (90.6 MHz, DMSO):  $\delta$  [ppm] = 170.7, 139.6, 128.2, 127.2, 126.7, 63.8, 45.3, 41.9, 39.5, 23.4; **HRMS (ESI)**: calcd. for  $C_{11}H_{16}NO_2$   $[M+H]^+$  : 194.1176; found: 194.1175.

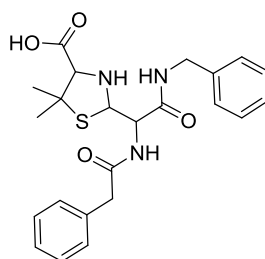
**3-Hydroxy-*N*-phenethylbutanamide (7-p)**

**7-p**  
 $C_{12}H_{17}NO_2$   
Molecular Weight: 207.27

To a solution of 2-phenylethylamine (**7**) (127  $\mu$ L, 122 mg, 1.00 mmol, 1.00 eq) in a 9:1-mixture of  $H_2O$  and MeCN (30 mL) was added BBL (81.5  $\mu$ L, 1.00 mmol, 1.00 eq). The reaction mixture was stirred until HPLC-ESI-HRMS analysis showed no further increase in product formation. The solvent was evaporated under reduced pressure and purification by reversed-phase HPLC yielded **7-p** (120 mg, 0.58 mmol, 58%) as white powder.<sup>[180]</sup>

**$^1H$  NMR** (500 MHz, DMSO):  $\delta$  [ppm] = 7.89 (t,  $J$  = 4.9 Hz, 1H), 7.43 - 7.08 (m, 5 H), 4.89 (s, 1 H), 4.11 - 3.84 (m, 1 H), 3.37 - 3.12 (m, 2 H), 2.71 (t,  $J$  = 7.4 Hz, 2 H), 2.21 (dd,  $J$  = 13.8, 7.1 Hz, 1 H), 2.10 (dd,  $J$  = 13.8, 5.9 Hz, 1 H), 1.05 (d,  $J$  = 6.2 Hz, 3 H);  **$^{13}C$  NMR** (90.6 MHz, DMSO):  $\delta$  [ppm] = 170.6, 139.5, 128.6, 128.3, 126.0, 63.8, 45.3, 40.1, 35.2, 23.3; **HRMS (ESI)**: calcd. for  $C_{12}H_{18}NO_2$   $[M+H]^+$  : 208.1332; found: 208.1330.

2-(2-(Benzylamino)-2-oxo-1-(2-phenylacetamido)ethyl)-5,5-dimethylthiazolidine-4-carboxylic acid  
(10b-p)

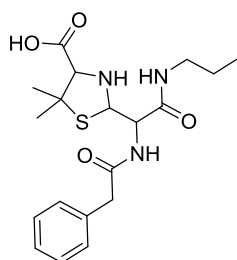


**10b-p**  
 $C_{23}H_{27}N_3O_4S$   
Molecular Weight: 441.55

To a solution of benzylamine (**6**) (31.5  $\mu$ L, 30.3 mg, 0.25 mmol, 1.00 eq) in a 9:1-mixture of  $H_2O$  and MeCN (5 mL) was added sodium benzylpenicillin (89 mg, 0.25 mmol, 1.00 eq). The reaction mixture was stirred until HPLC-ESI-HRMS analysis showed no further increase in product formation. The solvent was evaporated under reduced pressure and purification by reversed-phase HPLC yielded **10b-p** (58.5 mg, 0.13 mmol, 53%) as white powder (isolated as a mixture of diastereomers 45:55 dr as determined by NMR). The obtained NMR data is in accordance with previously published results.<sup>[181]</sup>

$^1H$  NMR (500 MHz, DMSO):  $\delta$  [ppm] = 8.70 (t,  $J$  = 5.7 Hz, 1 H), 8.55 (t,  $J$  = 5.8 Hz, 1 H), 8.45 (d,  $J$  = 8.6 Hz, 1 H), 8.34 (d,  $J$  = 9.2 Hz, 1 H), 7.34 - 7.17 (m, 20 H), 4.89 (dd,  $J$  = 12.3, 7.0 Hz, 2 H), 4.81 - 4.75 (m, 1 H), 4.51 (t,  $J$  = 8.5 Hz, 1 H), 4.38 - 4.15 (m, 6 H), 3.64 - 3.56 (m, 2 H), 3.56 - 3.43 (m, 4 H), 1.56 (s, 3 H), 1.52 (s, 3 H), 1.19 (s, 3 H), 1.14 (s, 3 H);  $^{13}C$  NMR (126 MHz, DMSO):  $\delta$  [ppm] = 170.5, 170.4, 170.3, 169.9, 169.6, 169.1, 139.1, 138.8, 136.6, 136.2, 129.14, 129.12, 128.24, 128.22, 128.2, 128.19, 128.1, 127.2, 127.1, 126.8, 126.7, 126.4, 126.2, 73.5, 72.2, 67.7, 66.9, 58.4, 57.2, 54.8, 42.2, 42.04, 42.01, 41.9, 28.4, 27.9, 27.7, 27.1; HRMS (ESI): calcd. for  $C_{22}H_{28}N_3O_4S$   $[M+H]^+$  : 442.1795; found: 442.1798.

5,5-Dimethyl-2-(2-oxo-1-(2-phenylacetamido)-2-(propylamino)ethyl)thiazolidine-4-carboxylic acid  
(10a-p)



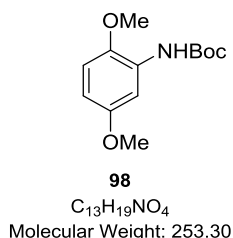
**10a-p**  
 $C_{19}H_{27}N_3O_4S$   
Molecular Weight: 393.50

To a solution of propylamine (**8**) (20.5  $\mu$ L, 30.3 mg, 0.25 mmol, 1.00 eq) in a 9:1-mixture of H<sub>2</sub>O and MeCN (5 mL) was added sodium benzylpenicillin (89 mg, 0.25 mmol, 1.00 eq). The reaction mixture was stirred until HPLC-ESI-HRMS analysis showed no further increase in product formation. The solvent was evaporated under reduced pressure and purification by reversed-phase HPLC yielded **10a-p** (66.8 mg, 0.17 mmol, 66%) as white powder (isolated as a mixture of diastereomers 45:55 dr as determined by NMR).

**<sup>1</sup>H NMR** (360 MHz, DMSO):  $\delta$  [ppm] = 8.38 (d,  $J$  = 8.7 Hz, 1 H), 8.28 (d,  $J$  = 9.1 Hz, 1 H), 8.17 (t,  $J$  = 5.5 Hz, 1 H), 8.02 (t,  $J$  = 5.5 Hz, 1 H), 7.33 - 7.15 (m, 10 H), 4.86 - 4.83 (m, 2 H), 4.71 - 4.67 (m, 1 H), 4.45 - 4.40 (t,  $J$  = 8.5 Hz, 1 H), 3.62 (d,  $J$  = 5.0 Hz, 2 H), 3.51 (dd,  $J$  = 9.7, 2.8 Hz, 4 H), 3.04–2.96 (m, 4 H), 1.55 (s, 3 H), 1.51 (s, 3 H), 1.44 - 1.34 (m, 4 H), 1.19 (s, 3 H), 1.13 (s, 3 H), 0.83 (q,  $J$  = 7.7 Hz, 6 H); **<sup>13</sup>C NMR** (90.6 MHz, DMSO):  $\delta$  [ppm] = 170.4, 170.2, 170.1, 169.6, 169.1, 168.6, 136.4, 136.0, 129.1, 129.0, 128.1, 128.0, 126.3, 126.1, 73.2, 72.0, 67.5, 66.7, 57.9, 57.0, 56.8, 56.7, 54.8, 54.2, 42.0, 41.8, 28.3, 27.7, 27.5, 26.9, 22.1, 22.0, 11.3; **HRMS (ESI)**: calcd. for C<sub>19</sub>H<sub>28</sub>N<sub>3</sub>O<sub>4</sub>S [M+H]<sup>+</sup>: 394.1795; found: 394.1796.

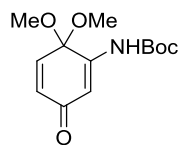
#### 1.2.2 EPOXY-CYCLOHEXENONES AND PRECURSORS

##### *N*-tert-Butoxycarbonyl-2,5-dimethoxyaniline (**98**)<sup>[121,182]</sup>



To a solution of 2,5-dimethoxyaniline (**50**) (5.01 g, 32.6 mmol, 1.00 eq) in dry THF (40 mL) under an inert atmosphere of nitrogen was given di-*tert*-butyl dicarbonate (8.55 g, 39.2 mmol, 1.20 eq) and the reaction mixture was heated under reflux for 16 h. The solvent was removed under reduced pressure and the residue was purified by flash column chromatography on silica gel (hexanes:EtOAc 4:1) to yield product **98** (8.20 g, 32.4 mmol, 99%) as colorless oil.

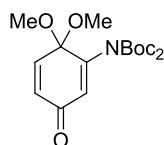
$R_f$  = 0.58 (hexanes:EtOAc 4:1); **<sup>1</sup>H NMR** (360.13 MHz, CDCl<sub>3</sub>):  $\delta$  [ppm] = 7.79 (s, 1H), 7.10 (s, 1H), 6.75 (d,  $J$  = 8.9 Hz, 1H), 6.49 (dd,  $J$  = 8.8, 3.0 Hz, 1H), 3.81 (s, 3H), 3.78 (s, 3H), 1.53 (s, 9H); **<sup>13</sup>C NMR** (90.56 MHz, CDCl<sub>3</sub>):  $\delta$  [ppm] = 154.26, 152.73, 141.85, 129.03, 110.96, 107.24, 104.48, 80.47, 56.34, 55.90, 28.50; **HRMS (ESI)**: calc. for C<sub>13</sub>H<sub>20</sub>NO<sub>4</sub> [M]<sup>+</sup>: 254.1387, found: 254.1387, diff: 0.01 ppm.

**3-*tert*-Butoxycarbonylamino-4,4-dimethoxycyclohexa-2,5-dien-1-one (54)**<sup>[111,182]</sup>
**54**C<sub>13</sub>H<sub>19</sub>NO<sub>5</sub>

Molecular Weight: 269.30

To a solution of **98** (2.15 g, 8.50 mmol, 1.00 eq) in anhydrous MeOH (30 mL) at 0 °C under nitrogen atmosphere was added portion wise PhI(OPiv)<sub>2</sub> (5.00 g, 10.2 mmol, 1.20 eq) and stirred for 16 h at 0 °C. The reaction mixture was diluted with EtOAc (17 mL) and saturated citric acid solution (7 mL). After stirring for 30 min at room temperature, the mixture was extracted with EtOAc (3 x 20 mL) and the combined organic extracts were washed with saturated NaHCO<sub>3</sub> aqueous solution (40 mL), water (40 mL) and brine (20 mL). The combined organic extracts were dried over Na<sub>2</sub>SO<sub>4</sub>, concentrated under reduced pressure and purified by flash column chromatography (hexanes:EtOAc 2:1) to yield product **54** (1.93 g, 7.17 mmol, 84%) as pale yellow needles.

*R*<sub>f</sub> = 0.37 (hexanes:EtOAc 2:1); <sup>1</sup>H NMR (250.13 MHz, CDCl<sub>3</sub>): δ [ppm] = 7.01 (d, *J* = 2.0 Hz, 1H), 6.84 (s, 1H), 6.52 (d, *J* = 10.3 Hz, 1H), 6.41 (dd, *J* = 10.3, 2.0 Hz, 1H), 3.27 (s, 6H), 1.51 (s, 9H); <sup>13</sup>C NMR (90.56 MHz, CDCl<sub>3</sub>): δ [ppm] = 185.59, 151.62, 148.40, 138.29, 133.54, 111.48, 94.50, 82.45, 51.65, 28.20; HRMS (ESI): calc. for C<sub>13</sub>H<sub>20</sub>NO<sub>5</sub> [M+H]<sup>+</sup>: 270.1336, found: 270.1336, diff: -0.02 ppm.

**3-*N,N*-Bis-(*tert*-butoxycarbonyl)amino-4,4-dimethoxycyclohexa-2,5-dien-1-one (99)**<sup>[182]</sup>
**99**C<sub>18</sub>H<sub>27</sub>NO<sub>7</sub>

Molecular Weight: 369.41

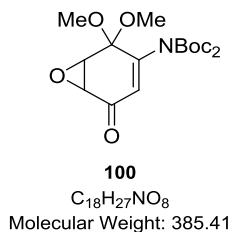
To a solution of **54** (8.40 g, 31.2 mmol, 2.00 eq) in dry THF (100 mL) were added DMAP (1.90 g, 15.6 mmol, 1.00 eq) and di-*tert*-butyl dicarbonate (13.6 g, 62.4 mmol, 4.00 eq) at room temperature. The reaction mixture was then heated to 80 °C and stirred for 16 h under nitrogen atmosphere. After addition of water (50 mL), the layers were separated and the aqueous layer was extracted with EtOAc (3 x 40 mL). The combined organic extracts were washed with brine (100 mL), dried over Na<sub>2</sub>SO<sub>4</sub>, concentrated under reduced pressure and purified by flash column chromatography (hexanes:EtOAc 2:1) to yield product **99** (7.80 g, 21.1 mmol, 68%) as white solid.

*R*<sub>f</sub> = 0.50 (hexanes:EtOAc 2:1); <sup>1</sup>H NMR (360.13 MHz, CDCl<sub>3</sub>): δ [ppm] = 6.81 (d, *J* = 10.4 Hz, 1H), 6.38 (dd, *J* = 10.4, 2.0 Hz, 1H), 6.30 (d, *J* = 2.0 Hz, 1H), 3.30 (s, 6H), 1.49 (s, 18H); <sup>13</sup>C NMR (90.56

MHz, CDCl<sub>3</sub>):  $\delta$  [ppm] = 185.78, 150.87, 149.51, 142.14, 130.87, 130.62, 94.86, 83.39, 51.36, 27.84;

HRMS (ESI): calc. for C<sub>18</sub>H<sub>28</sub>NO<sub>7</sub> [M+H]<sup>+</sup>: 370.1861, found: 370.1860, diff: -0.20 ppm.

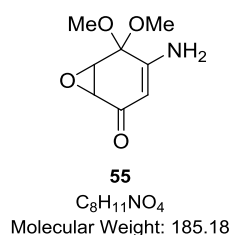
**5-*N,N*-Bis-(*tert*-butoxycarbonyl)amino-2,3-epoxy-4,4-dimethoxycyclohexa-6-en-1-one (100)**<sup>[118,121]</sup>



To a solution of **99** (1.80 g, 4.87 mmol, 1.00 eq) in THF (30 mL) were alternately added aqueous H<sub>2</sub>O<sub>2</sub> (30%, 9.70 mL) and aqueous NaOH (1.00 M, 19.5 mL) to keep a constant pH between 8 and 9. The reaction mixture was stirred at room temperature for 2 h and then diluted with EtOAc (10 mL). The phases were separated and the aqueous layer was extracted with EtOAc (3 x 10 mL). The combined organic extracts were washed with water (20 mL) and brine (20 mL), dried over Na<sub>2</sub>SO<sub>4</sub> and concentrated under reduced pressure. Purification was performed *via* flash column chromatography (hexanes:EtOAc 2:1) to yield **100** (1.01 g, 2.60 mmol, 53%) as pale yellow oil.

R<sub>f</sub> = 0.38 (hexanes:EtOAc 2:1); <sup>1</sup>H NMR (360.13 MHz, CDCl<sub>3</sub>):  $\delta$  [ppm] = 5.93 (d, *J* = 2.0 Hz, 1H), 3.82 (d, *J* = 4.1 Hz, 1H), 3.56 - 3.54 (m, 4H), 3.36 (s, 3H), 1.48 (s, 18H); HRMS (ESI): calc. for C<sub>18</sub>H<sub>28</sub>NO<sub>8</sub> [M+H]<sup>+</sup>: 386.1809, found: 386.1808, diff: -0.45 ppm.

**3-Amino-4,4-dimethoxy-5,6-epoxycyclohex-2-en-1-one (55)**<sup>[111,122,124]</sup>

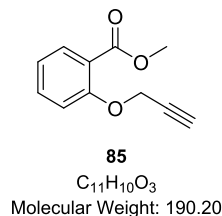


To a solution of **100** (4.71 g, 12.3 mmol, 1.00 eq) and anisole (2.67 mL, 24.5 mmol, 2.00 eq) in anhydrous DCM (140 mL) at room temperature was added TFA (34.6 mL, 453 mmol, 37.0 eq, TFA:DCM 1:4) dropwise over a period of 30 min. Stirring was continued for 2 h after which all volatile materials were evaporated under reduced pressure and the residue was purified by flash column chromatography on silica gel (hexanes:EtOAc 1:2 → EtOAc) to yield product **55** (2.17 g, 11.7 mmol, 96%) as pale green solid.

R<sub>f</sub> = 0.31 (EtOAc); <sup>1</sup>H NMR (360.13 MHz, CDCl<sub>3</sub>):  $\delta$  [ppm] = 5.14 (d, *J* = 2.1 Hz, 1H), 4.99 (s, 2H), 3.77 (d, *J* = 4.1 Hz, 1H), 3.62 (s, 3H), 3.44 (dd, *J* = 4.1, 2.1 Hz, 1H), 3.35 (s, 3H); <sup>13</sup>C NMR (90.56 MHz,

$\text{CDCl}_3$ ):  $\delta$  [ppm] = 188.83, 159.45, 95.76, 93.32, 52.64, 51.95, 51.07, 50.06; **HRMS (ESI)**: calc. for  $\text{C}_8\text{H}_{12}\text{NO}_4$   $[\text{M}+\text{H}]^+$ : 186.0761, found: 186.0760, diff: -0.31 ppm.

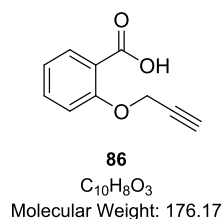
**Methyl-2-prop-2-ynylbenzoate (85)**<sup>[183]</sup>



To a solution of methyl salicylate (**84**) (1.52 g, 10.0 mmol, 1.00 eq) in acetone (25 mL) were added  $\text{K}_2\text{CO}_3$  (1.38 g, 10.0 mmol, 1.00 eq) followed by propargyl bromide (80% in toluene, 2.00 mL, 18.5 mmol, 1.85 eq). The reaction mixture was heated under reflux for 24 h under nitrogen atmosphere. After the addition of chilled water (10 mL) the layers were separated and the aqueous layer was extracted with  $\text{Et}_2\text{O}$  (3 x 10 mL). The combined organic extracts were washed with brine (80 mL), dried over  $\text{Na}_2\text{SO}_4$  and concentrated under reduced pressure. The crude product was purified by flash column chromatography (hexanes:EtOAc 4:1) giving compound **85** (1.83 g, 9.60 mmol, 96%) as pale yellow solid.

$R_f$  = 0.39 (hexanes:EtOAc 4:1);  $^1\text{H NMR}$  (360.13 MHz,  $\text{CDCl}_3$ ):  $\delta$  [ppm] = 7.81 (dd,  $J$  = 7.7, 1.8 Hz, 1H), 7.51 - 7.44 (m, 1H), 7.14 (d,  $J$  = 8.4 Hz, 1H), 7.04 (td,  $J$  = 7.6, 0.9 Hz, 1H), 4.79 (d,  $J$  = 2.4 Hz, 2H), 3.89 (s, 3H), 2.52 (t,  $J$  = 2.4 Hz, 1H);  $^{13}\text{C NMR}$  (90.56 MHz,  $\text{CDCl}_3$ ):  $\delta$  [ppm] = 166.02, 155.95, 133.23, 130.74, 120.96, 120.79, 114.19, 78.93, 78.64, 56.11, 51.97; **HRMS (ESI)**: calc. for  $\text{C}_{11}\text{H}_{11}\text{O}_3$   $[\text{M}+\text{H}]^+$ : 191.0703, found: 191.0703, diff: -0.01 ppm.

**2-Prop-2-ynyloxybenzoic acid (86)**<sup>[183]</sup>

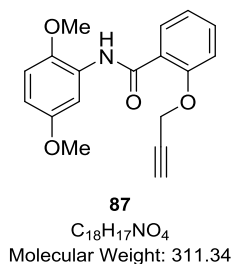


To a solution of **85** (1.50 g, 7.89 mmol, 1.00 eq) in EtOH (60 mL) was added a saturated aqueous solution of KOH (2.5 mL) and the reaction mixture was stirred for 4 h at room temperature. After addition of water (200 mL) and EtOAc (200 mL) the solution was acidified by adding aqueous 1 M HCl (20 mL) and the layers were separated. The aqueous layer was extracted with EtOAc (4 x 20 mL) and the combined organic extracts were washed with brine (100 mL), dried over  $\text{Na}_2\text{SO}_4$  and concentrated under reduced pressure giving compound **86** (1.31 g, 7.44 mmol, 94%) as pale yellow solid without further purification.



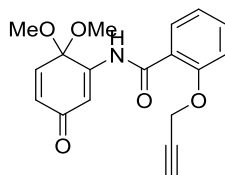
**<sup>1</sup>H NMR** (360.13 MHz, CDCl<sub>3</sub>): δ [ppm] = 12.72 (s, 1H), 7.65 (dd, *J* = 7.7, 1.7 Hz, 1H), 7.50 (ddd, *J* = 8.4, 7.4, 1.8 Hz, 1H), 7.18 (dd, *J* = 8.4, 0.6 Hz, 1H), 7.04 (td, *J* = 7.5, 1.0 Hz, 1H), 4.87 (d, *J* = 2.4 Hz, 2H), 3.59 (t, *J* = 2.4 Hz, 1H); **<sup>13</sup>C NMR** (90.56 MHz, CDCl<sub>3</sub>): δ [ppm] = 167.24, 155.92, 132.74, 130.74, 122.11, 120.91, 114.09, 79.11, 78.58, 56.08; **HRMS (ESI)**: calc. for C<sub>10</sub>H<sub>9</sub>O<sub>3</sub> [M+H]<sup>+</sup>: 177.0546, found: 177.0546, diff: -0.28 ppm.

***N*-(2,5-Dimethoxyphenyl)-2-(prop-2-yn-1-yloxy)benzamide (87)**<sup>[183]</sup>



**86** (10.0 g, 56.7 mmol, 1.20 eq) was added to a solution of thionyl chloride (50 mL) and *N,N*-dimethylformamide (cat.) and the reaction mixture was heated under reflux for 4 h under an inert atmosphere of nitrogen at 75°C. The solvent was evaporated and the residue redissolved in toluene (20 mL). After removing the solvent under reduced pressure the corresponding acetylenic acid chloride was redissolved in anhydrous THF (200 mL) and 2,5-dimethoxyaniline (**50**) (7.24 g, 47.3 mmol, 1.00 eq) was added. After cooling the reaction mixture to 0 °C, pyridine (7.60 mL, 94.5 mmol, 2.00 eq) was added slowly and the mixture was stirred for 15 min at 0 °C followed by 6 h at room temperature. The reaction was quenched by adding aqueous 1 M HCl (50 mL) and extracted with EtOAc (4 x 30 mL). The combined organic extracts were washed with brine (100 mL), dried over Na<sub>2</sub>SO<sub>4</sub> and concentrated under reduced pressure. The crude product was purified by flash column chromatography (hexanes:EtOAc 2:1) giving compound **87** (13.7 g, 44.0 mmol, 93% over two steps) as white solid.

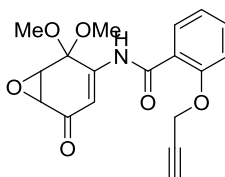
**R<sub>f</sub>** = 0.57 (hexanes:EtOAc 2:1); **<sup>1</sup>H NMR** (360.13 MHz, CDCl<sub>3</sub>): δ [ppm] = 8.38 (d, *J* = 3.0 Hz, 1H), 8.29 (dd, *J* = 8.0, 1.7 Hz, 1H), 7.54 - 7.46 (m, 1H), 7.24 - 7.13 (m, 2H), 6.84 (d, *J* = 8.9 Hz, 1H), 6.60 (dd, *J* = 8.9, 3.1 Hz, 1H), 4.94 (d, *J* = 2.4 Hz, 2H), 3.91 (s, 3H), 3.83 (s, 3H), 2.59 (t, *J* = 2.4 Hz, 1H); **<sup>13</sup>C NMR** (90.56 MHz, CDCl<sub>3</sub>): δ [ppm] = 162.91, 155.35, 154.14, 142.81, 133.02, 132.62, 129.30, 123.20, 122.53, 113.32, 111.13, 108.89, 106.43, 77.54, 76.85, 56.94, 56.72, 55.95; **HRMS (ESI)**: calc. for C<sub>18</sub>H<sub>18</sub>NO<sub>4</sub> [M+H]<sup>+</sup>: 312.1230, found: 312.1231, diff: 0.06 ppm.

***N*-(6,6-dimethoxy-3-oxocyclohexa-1,4-dien-1-yl)-2-(prop-2-yn-1-yloxy)benzamide (**88**)**<sup>[182]</sup>

**88**  
 $C_{18}H_{17}NO_5$   
 Molecular Weight: 327.34

To a solution of **87** (2.00 g, 6.42 mmol, 1.00 eq) in anhydrous MeOH (70 mL) at 0 °C under nitrogen atmosphere was added portion wise  $PhI(OAc)_2$  (3.92 g, 9.64 mmol, 1.50 eq). The mixture was allowed to warm to room temperature, further stirred for 4 h and then diluted with EtOAc (50 mL) and saturated citric acid solution (25 mL). After stirring for 30 min at room temperature, the mixture was extracted with EtOAc (3 x 50 mL) and the combined organic extracts were washed with saturated  $NaHCO_3$  aqueous solution (50 mL), water (50 mL) and brine (80 mL). The combined organic extracts were dried over  $Na_2SO_4$ , concentrated under reduced pressure and purified by flash column chromatography (hexanes:EtOAc 2:1) to yield product **88** (1.24 g, 3.80 mmol, 59%) as pale yellow needles.

$R_f$  = 0.15 (hexanes:EtOAc 2:1);  $^1H$  NMR (360.13 MHz,  $CDCl_3$ ):  $\delta$  [ppm] = 10.07 (s, 1H), 8.20 (dd,  $J$  = 8.1, 1.8 Hz, 1H), 7.59 (d,  $J$  = 2.0 Hz, 1H), 7.57 - 7.49 (m, 1H), 7.24 - 7.14 (m, 2H), 6.58 (d,  $J$  = 10.3 Hz, 1H), 6.47 (dd,  $J$  = 10.3, 2.0 Hz, 1H), 4.94 (d,  $J$  = 2.4 Hz, 2H), 3.31 (s, 6H), 2.58 (t,  $J$  = 2.4 Hz, 1H);  $^{13}C$  NMR (90.56 MHz,  $CDCl_3$ ):  $\delta$  [ppm] = 186.38, 164.40, 155.30, 148.08, 138.87, 134.06, 133.41, 132.66, 122.65, 121.93, 114.24, 113.63, 94.59, 77.22, 77.01, 56.97, 51.60; HRMS (ESI): calc. for  $C_{18}H_{18}NO_5$   $[M+H]^+$ : 328.1180, found: 328.1180, diff: -0.17 ppm.

***N*-(2,2-Dimethoxy-5-oxo-7-oxabicyclo[4.1.0]hept-3-en-3-yl)-2-(prop-2-yn-1-yloxy)benzamide (**89**)**<sup>[124]</sup>

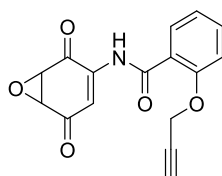
**89**  
 $C_{18}H_{17}NO_6$   
 Molecular Weight: 343.33

To a solution of **86** (0.31 g, 1.77 mmol, 1.10 eq) in anhydrous DCM (10 mL) at 0 °C containing 1 drop of *N,N*-dimethylformamide (cat.) was slowly added oxalyl chloride (168  $\mu$ L, 1.98 mmol, 1.22 eq). The reaction mixture was stirred at 0 °C for 1 h after which the solvent was removed under reduced pressure and the corresponding acetylenic acid chloride was redissolved in anhydrous THF (5 mL) at 0 °C. A solution of lithium *tert*-butoxide (1 M in THF, 1.80 mL, 1.81 mmol) was added dropwise over 15 min to a stirred solution of **55** (0.30 g, 1.62 mmol, 1.00 eq) in dry THF at 0 °C.

After stirring the reaction mixture at 0 °C for 30 min, the solution of acetylenic acid chloride in THF was added dropwise over 1 h. The mixture was then allowed to warm to room temperature and stirred for further 5 h until HPLC-MS measurements showed complete conversion of the starting material. The reaction was quenched by adding aqueous NH<sub>4</sub>Cl (5 mL) and water (5 mL) and extracted with EtOAc (3 x 30 mL). The combined organic extracts were washed with brine (50 mL), dried over Na<sub>2</sub>SO<sub>4</sub> and concentrated under reduced pressure. The crude product was purified by preparative reversed-phase HPLC (C18 5.0 µm, 30 x 150 mm column, gradient 2% B → 98% B over 17 min, *t<sub>R</sub>* = 7.4 - 8.4 min) giving compound **89** (0.33 g, 0.96 mmol, 59% over two steps) as yellow powder.

**<sup>1</sup>H NMR** (500.13 MHz, CDCl<sub>3</sub>): δ [ppm] = 10.32 (s, 1H), 8.19 (dd, *J* = 7.9, 1.8 Hz, 1H), 7.54 (ddd, *J* = 8.4, 7.4, 1.8 Hz, 1H), 7.36 (d, *J* = 2.1 Hz, 1H), 7.24 - 7.08 (m, 2H), 4.93 (dd, *J* = 5.7, 2.4 Hz, 2H), 3.86 (d, *J* = 4.2 Hz, 1H), 3.72 (s, 3H), 3.54 (dd, *J* = 4.2, 2.1 Hz, 1H), 3.36 (s, 3H), 2.61 (t, *J* = 2.4 Hz, 1H); **<sup>13</sup>C NMR** (75,48 MHz, CDCl<sub>3</sub>): δ [ppm] = 193.37, 163.65, 155.06, 146.86, 134.59, 131.75, 122.31, 120.75, 114.34, 107.44, 95.21, 79.55, 78.01, 56.91, 51.41, 51.06, 50.80, 50.59; **HRMS (ESI)**: calc. for C<sub>18</sub>H<sub>18</sub>NO<sub>6</sub> [M+H]<sup>+</sup>: 344.1129, found: 344.1128, diff: -0.22 ppm.

***N*-(2,5-Dioxo-7-oxabicyclo[4.1.0]hept-3-en-3-yl)-2-(prop-2-yn-1-yloxy)benzamide (FM141)<sup>[182]</sup>**

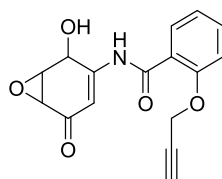


**FM141**  
C<sub>16</sub>H<sub>11</sub>NO<sub>5</sub>  
Molecular Weight: 297.27

To a solution of **89** (0.10 g, 0.29 mmol, 1.00 eq) in anhydrous DCM (15 mL) at -20 °C was added BF<sub>3</sub>·OEt<sub>2</sub> (92.0 µL, 0.73 mmol, 2.50 eq). The mixture was allowed to warm to room temperature and further stirred for 14 h. The reaction was quenched by adding water (5 mL) and extracted with CHCl<sub>3</sub> (3 x 10 mL). The combined organic extracts were washed with brine (20 mL), dried over Na<sub>2</sub>SO<sub>4</sub> and concentrated under reduced pressure. The crude product was purified by flash column chromatography (hexanes:EtOAc 2:1) giving **FM141** (80.0 mg, 0.27 mmol, 93%) as yellow solid.

**R<sub>f</sub>** = 0.39 (hexanes:EtOAc 2:1); **<sup>1</sup>H NMR** (360.13 MHz, CDCl<sub>3</sub>): δ [ppm] = 10.59 (s, 1H), 8.20 (dd, *J* = 8.1, 1.6 Hz, 1H), 7.74 (d, *J* = 2.2 Hz, 1H), 7.62 - 7.44 (m, 1H), 7.23 - 7.04 (m, 2H), 5.01 (d, *J* = 2.2 Hz, 2H), 3.94 (d, *J* = 3.7 Hz, 1H), 3.85 (dd, *J* = 3.6, 2.3 Hz, 1H), 2.64 (t, *J* = 2.3 Hz, 1H); **<sup>13</sup>C NMR** (90.56 MHz, CDCl<sub>3</sub>): δ [ppm] = 191.63, 188.40, 164.34, 155.60, 139.97, 134.61, 132.97, 122.76, 121.19, 115.88, 113.43, 77.61, 76.95, 57.15, 54.04, 52.76; **HRMS (ESI)**: calc. for C<sub>16</sub>H<sub>12</sub>NO<sub>5</sub> [M+H]<sup>+</sup>: 298.0710, found: 298.0711, diff: 0.38 ppm.

***N*-(2-Hydroxy-5-oxo-7-oxabicyclo[4.1.0]hept-3-en-3-yl)-2-(prop-2-yn-1-yloxy)benzamide**  
**(FM146)**<sup>[133,182]</sup>

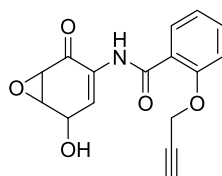


**FM146**  
 $C_{16}H_{13}NO_5$   
 Molecular Weight: 299.28

To a solution of **FM141** (80.0 mg, 0.27 mmol, 1.00 eq) in anhydrous MeOH (5 mL) was added  $NaBH(OAc)_3$  (57.0 mg, 0.27 mmol, 1.00 eq) at 0 °C. The mixture was stirred for 20 min at 0 °C and then allowed to warm to room temperature. After stirring for 2 h TLC showed complete consumption of the starting material and the mixture was therefore quenched with water (10 mL) and extracted with EtOAc (3 x 10 mL). The combined organic extracts were washed with brine (10 mL), dried over  $Na_2SO_4$  and concentrated under reduced pressure. The crude product was purified by preparative reversed-phase HPLC (C18 5.0  $\mu$ m, 30 x 150 mm column, gradient 2% B  $\rightarrow$  98% B over 17 min,  $t_R$  = 5.2 - 6.6 min) giving compound FM146 (32.0 mg, 0.11 mmol, 741%) as pale yellow powder.

$R_f$  = 0.05 (hexanes:EtOAc 2:1);  $^1H$  NMR (360.13 MHz,  $CDCl_3$ ):  $\delta$  [ppm] = 10.35 (s, 1H), 8.18 (dd,  $J$  = 7.9, 1.8 Hz, 1H), 7.62 - 7.44 (m, 1H), 7.22 - 7.05 (m, 2H), 7.01 - 6.90 (m, 1H), 4.92 (d,  $J$  = 2.4 Hz, 2H), 4.76 (dd,  $J$  = 2.8, 1.0 Hz, 1H), 3.91 (dd,  $J$  = 4.1, 2.9 Hz, 1H), 3.56 (dd,  $J$  = 4.1, 2.2 Hz, 1H), 2.65 (t,  $J$  = 2.4 Hz, 1H);  $^{13}C$  NMR (90.56 MHz,  $CDCl_3$ ):  $\delta$  [ppm] = 193.45, 164.53, 155.47, 149.61, 134.43, 133.03, 122.87, 121.50, 113.37, 107.71, 77.36, 77.04, 65.84, 57.30, 53.99, 53.61; HRMS (ESI): calc. for  $C_{16}H_{14}NO_5$   $[M+H]^+$ : 300.0867, found: 300.0867, diff: 0.15 ppm.

***N*-(5-Hydroxy-2-oxo-7-oxabicyclo[4.1.0]hept-3-en-3-yl)-2-(prop-2-yn-1-yloxy)benzamide**  
**(FM253)**<sup>[123,134]</sup>



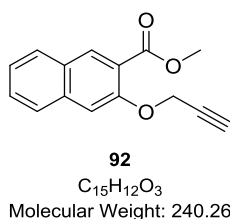
**FM253**  
 $C_{16}H_{13}NO_5$   
 Molecular Weight: 299.28

To a solution of **89** (0.10 g, 0.29 mmol, 1.00 eq) in anhydrous THF (25 mL) was added dropwise  $LiBHET_3$  (1 M in THF, 0.58 mL, 0.58 mmol, 2.00 eq) at -78 °C. The mixture was stirred for 1 h at -78 °C and then allowed to warm to room temperature. After stirring for 3 h TLC showed complete

consumption of the starting material and the mixture was therefore quenched with water and extracted with EtOAc (3 x 10 mL). The combined organic extracts were washed with brine (10 mL), dried over Na<sub>2</sub>SO<sub>4</sub> and concentrated under reduced pressure. The crude product (**90**) was directly redissolved in DCM (20 mL) without further purification. Montmorillonite K10 (50 mg) was added in one portion and the reaction was stirred for 16 h at room temperature. The solution was filtered through Celite, which was additionally washed with DCM (3 x 20 mL). The combined filtrates were washed with brine (10 mL), dried over Na<sub>2</sub>SO<sub>4</sub> and concentrated under reduced pressure giving compound **FM253** (56.9 mg, 0.19 mmol, 66% over two steps) as pale yellow powder.

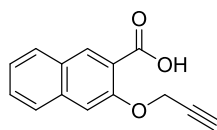
$R_f$  = 0.28 (hexanes:EtOAc 2:1); <sup>1</sup>H NMR (500.36 MHz, CDCl<sub>3</sub>): δ [ppm] = 10.02 (s, 1H), 7.98 (dd,  $J$  = 7.8, 1.7 Hz, 1H), 7.64 - 7.52 (m, 1H), 7.39 (t,  $J$  = 2.6 Hz, 1H), 7.33 (d,  $J$  = 8.3 Hz, 1H), 7.17 (t,  $J$  = 7.5 Hz, 1H), 5.89 (d,  $J$  = 6.6 Hz, 1H), 5.10 (d,  $J$  = 2.3 Hz, 2H), 4.92 - 4.77 (m, 1H), 3.83 (dt,  $J$  = 4.0, 2.8 Hz, 1H), 3.70 (t,  $J$  = 2.3 Hz, 1H), 3.64 (d,  $J$  = 4.1 Hz, 1H); <sup>13</sup>C NMR (125.83 MHz, CDCl<sub>3</sub>): δ [ppm] = 189.38, 163.04, 154.93, 133.65, 131.37, 128.08, 127.66, 122.02, 121.56, 114.26, 79.53, 78.13, 63.36, 56.90, 53.89, 51.94; HRMS (ESI): calc. for C<sub>16</sub>H<sub>14</sub>NO<sub>5</sub> [M+H]<sup>+</sup>: 300.0867, found: 300.0867, diff: -0.26 ppm.

#### Methyl-3-(prop-2-yn-1-yloxy)-2-naphthoate (**92**)<sup>[183]</sup>



To a solution of methyl-3-hydroxy-2-naphthoate (**91**) (10.0 g, 49.5 mmol, 1.00 eq) in acetone (100 mL) were added K<sub>2</sub>CO<sub>3</sub> (6.85 g, 49.5 mmol, 1.00 eq) followed by propargyl bromide (80% in toluene, 10.0 mL, 91.5 mmol, 1.85 eq). The reaction mixture was heated under reflux for 24 h under nitrogen atmosphere. After addition of chilled water (20 mL) the layers were separated and the aqueous layer was extracted with Et<sub>2</sub>O (3 x 50 mL). The combined organic extracts were washed with brine (100 mL), dried over Na<sub>2</sub>SO<sub>4</sub> and concentrated under reduced pressure. The crude product was purified by flash column chromatography (hexanes:EtOAc 4:1) giving compound **92** (10.8 g, 45.0 mmol, 91%) as yellow solid.

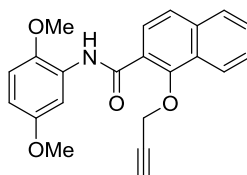
$R_f$  = 0.37 (hexanes:EtOAc 4:1); <sup>1</sup>H NMR (360.13 MHz, CDCl<sub>3</sub>): δ [ppm] = 8.34 (s, 1H), 7.83 (d,  $J$  = 8.2 Hz, 1H), 7.77 (d,  $J$  = 8.0 Hz, 1H), 7.53 (ddd,  $J$  = 8.2, 6.9, 1.2 Hz, 1H), 7.44 - 7.36 (m, 2H), 4.89 (d,  $J$  = 2.4 Hz, 2H), 3.96 (s, 3H), 2.55 (t,  $J$  = 2.4 Hz, 1H); <sup>13</sup>C NMR (90.56 MHz, CDCl<sub>3</sub>): δ [ppm] = 166.57, 153.64, 135.90, 133.15, 128.82, 128.60, 128.20, 126.83, 125.00, 122.28, 109.54, 78.38, 76.22, 56.95, 52.42; HRMS (ESI): calc. for C<sub>15</sub>H<sub>13</sub>O<sub>3</sub> [M+H]<sup>+</sup>: 241.0859, found: 241.0859, diff: -0.15 ppm.

**3-(Prop-2-yn-1-yloxy)-2-naphthoic acid (93)<sup>[183]</sup>****93**C<sub>14</sub>H<sub>10</sub>O<sub>3</sub>

Molecular Weight: 226.23

To a solution of **92** (1.50 g, 7.89 mmol, 1.00 eq) in EtOH (60 mL) was added a saturated aqueous solution of KOH (2.5 mL) and the reaction mixture was stirred for 4 h at room temperature. After addition of water (200 mL) the solution was acidified by adding aqueous 1M HCl (20 mL) and the layers were separated. The aqueous layer was extracted with EtOAc (4 x 20 mL) and the combined organic extracts were washed with brine (100 mL), dried over Na<sub>2</sub>SO<sub>4</sub> and concentrated under reduced pressure giving compound **93** (1.31 g, 7.44 mmol, 94%) as yellowish solid without further purification.

$R_f$  = 0.54 (hexanes:EtOAc 2:1); <sup>1</sup>H NMR (360.13 MHz, CDCl<sub>3</sub>): δ [ppm] = 10.62 (s, 1H), 8.81 (s, 1H), 7.93 (d, *J* = 7.9 Hz, 1H), 7.80 (d, *J* = 8.3 Hz, 1H), 7.61 (ddd, *J* = 8.2, 6.9, 1.2 Hz, 1H), 7.48 (ddd, *J* = 8.1, 6.9, 1.1 Hz, 1H), 7.46 - 7.38 (m, 1H), 5.05 (d, *J* = 2.4 Hz, 2H), 2.69 (t, *J* = 2.4 Hz, 1H); <sup>13</sup>C NMR (90.56 MHz, CDCl<sub>3</sub>): δ [ppm] = 165.26, 152.48, 136.62, 136.45, 129.72, 129.60, 128.87, 126.86, 125.91, 118.52, 109.00, 78.11, 76.49, 57.74; HRMS (ESI): calc. for C<sub>14</sub>H<sub>11</sub>O<sub>3</sub> [M+H]<sup>+</sup>: 227.0703, found: 227.0703, diff: -0.04 ppm.

***N*-(2,5-Dimethoxyphenyl)-1-(prop-2-yn-1-yloxy)-2-naphthamide (94)<sup>[183]</sup>****94**C<sub>22</sub>H<sub>19</sub>NO<sub>4</sub>

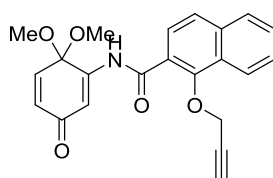
Molecular Weight: 361.40

**93** (1.00 g, 4.42 mmol, 1.20 eq) was added to thionyl chloride (8 mL) and *N,N*-dimethylformamide (cat.) and the reaction mixture was heated under reflux for 3 h under an inert atmosphere of nitrogen at 75°C. All volatile material was evaporated and the residue dissolved in toluene. After removing the solvent under reduced pressure the corresponding acetylenic acid chloride was redissolved in anhydrous THF (23 mL) and 2,5-dimethoxyaniline (0.56 g, 3.68 mmol, 1.00 eq) was added. After cooling the reaction mixture to 0 °C, pyridine (0.59 mL, 7.37 mmol, 2.00 eq) was added slowly and the mixture was stirred for 15 min at 0 °C followed by 16 h at room temperature. The reaction was quenched by adding aqueous 1 M HCl (10 mL) and extracted with EtOAc (3 x 20

mL). The combined organic extracts were washed with brine (100 mL), dried over Na<sub>2</sub>SO<sub>4</sub> and concentrated under reduced pressure. The crude product was purified by flash column chromatography (hexanes:EtOAc 3:1) giving compound **94** (0.96 g, 2.65 mmol, 72% over two steps) as yellow solid.

$R_f$  = 0.58 (hexanes:EtOAc 2:1); <sup>1</sup>H NMR (360.13 MHz, CDCl<sub>3</sub>): δ [ppm] = 10.48 (s, 1H), 8.86 (s, 1H), 8.43 (d,  $J$  = 3.0 Hz, 1H), 7.93 (d,  $J$  = 8.2 Hz, 1H), 7.80 (d,  $J$  = 8.2 Hz, 1H), 7.58 - 7.52 (m, 1H), 7.49 - 7.38 (m, 2H), 6.85 (d,  $J$  = 8.9 Hz, 1H), 6.63 (dd,  $J$  = 8.9, 3.1 Hz, 1H), 5.05 (d,  $J$  = 2.4 Hz, 2H), 3.93 (s, 3H), 3.85 (s, 3H), 2.62 (t,  $J$  = 2.4 Hz, 1H); <sup>13</sup>C NMR (90.56 MHz, CDCl<sub>3</sub>): δ [ppm] = 162.85, 154.23, 152.50, 142.95, 135.69, 134.49, 129.39, 129.35, 128.95, 128.65, 126.61, 125.25, 123.63, 111.21, 109.13, 108.74, 106.57, 77.62, 76.91, 56.95, 56.79, 56.00; HRMS (ESI): calc. for C<sub>22</sub>H<sub>20</sub>NO<sub>4</sub> [M+H]<sup>+</sup>: 362.1387, found: 362.1385, diff: -0.43 ppm.

***N*-(6,6-Dimethoxy-3-oxocyclohexa-1,4-dien-1-yl)-1-(prop-2-yn-1-yloxy)-2-naphthamide (95)<sup>[182]</sup>**

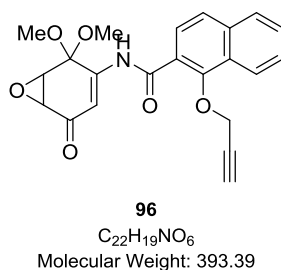


**95**  
C<sub>22</sub>H<sub>19</sub>NO<sub>5</sub>  
Molecular Weight: 377.40

To a solution of **94** (0.50 g, 1.38 mmol, 1.00 eq) in anhydrous MeOH (60 mL) at 0 °C under nitrogen atmosphere was added portion wise PhI(OPiv)<sub>2</sub> (0.84 g, 2.08 mmol, 1.50 eq). The mixture was allowed to warm to room temperature, further stirred for 6 h and then diluted with EtOAc (50 mL). After stirring for 30 min at room temperature, the mixture was extracted with EtOAc (3 x 50 mL). The combined organic extracts were washed with water (40 mL) and brine (40 mL), dried over Na<sub>2</sub>SO<sub>4</sub>, concentrated under reduced pressure and purified by flash column chromatography (hexanes:EtOAc 1:1) to yield product **95** (0.36 g, 0.95 mmol, 69%) as yellow solid.

$R_f$  = 0.47 (hexanes:EtOAc 2:1); <sup>1</sup>H NMR (360.13 MHz, CDCl<sub>3</sub>): δ [ppm] = 10.17 (s, 1H), 8.78 (s, 1H), 7.94 (d,  $J$  = 8.3 Hz, 1H), 7.80 (d,  $J$  = 8.0 Hz, 1H), 7.64 (d,  $J$  = 2.0 Hz, 1H), 7.61 - 7.56 (m, 1H), 7.50 - 7.40 (m, 2H), 6.61 (d,  $J$  = 10.3 Hz, 1H), 6.49 (dd,  $J$  = 10.3, 2.0 Hz, 1H), 5.04 (d,  $J$  = 2.4 Hz, 2H), 3.34 (s, 6H), 2.61 (t,  $J$  = 2.4 Hz, 1H); <sup>13</sup>C NMR (90.56 MHz, CDCl<sub>3</sub>): δ [ppm] = 186.49, 164.42, 151.96, 148.10, 138.96, 136.02, 134.97, 133.55, 129.44, 129.18, 128.76, 126.68, 125.51, 122.30, 114.59, 109.13, 94.73, 77.36, 77.22, 56.99, 51.71; HRMS (ESI): calc. for C<sub>22</sub>H<sub>20</sub>NO<sub>5</sub> [M+H]<sup>+</sup>: 378.1336, found: 378.1336, diff: 0.04.

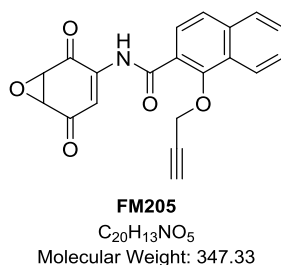
***N*-(2,2-Dimethoxy-5-oxo-7-oxabicyclo[4.1.0]hept-3-en-3-yl)-1-(prop-2-yn-1-yloxy)-2-naphthamide (96)<sup>[118]</sup>**



To a solution of **95** (0.50 g, 1.30 mmol, 1.00 eq) in THF (100 mL) were alternately added aqueous H<sub>2</sub>O<sub>2</sub> (30%, 16.8 mL) and aqueous K<sub>2</sub>CO<sub>3</sub> (0.40 M, 41 mL) to keep a constant pH between 8 and 9. The reaction mixture was stirred at room temperature for 16 h and then diluted with EtOAc (40 mL). The phases were separated and the aqueous layer was extracted with EtOAc (3 x 30 mL). The combined organic extracts were washed with water (40 mL) and brine (30 mL), dried over Na<sub>2</sub>SO<sub>4</sub> and concentrated under reduced pressure. The crude product was purified by preparative reversed-phase HPLC (C18 5.0 μm, 30 x 150 mm column, gradient 50% B → 80% B over 25 min, *t<sub>R</sub>* = 5.5 - 6.0 min) giving compound **96** (0.19 g, 0.49 mmol, 38%) as white solid.

*R<sub>f</sub>* = 0.47 (hexanes:EtOAc 1:1); <sup>1</sup>H NMR (500.13 MHz, CDCl<sub>3</sub>): δ [ppm] = 10.55 (s, 1H), 8.67 (s, 1H), 8.08 (d, *J* = 8.2 Hz, 1H), 7.91 (d, *J* = 8.3 Hz, 1H), 7.75 (s, 1H), 7.69 - 7.60 (m, 1H), 7.53 - 7.46 (m, 1H), 7.13 (d, *J* = 2.1 Hz, 1H), 5.25 (d, *J* = 2.3 Hz, 2H), 4.29 (d, *J* = 4.3 Hz, 1H), 3.78 (t, *J* = 2.3 Hz, 1H), 3.69 (s, 3H), 3.64 (dd, *J* = 4.2, 2.1 Hz, 1H), 3.33 (s, 3H); <sup>13</sup>C NMR (125.83 MHz, CDCl<sub>3</sub>): δ [ppm] = 193.49, 163.68, 151.43, 146.93, 135.73, 133.83, 129.32, 129.26, 127.95, 126.62, 125.40, 121.72, 109.46, 107.66, 95.26, 79.55, 78.13, 56.90, 51.45, 51.10, 50.88, 50.62; HRMS (ESI): calc. for C<sub>22</sub>H<sub>18</sub>NO<sub>6</sub> [M+H]<sup>+</sup>: 394.1285, found: 394.1284, diff: -0.27 ppm.

***N*-(2,5-Dioxo-7-oxabicyclo[4.1.0]hept-3-en-3-yl)-1-(prop-2-yn-1-yloxy)-2-naphthamid (FM205)<sup>[133]</sup>**



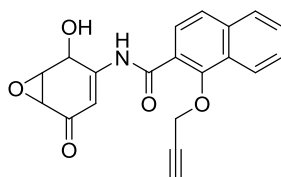
To a solution of **96** (8.00 mg, 22.0 μmol, 1.00 eq) in anhydrous DCM (5 mL) was added BF<sub>3</sub> · OEt<sub>2</sub> (7.15 μL, 56.0 μmol, 2.50 eq) at -20 °C. The mixture was stirred at -10 °C for 30 min, then allowed to warm to room temperature and further stirred for 14 h. The reaction was quenched by adding water (1 mL) and extracted with CHCl<sub>3</sub> (3 x 5 mL). The combined organic extracts were washed with brine (15 mL), dried over Na<sub>2</sub>SO<sub>4</sub> and concentrated under reduced pressure. The crude product



was purified by preparative reversed-phase HPLC (C18 3.5  $\mu$ m, 10 x 250 mm column, gradient 2% B  $\rightarrow$  98% B over 17 min,  $t_R$  = 12.0 - 12.4 min) giving compound **FM205** (5.20 mg, 15.0  $\mu$ mol, 68%) as yellow solid.

$R_f$  = 0.46 (hexanes:EtOAc 2:1);  $^1\text{H NMR}$  (360.13 MHz,  $\text{CDCl}_3$ ):  $\delta$  [ppm] = 10.62 (s, 1H), 8.63 (s, 1H), 8.07 (d,  $J$  = 8.1 Hz, 1H), 7.91 (d,  $J$  = 8.2 Hz, 1H), 7.71 (s, 1H), 7.66 - 7.61 (m, 1H), 7.52 - 7.47 (m, 1H), 7.45 (d,  $J$  = 2.3 Hz, 1H), 5.21 (d,  $J$  = 2.2 Hz, 2H), 4.21 (d,  $J$  = 3.9 Hz, 1H), 4.00 (dd,  $J$  = 3.9, 2.3 Hz, 1H), 3.76 (t,  $J$  = 2.3 Hz, 1H);  $^{13}\text{C NMR}$  (125.83 MHz,  $\text{CDCl}_3$ ):  $\delta$  [ppm] = 192.32, 187.81, 164.18, 151.62, 139.70, 135.76, 133.63, 129.31, 129.23, 127.89, 126.64, 125.37, 121.69, 114.34, 109.49, 79.73, 78.00, 57.15, 53.82, 52.98; **HRMS (ESI)**: calc. for  $\text{C}_{20}\text{H}_{14}\text{NO}_5$   $[\text{M}+\text{H}]^+$ : 348.0867, found: 348.0877, diff: 2.95 ppm.

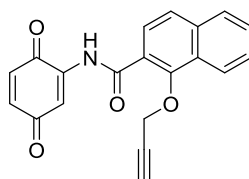
***N*-(2-Hydroxy-5-oxo-7-oxabicyclo[4.1.0]hept-3-en-3-yl)-1-(prop-2-yn-1-yloxy)-2-naphthamide**  
**(FM247)**<sup>[133,182]</sup>



**FM247**  
 $\text{C}_{20}\text{H}_{15}\text{NO}_5$   
Molecular Weight: 349.34

To a solution of **FM205** (54.0 mg, 0.16 mmol, 1.00 eq) in anhydrous MeOH (5 mL) was added  $\text{NaBH}(\text{OAc})_3$  (33.0 mg, 0.16 mmol, 1.00 eq) at 0  $^\circ\text{C}$ . The mixture was stirred for 20 min at 0  $^\circ\text{C}$  and then allowed to warm to room temperature. After stirring for 16 h TLC showed complete consumption of the starting material and the mixture was therefore quenched with water (1 mL) and extracted with EtOAc (3 x 10 mL). The combined organic extracts were washed with brine (10 mL), dried over  $\text{Na}_2\text{SO}_4$  and concentrated under reduced pressure. The crude product was purified by preparative reversed-phase HPLC (C18 5.0  $\mu$ m, 30 x 150 mm column, gradient 2% B  $\rightarrow$  98% B over 17 min,  $t_R$  = 7.0 - 8.0 min) giving compound **FM247** (32.0 mg, 0.11 mmol, 50%) as slightly yellow powder.

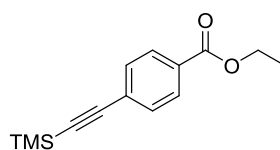
$R_f$  = 0.51 (hexanes:EtOAc 2:1);  $^1\text{H NMR}$  (500.36 MHz,  $\text{CDCl}_3$ ):  $\delta$  [ppm] = 10.60 (s, 1H), 8.64 (s, 1H), 8.07 (d,  $J$  = 8.1 Hz, 1H), 7.92 (d,  $J$  = 8.2 Hz, 1H), 7.70 (s, 1H), 7.65 - 7.61 (m, 1H), 7.51 - 7.46 (m, 1H), 6.93 - 6.90 (m, 1H), 6.82 (d,  $J$  = 7.3 Hz, 1H), 5.19 - 5.15 (m, 2H), 4.87 (d,  $J$  = 4.3 Hz, 1H), 3.88 (dd,  $J$  = 4.3, 2.5 Hz, 1H), 3.72 (t,  $J$  = 2.3 Hz, 1H), 3.46 (dd,  $J$  = 4.3, 2.2 Hz, 1H);  $^{13}\text{C NMR}$  (90.56 MHz,  $\text{CDCl}_3$ ):  $\delta$  [ppm] = 194.09, 164.04, 151.48, 150.98, 135.59, 133.51, 129.20, 129.18, 127.93, 126.62, 125.30, 122.25, 109.40, 105.84, 79.68, 78.24, 64.20, 56.74, 53.49, 52.94; **HRMS (ESI)**: calc. for  $\text{C}_{20}\text{H}_{16}\text{NO}_5$   $[\text{M}+\text{H}]^+$ : 350.1023, found: 350.1023, diff: 0.01 ppm.

***N*-(3,6-Dioxocyclohexa-1,4-dien-1-yl)-1-(prop-2-yn-1-yloxy)-2-naphthamide (FM321)<sup>[134]</sup>**

**FM321**  
 $C_{20}H_{13}NO_4$   
 Molecular Weight: 331.33

To a solution of **95** (50.0 mg, 0.13 mmol, 1.00 eq) in anhydrous DCM (5 mL) Montmorillonite K10 (100 mg) was added in small portions and the reaction was stirred for 16 h at room temperature. The solution was filtered through Celite, which was additionally washed with DCM (3 x 10 mL). The combined filtrates were washed with brine (10 mL), dried over  $Na_2SO_4$  and concentrated under reduced pressure. The residue was purified by flash column chromatography (hexanes:EtOAc 2:1) to yield product **FM321** (20.0 mg, 60.4  $\mu$ mol, 46%) as orange solid.

$R_f$  = 0.73 (hexanes:EtOAc 1:1);  $^1H$  NMR (500.36 MHz,  $CDCl_3$ ):  $\delta$  [ppm] = 10.73 (s, 1H), 8.70 (s, 1H), 8.09 (d,  $J$  = 8.2 Hz, 1H), 7.92 (d,  $J$  = 8.2 Hz, 1H), 7.74 (s, 1H), 7.64 (t,  $J$  = 7.4 Hz, 1H), 7.54 (d,  $J$  = 2.5 Hz, 1H), 7.49 (t,  $J$  = 7.5 Hz, 1H), 7.01 (d,  $J$  = 10.1 Hz, 1H), 6.87 (dd,  $J$  = 10.1, 2.5 Hz, 1H), 5.24 (d,  $J$  = 2.2 Hz, 2H), 3.75 (t,  $J$  = 2.2 Hz, 1H);  $^{13}C$  NMR (125.83 MHz,  $CDCl_3$ ):  $\delta$  [ppm] = 188.40, 182.41, 163.78, 151.63, 139.49, 137.56, 135.79, 134.20, 133.81, 129.34, 129.28, 127.93, 126.64, 125.39, 121.59, 114.03, 109.57, 79.78, 78.00, 57.15; HRMS (ESI): calc. for  $C_{20}H_{12}NO_4$   $[M-H]^-$ : 330.0761 found: 330.0772, diff: 3.29 ppm.

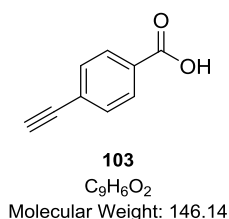
**Ethyl-4-((trimethylsilyl)ethynyl)benzoate (**108**)<sup>[184]</sup>**

**108**  
 $C_{14}H_{18}O_2Si$   
 Molecular Weight: 246.38

To a solution of ethyl-4-iodobenzoate (4.41 g, 16.0 mmol, 1.00 eq) in  $NEt_3$  (30 mL) were added CuI (0.30 g, 1.60 mmol, 0.10 eq) and  $PdCl_2(PPh_3)_2$  (0.56 g, 0.80 mmol, 0.05 eq) at room temperature under an inert atmosphere of nitrogen. Ethynyltrimethylsilane (1.73 g, 17.6 mmol, 1.10 eq) was slowly added and the reaction mixture was heated under reflux for 3 h.  $NEt_3$  was evaporated under reduced pressure and the residue was dissolved in EtOAc (20 mL) and filtered. The solvent was again evaporated and the crude product was purified by flash column chromatography (hexanes:EtOAc 4:1) giving compound **108** (3.80 g, 15.4 mmol, 96%) as yellow solid.

$R_f$  = 0.70 (hexanes:EtOAc 4:1);  $^1\text{H NMR}$  (500.36 MHz,  $\text{CDCl}_3$ ):  $\delta$  [ppm] = 7.92 (d,  $J$  = 8.2 Hz, 2H), 7.58 (d,  $J$  = 8.2 Hz, 2H), 4.30 (q,  $J$  = 7.1 Hz, 2H), 1.31 (t,  $J$  = 7.1 Hz, 3H), 0.24 (s, 9H);  $^{13}\text{C NMR}$  (125.83 MHz,  $\text{CDCl}_3$ ):  $\delta$  [ppm] = 165.01, 131.89, 129.79, 129.30, 126.73, 104.06, 97.65, 61.01, 14.12, -0.27; **HRMS (ESI)**: calc. for  $\text{C}_{14}\text{H}_{19}\text{O}_2\text{Si}$   $[\text{M}+\text{H}]^+$ : 247.1149, found: 247.1150, diff: 0.26 ppm.

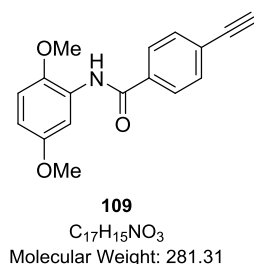
#### 4-Ethynylbenzoic acid (**103**)<sup>[183]</sup>



To a solution of **108** (3.90 g, 15.8 mmol, 1.00 eq) in MeOH (80 mL) was added LiOH (3.79 g, 0.16 mol, 10.0 eq) at room temperature and stirred for 3 h. The reaction was acidified to pH 1 by adding HCl (2 M, 30 mL) and the layers were separated. The aqueous layer was extracted with EtOAc (3 x 20 mL) and the combined organic extracts were washed with brine (100 mL), dried over  $\text{Na}_2\text{SO}_4$  and concentrated under reduced pressure giving compound **103** (2.30 g, 15.7 mmol, 99%) as copper colored solid without further purification.

$^1\text{H NMR}$  (500.36 MHz,  $\text{CDCl}_3$ ):  $\delta$  [ppm] = 13.19 (s, 1H), 7.93 (d,  $J$  = 8.0 Hz, 2H), 7.59 (d,  $J$  = 8.0 Hz, 2H), 4.45 (s, 1H);  $^{13}\text{C NMR}$  (125.83 MHz,  $\text{CDCl}_3$ ):  $\delta$  [ppm] = 13C NMR (126 MHz, DMSO)  $\delta$  166.73, 131.97, 130.93, 129.56, 126.08, 83.69, 82.82; **HRMS (ESI)**: calc. for  $\text{C}_9\text{H}_5\text{O}_2$   $[\text{M}-\text{H}]^-$ : 145.0284, found: 145.0295, diff: 7.28 ppm.

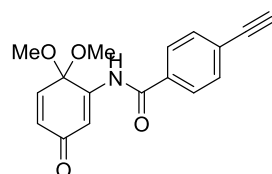
#### *N*-(2,5-Dimethoxyphenyl)-4-ethynylbenzamide (**109**)



To a solution of **103** (0.12 g, 0.82 mmol, 1.00 eq) in anhydrous DMF (25 mL) were added DIPEA (0.42 mL, 2.46 mol, 3.00 eq), PyBOP (0.47 g, 0.90 mmol, 1.10 eq) and HOBt (0.13 mg, 0.99 mmol, 1.2 eq) at room temperature under an inert atmosphere of nitrogen. After stirring for 10 min 2,5-dimethoxyaniline (0.15 g, 0.99 mmol, 1.20 eq) was added to the reaction mixture and stirred at room temperature for 16 h. DMF was evaporated under reduced pressure and the crude product was purified by flash column chromatography (hexanes:EtOAc 2:1) giving compound **109** (0.15 g, 0.53 mmol, 65%) as brown solid.

$R_f$  = 0.63 (hexanes:EtOAc 2:1);  $^1\text{H NMR}$  (360.13 MHz,  $\text{CDCl}_3$ ):  $\delta$  [ppm] = 8.55 (s, 1H), 8.26 (d,  $J$  = 3.0 Hz, 1H), 7.85 (d,  $J$  = 8.5 Hz, 2H), 7.61 (d,  $J$  = 8.4 Hz, 2H), 6.84 (d,  $J$  = 8.9 Hz, 1H), 6.63 (dd,  $J$  = 8.9, 3.0 Hz, 1H), 3.89 (s, 3H), 3.82 (s, 3H), 3.22 (s, 1H);  $^{13}\text{C NMR}$  (125.83 MHz,  $\text{CDCl}_3$ ):  $\delta$  [ppm] = 164.41, 154.09, 142.49, 135.23, 132.65, 132.59, 130.50, 128.35, 127.11, 125.79, 110.86, 109.19, 106.12, 82.83, 79.90, 56.46, 55.95; **HRMS (ESI)**: calc. for  $\text{C}_{17}\text{H}_{16}\text{NO}_3$   $[\text{M}+\text{H}]^+$ : 282.1125, found: 282.1125, diff: -0.09 ppm.

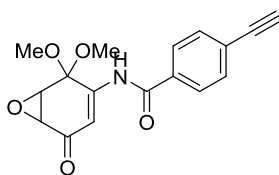
***N*-(6,6-Dimethoxy-3-oxocyclohexa-1,4-dien-1-yl)-4-ethynylbenzamide (110)**<sup>[182]</sup>



**110**  
 $\text{C}_{17}\text{H}_{15}\text{NO}_4$   
 Molecular Weight: 297.31

To a solution of **109** (0.10 g, 0.35 mmol, 1.00 eq) in anhydrous MeOH (10 mL) at 0 °C under nitrogen atmosphere was added portion wise  $\text{PhI}(\text{OPiv})_2$  (0.22 g, 0.53 mmol, 1.50 eq). The mixture was allowed to warm to room temperature, further stirred for 3 h and then diluted with EtOAc (10 mL) and saturated aqueous citric acid solution (5 mL). After stirring for another 30 min at room temperature, the mixture was extracted with EtOAc (3 x 20 mL). The combined organic extracts were washed with saturated aqueous  $\text{NaHCO}_3$  solution (20 mL), water (10 mL) and brine (30 mL), dried over  $\text{Na}_2\text{SO}_4$ , concentrated under reduced pressure and purified by flash column chromatography (hexanes:EtOAc 2:1) to yield product **110** (86.0 g, 0.29 mmol, 83%) as yellow solid.  $R_f$  = 0.14 (hexanes:EtOAc 1:1);  $^1\text{H NMR}$  (500.36 MHz,  $\text{CDCl}_3$ ):  $\delta$  [ppm] = 9.38 (s, 1H), 7.80 (d,  $J$  = 8.4 Hz, 2H), 7.63 (d,  $J$  = 8.3 Hz, 2H), 7.26 (d,  $J$  = 2.0 Hz, 1H), 6.98 (d,  $J$  = 10.4 Hz, 1H), 6.41 (dd,  $J$  = 10.4, 2.1 Hz, 1H), 4.48 (s, 1H), 3.26 (s, 6H);  $^{13}\text{C NMR}$  (125.83 MHz,  $\text{CDCl}_3$ ):  $\delta$  [ppm] = 185.63, 166.76, 148.81, 140.38, 133.66, 131.80, 131.48, 128.38, 125.62, 112.90, 93.77, 83.73, 82.73, 51.13; **HRMS (ESI)**: calc. for  $\text{C}_{17}\text{H}_{16}\text{NO}_4$   $[\text{M}+\text{H}]^+$ : 298.1074, found: 298.1074, diff: 0.16 ppm.

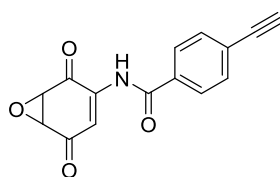
***N*-(2,2-Dimethoxy-5-oxo-7-oxabicyclo[4.1.0]hept-3-en-3-yl)-4-ethynylbenzamide (111)**<sup>[124,182]</sup>



**111**  
 $\text{C}_{17}\text{H}_{15}\text{NO}_5$   
 Molecular Weight: 313.31

To a solution of **103** (42.0 mg, 0.29 mmol, 1.10 eq) in anhydrous DCM (5 mL) at 0 °C containing 1 drop of *N,N*-dimethylformamide (cat.) was slowly added oxalyl chloride (28.0  $\mu$ L, 0.33 mmol, 1.22 eq). The reaction mixture was stirred at 0 °C for 1 h after which the solvent was evaporated and the corresponding acetylenic acid chloride was redissolved in anhydrous THF (5 mL) at 0 °C. A solution of lithium *tert*-butoxide (1 M in THF, 0.30 mL, 0.30 mmol, 1.12 eq) was added dropwise over 15 min to a stirred solution of **55** (50.0 mg, 0.27 mmol, 1.00 eq) in dry THF at 0 °C. After stirring the reaction mixture at 0 °C for 30 min, the solution of acetylenic acid chloride in THF was added dropwise over 1 h. The solution was then allowed to warm to room temperature and stirred for further 16 h until HPLC-MS analysis showed complete conversion of the starting material. The reaction was quenched by adding aqueous  $\text{NH}_4\text{Cl}$  (5 mL) and water (5 mL) and extracted with EtOAc (3 x 30 mL). The combined organic extracts were washed with brine (50 mL), dried over  $\text{Na}_2\text{SO}_4$  and concentrated under reduced pressure. The crude product was purified by preparative reversed-phase HPLC (C18 3.5  $\mu$ m, 10 x 250 mm column, gradient 2% B  $\rightarrow$  98% B over 17 min,  $t_R$  = 9.4 - 11.0 min) giving compound **111** (40.0 mg, 0.13 mmol, 48% over two steps) as white powder.  $R_f$  = 0.59 (hexanes:EtOAc 1:1);  $^1\text{H NMR}$  (500.36 MHz,  $\text{CDCl}_3$ ):  $\delta$  [ppm] = 9.33 (s, 1H), 7.80 (d,  $J$  = 8.3 Hz, 2H), 7.63 (d,  $J$  = 8.3 Hz, 2H), 7.01 (d,  $J$  = 2.1 Hz, 1H), 4.48 (s, 1H), 4.25 (d,  $J$  = 4.3 Hz, 1H), 3.63 (dd,  $J$  = 4.2, 2.1 Hz, 1H), 3.59 (s, 3H), 3.32 (s, 3H);  $^{13}\text{C NMR}$  (125.83 MHz,  $\text{CDCl}_3$ ):  $\delta$  [ppm] = 193.33, 166.26, 147.07, 133.54, 131.91, 128.25, 125.79, 107.84, 95.35, 83.86, 82.67, 51.52, 51.30, 51.11, 50.34; **HRMS (ESI)**: calc. for  $\text{C}_{17}\text{H}_{16}\text{NO}_5$   $[\text{M}+\text{H}]^+$ : 314.1023, found: 314.1023, diff: -0.10 ppm.

***N*-(2,5-Dioxo-7-oxabicyclo[4.1.0]hept-3-en-3-yl)-4-ethynylbenzamide (FM239)<sup>[182]</sup>**

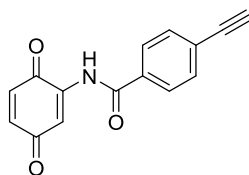


**FM239**  
 $\text{C}_{15}\text{H}_9\text{NO}_4$   
 Molecular Weight: 267.24

To a solution of **111** (87.0 mg, 0.28 mmol, 1.00 eq) in anhydrous DCM (5 mL) was added  $\text{BF}_3 \cdot \text{OEt}_2$  (88.0  $\mu$ L, 0.70 mmol, 2.50 eq) at -20 °C. The mixture was stirred at -10 °C for 30 min, then allowed to warm to room temperature and further stirred for 14 h. The reaction was quenched by adding water (1 mL) and extracted with  $\text{CHCl}_3$  (3 x 5 mL). The combined organic extracts were washed with brine (15 mL), dried over  $\text{Na}_2\text{SO}_4$  and concentrated under reduced pressure. The crude product was purified by preparative reversed-phase HPLC (C18 5.0  $\mu$ m, 30 x 150 mm column, gradient 2% B  $\rightarrow$  98% B over 17 min,  $t_R$  = 7.2 - 8.4 min) giving compound **FM239** (5.20 mg, 15.0  $\mu$ mol, 68%) as yellow solid.

$R_f$  = 0.47 (hexanes:EtOAc 2:1);  $^1\text{H NMR}$  (500.36 MHz,  $\text{CDCl}_3$ ):  $\delta$  [ppm] = 9.89 (s, 1H), 7.89 (d,  $J$  = 8.3 Hz, 2H), 7.65 (d,  $J$  = 8.3 Hz, 2H), 7.23 (d,  $J$  = 2.2 Hz, 1H), 4.49 (s, 1H), 4.19 (d,  $J$  = 4.0 Hz, 1H), 3.99 (dd,  $J$  = 3.9, 2.4 Hz, 1H);  $^{13}\text{C NMR}$  (125.83 MHz,  $\text{CDCl}_3$ ):  $\delta$  [ppm] = 192.21, 187.85, 166.09, 140.77, 132.99, 131.95, 128.38, 125.96, 115.44, 83.95, 82.66, 53.95, 53.15; **HRMS (ESI)**: calc. for  $\text{C}_{15}\text{H}_{10}\text{NO}_4$   $[\text{M}+\text{H}]^+$ : 268.0604, found: 268.0602, diff: -1.00 ppm.

***N*-(3,6-Dioxocyclohexa-1,4-dien-1-yl)-4-ethynylbenzamide (FM257)<sup>[134]</sup>**

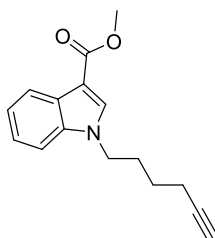


**FM257**  
 $\text{C}_{15}\text{H}_9\text{NO}_3$   
Molecular Weight: 251.24

To a solution of **110** (30.0 mg, 0.10 mmol, 1.00 eq) in anhydrous DCM (5 mL) Montmorillonite K10 (100 mg) was added in small portions and the reaction was stirred for 16 h at room temperature. The solution was filtered through Celite, which was additionally washed with DCM (3 x 10 mL). The combined filtrates were washed with brine (10 mL), dried over  $\text{Na}_2\text{SO}_4$  and concentrated under reduced pressure. The crude product was purified by preparative reversed-phase HPLC (C18 5.0  $\mu\text{m}$ , 30 x 150 mm column, gradient 2% B  $\rightarrow$  98% B over 17 min,  $t_R$  = 7.4 - 8.6 min) giving compound **FM257** (21.0 mg, 83.6  $\mu\text{mol}$ , 84%) as pale brown solid.

$^1\text{H NMR}$  (500.36 MHz,  $\text{CDCl}_3$ ):  $\delta$  [ppm] = 9.67 (s, 1H), 7.92 (d,  $J$  = 8.3 Hz, 2H), 7.66 (d,  $J$  = 8.3 Hz, 2H), 7.48 (d,  $J$  = 2.5 Hz, 1H), 7.01 (d,  $J$  = 10.1 Hz, 1H), 6.88 (dd,  $J$  = 10.1, 2.5 Hz, 1H), 4.50 (s, 1H);  $^{13}\text{C NMR}$  (125.83 MHz,  $\text{CDCl}_3$ ):  $\delta$  [ppm] = 13C NMR (126 MHz, DMSO)  $\delta$  191.17, 188.66, 182.49, 166.29, 139.99, 137.84, 134.86, 133.59, 132.43, 128.70, 126.34, 115.24, 84.37, 83.08; **HRMS (ESI)**: calc. for  $\text{C}_{15}\text{H}_{10}\text{NO}_3$   $[\text{M}+\text{H}]^+$ : 252.0655, found: 252.0655, diff: -0.19 ppm.

**Methyl-1-(hex-5-yn-1-yl)-1*H*-indole-3-carboxylate (112)**



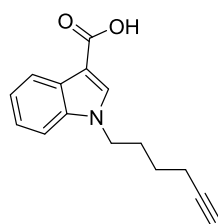
**112**  
 $\text{C}_{16}\text{H}_{17}\text{NO}_2$   
Molecular Weight: 255.32

To a solution of methyl-1*H*-indole-3-carboxylate (4.38 g, 25.0 mmol, 1.00 eq) in anhydrous THF (150 mL) under an inert atmosphere of nitrogen at 0 °C was added NaH (60% dispersion in mineral

oil, 1.50 g, 37.5 mmol, 1.50 eq) and the reaction mixture was stirred for 30 min at 0 °C. Subsequently hex-5-yn-1-yl 4-methylbenzenesulfonate (6.00 g, 23.8 mmol, 0.95 eq) was added dropwise over 30 min and the mixture was allowed to warm to room temperature and stirred for 16 h. After quenching the reaction with saturated  $\text{NH}_4\text{Cl}$  aqueous solution (20 mL) the layers were separated and the aqueous layer was extracted with EtOAc (3 x 50 mL). The combined organic extracts were washed with brine (100 mL), dried over  $\text{Na}_2\text{SO}_4$  and concentrated under reduced pressure. The crude product was purified by flash column chromatography (hexanes:EtOAc 2:1) giving compound **112** (4.72 g, 18.5 mmol, 78%) as pale yellow oil.

$R_f$  = 0.69 (hexanes:EtOAc 2:1);  $^1\text{H NMR}$  (360.13 MHz,  $\text{CDCl}_3$ ):  $\delta$  [ppm] = 8.23 - 8.15 (m, 1H), 7.83 (s, 1H), 7.40 - 7.35 (m, 1H), 7.33 - 7.27 (m, 2H), 4.19 (t,  $J$  = 7.1 Hz, 2H), 3.91 (s, 3H), 2.23 (td,  $J$  = 6.9, 2.7 Hz, 2H), 2.07 - 2.03 (m, 2H), 1.97 (t,  $J$  = 2.7 Hz, 1H), 1.60 - 1.55 (m, 2H); **HRMS (ESI)**: calc. for  $\text{C}_{16}\text{H}_{18}\text{NO}_2$   $[\text{M}+\text{H}]^+$ : 256.1332, found: 256.1331, diff: -0.45 ppm.

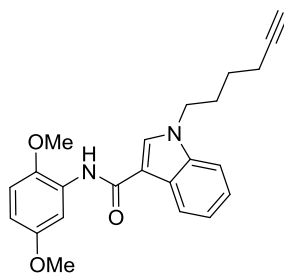
**1-(Hex-5-yn-1-yl)-1H-indole-3-carboxylic acid (**105**)**<sup>[183]</sup>



**105**  
 $\text{C}_{15}\text{H}_{15}\text{NO}_2$   
Molecular Weight: 241.29

To a solution of **112** (4.15 g, 16.3 mmol, 1.00 eq) in EtOH (100 mL) was added a saturated aqueous solution of KOH (50 mL) and the reaction mixture was stirred for 16 h at room temperature. After addition of water (200 mL) the solution was acidified by adding HCl (37%, 20 mL) and the layers were separated. The aqueous layer was extracted with EtOAc (4 x 50 mL) and the combined organic extracts were washed with brine (100 mL), dried over  $\text{Na}_2\text{SO}_4$  and concentrated under reduced pressure giving compound **105** (3.59 g, 15.0 mmol, 92%) as orange solid without further purification.

$R_f$  = 0.57 (hexanes:EtOAc 2:1);  $^1\text{H NMR}$  (360.13 MHz,  $\text{CDCl}_3$ ):  $\delta$  [ppm] = 8.42 - 8.00 (m, 1H), 7.93 (s, 1H), 7.43 - 7.36 (m, 1H), 7.35 - 7.28 (m, 2H), 4.21 (t,  $J$  = 7.1 Hz, 2H), 2.25 (td,  $J$  = 6.9, 2.6 Hz, 2H), 2.10 - 2.00 (m, 2H), 1.98 (t,  $J$  = 2.6 Hz, 1H), 1.58 (dt,  $J$  = 14.3, 6.9 Hz, 2H);  $^{13}\text{C NMR}$  (90.56 MHz,  $\text{CDCl}_3$ ):  $\delta$  [ppm] = 170.57, 136.80, 135.54, 127.14, 123.08, 122.36, 122.13, 110.16, 106.57, 83.47, 69.39, 46.78, 28.94, 25.63, 18.16; **HRMS (ESI)**: calc. for  $\text{C}_{15}\text{H}_{16}\text{NO}_2$   $[\text{M}+\text{H}]^+$ : 242.1176, found: 242.1174, diff: -0.63 ppm.

***N*-(2,5-Dimethoxyphenyl)-1-(hex-5-yn-1-yl)-1*H*-indole-3-carboxamide (**113**)<sup>[183]</sup>**

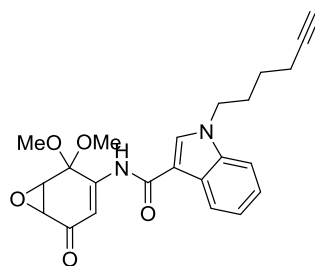
**113**  
 $C_{23}H_{24}N_2O_3$   
Molecular Weight: 376.46

A solution of **105** (0.50 g, 2.07 mmol, 1.20 eq) in thionyl chloride (10 mL) was heated under reflux for 2 h after which the solvent was evaporated and the corresponding acetylenic acid chloride was redissolved in anhydrous THF (5 mL) at 0 °C. 2,5-Dimethoxyaniline (0.26 g, 1.72 mmol, 1.00 eq) was added to the reaction mixture and cooled to 0 °C before pyridine (0.28 mL, 3.44 mmol, 2.00 eq) was added slowly and the mixture was stirred for 15 min at 0 °C followed by 16 h at room temperature. The reaction was quenched by adding aqueous HCl (1 M, 10 mL) and extracted with EtOAc (3 x 20 mL). The combined organic extracts were washed with brine (20 mL), dried over  $Na_2SO_4$  and concentrated under reduced pressure. The crude product was purified by flash column chromatography (hexanes:EtOAc 1:1) giving compound **113** (0.37 g, 0.98 mmol, 57% over two steps) as pale gray solid.

$R_f$  = 0.64 (hexanes:EtOAc 1:1);  $^1H$  NMR (500.13 MHz,  $CDCl_3$ ):  $\delta$  [ppm] = 8.79 (s, 1H), 8.34 (s, 1H), 8.15 (d,  $J$  = 7.5 Hz, 1H), 7.80 (d,  $J$  = 3.0 Hz, 1H), 7.61 (d,  $J$  = 8.0 Hz, 1H), 7.24 (ddd,  $J$  = 14.9, 14.0, 6.9 Hz, 2H), 6.99 (d,  $J$  = 8.9 Hz, 1H), 6.65 (dd,  $J$  = 8.9, 3.0 Hz, 1H), 4.28 (t,  $J$  = 7.0 Hz, 2H), 3.85 (s, 3H), 3.73 (s, 3H), 2.79 (t,  $J$  = 2.5 Hz, 1H), 2.21 (td,  $J$  = 7.0, 2.5 Hz, 2H), 2.00 – 1.78 (m, 2H), 1.45 (dt,  $J$  = 14.6, 7.2 Hz, 2H);  $^{13}C$  NMR (125.83 MHz,  $CDCl_3$ ):  $\delta$  [ppm] = 162.46, 153.00, 143.65, 136.28, 132.17, 128.42, 126.13, 122.31, 121.24, 120.67, 111.57, 110.81, 109.62, 108.37, 107.69, 84.19, 71.60, 56.32, 55.37, 45.54, 28.81, 25.23, 17.34; HRMS (ESI): calc. for  $C_{23}H_{25}N_2O_3$   $[M+H]^+$ : 377.1860, found: 377.1857, diff: -0.85 ppm.



***N*-(2,2-Dimethoxy-5-oxo-7-oxabicyclo[4.1.0]hept-3-en-3-yl)-1-(hex-5-yn-1-yl)-1*H*-indole-3-carboxamide (**114**)<sup>[124]</sup>**

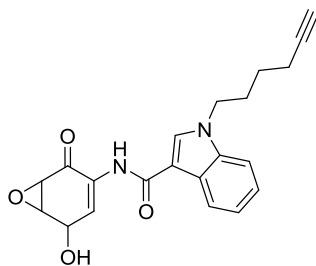


**114**  
 $C_{23}H_{24}N_2O_5$   
 Molecular Weight: 408.45

To a solution of **105** (70.0 mg, 0.29 mmol, 1.10 eq) in anhydrous DCM (10 mL) at 0 °C containing 1 drop of *N,N*-dimethylformamide (cat.) was slowly added oxalyl chloride (28.0  $\mu$ L, 0.33 mmol, 1.22 eq). The reaction mixture was stirred at room temperature for 1 h after which the solvent was evaporated and the corresponding acetylenic acid chloride was redissolved in anhydrous THF (5 mL) and cooled to 0 °C. A solution of lithium *tert*-butoxide (1 M in THF, 0.30 mL, 0.30 mmol, 1.12 eq) was added dropwise over 15 min to a stirred solution of **55** (50.0 mg, 0.27 mmol, 1.00 eq) in dry THF at 0 °C. After stirring the reaction mixture at 0 °C for 30 min, the solution of acetylenic acid chloride in THF was added dropwise over 1 h. The solution was then allowed to warm to room temperature and stirred for further 2 h until HPLC-MS measurements showed complete conversion of the starting material. The reaction was quenched by adding aqueous  $NH_4Cl$  (5 mL) and water (5 mL) and extracted with EtOAc (3 x 30 mL). The combined organic extracts were washed with brine (50 mL), dried over  $Na_2SO_4$  and concentrated under reduced pressure. The crude product was purified by preparative reversed-phase HPLC (C18 5.0  $\mu$ m, 30 x 150 mm column, gradient 2% B  $\rightarrow$  98% B over 17 min,  $t_R$  = 9.2 - 9.8 min) giving compound **114** (73.5 mg, 0.18 mmol, 65% over two steps) as yellow powder.

$R_f$  = 0.39 (hexanes: EtOAc 1:1);  $^1H$  NMR (500.13 MHz,  $CDCl_3$ ):  $\delta$  [ppm] = 8.63 (s, 1H), 8.39 (s, 1H), 8.05 (d,  $J$  = 7.9 Hz, 1H), 7.66 (d,  $J$  = 8.4 Hz, 1H), 7.32 - 7.23 (m, 2H), 7.04 - 7.00 (m, 1H), 4.31 (t,  $J$  = 7.1 Hz, 2H), 4.25 (dd,  $J$  = 4.2, 1.3 Hz, 1H), 3.66 (s, 3H), 3.62 - 3.59 (m, 1H), 3.34 (s, 3H), 2.81 - 2.78 (m, 1H), 2.21 (td,  $J$  = 7.0, 2.5 Hz, 2H), 1.94 - 1.85 (m, 2H), 1.49 - 1.41 (m, 2H);  $^{13}C$  NMR (125.83 MHz,  $CDCl_3$ ):  $\delta$  [ppm] = 192.89, 163.02, 147.39, 136.41, 133.72, 125.84, 122.86, 122.00, 120.38, 111.23, 108.62, 106.03, 95.36, 84.18, 71.64, 51.53, 51.20, 51.06, 50.58, 45.78, 28.84, 25.17, 17.32; HRMS (ESI): calc. for  $C_{23}H_{25}N_2O_5$   $[M+H]^+$ : 409.1758, found: 409.1757, diff: -0.28 ppm.

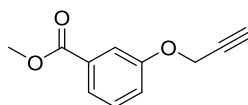
**1-(Hex-5-yn-1-yl)-*N*-(5-hydroxy-2-oxo-7-oxabicyclo[4.1.0]hept-3-en-3-yl)-1*H*-indole-3-carboxamide (FM255)<sup>[134]</sup>**



**FM255**  
 $C_{21}H_{20}N_2O_4$   
Molecular Weight: 364.40

To a solution of **114** (80.0 mg, 0.20 mmol, 1.00 eq) in anhydrous THF (25 mL) was added dropwise  $LiBHET_3$  (1 M in THF, 0.40 mL, 0.40 mmol, 2.00 eq) at  $-78\text{ }^{\circ}C$ . The mixture was stirred for 1 h at  $-78\text{ }^{\circ}C$  and then allowed to warm to room temperature. After stirring for 3 h TLC showed complete consumption of the starting material and the mixture was therefore quenched with water (10 mL) and extracted with EtOAc (3 x 10 mL). The combined organic extracts were washed with brine (10 mL), dried over  $Na_2SO_4$  and concentrated under reduced pressure. The crude product was directly redissolved in DCM (20 mL) without further purification. Montmorillonite K10 (200 mg) was added in one portion and the reaction was stirred for 16 h at room temperature. The solution was filtered through Celite, which was additionally washed with DCM (3 x 20 mL). The combined filtrates were washed with brine (10 mL), dried over  $Na_2SO_4$  and concentrated under reduced pressure. The crude product was purified by preparative reversed-phase HPLC (C18 5.0  $\mu m$ , 30 x 150 mm column, gradient 2% B  $\rightarrow$  98% B over 17 min,  $t_R = 7.4 - 8.2$  min) giving compound **FM255** (50.0 mg, 0.14 mmol, 70% over two steps) as white powder.

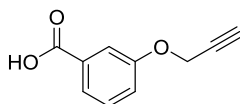
$^1H$  NMR (500.36 MHz,  $CDCl_3$ ):  $\delta$  [ppm] = 8.69 (s, 1H), 8.29 (s, 1H), 8.08 (dd,  $J = 7.3, 0.6$  Hz, 1H), 7.60 (d,  $J = 8.1$  Hz, 1H), 7.27 - 7.22 (m, 1H), 7.22 - 7.17 (m, 1H), 7.03 (t,  $J = 2.6$  Hz, 1H), 5.83 (s, 1H), 4.87 (t,  $J = 2.8$  Hz, 1H), 4.26 (t,  $J = 7.0$  Hz, 2H), 3.82 (dt,  $J = 4.2, 2.7$  Hz, 1H), 3.63 (d,  $J = 4.2$  Hz, 1H), 2.79 (t,  $J = 2.6$  Hz, 1H), 2.20 (td,  $J = 7.1, 2.6$  Hz, 2H), 1.88 (dt,  $J = 14.9, 7.2$  Hz, 2H), 1.48 - 1.40 (m, 2H);  $^{13}C$  NMR (125.83 MHz,  $CDCl_3$ ):  $\delta$  [ppm] = 189.97, 162.96, 136.22, 132.27, 128.66, 128.40, 126.21, 122.38, 121.26, 120.77, 110.78, 108.95, 84.18, 71.63, 63.54, 53.84, 52.41, 45.54, 28.74, 25.21, 17.33; HRMS (ESI): calc. for  $C_{21}H_{21}N_2O_4$   $[M+H]^+$ : 365.1496, found: 365.1493, diff: -0.70 ppm.

**Methyl-3-(prop-2-yn-1-yloxy)benzoate (115)<sup>[183]</sup>**

**115**  
 $C_{11}H_{10}O_3$   
Molecular Weight: 190.20

To a solution of methyl-3-hydroxybenzoate (5.00 g, 32.8 mmol, 1.00 eq) in acetone (100 mL) were added  $K_2CO_3$  (4.53 g, 32.8 mmol, 1.00 eq) followed by propargyl bromide (80% in toluene, 6.54 mL, 60.1 mmol, 1.85 eq). The suspension was heated under reflux for 24 h under nitrogen atmosphere. After addition of chilled water (20 mL) the layers were separated and the aqueous layer was extracted with  $Et_2O$  (3 x 40 mL). The combined organic extracts were washed with brine (100 mL), dried over  $Na_2SO_4$  and concentrated under reduced pressure giving compound **115** (6.24 g, 32.8 mmol, quant.) as yellow solid without further purification.

$R_f$  = 0.37 (hexanes:EtOAc 4:1);  $^1H$  NMR (360.13 MHz,  $CDCl_3$ ):  $\delta$  [ppm] = 7.71 - 7.66 (m, 1H), 7.64 (dd,  $J$  = 2.4, 1.3 Hz, 1H), 7.36 (t,  $J$  = 8.0 Hz, 1H), 7.18 (ddd,  $J$  = 8.3, 2.7, 1.0 Hz, 1H), 4.74 (d,  $J$  = 2.4 Hz, 2H), 3.91 (s, 3H), 2.53 (t,  $J$  = 2.4 Hz, 1H);  $^{13}C$  NMR (90.56 MHz,  $CDCl_3$ ):  $\delta$  [ppm] = 166.90, 157.63, 131.68, 129.62, 123.02, 120.40, 115.39, 78.25, 76.00, 56.14, 52.38; HRMS (ESI): calc. for  $C_{11}H_{11}O_3$   $[M+H]^+$ : 191.0703, found: 191.0703, diff: -0.02 ppm.

**3-(Prop-2-yn-1-yloxy)benzoic acid (106)<sup>[183]</sup>**

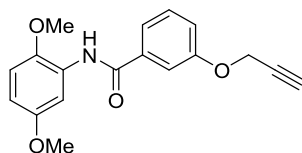
**106**  
 $C_{10}H_8O_3$   
Molecular Weight: 176.17

To a solution of **115** (5.00 g, 26.3 mmol, 1.00 eq) in EtOH (60 mL) was added a saturated aqueous solution of KOH (2.50 mL) and the reaction mixture was stirred for 16 h at room temperature. After addition of water (200 mL) and EtOAc (200 mL) the mixture was acidified by adding aqueous 1 M HCl (20 mL) and the layers were separated. The aqueous layer was extracted with EtOAc (4 x 20 mL) and the combined organic extracts were washed with brine (100 mL), dried over  $Na_2SO_4$  and concentrated under reduced pressure giving compound **106** (4.58 g, 26.0 mmol, 99%) as slightly yellow solid without further purification.

$R_f$  = 0.31 (hexanes:EtOAc 2:1);  $^1H$  NMR (360.13 MHz,  $CDCl_3$ ):  $\delta$  [ppm] = 12.94 (s, 1H), 7.57 (d,  $J$  = 7.6 Hz, 1H), 7.53 - 7.50 (m, 1H), 7.43 (t,  $J$  = 7.9 Hz, 1H), 7.23 (dd,  $J$  = 7.8, 2.3 Hz, 1H), 4.86 (d,  $J$  = 2.4 Hz, 2H), 3.59 (t,  $J$  = 2.3 Hz, 1H);  $^{13}C$  NMR (90.56 MHz,  $CDCl_3$ ):  $\delta$  [ppm] = 166.98, 157.16, 132.17, 129.72,

122.24, 119.82, 114.94, 78.97, 78.52, 55.57; **HRMS (ESI)**: calc. for  $C_{10}H_7O_3$   $[M-H]^-$ : 175.0390, found: 175.0400, diff: 5.83 ppm.

***N*-(2,5-Dimethoxyphenyl)-3-(prop-2-yn-1-yloxy)benzamide (116)**<sup>[183]</sup>

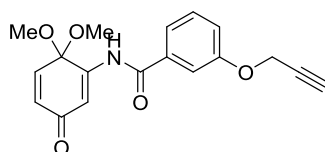


**116**  
 $C_{18}H_{17}NO_4$   
 Molecular Weight: 311.34

**106** (4.36 g, 24.8 mmol, 1.20 eq) was added to a solution of thionyl chloride (50 mL) containing a drop of *N,N*-dimethylformamide (cat.) and the reaction mixture was heated under reflux for 4 h under an inert atmosphere of nitrogen at 75 °C. The solvent was evaporated and the residue was dissolved in toluene (20 mL). After removing the solvent under reduced pressure the corresponding acetylenic acid chloride was redissolved in anhydrous THF (200 mL) and 2,5-dimethoxyaniline (3.16 g, 20.6 mmol, 1.00 eq) was added. After cooling the reaction mixture to 0 °C, pyridine (3.33 mL, 41.3 mmol, 2.00 eq) was added slowly and the mixture was stirred for 15 min at 0 °C followed by 6 h at room temperature. The reaction was quenched by adding aqueous 1 M HCl (50 mL) and extracted with EtOAc (4 x 30 mL). The combined organic extracts were washed with brine (100 mL), dried over  $Na_2SO_4$  and concentrated under reduced pressure. The crude product was purified by flash column chromatography (hexanes:EtOAc 2:1) giving compound **116** (6.29 g, 20.2 mmol, 98% over two steps) as a white solid.

$R_f$  = 0.55 (hexanes:EtOAc 2:1);  $^1H$  NMR (360.13 MHz,  $CDCl_3$ ):  $\delta$  [ppm] = 9.37 (s, 1H), 7.57 (t,  $J$  = 5.6 Hz, 2H), 7.52 (d,  $J$  = 3.1 Hz, 1H), 7.46 (t,  $J$  = 7.9 Hz, 1H), 7.21 (ddd,  $J$  = 8.3, 2.5, 0.8 Hz, 1H), 7.01 (d,  $J$  = 9.0 Hz, 1H), 6.74 (dd,  $J$  = 8.9, 3.1 Hz, 1H), 4.90 (d,  $J$  = 2.4 Hz, 2H), 3.79 (s, 3H), 3.72 (s, 3H), 3.63 (t,  $J$  = 2.4 Hz, 1H);  $^{13}C$  NMR (90.56 MHz,  $CDCl_3$ ):  $\delta$  [ppm] = 13C NMR (126 MHz, DMSO)  $\delta$  164.57, 157.25, 152.85, 145.28, 135.91, 129.77, 127.52, 120.29, 118.44, 113.70, 112.05, 110.18, 109.65, 79.07, 78.59, 56.24, 55.63, 55.43; **HRMS (ESI)**: calc. for  $C_{18}H_{18}NO_4$   $[M+H]^+$ : 312.1230, found: 312.1229, diff: -0.41 ppm.

***N*-(6,6-Dimethoxy-3-oxocyclohexa-1,4-dien-1-yl)-3-(prop-2-yn-1-yloxy)benzamide (117)**<sup>[182]</sup>

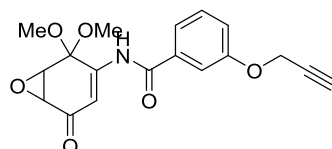


**117**  
 $C_{18}H_{17}NO_5$   
 Molecular Weight: 327.34

To a solution of **116** (2.00 g, 7.07 mmol, 1.00 eq) in anhydrous MeOH (70 mL) at 0 °C under nitrogen atmosphere was added portion wise  $\text{PhI}(\text{OPiv})_2$  (4.30 g, 10.6 mmol, 1.50 eq). The mixture was allowed to warm to room temperature, further stirred for 4 h and then diluted with EtOAc (50 mL) and saturated citric acid solution (25 mL). After stirring for 30 min at room temperature, the mixture was extracted with EtOAc (3 x 50 mL) and the combined organic extracts were washed with saturated  $\text{NaHCO}_3$  aqueous solution (20 mL), water (20 mL) and brine (50 mL). The combined organic extracts were dried over  $\text{Na}_2\text{SO}_4$ , concentrated under reduced pressure and purified by flash column chromatography (hexanes:EtOAc 2:1) to yield product **117** (2.07 g, 6.30 mmol, 89%) as brown solid.

$R_f$  = 0.13 (hexanes:EtOAc 2:1);  $^1\text{H}$  NMR (500.36 MHz,  $\text{CDCl}_3$ ):  $\delta$  [ppm] = 9.16 (s, 1H), 7.49 (t,  $J$  = 7.9 Hz, 1H), 7.40 (ddd,  $J$  = 10.1, 5.2, 1.3 Hz, 2H), 7.30 - 7.22 (m, 2H), 6.98 (d,  $J$  = 10.4 Hz, 1H), 6.41 (dd,  $J$  = 10.4, 2.1 Hz, 1H), 4.91 (d,  $J$  = 2.4 Hz, 2H), 3.63 (t,  $J$  = 2.4 Hz, 1H), 3.26 (s, 6H);  $^{13}\text{C}$  NMR (125.83 MHz,  $\text{CDCl}_3$ ):  $\delta$  [ppm] = 185.59, 166.84, 157.15, 148.72, 140.22, 134.95, 131.56, 129.91, 120.60, 119.24, 114.19, 112.72, 93.74, 78.93, 78.73, 55.70, 51.14; HRMS (ESI): calc. for  $\text{C}_{18}\text{H}_{18}\text{NO}_5$   $[\text{M}+\text{H}]^+$ : 328.1180, found: 328.1179, diff: -0.04 ppm.

*N*-(2,2-Dimethoxy-5-oxo-7-oxabicyclo[4.1.0]hept-3-en-3-yl)-3-(prop-2-yn-1-yloxy)benzamide (**118**)<sup>[124]</sup>



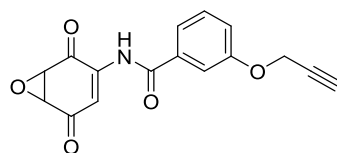
**118**  
 $\text{C}_{18}\text{H}_{17}\text{NO}_6$   
Molecular Weight: 343.33

To a solution of **106** (0.10 g, 0.59 mmol, 1.10 eq) in anhydrous DCM (10 mL) at 0 °C containing 1 drop of *N,N*-dimethylformamide (cat.) was slowly added oxalyl chloride (56.0  $\mu\text{L}$ , 0.66 mmol, 1.22 eq). The reaction mixture was stirred at room temperature for 2 h after which the solvent was evaporated and the corresponding acetylenic acid chloride was redissolved in anhydrous THF (5 mL) at 0 °C. A solution of lithium *tert*-butoxide (1 M in THF, 0.60 mL, 0.60 mmol, 1.12 eq) was added dropwise over 15 min to a stirred solution of **55** (0.10 g, 0.59 mmol, 1.00 eq) in dry THF at 0 °C. After stirring the reaction mixture at 0 °C for 30 min, the solution of acetylenic acid chloride in THF was added dropwise over 1 h. The solution was then allowed to warm to room temperature and stirred for further 5 h until HPLC-MS measurements showed complete conversion of the starting material. The reaction was quenched by adding aqueous  $\text{NH}_4\text{Cl}$  (5 mL) and water (5 mL) and extracted with EtOAc (3 x 30 mL). The combined organic extracts were washed with brine (50 mL), dried over  $\text{Na}_2\text{SO}_4$  and concentrated under reduced pressure. The crude product was purified

by preparative reversed-phase HPLC (C18 5.0  $\mu$ m, 30 x 150 mm column, gradient 2% B  $\rightarrow$  98% B over 17 min,  $t_R$  = 8.0 - 8.6 min) giving compound **118** (0.11 g, 0.32 mmol, 59% over two steps) as yellow needles.

**$^1\text{H}$  NMR** (500.13 MHz,  $\text{CDCl}_3$ ):  $\delta$  [ppm] = 9.17 (s, 1H), 7.50 (t,  $J$  = 7.9 Hz, 1H), 7.43 - 7.40 (m, 1H), 7.37 (dd,  $J$  = 2.4, 1.7 Hz, 1H), 7.27 (ddd,  $J$  = 8.2, 2.6, 0.9 Hz, 1H), 7.00 (d,  $J$  = 2.1 Hz, 1H), 4.91 (d,  $J$  = 2.4 Hz, 2H), 4.25 (d,  $J$  = 4.3 Hz, 1H), 3.64 (dt,  $J$  = 6.4, 2.2 Hz, 2H), 3.60 (s, 3H), 3.33 (s, 3H);  **$^{13}\text{C}$  NMR** (75,48 MHz,  $\text{CDCl}_3$ ):  $\delta$  [ppm] = 193.32, 166.36, 157.20, 146.98, 134.83, 130.06, 120.50, 119.46, 113.89, 107.63, 95.32, 78.90, 78.78, 55.66, 51.52, 51.23, 51.07, 50.39; **HRMS (ESI)**: calc. for  $\text{C}_{18}\text{H}_{18}\text{NO}_6$   $[\text{M}+\text{H}]^+$ : 344.1129, found: 344.1128, diff: -0.14 ppm.

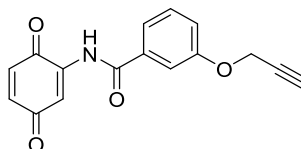
***N*-(2,5-Dioxo-7-oxabicyclo[4.1.0]hept-3-en-3-yl)-3-(prop-2-yn-1-yloxy)benzamide (FM242)<sup>[182]</sup>**



**FM242**  
 $\text{C}_{16}\text{H}_{11}\text{NO}_5$   
Molecular Weight: 297.27

To a solution of **118** (80.0 mg, 0.23 mmol, 1.00 eq) in anhydrous DCM (7 mL) at -20  $^{\circ}\text{C}$  was added  $\text{BF}_3 \cdot \text{OEt}_2$  (74.0  $\mu\text{L}$ , 0.58 mmol, 2.50 eq). The mixture was allowed to warm to room temperature and further stirred for 14 h. The reaction was quenched by adding water (5 mL) and extracted with  $\text{CHCl}_3$  (3 x 10 mL). The combined organic extracts were washed with brine (20 mL), dried over  $\text{Na}_2\text{SO}_4$  and concentrated under reduced pressure. The crude product was purified by preparative reversed-phase HPLC (C18 5.0  $\mu$ m, 30 x 150 mm column, gradient 2% B  $\rightarrow$  98% B over 17 min,  $t_R$  = 7.2 - 8.4 min) giving compound **FM242** (48.0 mg, 0.16 mmol, 70%) as white powder.

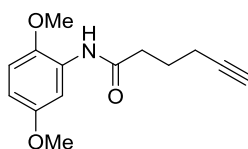
$R_f$  = 0.61 (hexanes:EtOAc 2:1;  **$^1\text{H}$  NMR** (500.36 MHz,  $\text{CDCl}_3$ ):  $\delta$  [ppm] = 9.75 (s, 1H), 7.54 - 7.45 (m, 3H), 7.31 - 7.25 (m, 1H), 7.23 (d,  $J$  = 2.4 Hz, 1H), 4.90 (d,  $J$  = 2.4 Hz, 2H), 4.19 (d,  $J$  = 4.0 Hz, 1H), 3.99 (dd,  $J$  = 4.0, 2.4 Hz, 1H), 3.63 (t,  $J$  = 2.4 Hz, 1H);  **$^{13}\text{C}$  NMR** (125.83 MHz,  $\text{CDCl}_3$ ):  $\delta$  [ppm] = 192.21, 187.86, 166.35, 157.24, 140.79, 134.38, 130.00, 120.79, 119.51, 115.33, 114.15, 78.92, 78.73, 55.73, 53.94, 53.15; **HRMS (ESI)**: calc. for  $\text{C}_{16}\text{H}_{12}\text{NO}_5$   $[\text{M}+\text{H}]^+$ : 298.0710, found: 298.0709, diff: -0.32 ppm.

***N*-(3,6-Dioxocyclohexa-1,4-dien-1-yl)-3-(prop-2-yn-1-yloxy)benzamide (FM272)**<sup>[134]</sup>

**FM272**  
 $C_{16}H_{11}NO_4$   
 Molecular Weight: 281.27

To a solution of **117** (0.20 g, 0.61 mmol, 1.00 eq) in anhydrous DCM (10 mL) Montmorillonite K10 (400 mg) was added in small portions and the reaction was stirred for 16 h at room temperature. The solution was filtered through Celite, which was additionally washed with DCM (3 x 10 mL). The combined filtrates were washed with brine (10 mL), dried over  $Na_2SO_4$  and concentrated under reduced pressure. The residue was purified by flash column chromatography (hexanes:EtOAc 2:1) to yield product **FM272** (80.0 mg, 0.28 mmol, 46%) as orange solid.

$R_f$  = 0.34 (hexanes:EtOAc 2:1);  $^1H$  NMR (500.36 MHz,  $CDCl_3$ ):  $\delta$  [ppm] = 9.50 (s, 1H), 7.55 – 7.48 (m, 3H), 7.46 (d,  $J$  = 2.6 Hz, 1H), 7.28 (ddd,  $J$  = 7.5, 2.6, 1.7 Hz, 1H), 7.01 (d,  $J$  = 10.1 Hz, 1H), 6.87 (dd,  $J$  = 10.1, 2.6 Hz, 1H), 4.91 (d,  $J$  = 2.4 Hz, 2H), 3.63 (t,  $J$  = 2.4 Hz, 1H);  $^{13}C$  NMR (125.83 MHz,  $CDCl_3$ ):  $\delta$  [ppm] = 188.22, 182.19, 166.08, 157.29, 139.50, 137.45, 134.56, 134.38, 130.08, 120.58, 119.50, 114.68, 114.03, 78.92, 78.75, 55.73; HRMS (ESI): calc. for  $C_{16}H_{10}NO_4$   $[M-H]^-$ : 280.0604, found: 280.0615, diff: 3.91 ppm.

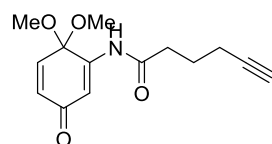
***N*-(2,5-Dimethoxyphenyl)hex-5-ynamide (119)**

**119**  
 $C_{14}H_{17}NO_3$   
 Molecular Weight: 247.29

To a solution of 2,5-dimethoxyaniline (**50**) (5.00 g, 32.6 mmol, 1.00 eq) and hex-5-ynoic acid (**102**) (4.30 mL, 39.2 mmol, 1.20 eq) in anhydrous DCM (200 mL) was added dropwise DIC (6.10 mL, 39.3 mmol, 1.20 eq) at room temperature. The reaction was stirred at room temperature for 16 h, quenched by adding aqueous HCl (1 M, 50 mL), filtered and extracted with DCM (3 x 50 mL). The combined organic extracts were washed with brine (100 mL), dried over  $Na_2SO_4$  and concentrated under reduced pressure. The crude product was purified by flash column chromatography (hexanes:EtOAc 2:1) followed by recrystallization (hexanes:EtOAc 9:1, 50 mL) giving compound **119** (6.30 g, 25.5 mmol, 78%) as white needles.

$R_f$  = 0.40 (hexanes:EtOAc 2:1);  $^1\text{H NMR}$  (360.13 MHz,  $\text{CDCl}_3$ ):  $\delta$  [ppm] = 8.12 (d,  $J$  = 2.7 Hz, 1H), 7.82 (s, 1H), 6.78 (d,  $J$  = 8.9 Hz, 1H), 6.56 (dd,  $J$  = 8.9, 3.0 Hz, 1H), 3.84 (s, 3H), 3.78 (s, 3H), 2.54 (t,  $J$  = 7.3 Hz, 2H), 2.33 (td,  $J$  = 6.8, 2.6 Hz, 2H), 2.01 - 1.91 (m, 3H);  $^{13}\text{C NMR}$  (90.56 MHz,  $\text{CDCl}_3$ ):  $\delta$  [ppm] = 170.51, 154.04, 142.01, 128.45, 110.88, 108.74, 105.96, 83.56, 69.41, 56.36, 55.92, 36.45, 24.09, 17.99; **HRMS (ESI)**: calc. for  $\text{C}_{14}\text{H}_{17}\text{NO}_3$   $[\text{M}+\text{H}]^+$ : 248.1281, found: 248.1281, diff: -0.02 ppm.

***N*-(6,6-Dimethoxy-3-oxocyclohexa-1,4-dien-1-yl)hex-5-ynamide (120)**<sup>[182]</sup>

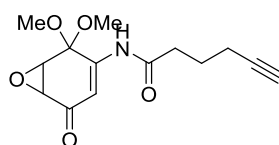


**120**  
 $\text{C}_{14}\text{H}_{17}\text{NO}_4$   
 Molecular Weight: 263.29

To a solution of **119** (2.00 g, 8.09 mmol, 1.00 eq) in anhydrous MeOH (100 mL) at 0 °C under nitrogen atmosphere was added portion wise  $\text{PhI}(\text{OPiv})_2$  (3.78 g, 9.30 mmol, 1.10 eq). The mixture was allowed to warm to room temperature, further stirred for 16 h and then diluted with EtOAc (50 mL) and saturated citric acid solution (25 mL). After stirring for 30 min at room temperature, the mixture was extracted with EtOAc (3 x 50 mL) and the combined organic extracts were washed with saturated  $\text{NaHCO}_3$  aqueous solution (30 mL), water (30 mL) and brine (50 mL). The combined organic extracts were dried over  $\text{Na}_2\text{SO}_4$ , concentrated under reduced pressure and purified by flash column chromatography (hexanes:EtOAc 1:1) to yield product **120** (1.86 g, 7.07 mmol, 87%) as yellow solid.

$R_f$  = 0.39 (hexanes:EtOAc 1:1);  $^1\text{H NMR}$  (360.13 MHz,  $\text{CDCl}_3$ ):  $\delta$  [ppm] = 7.44 (s, 1H), 7.37 (d,  $J$  = 2.0 Hz, 1H), 6.55 (d,  $J$  = 10.4 Hz, 1H), 6.43 (dd,  $J$  = 10.4, 2.0 Hz, 1H), 3.27 (s, 6H), 2.55 (t,  $J$  = 7.3 Hz, 2H), 2.31 (td,  $J$  = 6.8, 2.6 Hz, 2H), 2.01 (t,  $J$  = 2.6 Hz, 1H), 1.92 (p,  $J$  = 7.0 Hz, 2H);  $^{13}\text{C NMR}$  (90.56 MHz,  $\text{CDCl}_3$ ):  $\delta$  [ppm] = 185.99, 171.99, 146.96, 138.41, 133.55, 114.10, 94.40, 83.03, 69.79, 51.65, 36.24, 23.50, 17.73; **HRMS (ESI)**: calc. for  $\text{C}_{14}\text{H}_{18}\text{NO}_4$   $[\text{M}+\text{H}]^+$ : 264.1230, found: 264.1220, diff: -4.12 ppm.

***N*-(2,2-Dimethoxy-5-oxo-7-oxabicyclo[4.1.0]hept-3-en-3-yl)hex-5-ynamide (121)**<sup>[124]</sup>



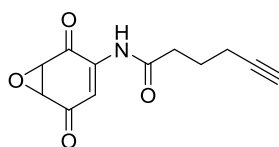
**121**  
 $\text{C}_{14}\text{H}_{17}\text{NO}_5$   
 Molecular Weight: 279.29



A solution of lithium *tert*-butoxide (1M in THF, 1.20 mL, 1.20 mmol, 1.12 eq) was added dropwise over 15 min to a stirred solution of **55** (0.20 g, 1.08 mmol, 1.00 eq) in dry THF (30 mL) at 0 °C. After stirring the reaction mixture at 0 °C for 30 min, a solution of **102** (0.14 mL, 1.18 mmol, 1.10 eq) in THF (5 mL) was added dropwise over 1 h. The solution was then allowed to warm to room temperature and stirred for further 16 h until HPLC-MS measurements showed complete conversion of the starting material. The reaction was quenched by adding aqueous NH<sub>4</sub>Cl (5 mL) and water (5 mL) and extracted with EtOAc (3 x 30 mL). The combined organic extracts were washed with brine (50 mL), dried over Na<sub>2</sub>SO<sub>4</sub> and concentrated under reduced pressure. The crude product was purified flash column chromatography (hexanes:EtOAc 1:1) giving compound **121** (90.0 mg, 0.32 mmol, 30%) as white solid.

$R_f$  = 0.38 (hexanes:EtOAc 1:1); <sup>1</sup>H NMR (360.13 MHz, CDCl<sub>3</sub>):  $\delta$  [ppm] = 7.72 (s, 1H), 7.11 (d,  $J$  = 2.1 Hz, 1H), 3.81 (d,  $J$  = 4.2 Hz, 1H), 3.63 (s, 3H), 3.50 (dd,  $J$  = 4.2, 2.1 Hz, 1H), 3.28 (s, 3H), 2.51 (t,  $J$  = 7.3 Hz, 2H), 2.27 (td,  $J$  = 6.8, 2.6 Hz, 2H), 1.99 (t,  $J$  = 2.6 Hz, 1H), 1.86 (dd,  $J$  = 14.0, 6.9 Hz, 2H); <sup>13</sup>C NMR (90.56 MHz, CDCl<sub>3</sub>):  $\delta$  [ppm] = 192.88, 171.62, 145.18, 108.95, 95.53, 83.05, 69.77, 52.18, 51.54, 51.39, 50.79, 36.45, 23.45, 17.71; HRMS (ESI): calc. for C<sub>14</sub>H<sub>18</sub>NO<sub>5</sub> [M+H]<sup>+</sup>: 280.1180, found: 280.1184, diff: 1.52 ppm.

***N*-(2,5-Dioxo-7-oxabicyclo[4.1.0]hept-3-en-3-yl)hex-5-ynamide (FM209)<sup>[182]</sup>**



**FM209**  
C<sub>12</sub>H<sub>11</sub>NO<sub>4</sub>  
Molecular Weight: 233.22

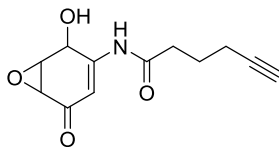
To a solution of **121** (0.10 g, 0.36 mmol, 1.00 eq) in anhydrous DCM (15 mL) at -10 °C was added BF<sub>3</sub> · OEt<sub>2</sub> (0.23 mL, 1.80 mmol, 5.00 eq). The mixture was allowed to warm to room temperature and further stirred for 2 h. The reaction was quenched by adding water (5 mL) and extracted with CHCl<sub>3</sub> (3 x 10 mL). The combined organic extracts were washed with brine (20 mL), dried over Na<sub>2</sub>SO<sub>4</sub> and concentrated under reduced pressure. The crude product was purified by flash column chromatography (hexanes:EtOAc 1:1) giving compound **FM209** (72.0 mg, 0.31 mmol, 86%) as yellow solid.

$R_f$  = 0.35 (hexanes:EtOAc 1:1); <sup>1</sup>H NMR (360.13 MHz, CDCl<sub>3</sub>):  $\delta$  [ppm] = 7.90 (s, 1H), 7.52 (d,  $J$  = 2.3 Hz, 1H), 3.91 (d,  $J$  = 3.7 Hz, 1H), 3.82 (dd,  $J$  = 3.6, 2.3 Hz, 1H), 2.58 (t,  $J$  = 7.3 Hz, 2H), 2.29 (td,  $J$  = 6.7, 2.6 Hz, 2H), 2.01 (t,  $J$  = 2.6 Hz, 1H), 1.88 (dd,  $J$  = 14.0, 7.0 Hz, 2H); <sup>13</sup>C NMR (90.56 MHz, CDCl<sub>3</sub>):

$\delta$  [ppm] = 191.17, 188.21, 171.84, 138.63, 115.63, 82.91, 69.96, 53.96, 52.61, 36.16, 23.32, 17.74;

**HRMS (ESI):** calc. for  $C_{12}H_{12}NO_4$   $[M+H]^+$ : 235.0839, found: 234.0761, diff: 0.08 ppm.

***N*-(2-Hydroxy-5-oxo-7-oxabicyclo[4.1.0]hept-3-en-3-yl)hex-5-ynamide (FM249)<sup>[133]</sup>**

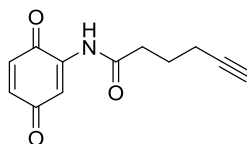


**FM249**  
 $C_{12}H_{13}NO_4$   
Molecular Weight: 235.24

To a solution of **FM209** (44.0 mg, 0.19 mmol, 1.00 eq) in anhydrous MeOH (5 mL) was added  $NaBH(OAc)_3$  (40.0 mg, 0.19 mmol, 1.00 eq) at 0 °C. The mixture was stirred for 20 min at 0 °C and then allowed to warm to room temperature. After stirring for 2 h TLC showed complete consumption of the starting material and the mixture was therefore quenched with water (5 mL) and extracted with EtOAc (3 x 10 mL). The combined organic extracts were washed with brine (10 mL), dried over  $Na_2SO_4$  and concentrated under reduced pressure. The crude product was purified by preparative reversed-phase HPLC (C18 5.0  $\mu$ m, 30 x 150 mm column, gradient 2% B  $\rightarrow$  20% B over 13 min,  $t_R$  = 7.6 - 9.2 min) giving racemic compound **FM249** (24.0 mg, 0.10 mmol, 53%) as colorless oil.

**$^1H$  NMR** (500.36 MHz,  $CDCl_3$ ):  $\delta$  [ppm] = 10.00 (s, 1H), 9.36 (s, 1H), 6.67 (d,  $J$  = 1.8 Hz, 1H), 6.65 (dd,  $J$  = 2.1, 1.2 Hz, 1H), 6.21 (d,  $J$  = 7.8 Hz, 1H), 6.08 (d,  $J$  = 8.7 Hz, 1H), 4.65 (ddd,  $J$  = 7.8, 2.8, 1.1 Hz, 1H), 4.50 (d,  $J$  = 8.6 Hz, 1H), 3.79 (dd,  $J$  = 4.2, 2.9 Hz, 1H), 3.71 (dd,  $J$  = 3.8, 1.5 Hz, 1H), 3.40 - 3.36 (m, 1H), 2.85 - 2.81 (m, 1H), 2.50 (m, 2H), 2.45 (t,  $J$  = 7.4 Hz, 1H), 2.18 (td,  $J$  = 7.1, 2.6 Hz, 2H), 1.69 (m, 2H);  **$^{13}C$  NMR** (125.83 MHz,  $CDCl_3$ ):  $\delta$  [ppm] = 194.35, 194.18, 173.75, 173.55, 152.29, 151.88, 106.68, 106.10, 84.32, 84.31, 72.27, 72.24, 63.98, 63.72, 55.12, 54.24, 53.28, 51.97, 35.88, 35.74, 24.01, 23.85, 17.66; **HRMS (ESI):** calc. for  $C_{12}H_{14}NO_4$   $[M+H]^+$ : 236.0917, found: 236.0917, diff: -0.05 ppm.

***N*-(3,6-Dioxocyclohexa-1,4-dien-1-yl)hex-5-ynamide (FM256)<sup>[134]</sup>**



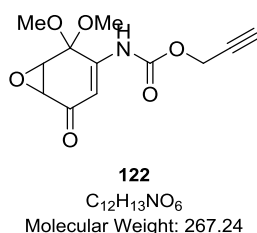
**FM256**  
 $C_{12}H_{11}NO_3$   
Molecular Weight: 217.22

To a solution of **120** (87.0 mg, 0.33 mmol, 1.00 eq) in anhydrous DCM (10 mL) Montmorillonite K10 (200 mg) was added in small portions and the reaction was stirred for 16 h at room temperature.

The solution was filtered through Celite, which was additionally washed with DCM (3 x 10 mL). The combined filtrates were washed with brine (10 mL), dried over Na<sub>2</sub>SO<sub>4</sub> and concentrated under reduced pressure. The crude product was purified by preparative reversed-phase HPLC (C18 5.0 µm, 30 x 150 mm column, gradient 2% B → 98% B over 17 min, *t<sub>R</sub>* = 5.4 - 7.0 min) giving compound **FM256** (53.0 mg, 0.24 mmol, 73%) as yellow solid.

<sup>1</sup>H NMR (500.36 MHz, CDCl<sub>3</sub>): δ [ppm] = 9.76 (s, 1H), 7.40 (d, *J* = 2.6 Hz, 1H), 6.90 (d, *J* = 10.1 Hz, 1H), 6.79 (dd, *J* = 10.1, 2.6 Hz, 1H), 2.82 (t, *J* = 2.6 Hz, 1H), 2.62 (t, *J* = 7.3 Hz, 2H), 2.18 (td, *J* = 7.1, 2.6 Hz, 2H), 1.71 (dd, *J* = 14.5, 7.2 Hz, 2H); <sup>13</sup>C NMR (125.83 MHz, CDCl<sub>3</sub>): δ [ppm] = 188.52, 182.69, 173.61, 139.81, 136.98, 134.41, 113.96, 83.88, 71.80, 35.25, 23.63, 17.27; HRMS (ESI): calc. for C<sub>12</sub>H<sub>12</sub>NO<sub>3</sub> [M+H]<sup>+</sup>: 218.0812, found: 218.0812, diff: 0.09 ppm.

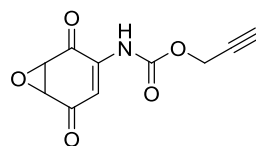
**Prop-2-yn-1-yl (2,2-dimethoxy-5-oxo-7-oxabicyclo[4.1.0]hept-3-en-3-yl)carbamate (122)**<sup>[124]</sup>



A solution of lithium *tert*-butoxide (1 M in THF, 0.22 mL, 0.22 mmol, 1.20 eq) was added dropwise over 15 min to a stirred solution of **55** (33.0 mg, 0.18 mmol, 1.00 eq) in dry THF (10 mL) at 0 °C. After stirring the reaction mixture at 0 °C for 30 min, a solution of prop-2-yn-1-yl carbonochloridate (**107**) (19.0 µL, 0.19 mmol, 1.10 eq) in THF (2 mL) was added dropwise over 1 h at 0 °C. The solution was then allowed to warm to room temperature and stirred for further 2 h until HPLC-MS analysis showed complete conversion of the starting material. The reaction was quenched by adding aqueous NH<sub>4</sub>Cl (2 mL) and water (2 mL) and extracted with EtOAc (3 x 10 mL). The combined organic extracts were washed with brine (20 mL), dried over Na<sub>2</sub>SO<sub>4</sub> and concentrated under reduced pressure. The crude product was purified by preparative reversed-phase HPLC (C18 5.0 µm, 30 x 150 mm column, gradient 2% B → 98% B over 17 min, *t<sub>R</sub>* = 8.0 - 8.6 min) giving compound **122** (30.0 mg, 0.11 mmol, 61%) as white solid.

*R<sub>f</sub>* = 0.42 (hexanes:EtOAc 1:1); <sup>1</sup>H NMR (500.36 MHz, CDCl<sub>3</sub>): δ [ppm] = 9.32 (s, 1H), 6.55 (d, *J* = 2.1 Hz, 1H), 4.79 (dd, *J* = 3.1, 2.5 Hz, 2H), 4.14 (d, *J* = 4.2 Hz, 1H), 3.64 (t, *J* = 2.4 Hz, 1H), 3.55 (dd, *J* = 4.2, 2.1 Hz, 1H), 3.48 (s, 3H), 3.26 (s, 3H); <sup>13</sup>C NMR (125.83 MHz, CDCl<sub>3</sub>): δ [ppm] = 192.74, 152.23, 148.28, 106.08, 95.24, 78.37, 78.22, 53.14, 51.48, 51.47, 51.11, 49.84; HRMS (ESI): calc. for C<sub>12</sub>H<sub>14</sub>NO<sub>6</sub> [M+H]<sup>+</sup>: 268.0816, found: 268.0815, diff: -0.17 ppm.

Prop-2-yn-1-yl (2,5-dioxo-7-oxabicyclo[4.1.0]hept-3-en-3-yl)carbamate (FM233)<sup>[182]</sup>

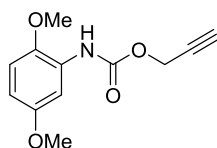


**FM233**  
C<sub>10</sub>H<sub>7</sub>NO<sub>5</sub>  
Molecular Weight: 221.17

To a solution of **122** (0.12 g, 0.45 mmol, 1.00 eq) in anhydrous DCM (15 mL) at -10 °C was added BF<sub>3</sub> · OEt<sub>2</sub> (0.14 mL, 1.12 mmol, 2.50 eq). The mixture was allowed to warm to room temperature and further stirred for 6 h. The reaction was quenched by adding water (5 mL) and extracted with CHCl<sub>3</sub> (3 x 10 mL). The combined organic extracts were washed with brine (20 mL), dried over Na<sub>2</sub>SO<sub>4</sub> and concentrated under reduced pressure. The crude product was purified by preparative reversed-phase HPLC (C18 5.0 μm, 30 x 150 mm column, gradient 2% B → 98% B over 17 min, *t<sub>R</sub>* = 4.8 - 6.2 min) giving compound **FM233** (81.0 mg, 0.37 mmol, 81%) as slightly red solid.

*R<sub>f</sub>* = 0.58 (hexanes:EtOAc 1:1); <sup>1</sup>H NMR (500.36 MHz, CDCl<sub>3</sub>): δ [ppm] = 7.50 (s, 1H), 7.20 (d, *J* = 2.2 Hz, 1H), 4.78 (d, *J* = 2.5 Hz, 2H), 3.92 (d, *J* = 3.7 Hz, 1H), 3.83 (dd, *J* = 3.6, 2.3 Hz, 1H), 2.55 (t, *J* = 2.4 Hz, 1H); <sup>13</sup>C NMR (125.83 MHz, CDCl<sub>3</sub>): δ [ppm] = 190.58, 187.40, 151.28, 139.19, 114.35, 76.70, 76.18, 53.99, 52.63; HRMS (ESI): calc. for C<sub>10</sub>H<sub>7</sub>NO<sub>5</sub> [M+H]<sup>+</sup>: 222.0397, found: 222.0397, diff: 0.01 ppm.

Prop-2-yn-1-yl (2,5-dimethoxyphenyl)carbamate (**123**)

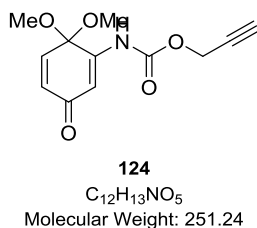


**123**  
C<sub>12</sub>H<sub>13</sub>NO<sub>4</sub>  
Molecular Weight: 235.24

**107** (1.9 mL, 19.6 mmol, 10.0 eq) and trimethylamine (0.54 mL, 3.92 mmol, 2.00 eq) were added to anhydrous DCM (3 mL) under an inert atmosphere of nitrogen at 0 °C and *N,N*-dimethylformamide (cat.) was added. 2,5-Dimethoxyaniline (**50**) (0.30 mg, 2.00 mmol, 1.00 eq) was dissolved in anhydrous DCM (20 mL) and the solution was slowly added dropwise to the reaction mixture, which was then allowed to warm to room temperature and further stirred for 16 h. The reaction was quenched by adding aqueous 2 M HCl (10 mL) and extracted with DCM (4 x 30 mL). The combined organic extracts were washed with brine (100 mL), dried over Na<sub>2</sub>SO<sub>4</sub> and concentrated under reduced pressure. The crude product was purified by flash column chromatography (hexanes:EtOAc 2:1) giving compound **123** (0.30 g, 1.28 mmol, 64%) as white solid.

$R_f$  = 0.56 (hexanes:EtOAc 2:1);  $^1\text{H NMR}$  (500.13 MHz,  $\text{CDCl}_3$ ):  $\delta$  [ppm] = 8.72 (s, 1H), 7.29 (s, 1H), 6.93 (d,  $J$  = 8.9 Hz, 1H), 6.63 (dd,  $J$  = 8.9, 3.0 Hz, 1H), 4.74 (d,  $J$  = 2.4 Hz, 2H), 3.73 (s, 3H), 3.68 (s, 3H), 3.57 (t,  $J$  = 2.4 Hz, 1H);  $^{13}\text{C NMR}$  (125.83 MHz,  $\text{CDCl}_3$ ):  $\delta$  [ppm] = 152.99, 152.93, 144.38, 127.56, 112.17, 108.37, 79.02, 77.63, 56.23, 55.35, 52.10; **HRMS (ESI)**: calc. for  $\text{C}_{12}\text{H}_{14}\text{NO}_4$   $[\text{M}+\text{H}]^+$ : 236.0917, found: 236.0917, diff: -0.07 ppm.

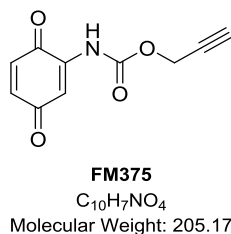
**Prop-2-yn-1-yl (6,6-dimethoxy-3-oxocyclohexa-1,4-dien-1-yl)carbamate (124)**<sup>[182]</sup>



To a solution of **123** (0.25 g, 1.10 mmol, 1.00 eq) in anhydrous MeOH (20 mL) at 0 °C under nitrogen atmosphere was added portion wise  $\text{PhI}(\text{OPiv})_2$  (0.48 g, 1.17 mmol, 1.10 eq). The mixture was allowed to warm to room temperature, further stirred for 16 h and then diluted with EtOAc (50 mL). After stirring for 30 min at room temperature, the mixture was extracted with EtOAc (3 x 50 mL) and the combined organic extracts were washed with saturated  $\text{NaHCO}_3$  aqueous solution, water and brine. The combined organic extracts were dried over  $\text{Na}_2\text{SO}_4$ , concentrated under reduced pressure and purified by flash column chromatography (hexanes:EtOAc 2:1) to yield product **124** (0.20 g, 0.80 mmol, 75%) as yellow solid.

$R_f$  = 0.36 (hexanes:EtOAc 2:1);  $^1\text{H NMR}$  (500.36 MHz,  $\text{CDCl}_3$ ):  $\delta$  [ppm] = 9.48 (s, 1H), 6.89 (d,  $J$  = 10.3 Hz, 1H), 6.82 (d,  $J$  = 2.1 Hz, 1H), 6.32 (dd,  $J$  = 10.3, 2.1 Hz, 1H), 4.78 (d,  $J$  = 2.4 Hz, 2H), 3.63 (t,  $J$  = 2.4 Hz, 1H), 3.18 (s, 6H);  $^{13}\text{C NMR}$  (125.83 MHz,  $\text{CDCl}_3$ ):  $\delta$  [ppm] = 185.21, 152.64, 149.88, 140.26, 131.02, 110.84, 93.59, 78.40, 78.19, 52.91, 50.87; **HRMS (ESI)**: calc. for  $\text{C}_{12}\text{H}_{14}\text{NO}_5$   $[\text{M}+\text{H}]^+$ : 252.0867, found: 371.0967, diff: 0.02 ppm.

**Prop-2-yn-1-yl (3,6-dioxocyclohexa-1,4-dien-1-yl)carbamate (FM375)**<sup>[134]</sup>

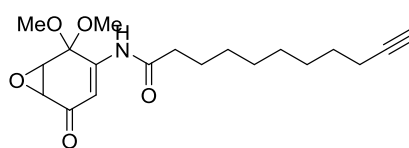


To a solution of **124** (0.10 g, 0.40 mmol, 1.00 eq) in anhydrous DCM (10 mL) Montmorillonite K10 (200 mg) was added in small portions and the reaction was stirred for 16 h at room temperature. The solution was filtered through Celite, which was additionally washed with DCM (3 x 10 mL). The

combined filtrates were washed with brine (10 mL), dried over Na<sub>2</sub>SO<sub>4</sub> and concentrated under reduced pressure. The crude product was purified by flash column chromatography (hexanes:EtOAc 2:1) giving compound **FM375** (21.0 mg, 0.10 mmol, 25%) as orange solid.

$R_f$  = 0.44 (hexanes:EtOAc 2:1); <sup>1</sup>H NMR (360.13 MHz, CDCl<sub>3</sub>): δ [ppm] = 7.64 (s, 1H), 7.27 (d,  $J$  = 2.2 Hz, 1H), 6.79 (d,  $J$  = 10.1 Hz, 1H), 6.74 (dd,  $J$  = 10.1, 2.3 Hz, 1H), 4.81 (d,  $J$  = 2.5 Hz, 2H), 2.55 (t,  $J$  = 2.5 Hz, 1H); <sup>13</sup>C NMR (90.56 MHz, CDCl<sub>3</sub>): δ [ppm] = 187.33, 182.05, 151.38, 138.84, 138.35, 133.36, 113.75, 77.36, 76.03, 53.87; HRMS (ESI): calc. for C<sub>10</sub>H<sub>8</sub>NO<sub>4</sub> [M+H]<sup>+</sup>: 206.0448, found: 206.0444, diff: -1.93 ppm.

***N*-(2,2-Dimethoxy-5-oxo-7-oxabicyclo[4.1.0]hept-3-en-3-yl)undec-10-ynamide (**125**)<sup>[124]</sup>**



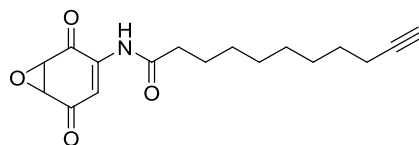
**125**  
C<sub>19</sub>H<sub>27</sub>NO<sub>5</sub>  
Molecular Weight: 349.43

To a solution of undec-10-ynoic acid (**104**) (0.16 g, 0.88 mmol, 1.5 eq) in anhydrous DCM (5 mL) at 0 °C containing 1 drop of *N,N*-dimethylformamide (cat.) was slowly added oxalyl chloride (84.0 μL, 1.00 mmol, 1.22 eq). The reaction mixture was stirred at 0 °C for 1 h after which the solvent was evaporated under reduced pressure and the corresponding acetylenic acid chloride was redissolved in anhydrous THF (5 mL) at -10 °C. A solution of lithium *tert*-butoxide (1 M in THF, 0.90 mL, 0.90 mmol, 1.12 eq) was added dropwise over 15 min to a stirred solution of **55** (0.15 g, 0.81 mmol, 1.00 eq) in dry THF at -10 °C. After stirring the reaction mixture at 0 °C for 30 min, the solution of acetylenic acid chloride in THF was added dropwise over 1 h. The solution was then allowed to warm to room temperature and stirred for further 3 h until HPLC-MS analysis showed complete conversion of the starting material. The reaction was quenched by adding aqueous NH<sub>4</sub>Cl (5 mL) and water (5 mL) and extracted with EtOAc (3 x 30 mL). The combined organic extracts were washed with brine (50 mL), dried over Na<sub>2</sub>SO<sub>4</sub> and concentrated under reduced pressure. The crude product was purified by preparative reversed-phase HPLC (C18 5.0 μm, 30 x 150 mm column, gradient 2% B → 98% B over 17 min,  $t_R$  = 9.2 - 10.0 min) giving compound **125** (0.14 g, 0.41 mmol, 51% over two steps) as slightly yellow solid.

$R_f$  = 0.31 (hexanes:EtOAc 2:1); <sup>1</sup>H NMR (500.36 MHz, CDCl<sub>3</sub>): δ [ppm] = 9.23 (s, 1H), 6.94 (d,  $J$  = 2.1 Hz, 1H), 4.14 (d,  $J$  = 4.2 Hz, 1H), 3.54 (dd,  $J$  = 4.2, 2.1 Hz, 1H), 3.53 (s, 3H), 3.25 (s, 3H), 2.74 (t,  $J$  = 2.6 Hz, 1H), 2.49 - 2.42 (m, 2H), 2.13 (td,  $J$  = 7.0, 2.6 Hz, 2H), 1.54 - 1.46 (m, 2H), 1.41 (dd,  $J$  = 14.7, 7.3 Hz, 2H), 1.35 - 1.22 (m, 8H); <sup>13</sup>C NMR (125.83 MHz, CDCl<sub>3</sub>): δ [ppm] = 193.26, 174.15, 147.31,

107.33, 95.20, 84.58, 71.21, 51.54, 51.38, 51.00, 50.18, 36.59, 28.69, 28.48, 28.41, 28.13, 27.95, 24.73, 17.69; **HRMS (ESI)**: calc. for  $C_{19}H_{28}NO_5$   $[M+H]^+$ : 350.1962, found: 350.1972, diff: 2.82 ppm.

***N*-(2,5-Dioxo-7-oxabicyclo[4.1.0]hept-3-en-3-yl)undec-10-ynamide (FM243)**<sup>[182]</sup>

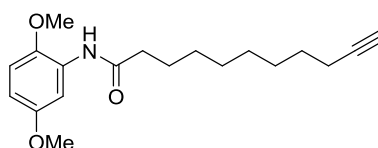


**FM243**  
 $C_{17}H_{21}NO_4$   
Molecular Weight: 303.36

To a solution of **125** (0.10 g, 0.29 mmol, 1.00 eq) in anhydrous DCM (7 mL) at -10 °C was added  $BF_3 \cdot OEt_2$  (91.0  $\mu$ L, 0.72 mmol, 2.50 eq). The mixture was allowed to warm to room temperature and further stirred for 16 h after which the reaction was quenched by adding water (5 mL) and extracted with  $CHCl_3$  (3 x 10 mL). The combined organic extracts were washed with brine (20 mL), dried over  $Na_2SO_4$  and concentrated under reduced pressure. The crude product was purified by preparative reversed-phase HPLC (C18 5.0  $\mu$ m, 30 x 150 mm column, gradient 2% B  $\rightarrow$  98% B over 17 min,  $t_R$  = 9.2 - 10.2 min) giving compound **FM243** (73.0 mg, 0.24 mmol, 83%) as white powder.

$R_f$  = 0.61 (hexanes:EtOAc 2:1);  $^1H$  NMR (500.13 MHz,  $CDCl_3$ ):  $\delta$  [ppm] = 7.80 (s, 1H), 7.54 (d,  $J$  = 2.3 Hz, 1H), 3.91 (d,  $J$  = 3.7 Hz, 1H), 3.83 (dd,  $J$  = 3.7, 2.3 Hz, 1H), 2.42 – 2.38 (m, 2H), 2.20 – 2.16 (m, 2H), 1.94 (t,  $J$  = 2.6 Hz, 1H), 1.67 (d,  $J$  = 7.4 Hz, 2H), 1.57 – 1.50 (m, 8H), 1.40 (s, 2H);  $^{13}C$  NMR (125.83 MHz,  $CDCl_3$ ):  $\delta$  [ppm] = 191.21, 188.32, 172.57, 138.67, 115.53, 84.81, 68.29, 53.96, 52.61, 38.01, 29.23, 29.10, 28.98, 28.75, 28.53, 25.02, 18.51; **HRMS (ESI)**: calc. for  $C_{17}H_{22}NO_4$   $[M+H]^+$ : 304.1543, found: 304.1543, diff: -0.13 ppm.

***N*-(2,5-Dimethoxyphenyl)undec-10-ynamide (126)**



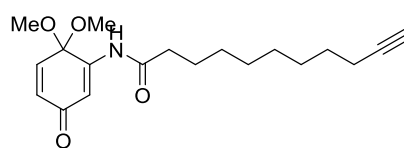
**126**  
 $C_{19}H_{27}NO_3$   
Molecular Weight: 317.43

To a solution of **104** (0.29 mg, 1.57 mmol, 1.20 eq), EDC (0.30 mg, 1.57 mmol, 1.20 eq) and DMAP (cat.) in anhydrous DCM (20 mL) under an inert atmosphere of nitrogen at room temperature was slowly added dropwise a solution of 2,5-dimethoxyaniline (0.20 mg, 1.31 mmol, 1.00 eq) in anhydrous DCM (5 mL). The reaction was stirred at room temperature for 16 h, then quenched by adding aqueous 1 M HCl (10 mL) and extracted with DCM (4 x 30 mL). The combined organic extracts were washed with brine (100 mL), dried over  $Na_2SO_4$  and concentrated under reduced

pressure. The crude product was purified by flash column chromatography (hexanes:EtOAc 4:1) giving compound **126** (0.34 g, 1.02 mmol, 78%) as white solid.

$R_f$  = 0.24 (hexanes:EtOAc 4:1);  $^1\text{H NMR}$  (500.36 MHz,  $\text{CDCl}_3$ ):  $\delta$  [ppm] = 9.00 (s, 1H), 7.70 (d,  $J$  = 3.0 Hz, 1H), 6.92 (d,  $J$  = 8.9 Hz, 1H), 6.59 (dd,  $J$  = 8.9, 3.1 Hz, 1H), 3.76 (s, 3H), 3.67 (s, 3H), 2.74 (t,  $J$  = 2.7 Hz, 1H), 2.37 (t,  $J$  = 7.4 Hz, 2H), 2.13 (td,  $J$  = 7.0, 2.7 Hz, 2H), 1.59 - 1.51 (m, 2H), 1.47 - 1.39 (m, 2H), 1.36 - 1.23 (m, 8H);  $^{13}\text{C NMR}$  (125.83 MHz,  $\text{CDCl}_3$ ):  $\delta$  [ppm] = 171.58, 152.86, 143.41, 128.30, 111.70, 108.18, 107.72, 84.59, 71.20, 56.17, 55.31, 36.14, 28.78, 28.66, 28.47, 28.17, 27.98, 25.20, 17.70; **HRMS (ESI)**: calc. for  $\text{C}_{19}\text{H}_{28}\text{NO}_3$   $[\text{M}+\text{H}]^+$ : 318.20637, found: 318.2064, diff: -0.01 ppm.

***N*-(6,6-Dimethoxy-3-oxocyclohexa-1,4-dien-1-yl)undec-10-ynamide (**127**)<sup>[182]</sup>**

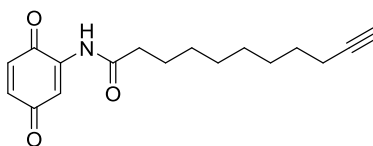


**127**  
 $\text{C}_{19}\text{H}_{27}\text{NO}_4$   
Molecular Weight: 333.43

To a solution of **126** (0.30 g, 0.95 mmol, 1.00 eq) in anhydrous MeOH (20 mL) at 0 °C under nitrogen atmosphere was added portion wise  $\text{PhI}(\text{OPiv})_2$  (0.42 g, 1.04 mmol, 1.10 eq). The mixture was allowed to warm to room temperature, further stirred for 16 h and then diluted with EtOAc (50 mL). After stirring for 30 min at room temperature, the mixture was extracted with EtOAc (3 x 50 mL) and the combined organic extracts were washed with saturated  $\text{NaHCO}_3$  aqueous solution (30 mL), water (30 mL) and brine (50 mL). The combined organic extracts were dried over  $\text{Na}_2\text{SO}_4$ , concentrated under reduced pressure and purified by flash column chromatography (hexanes:EtOAc 1:1) to yield product **127** (0.31 g, 0.94 mmol, 94%) as yellow solid.

$R_f$  = 0.39 (hexanes:EtOAc 1:1);  $^1\text{H NMR}$  (500.36 MHz,  $\text{CDCl}_3$ ):  $\delta$  [ppm] = 9.48 (s, 1H), 7.19 (d,  $J$  = 2.1 Hz, 1H), 6.84 (d,  $J$  = 10.3 Hz, 1H), 6.34 (dd,  $J$  = 10.3, 2.1 Hz, 1H), 3.18 (s, 6H), 2.73 (t,  $J$  = 2.7 Hz, 1H), 2.47 (t,  $J$  = 7.4 Hz, 2H), 2.13 (td,  $J$  = 7.0, 2.7 Hz, 2H), 1.56 - 1.47 (m, 2H), 1.42 (dd,  $J$  = 14.7, 7.3 Hz, 2H), 1.30 (dt,  $J$  = 40.9, 6.6 Hz, 8H);  $^{13}\text{C NMR}$  (125.83 MHz,  $\text{CDCl}_3$ ):  $\delta$  [ppm] = 185.84, 179.42, 174.46, 148.98, 140.34, 131.48, 112.22, 84.56, 71.19, 50.94, 36.29, 28.69, 28.50, 28.44, 28.15, 27.97, 27.04, 24.97, 17.70; **HRMS (ESI)**: calc. for  $\text{C}_{19}\text{H}_{28}\text{NO}_4$   $[\text{M}+\text{H}]^+$ : 334.2013, found: 334.2013, diff: 0.04 ppm.



***N*-(3,6-Dioxocyclohexa-1,4-dien-1-yl)undec-10-ynamide (FM310)<sup>[134]</sup>**

**FM310**  
 $C_{17}H_{21}NO_3$   
Molecular Weight: 287.36

To a solution of **127** (0.10 g, 0.30 mmol, 1.00 eq) in anhydrous DCM (10 mL) Montmorillonite K10 (200 mg) was added in small portions and the reaction was stirred for 16 h at room temperature. The solution was filtered through Celite, which was additionally washed with DCM (3 x 10 mL). The combined filtrates were washed with brine (10 mL), dried over  $Na_2SO_4$  and concentrated under reduced pressure. The crude product was purified by preparative reversed-phase HPLC (C18 5.0  $\mu$ m, 30 x 150 mm column, gradient 2% B  $\rightarrow$  98% B over 17 min,  $t_R$  = 9.4 - 10.2 min) giving compound **FM310** (70.0 mg, 0.24 mmol, 81%) as yellow solid.

$R_f$  = 0.76 (hexanes:EtOAc 1:1);  $^1H$  NMR (360.13 MHz,  $CDCl_3$ ):  $\delta$  [ppm] = 7.64 (s, 1H), 7.27 (d,  $J$  = 2.2 Hz, 1H), 6.79 (d,  $J$  = 10.1 Hz, 1H), 6.74 (dd,  $J$  = 10.1, 2.3 Hz, 1H), 4.81 (d,  $J$  = 2.5 Hz, 2H), 2.55 (t,  $J$  = 2.5 Hz, 1H);  $^{13}C$  NMR (90.56 MHz,  $CDCl_3$ ):  $\delta$  [ppm] = 187.33, 182.05, 151.38, 138.84, 138.35, 133.36, 113.75, 77.36, 76.03, 53.87; **HRMS (ESI)**: calc. for  $C_{17}H_{22}NO_3$   $[M+H]^+$ : 288.1594, found: 288.1594, diff: 0.08 ppm.

## 2 MICROBIOLOGY

### 2.1 BACTERIAL STRAINS AND MEDIA

**Table 12:** Bacterial strains and their appropriate cultivation media.

Species	Microbial strain	Medium for cultivation
<b>S1 (non-pathogenic)</b>		
<i>Bacillus licheniformis</i>	ATC 14580	LB
<i>Bacillus subtilis</i>	168	LB
<i>Burkholderia thailandensis</i>	E264	CASO
<i>Escherichia coli</i>	K12	LB
<i>Escherichia coli</i>	BL21	LB
<i>Listeria welshimeri</i>	SLCC 5334 serovar 6b	BHB
<i>Mycobacterium vanbalenii</i>	Pyr-1	LB + 0.25% Tween
<i>Pseudomonas putida</i>	KT2440	LB
<b>S2 (pathogenic)</b>		
<i>Burkholderia cenocepacia</i>	J2315	CASO
<i>Enterococcus faecalis</i>	OG1RF	B
<i>Listeria monocytogenes</i>	EGD-e	BHB
<i>Mycobacterium smegmatis</i>	MC2 155	LB + 0.25% Tween
<i>Pseudomonas aeruginosa</i>	PAO1	LB
<i>Salmonella enteritidis</i>		LB
<i>Salmonella typhimurium</i>	LT2	LB
<i>Salmonella typhimurium</i>	TA100	LB
<i>Staphylococcus aureus</i>	NCTC 8325	B
<i>Staphylococcus aureus</i>	Mu50	B
<i>Staphylococcus aureus</i>	USA300	B

**Table 13:** Composition of the different media used for the cultivation of bacteria. Amounts of the single ingredients were calculated for 1 L total volume.

Name	Composition
LB	10.0 g peptone ex casein
	5.00 g NaCl
	5.00 g yeast extract
	in 1 L ddH <sub>2</sub> O, pH = 7.5
BHB	17.5 g brain heart infusion
	2.50 g Na <sub>2</sub> HPO <sub>4</sub>
	2.00 g D-(+)-glucose
	10.0 g peptone ex casein
	5.00 g NaCl
	in 1 L ddH <sub>2</sub> O, pH = 7.4

<b>B</b>	10.0 g peptone ex casein
	5.00 g NaCl
	5.00 g yeast extract
	1.00 g K <sub>2</sub> HPO <sub>4</sub>
	in 1 L ddH <sub>2</sub> O, pH = 7.5
<b>CASO</b>	17.0 g peptone ex casein
	3.00 g peptone ex soy
	2.00 g D-(+)-glucose
	5.00 g NaCl
	2.50 g Na <sub>2</sub> HPO <sub>4</sub>
<b>SOC</b>	in 1 L ddH <sub>2</sub> O, pH = 7.3
	20.0 g yeast extract
	5.00 g tryptone
	0.50 g NaCl
	0.20 g KCl
	1.00 g MgCl <sub>2</sub>
	1.20 g MgSO <sub>4</sub>
	3.60 g glucose
	in 1 L ddH <sub>2</sub> O, pH = 7.3

## 2.2 CULTIVATION METHODS

### Overnight cultures

5 mL of the particular medium for cultivation were inoculated with 5 µL of the desired bacterial cryostock (1:1000) with a sterile pipet tip in a plastic culture tube. The culture was then incubated overnight (16 h, 37 °C, 200 rpm) in an Innova incubator shaker. Overnight cultures were always prepared freshly to avoid genetic variations. A sterile control (medium containing no bacteria) was added each time.

### Cryostocks

1 mL of an overnight culture of the desired bacteria were harvested by centrifugation (10 min, 4 °C, 6000 rpm) and the pelletized cells were resuspended in 250 µL fresh, sterile medium. 250 µL of sterilized glycerin were added, the stocks were mixed, frozen in liquid nitrogen and stored at -80 °C in 20 µL aliquots prior to use. After inoculating fresh media with the aliquot, the leftover amount of the cryostock was discarded.

## 2.3 MIC ASSAY

The minimal inhibitory concentration (MIC) describes by definition the lowest concentration of a compound that will inhibit the visible growth of bacteria. For the assay the bacteria were grown as overnight culture and then diluted by the appropriate media to an OD<sub>600</sub> of 0.01. Various dilutions of the small molecule inhibitor in DMSO were prepared and 1 µL of this stock was put in a 96 flat

bottom well-plate in triplicates, including a DMSO-control. Then, 99  $\mu\text{L}$  of the diluted bacterial suspension was given to each well and a growth control without any substances added was additionally applied. The free floating bacteria were incubated for 16 h at 37 °C in a shaker at 200 rpm. The MIC of the substances was visually defined as the lowest concentration at which no growth could be observed.

### 3 PROTEOMICS

#### 3.1 GEL-BASED PROTEIN PROFILING PROTEOMICS

**Table 14:** Buffers and solutions used for analytical and preparative labeling including Click-chemistry.

Name	Composition
PBS buffer	137 mM NaCl 10 mM Na <sub>2</sub> HPO <sub>4</sub> 2.7 mM KH <sub>2</sub> PO <sub>4</sub> 1.8 mM KCl in ddH <sub>2</sub> O, pH = 7.4
21.5% SDS	0.75 M sodium dodecyl sulfate in ddH <sub>2</sub> O
20 x RhN <sub>3</sub>	100 mM RhN <sub>3</sub> in MeOH (dry)
1 x RhN <sub>3</sub>	5 mM RhN <sub>3</sub> in MeOH
1 x Trifunctional linker	10 mM trifunctional linker in DMSO (dry)
1 x Biotin-PEG-N <sub>3</sub>	10 mM biotin-PEG-N <sub>3</sub> in DMSO (dry)
TCEP solution	53 mM tris(2-carboxyethylphosphin) in ddH <sub>2</sub> O
50 x TBTA	83.4 mM TBTA ligand in DMSO (dry)
1 x TBTA ligand	20 µL 50 x TBTA 180 µL DMSO (dry) 800 µL t-BuOH (dry)
CuSO <sub>4</sub> solution	50 mM CuSO <sub>4</sub> in ddH <sub>2</sub> O
2 x SDS loading buffer	63 mM Tris · HCl 10% (v/v) glycerin 0.0025% (w/v) bromophenol blue 2.0% (w/v) sodium dodecyl sulfate 5.0% (v/v) mercaptoethanol in ddH <sub>2</sub> O
0.4% SDS	13.9 mM sodium dodecyl sulfate in ddH <sub>2</sub> O
6 M Urea	6 M urea in ddH <sub>2</sub> O

##### 3.1.1 ANALYTICAL *IN SITU* LABELING AND CLICK REACTION

For analytical *in situ* labeling, 100 mL of the respective cultivation media were inoculated with 10 mL of an overnight culture of the desired bacterial strain (1:10 v/v) in a 500 mL flask and incubated at 37 °C and 200 rpm in an Innova incubator shaker until stationary phase was reached. The cells were harvested by centrifugation (10 min, 4 °C, 6000 rpm), washed with 20 mL PBS and resuspended in PBS to a theoretical OD<sub>600</sub> of 40. 200 µL of the bacterial suspension were then incubated with 2 µL of probe in DMSO in varying concentrations (see preparation of probe stocks) for 1 h at room temperature. A DMSO control containing no probe was additionally added to each experiment. After centrifugation (10 min, 4 °C, 6000 rpm), the bacterial cells were washed with 800

$\mu\text{L}$  PBS and lysed by sonication (3 x 20 sec, 85% max. intensity, on ice). Membrane and cytosol fraction were separated by centrifugation (30 min, 13.000 rpm, 4 °C) and the membrane fraction was additionally washed with 800  $\mu\text{L}$  PBS. The click reaction was carried out with 44  $\mu\text{L}$  of proteome, so that after addition of all reagents a total volume of 50  $\mu\text{L}$  was reached. Therefore, 1  $\mu\text{L}$  1 x  $\text{RhN}_3$ , followed by 3  $\mu\text{L}$  1 x TBTA ligand and 1  $\mu\text{L}$  TCEP solution were added to the cells. After gently vortexing the samples, the cycloaddition reaction was initiated by adding 1  $\mu\text{L}$   $\text{CuSO}_4$  solution. The reaction was incubated for 1 h at room temperature and stopped by adding 50  $\mu\text{L}$  2 x SDS loading buffer. After vortexing the samples, 45  $\mu\text{L}$  were applied on an analytical SDS gel, which was developed for 2 - 3 h (150 V). Bands were then visualized by fluorescent scanning (see section 3.1.3).<sup>[185,186]</sup>

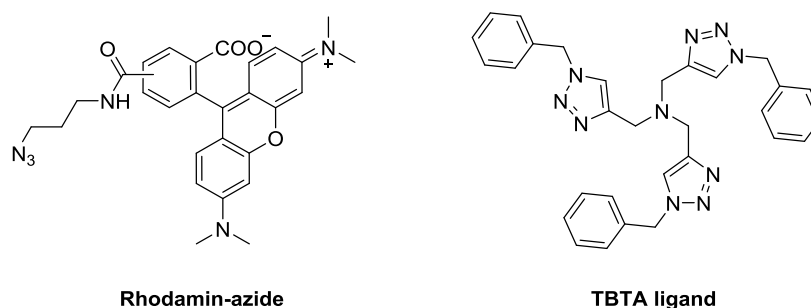
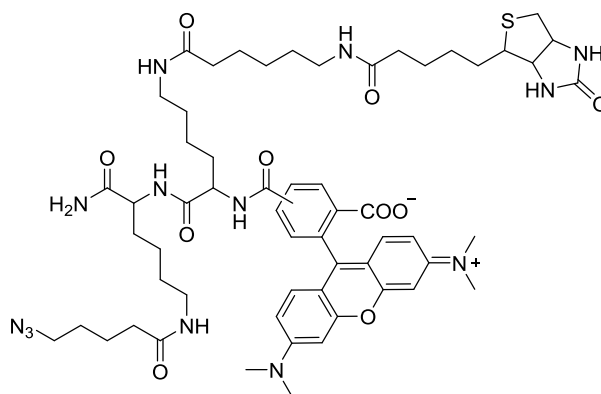


**Figure 56:** Molecular structures of the fluorescent dye Rhodamine-azide ( $\text{RhN}_3$ , left) and the CuAAC-accelerating ligand tris[(1-benzyl-1H-1,2,3-triazol-4-yl)methyl]amine (TBTA, right).

### 3.1.2 PREPARATIVE IN SITU LABELING INCLUDING CLICK REACTION

For preparative *in situ* labeling, 100 mL of the respective cultivation media were inoculated with 10 mL of an overnight culture of the desired bacterial strain (1:10 v/v) in a 500 mL flask and incubated at 37 °C and 200 rpm in an Innova incubator shaker until stationary phase was reached. The cells were harvested by centrifugation (10 min, 6000 rpm, 4 °C), washed with 20 mL PBS and resuspended in PBS to a theoretical  $\text{OD}_{600}$  of 40. 500  $\mu\text{L}$  of the bacterial suspension were then incubated with 5  $\mu\text{L}$  of probe in DMSO in varying concentrations (see probe stocks) for 1 h at room temperature. A DMSO control containing no probe was additionally added to each experiment to compare the results of the biotin-avidin enriched samples with the background of unspecific protein binding on avidin-agarose beads. After centrifugation (10 min, 6000 rpm, 4 °C), the bacterial cells were washed twice with 1 mL PBS, resuspended in 500  $\mu\text{L}$  PBS and lysed by sonication (5 x 20 sec, 85% max. intensity, on ice). Membrane and cytosol fraction were separated by centrifugation (30 min, 13.000 rpm, 4 °C), the membrane fraction was additionally washed with 1 mL PBS and resuspended in 500  $\mu\text{L}$  PBS. For the Click reaction 3  $\mu\text{L}$  1 x trifunctional linker, followed by 30  $\mu\text{L}$  1 x TBTA ligand and 10  $\mu\text{L}$  TCEP solution were subsequently added to each sample. After gently vortexing the probes, the click-reaction was initiated by adding 10  $\mu\text{L}$   $\text{CuSO}_4$

solution. The reaction was incubated for 1 h at room temperature after which the proteins were precipitated over night at -20 °C by adding 4 mL chilled acetone and pelletized by centrifugation (10 min, 8000 rpm, 4 °C). The supernatant was discarded and the pellet was washed two times with 500 µL chilled MeOH (resuspension by sonication, 1 x 10 sec, 10% max. intensity). After centrifugation (10 min, 13000 rpm, 4 °C), the pellet was resuspended in 1 mL 0.4% SDS by sonication (4 x 10 sec, 10% max. intensity) and incubated under gentle mixing with 50 µL pre washed avidin-agarose beads (3 x 1 mL 0.4% SDS solution, centrifugation was performed at 2500 rpm for 5 min at RT) for 1 h at room temperature. The beads were washed three times with 1 mL 0.4% SDS, twice with 1 mL 6 M urea and again three times with 1 mL PBS. All supernatants were discarded carefully and 50 µL 2 x SDS loading buffer was added to the beads. The proteins were released for preparative SDS-PAGE by incubation for 6 min at 96 °C and 350 rpm in an eppi shaker. After centrifugation (2 min, 13000 rpm, RT), the supernatant was isolated and applied on a preparative SDS gel, which was developed for 4 - 5 h (300 V). Bands were then visualized by fluorescent scanning (see chapter 3.1.3). The enriched bands as well as the DMSO control were cut out, dismembered into small pieces using a razor blade and stored at -20 °C until further usage.<sup>[187]</sup>



**Trifunctional linker**

**Figure 57:** Molecular structure of the trifunctional linker containing a rhodamine fluorophore, a biotin and an aliphatic azide moiety.

### 3.1.3 SDS-PAGE AND COOMASSIE STAINING

**Table 15:** Buffers and solutions used for gel electrophoresis including solutions for Coomassie staining and destaining.

Name	Composition
10 x SDS buffer	0.25 M Tris HCl
	1.92 M glycine
	35 mM sodium dodecyl sulfate
	in ddH <sub>2</sub> O
10 x SDS resolving gel buffer	3 M Tris base in ddH <sub>2</sub> O, pH = 8.8

10 x SDS stacking gel buffer	0.5 M Tris base in ddH <sub>2</sub> O, pH = 6.8
10% APS	10% (w/v) ammonium persulfate in ddH <sub>2</sub> O
10% SDS	10% (w/v) sodium dodecyl sulfate in ddH <sub>2</sub> O
Coomassie-stain	0.25% (w/v) Coomassie Brilliant Blue
	9.2% (v/v) glacial acetic acid
	45.4% bio grade ethanol
	in ddH <sub>2</sub> O, pH = 6.8
Coomassie-destainer	10% (v/v) glacial acetic acid
	20% bio grade ethanol
	in ddH <sub>2</sub> O, pH = 6.8

Gels for sodium dodecyl sulfate polyacrylamide gel electrophoresis (SDS-PAGE) were produced in two steps: first, the respective resolving gel mixture (composition of gels with different acrylamide concentrations are given in table 16) was carefully added between two glass plates in a gel chamber until complete polymerization occurred. Second, the stacking gel solution (composition given in table 16) was filled on top of the resolving gel, a gel comb was plunged into the solution and the mixture was allowed to harden. Before the samples were applied the gel chamber was filled with 1 x SDS running buffer and the comb was removed. To later determine the protein mass of the samples, Roti®-Mark STANDARD protein marker (16 µL, for Coomassie staining) and BenchMark™ Fluorescent Protein Standard (8 µL) were given together into one gel pocket. After adding 45 µL of the samples in the remaining pockets of the gel, 45 µL of 2 x SDS loading buffer was filled in all empty pockets and the gel was developed for 2 -3 h at 150 V for small gels and 4 - 5 h at 300 V for large gels in a EV261 or EC265 Electrophoresis Power Supply (Consort BVAB). Fluorescence scans were performed with a Fujifilm Las-4000 luminescent image analyzer equipped with a Fujinon VRF43LMD3 lens or a Fujifilm Las-3000 fluorescence darkbox equipped with a Fujinon VRF43LMD3 lens, 605DF40 filter and 520 nm EPI excitation wavelengths. Printouts of fluorescence gels were used to localize and cut the bands in preparative labeling experiments. After the fluorescence scans the gels were washed with ddH<sub>2</sub>O and incubated in a Coomassie Brilliant Blue G-250 dye at room temperature overnight. After the stain was removed, the gels were washed with water and then covered with a Coomassie-destainer, which was changed several times until proteins became visible as blue bands.

**Table 16:** Composition of resolving and stacking gels.

	Acrylamide [%]	H <sub>2</sub> O [mL]	Rotiph. [mL]	Buffer [mL]	10% SDS [µL]	10% APS [µL]	TEMED [µL]
Resolving gel							
Small	10	7.2	6	4.5	180	75	7.5
	12.5	5.7	7.5	4.5	180	75	7.5
	15	4.2	9	4.5	180	75	7.5



	10	21.6	18	13.5	540	225	22.5
Large	12.5	17.1	22.5	13.5	540	225	22.5
	15	12.6	27	13.5	540	225	22.5
<b>Stacking gel</b>							
Small	3.75	11	2.25	4.5	180	90	18
Large	3.75	3.7	0.75	1.5	60	30	6

### 3.1.4 IN-GEL DIGEST

The gel pieces of the preparative labeling experiment stored at -20 °C were washed with ddH<sub>2</sub>O (100 µL, 15 min, 550 rpm, RT), MeCN/50 mM ABC (200 µL, 15 min, 550 rpm, RT) and MeCN (100 µL, 10 min, 550 rpm, RT). Then, 100 µL 50 mM ABC was added to the gel pieces followed after 5 min at 550 rpm by additional MeCN (100 µL, 15 min, 550 rpm, RT). The supernatant was removed; the gel pieces were again washed with MeCN (100 µL, 15 min, 550 rpm, RT) and then dried under vacuum in a centrifugal evaporator (15 min, 1 mbar, RT). The proteins were reduced by adding DTT solution (100 µL, 45 min, 550 rpm, 56 °C) to the gel pieces, washed with MeCN (100 µL, 10 min, 550 rpm, RT) and then alkylated by the addition of IAA solution (100 µL, 30 min covered, 550 rpm, RT). After washing three times with MeCN/50 mM ABC (100 µL, 15 min, 550 rpm, RT) and MeCN (100 µL, 10 min, 550 rpm, RT), the gel pieces were again dried under vacuum in a centrifugal evaporator (15 min, 1 mbar, RT). Trypsin digest solution (100 µL, overnight, 300 rpm, 37 °C) was added and the next day the supernatant was transferred into a LoBind Eppendorf cup and 25 mM ABC solution (100 µL, 15 min, sonication, RT) was given to the gel pieces. MeCN (100 µL, 15 min, sonication, RT) was additionally added to the gel pieces and the supernatant was again transferred into the LoBind Eppendorf cup. The gel pieces were discarded and the solvent of the digested proteins was removed under vacuum in a centrifugal evaporator (5 h, 1 mbar, RT). The remaining peptides were stored at -80 °C until further use.

**Table 17:** Buffers and solution used for in gel digest.

Name	Composition
50 mM ABC	50 mM NH <sub>4</sub> HCO <sub>3</sub> in ddH <sub>2</sub> O
MeCN/50 mM ABC	50 mM NH <sub>4</sub> HCO <sub>3</sub> in MeCN/ddH <sub>2</sub> O (1:1 v/v)
DTT solution	10 mM dithiotreitol in 50 mM ABC
IAA solution	55 mM iodoacetamide in 50 mM ABC
5% FA	5% (v/v) formic acid in ddH <sub>2</sub> O
Trypsin digest solution	1% (v/v) trypsin stock solution in 25 mM ABC

## 3.2 GEL-FREE PROTEIN PROFILING PROTEOMICS

### 3.2.1 IN-SOLUTION DIGEST

For gel-free studies, cells were labeled in preparative scale as described in section 3.1.2 but for the Click reaction the trifunctional linker was replaced by adding 20  $\mu\text{L}$  of a bifunctional Biotin-PEG- $\text{N}_3$  linker, followed by 30  $\mu\text{L}$  1 x TBTA ligand and 10  $\mu\text{L}$  TCEP solution to the proteome samples. After gently vortexing the samples, the cycloaddition reaction was initiated by adding 10  $\mu\text{L}$   $\text{CuSO}_4$  solution. The reaction was incubated for 1 h at room temperature after which the proteins were precipitated over night at  $-20\text{ }^\circ\text{C}$  by adding 4 mL chilled acetone and pelletized by centrifugation (10 min, 8000 rpm,  $4\text{ }^\circ\text{C}$ ). The supernatant was discarded and the pellet was washed two times with 500  $\mu\text{L}$  chilled MeOH (resuspension by sonication, 1 x 10 sec, 10% max. intensity). After centrifugation (10 min, 13000 rpm,  $4\text{ }^\circ\text{C}$ ), the pellet was resuspended in 1 mL 0.4% SDS by sonication (4 x 10 sec, 10% max. intensity) and incubated under gentle mixing with 50  $\mu\text{L}$  pre washed avidin-agarose beads (3 x 1 mL 0.4% SDS solution, centrifugation was performed at 2500 rpm and RT for 5 min) for 1 h at room temperature. The beads were washed three times with 1 mL 0.4% SDS, twice with 1 mL 6 M urea and again three times with 1 mL PBS. After the last washing step, the supernatant was completely removed, digestion buffer (200  $\mu\text{L}$ ) was added to the beads and the proteins were reduced by adding DTT solution (1 M, 0.2  $\mu\text{L}$ , 45 min, 450 rpm, RT). After alkylation with IAA solution (550 mM, 2  $\mu\text{L}$ , 30 min in the dark, 450 rpm, RT), the reaction was quenched with DTT solution (1 M, 0.8  $\mu\text{L}$ , 30 min, 450 rpm, RT) and the proteins were digested by adding LysC (0.5  $\mu\text{g}/\mu\text{L}$ , 1  $\mu\text{L}$ , 2 h, 450 rpm, RT). The samples were diluted with TEAB solution (600  $\mu\text{L}$ ) and further digested with Trypsin (0.5  $\mu\text{g}/\mu\text{L}$ , 1.5  $\mu\text{L}$ , overnight, 450 rpm,  $37\text{ }^\circ\text{C}$ ). To finally quench the reaction, FA (10  $\mu\text{L}$ ) was added to the samples which were further desalted using 50 mg Sep-Pak C18 Vac Cartridges (Waters).

### 3.2.2 ON-COLUMN DIMETHYL LABELING

For on-column dimethyl labeling the cartridges had to be equilibrated with MeCN (1 x 1 mL), elution buffer (1 x 1 mL) and 0.5% FA (in ddH<sub>2</sub>O, 3 x 1 mL). The samples (about 800  $\mu\text{L}$ ) were loaded to the column via gravity flow and washed with 0.5% FA (in ddH<sub>2</sub>O, 5 x 1 mL) and then labeled with 5 mL of the respective dimethyl labeling solution (light (L): 30 mM  $\text{NaBH}_3\text{CN}$ , 0.2%  $\text{CH}_2\text{O}$ , 10 mM  $\text{NaH}_2\text{PO}_4$ , 35 mM  $\text{Na}_2\text{HPO}_4$ , pH 7.5; medium (M): 30 mM  $\text{NaBH}_3\text{CN}$ , 0.2%  $\text{CD}_2\text{O}$ , 10 mM  $\text{NaH}_2\text{PO}_4$ , 35 mM  $\text{Na}_2\text{HPO}_4$ , pH 7.5; heavy (H): 30 mM  $\text{NaBD}_3\text{CN}$ , 0.2%  $^{13}\text{CD}_2\text{O}$ , 10 mM  $\text{NaH}_2\text{PO}_4$ , 35 mM  $\text{Na}_2\text{HPO}_4$ , pH 7.5). The labeled peptides were eluted in a LoBind Eppendorf tube with elution buffer

(3 x 250 µL), mixed via label switch, dried under vacuum in a lyophilizer (16 h, 1 mbar, -80 °C) and stored at -80 °C.<sup>[81]</sup>

**Table 18:** Buffers and solutions used for gel free in solution digest.

Name	Composition
Digestion buffer	20 mM HEPES
	7 M urea
	2 M thiourea
TEAB solution	50 mM TEAB in ddH <sub>2</sub> O
DTT solution	1 M dithiotreitol in ddH <sub>2</sub> O
IAA solution	550 mM iodoacetamide in ddH <sub>2</sub> O
5% FA	5% (v/v) formic acid in ddH <sub>2</sub> O

### 3.3 SAMPLE PREPARATION AND STATISTICAL EVALUATION

Before MS measurements peptide samples were filtrated through centrifugal filters (VWR Centrifugal Filters, modified Nylon, 0.45 µm, low protein binding), which had to be pre-rinsed before usage: ddH<sub>2</sub>O (2 × 500 µL, 13000 rpm, 1 min, RT), aq. 0.05 M NaOH (2 × 500 µL, 13000 rpm, 1 min, RT) and 1% FA (2 × 500 µL, 13000 rpm, 1 min, RT). The peptides were dissolved in 1% FA (40 µL, 15 min sonication, RT) and then added to the pre-equilibrated filters (13000 rpm, 4 min, RT). The filtrate was transferred into a PP screw top vial and stored at -20 °C until the measurements were performed. Nano flow LC-MS/MS analysis was performed with an UltiMate 3000 Nano HPLC system (Thermo Scientific) coupled to a LTQ Orbitrap XL (Thermo Scientific) or an Orbitrap Fusion (Thermo Scientific). Peptides were loaded on a trap column (Acclaim C18 PepMap100 75 µm ID x 2 cm) and washed for 10 min with 0.1% FA (5 µL/min flow rate), then transferred to an analytical column (Acclaim C18 PepMap RSLC, 75 µm ID x 15 cm). Raw files were analyzed using MaxQuant software (version 1.5.1.2) with Andromeda as search engine. The search included carbamidomethylation of cysteines as a fixed modification and oxidation of methionines as variable modifications. Trypsin was specified as the proteolytic enzyme with N-terminal cleavage to proline and two missed cleavages allowed. Precursor mass tolerance was set to 4.5 ppm (main search) and fragment mass tolerance to 0.5 Da. Searches were performed against the Uniprot database for *Salmonella typhimurium* LT2 (taxon identifier: 99287, 10.07.2014). The second peptide identification option was enabled. False discovery rate determination was carried out using a decoy database and thresholds were set to 1% both at peptide-spectrum match and at protein levels. “I = L”, “requantification” and “match between runs” (0.7 min match and 20 min alignment time windows) options were enabled. Label-free quantification was enabled with a minimum ratio count

of 2. Quantification of dimethyl triplets was carried out based on unique peptides only using “DimethLys0,” and “DimethNter0” as “light”, “DimethLys4,” and “DimethNter4” as “medium” and “DimethLys8,” and “DimethNter8” as “heavy” isotope identifiers requiring a minimum ratio count of 2. In case of gel-based target identification, analysis of the resulting *proteingroups.txt*-table was performed with Perseus 1.5.1.6. Putative contaminants, reverse hits and proteins, that were identified by site only, were removed. Ratios were calculated by dividing the LFQ intensity signal of the excised band by the LFQ intensity of corresponding gel area for the untreated sample. Rows were filtered to contain seven valid values. Ratios were transformed using  $\log_2(x)$  and normalized using z-score. *P*-values were obtained using a two sided one sample t-test. (Benjamini Hochberg FDR of 0.01). Statistical analysis of gel-free target identification was performed with Perseus 1.5.1.6. MaxQuant result table *proteingroups.txt* was used for further analysis. Putative contaminants, reverse hits and proteins, that were identified by site only, were removed. Dimethyl isotope ratios were  $\log_2(x)$ -transformed, filtered to have six valid values per row (from three replicates in total), and z-score-normalized.  $-\log_{10}$  p-values were obtained by a two sided one sample t-test (Benjamini-Hochberg FDR of 0.01).

## 4 GENOMICS

**Table 19:** Buffers and solutions used for Gateway cloning, protein overexpression, purification and storage.

Name	Composition
TE buffer	10 mM Tris base
	1 mM EDTA
	in ddH <sub>2</sub> O, pH = 8.0
IPTG solution	1 M IPTG in ddH <sub>2</sub> O
ATET solution	2 mg/mL anhydrotetracylin in DMF
Strep binding buffer	100 mM Tris-HCl
	150 mM NaCl
	1 mM EDTA
	in ddH <sub>2</sub> O, pH = 8.0
Strep elution buffer	26.8 mg DTT
	in 50 mL strep binding buffer
His-binding buffer	20 mM Tris base
	10 mM imidazole
	150 mM NaCl
	2 mM <i>beta</i> -mercaptoethanol
	in ddH <sub>2</sub> O, pH = 8.0
His-elution buffer	20 mM Tris base
	500 mM imidazole
	150 mM NaCl
	2 mM <i>beta</i> -mercaptoethanol
	in ddH <sub>2</sub> O, pH 8.0
SCRP storage buffer	20 mM HEPES
	500 mM NaCl
	0.1 mM EDTA
	0.1 mM DTT
	in ddH <sub>2</sub> O, pH = 7.0

### 4.1 PCR FOR GATEWAY

For the recombinant expression of sigma cross-reacting protein 27A of *Salmonella typhimurium* LT2, the Invitrogen™ Gateway® Technology was used. As this cloning method requires *attB* recombination sites at first, the following *attB1* forward (for) and *attB2* reverse (rev) primers were designed:

**for\_ *attB1*\_SCRP:** 5'-ggggacaagtttgtaaaaaagcaggctttgagaatctttatcttcaggggcaaaaaattggcgtagtgctc-3'

**rev\_ *attB2*\_SCRP:** 5'-ggggaccactttgtacaagaaagctgggtgttattccgccagaaccag-3'

The PCR reaction was performed with a CFX96 Real-time System combined with a C1000 Thermal Cycler (BioRad) with 100 ng of genomic DNA of *Salmonella typhimurium* LT2, prepared according to

the protocol provided in the peqGOLD Bacterial DNA Kit (peqlab biotechnology GmbH), applying the following temperature program:

**Table 20:** PCR temperature program performed for the Gateway technology.

Step	Temperature [C°]	Time [min]
Initial denaturation	98	00:30
35 Cycles	98	00:10
	50 - 72	00:30
	72	00:30/kb
Final extension	72	05:00
	4	hold

According to Phusion manufacturer's protocol, 50 µL PCR reaction mixture were prepared containing 30.5 µL ddH<sub>2</sub>O, 10 µL 5x GC or 5x HF buffer (NEB), 10 µL forward and 10 µL reverse primer (10 µM), 1.0 µL dNTPs (10 mM), 1.5 µL DMSO and 1.5 µL genomic template DNA (70 ng/µL). Finally 0.5 µL Phusion® High Fidelity DNA polymerase (NEB) were added and the PCR reaction was subsequently performed. After 35 cycles a comparable amplification was detected over a broad range of annealing temperatures (50 - 72 °C). The PCR products were identified on an agarose gel, purified by the MicroElute® Cycle-Pure Kit using the centrifugation protocol (OMEGA bio-tek) and finally the DNA concentration was measured on an Infinite® M200 Pro NanoQuant multiplate reader (Tecan).

## 4.2 GATEWAY CLONING

### 4.2.1 BP CLONING REACTION

To transfer the *attB*-PCR product into the destination vector pDONR™207, containing an *attP* recombination site, a BP reaction with BP Clonase™II Enzyme Mix was performed. Therefor 1.0 µL of the vector (150 ng/µL) was added to 1.5 µL of the purified *attB*-PCR product (total amount of 150 ng) and 5.5 µL TE buffer at room temperature in a 1.5 mL Eppendorf cup and mixed. 2.0 µL of BP Clonase™II Enzyme Mix, thawed on ice, were added and the solution was incubated for 12 h at room temperature. 7 µL of the BP solution were then added to 200 µL of super competent *E. coli* XL1-Blue cells, which were thawed on ice and incubated for 30 min on ice. The transformation was initiated by heat shock at 42 °C in a water bath for 30 sec and the eppi was placed back on ice for 2 min. The cells were grown for 2 h in 500 µL preheated (37 °C) SOC medium (see table 13) at 37 °C, plated on gentamycin LB agar plates for clone selection (50 - 100 µL per plate) and incubated for 12 - 24 h at 37 °C. Single clones were picked and grown in 10 mL LB medium containing gentamycin (15 µg/mL) for 16 h at 37 °C. Cryostocks of the overnight culture were prepared according to chapter 2.2 and additionally 5 mL of the cells were harvested (6000 rpm, 4 °C, 5 min) and the

plasmid DNA was isolated using E.Z.N.A. Plasmid Mini Kit I (OMEGA Bio-Tek) according to the manufacturer's protocol. The DNA concentration was measured using Infinite® M200 Pro NanoQuant multiplate reader (Tecan) and the validity of the expression vector was proved by DNA sequencing by GATC Biotech AG.

#### 4.2.2 LR CLONING REACTION

The gene of interest was then cloned into two different expression vector systems (pDest007 and pET300) enabled by the LR reaction. Therefore, 150 ng of the entry clone and 150 ng of the corresponding destination vector were added to 8 µL of TE buffer at room temperature in a 1.5 mL Eppendorf cup and mixed. LR Clonase™II Enzyme Mix was added and the reaction mixture was incubated overnight at room temperature. 10 µL of the resulting *attB*-expression clone were transformed into 200 µL of chemically competent *E. coli* BL21(DE3) cells as described in the BP reaction and selected on ampicillin LB agar plates (100 µg/mL). The plasmid DNA was isolated using E.Z.N.A. Plasmid Mini Kit I (OMEGA Bio-Tek) according to the manufacturer's protocol, the concentration was measured using Infinite® M200 Pro NanoQuant multiplate reader (Tecan) and the validity of the destination vector was proved via DNA sequencing by GATC Biotech AG.

#### 4.3 SITE-DIRECTED MUTAGENESIS

Site-directed mutagenesis is a molecular biology technique by which a mutation is inserted at a defined site in a known DNA sequence. To exchange cysteine 135 for alanine in SCRP-27A, the point mutation was introduced by mismatch PCR using two mismatching primers which were designed with the Quick Change Primer Design program (Agilent Technologies):

**for\_SCRP:C135A:** 5'-gcgggcgcgatagcgatgaatcccagcggc-3'

**rev\_SCRP\_C135A:** 5'-gccgctgggattcatcgctatcgccccc-3'

The mismatch PCR reaction was performed with a prime full size thermal cycler (Techne) with 10 ng of SCRP\_pET300 plasmid as template applying the following temperature program:

**Table 21:** PCR temperature program performed for site-directed mutagenesis.

Step	Temperature [C°]	Time [min]
Initial denaturation	98	00:30
30 Cycles	95	00:10
	64	00:30
	72	1:00/kb
	72	05:00
Final extension	4	hold

According to Phusion manufacturer's protocol, 50  $\mu$ L PCR reaction mixture were prepared containing 34.5  $\mu$ L ddH<sub>2</sub>O, 10  $\mu$ L 5x GC or 5x HF buffer (NEB), 0.75  $\mu$ L forward and 0.75  $\mu$ L reverse primer (10  $\mu$ M), 1.0  $\mu$ L dNTPs (10 mM), 1.5  $\mu$ L DMSO and 1.0  $\mu$ L template DNA (10 ng/ $\mu$ L). Finally, 0.5  $\mu$ L Phusion® High Fidelity DNA polymerase (NEB) were added and the PCR reaction was subsequently performed. After 30 cycles, a good amplification was detected at an annealing temperature of 64 ° for the GC buffer mix. The PCR products were identified on an agarose gel, purified by the MicroElute®Cycle-Pure Kit using the centrifugation protocol (OMEGA bio-tek) and finally the DNA concentration was measured on an Infinite® M200 Pro NanoQuant multiplate reader (Tecan). To remove unmutated parental DNA, the PCR product (GC buffer mix) was digested with the endonuclease DpnI, specific for methylated and hemimethylated DNA. Therefore 3.0  $\mu$ L of DpnI was added to 30  $\mu$ L purified PCR product and 3.0  $\mu$ L CutSmart® buffer (NEB) and the digestion mixture was incubated for 1 h at 37 °C. As the template DNA is implemented in a Gateway destination vector, the PCR products can directly be transformed into *E. coli* XL1-Blue competent cells as described in the BP reaction protocol. Plasmid DNA was isolated using again E.Z.N.A. Plasmid Mini Kit I (OMEGA Bio-Tek) according to the manufacturer's protocol. The DNA concentration was measured using Infinite® M200 Pro NanoQuant multiplate reader (Tecan) and the validity of the expression vector was proved by DNA sequencing by GATC Biotech AG. Finally, the plasmid was amplified in *E. coli* BL21(DE3) and further processed as described before in section 4.2.2.

#### 4.4 OVEREXPRESSION AND PURIFICATION OF RECOMBINANT PROTEINS

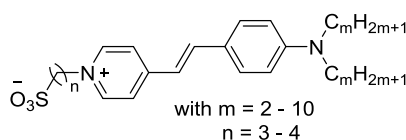
The recombinant pDest007- and pET300-BL21 clones of wild-type SCRP-27A and the pET300-BL21-SCRP-C135A mutant were grown in LB medium (1 L, inoculated 1:100 with an overnight culture) containing ampicillin (100  $\mu$ g/mL) at 37 °C until an OD<sub>600</sub> of 0.6 was reached. Afterwards the target gene expression was induced with IPTG solution (1:1000) in case of pET300-clones and ATET solution (1:10000) in case of pDest007-clones. The cultures were further incubated at 37 °C for 4 h and a not-induced control was added in case of test-overexpressions. The cells were harvested (6000 rpm, 4 °C, 10min), washed with PBS (25 mL) and resuspended in Strep-binding buffer in case of pDest007-constructs and His-binding buffer in case of pET300-clones. The bacterial pellets were lysed by sonication (20 min, 80% max. intensity, under ice cooling) and the soluble fractions were separated via centrifugation (40 min, 18000 rpm, 4 °C). Purification was performed by an ÄKTA system (GE Healthcare) using a StrepTrap™ HP 5 mL column or a HisTrap™ HP 5 mL column (GE Healthcare). After washing with the binding buffers, the proteins were eluted with the respective elution buffers and suitable fractions were concentrated with an Amicon filter unit (MWCO 10 kDa,



Millipore). In case of the HisTrap column an additional buffer exchange to SCRP storage buffer via dialysis was performed. Finally, the enzymes were purified via size exclusion with an ÄKTA system over a HiLoad 16/60 Superdex 200 prep grade column (GE Healthcare), concentrated again and stored at -80 °C in SCRP storage buffer containing 10% glycerin.

#### 4.5 THERMAL SHIFT ASSAY

Thermal denaturation temperatures of proteins were measured via thermal shift assay, performed with a CFX96 Real-time System in combination with a C1000 Thermal Cycler (BioRad). SYPRO Orange was added to the respective buffer (1:1000) containing a protein concentration of 5 µM. In case any inhibitor was added in various concentrations, the total amount of DMSO per well was at most 1%. A control containing the protein and DMSO was included. After vortexing 50 µL of each sample were pipetted in a 96-well PCR plate. Measurements were performed in triplicates.<sup>[146,147]</sup>



**SYPRO Orange**

**Figure 58:** Molecular structure of SYPRO Orange.

#### 4.6 CRYSTALLIZATION OF *SALMONELLA TYPHIMURIUM* LT2 SCRP-27A

Freshly purified SCRP-27A was concentrated to 10 mg/mL in SCRP-27A storage buffer and crystallized using the vapor diffusion method performed in sitting-drop format. Sitting-drop 96 well plates containing different buffers (40 µL per well) were used and for each condition 0.2 µL of protein solution were diluted by 0.2 µL of the reservoir solution. Crystals were grown in 0.5 M sodium acetate, pH 4.7 and 40% (v/v) PEG200 at 20 °C, cryo-protected with reservoir solution supplemented with 30 % ethylene glycol and cryo-cooled in liquid nitrogen. Diffraction data were collected at the ID23-2 microfocus beamline of the European Synchrotron Radiation Facility (ESRF), Grenoble, France. The data were processed with XDS and the crystals belonged to the space group P32.21.<sup>[188]</sup> The resolution cut-offs were chosen according to the correlation coefficient of random half-data sets (1/2 CC) at about 50%.<sup>[189-191]</sup> The structures were solved using the coordinates of the homologue from *E. coli* (PDB code 1VHQ) by molecular replacement in PHASER.<sup>[192]</sup> This was followed by iterative cycles of manual model building in COOT and restraint and TLS refinement in REFMAC5.<sup>[193]</sup> The number and positions of TLS groups was determined utilizing the TLSMD server.<sup>[194,195]</sup> For data processing and structure refinement statistics see table 22. Structural figures of SCRP-27A shown in section 2.4.4.1 were prepared with PyMol (Delano Scientific).

**Table 22:** Data collection and refinement statistics for SCRP-27A. Statistics for the highest-resolution shell are shown in parentheses.

<b>Wavelength</b>	0.873	<b>R-free</b>	0.198 (0.320)
<b>Resolution range</b>	44.86 - 1.75 (1.8 - 1.75)	<b>CC(work)</b>	0.961 (0.714)
<b>Space group</b>	P 3 <sub>2</sub> 2 1	<b>CC(free)</b>	0.963 (0.752)
<b>Unit cell</b>	99.7 99.7 52.5 90 90 120	<b>Number of non-hydrogen atoms</b>	1,696
<b>Total reflections</b>	258,019 (25,406)	<b>Macromolecules</b>	1632
<b>Unique reflections</b>	30,563 (3,005)	<b>Protein residues</b>	219
<b>Multiplicity</b>	8.4 (8.5)	<b>RMS(bonds)</b>	0.017
<b>Completeness (%)</b>	1.00 (0.99)	<b>RMS(angles)</b>	1.65
<b>Mean I/sigma(I)</b>	11.65 (0.97)	<b>Ramachandran favoured (%)</b>	98
<b>Wilson B-factor</b>	28.17	<b>Ramachandran allowed (%)</b>	1.8
<b>R-merge</b>	0.1022 (1.711)	<b>Ramachandran outliers (%)</b>	0
<b>R-meas</b>	0.109 (1.822)	<b>Rotamer outliers (%)</b>	0
<b>CC1/2</b>	0.999 (0.461)	<b>Clashscore</b>	1.5
<b>CC*</b>	1 (0.79)	<b>Average B-factor</b>	29.3
<b>Reflections used in refinement</b>	30,558 (3,005)	<b>Macromolecules</b>	29
<b>Reflections used for R-free</b>	1,409 (145)	<b>Solvent</b>	35.8
<b>R-work</b>	0.189 (0.358)		



## V – BIBLIOGRAPHY



- 
- [1] A. J. Alanis, "Resistance to Antibiotics: Are We in the Post-Antibiotic Era?", *Arch. Med. Res.* **2005**, 36, 697-705.
- [2] Antimicrobial resistance: global report on surveillance, WHO **2014**.
- [3] G.-S. L. Declaration. "Think Ahead. Act Together. An morgen denken. Gemeinsam handeln." *G7 Germany*. Schloss Elmau, Germany; **2015**.
- [4] A. Fleming. Penicillin - Nobel Lecture; 1945.
- [5] A. Fleming, "On the Antibacterial Action of Cultures of a *Penicillium*, with Special Reference to their Use in the Isolation of *B. influenzae*", *Br. J. Exp. Biol.* **1929**, 10, 226-236.
- [6] A. E. Clatworthy, E. Pierson, D. T. Hung, "Targeting virulence: a new paradigm for antimicrobial therapy", *Nat. Chem. Biol.* **2007**, 3, 541-548.
- [7] H. W. Boucher, G. H. Talbot, D. K. Benjamin, Jr., J. Bradley, R. J. Guidos, R. N. Jones, *et al.*, "10 x '20 Progress-development of new drugs active against gram-negative bacilli: an update from the Infectious Diseases Society of America", *Clin. Infect. Dis.* **2013**, 56, 1685-1694.
- [8] H. W. Boucher, G. H. Talbot, J. S. Bradley, J. E. Edwards, D. Gilbert, L. B. Rice, *et al.*, "Bad bugs, no drugs: no ESKAPE! An update from the Infectious Diseases Society of America", *Clin. Infect. Dis.* **2009**, 48, 1-12.
- [9] K. Le Doare, J. Bielicki, P. T. Heath, M. Sharland, "Systematic Review of Antibiotic Resistance Rates Among Gram-Negative Bacteria in Children With Sepsis in Resource-Limited Countries", *J. Pediatr. Infect. Dis. Soc.* **2015**, 4, 11-20.
- [10] B. Swaminathan, P. Gerner-Smidt, T. Barrett, "Focus on Salmonella", *Foodborne Pathog. Dis.* **2006**, 3, 154-156.
- [11] E. J. Threlfall, "Antimicrobial drug resistance in Salmonella: problems and perspectives in food- and water-borne infections", *FEMS Microbiol. Rev.* **2002**, 26, 141-148.
- [12] D. L. Paterson, R. A. Bonomo, "Extended-spectrum beta-lactamases: a clinical update", *Clin. Microbiol. Rev.* **2005**, 18, 657-686.
- [13] D. Rawat, D. Nair, "Extended-spectrum beta-lactamases in Gram Negative Bacteria", *J. Glob. Infect. Dis.* **2010**, 2, 263-274.
- [14] J. A. Beutler, "Natural Products as a Foundation for Drug Discovery", *Curr. Protoc. Pharmacol.* **2009**, 46, 9.11.11-19.11.21.
- [15] J. Singh, R. C. Petter, T. A. Baillie, A. Whitty, "The resurgence of covalent drugs", *Nat. Rev. Drug. Discov.* **2011**, 10, 307-317.
- [16] R. Mah, J. R. Thomas, C. M. Shafer, "Drug discovery considerations in the development of covalent inhibitors", *Bioorg. Med. Chem. Lett.* **2014**, 24, 33-39.

- [17] M. Gersch, J. Kreuzer, S. A. Sieber, "Electrophilic natural products and their biological targets", *Nat. Prod. Rep.* **2012**, *29*, 659-682.
- [18] C. Drahl, B. F. Cravatt, E. J. Sorensen, "Protein-reactive natural products", *Angew. Chem. Int. Ed. Engl.* **2005**, *44*, 5788-5809.
- [19] J. A. H. Schwöbel, Y. K. Koleva, S. J. Enoch, F. Bajot, M. Hewitt, J. C. Madden, *et al.*, "Measurement and Estimation of Electrophilic Reactivity for Predictive Toxicology", *Chem. Rev.* **2011**, *111*, 2562-2596.
- [20] D. J. Waxman, J. L. Strominger, "Penicillin-binding proteins and the mechanism of action of beta-lactam antibiotics", *Annu. Rev. Biochem.* **1983**, *52*, 825-869.
- [21] I. Staub, S. A. Sieber, "Beta-lactams as selective chemical probes for the in vivo labeling of bacterial enzymes involved in cell wall biosynthesis, antibiotic resistance, and virulence", *J. Am. Chem. Soc.* **2008**, *130*, 13400-13409.
- [22] M. I. Page, Laws, A. P. , "The Chemical Reactivity of beta-Lactams, beta-Sultams and beta-Phospholactams", *Tetrahedron* **2000**, *56*, 5631-5638.
- [23] P. G. Proctor, N.P.; Page, M.I., "The Chemical Reactivity of Penicillins and Other p-Lactam Antibiotics", *J. Chem. Soc. Perkin Trans. II* **1982**, 1185-1192.
- [24] T. Böttcher, S. A. Sieber, "β-Lactams and β-lactones as activity-based probes in chemical biology", *Med. Chem. Comm.* **2012**, *3*, 408-417.
- [25] A. Noel, B. Delpech, D. Crich, "Comparison of the reactivity of beta-thiolactones and beta-lactones toward ring-opening by thiols and amines", *Org. Biomol. Chem.* **2012**, *10*, 6480-6483.
- [26] A. S. Griesbeck, D., "Herstellung enantiomerenreiner Derivate von 3-Amino- und 3-Mercaptobuttersäure durch SN2-Ringöffnung des β-Lactons und eines 1,3-Dioxanons aus der 3-Hydroxybuttersäure", *Helv. Chim. Acta* **1987**, *70*, 1326-1332.
- [27] J. A. T. P.-P. Manso, M.; del Pilar García-Santos, M.; Calle, E.; Casado, J., "A Kinetic Approach to the Alkylating Potential of Carcinogenic Lactones", *Chem. Res. Toxicol.* **2005**, *18*, 1161-1166.
- [28] H. Mayr, M. Patz, "Scales of Nucleophilicity and Electrophilicity: A System for Ordering Polar Organic and Organometallic Reactions", *Angew. Chem. Int. Ed. Engl.* **1994**, *33*, 938-957.
- [29] O. Kaumanns, R. Appel, T. Lemek, F. Seeliger, H. Mayr, "Nucleophilicities of the Anions of Arylacetonitriles and Arylpropionitriles in Dimethyl Sulfoxide", *J. Org. Chem.* **2008**, *74*, 75-81.
- [30] H. Mayr, T. Bug, M. F. Gotta, N. Hering, B. Irrgang, B. Janker, *et al.*, "Reference Scales for the Characterization of Cationic Electrophiles and Neutral Nucleophiles", *J. Am. Chem. Soc.* **2001**, *123*, 9500-9512.

- [31] For a comprehensive listing of nucleophilicity parameters  $N$ ,  $s_N$  and electrophilicity parameters  $E$ , see <http://www.cup.lmu.de/oc/mayr/DBintro.html>.
- [32] F. A. Long, M. Purchase, "The Kinetics of Hydrolysis of  $\beta$ -Propiolactone in Acid, Neutral and Basic Solutions<sup>1</sup>", *J. Am. Chem. Soc.* **1950**, *72*, 3267-3273.
- [33] A. R. Olson, R. J. Miller, "The Mechanism of the Aqueous Hydrolysis of  $\beta$ -Butyrolactone", *J. Am. Chem. Soc.* **1938**, *60*, 2687-2692.
- [34] G. M. Blackburn, H. L. H. Dodds, "Strain effects in acyl transfer reactions. Part III. Hydroxide and buffer-catalysed hydrolysis of small and medium ring lactones", *J. Chem. Soc. Perkin Trans. II* **1974**, 377-382.
- [35] T. L. Gresham, J. E. Jansen, F. W. Shaver, J. T. Gregory, " $\beta$ -Propiolactone. II. Reactions with Salts of Inorganic Acids", *J. Am. Chem. Soc.* **1948**, *70*, 999-1001.
- [36] T. L. Gresham, J. E. Jansen, F. W. Shaver, " $\beta$ -Propiolactone. IV<sup>1,2</sup> Reactions with Salts of Carboxylic Acids", *J. Am. Chem. Soc.* **1948**, *70*, 1003-1004.
- [37] P. D. Bartlett, G. Small, " $\beta$ -Propiolactone. IX. The Kinetics of Attack by Nucleophilic Reagents upon the Alcoholic Carbon of  $\beta$ -Propiolactone", *J. Am. Chem. Soc.* **1950**, *72*, 4867-4869.
- [38] M. T. Pérez-Prior, J. A. Manso, M. del Pilar García-Santos, E. Calle, J. Casado, "Reactivity of Lactones and GHB Formation", *J. Org. Chem.* **2005**, *70*, 420-426.
- [39] J. Kussmann, M. Beer, C. Ochsenfeld, "Linear-scaling self-consistent field methods for large molecules", *Wiley Interdiscip. Rev. Comput. Mol. Sci.* **2013**, *3*, 614-636.
- [40] H. M. Senn, W. Thiel, "QM/MM Methods for Biomolecular Systems", *Angew. Chem. Int. Ed. Engl.* **2009**, *48*, 1198-1229.
- [41] A. Warshel, "Multiscale Modeling of Biological Functions: From Enzymes to Molecular Machines (Nobel Lecture)", *Angew. Chem. Int. Ed. Engl.* **2014**, *53*, 10020-10031.
- [42] C. W. Pemble, L. C. Johnson, S. J. Kridel, W. T. Lowther, "Crystal structure of the thioesterase domain of human fatty acid synthase inhibited by Orlistat", *Nat. Struct. Mol. Biol.* **2007**, *14*, 704-709.
- [43] M. Gersch, K. Famulla, M. Dahmen, C. Göbl, I. Malik, K. Richter, *et al.*, "AAA+ chaperones and acyldepsipeptides activate the ClpP protease via conformational control", *Nat. Commun.* **2015**, *6*, 1-12.
- [44] H. N. Po, N. M. Senozan, "The Henderson-Hasselbalch Equation: Its History and Limitations", *J. Chem. Educ.* **2001**, *78*, 1499.
- [45] F. Brotzel, Y. C. Chu, H. Mayr, "Nucleophilicities of Primary and Secondary Amines in Water", *J. Org. Chem.* **2007**, *72*, 3679-3688.
- [46] Y. Altun, "Study of Solvent Composition Effects on the Protonation Equilibria of Various Anilines by Multiple Linear Regression and Factor Analysis Applied to the Correlation

- Between Protonation Constants and Solvatochromic Parameters in Ethanol–Water Mixed Solvents", *J. Sol. Chem.* **2004**, *33*, 479-497.
- [47] D. Xiong, Z. Li, H. Wang, J. Wang, "Selective separation of aliphatic and aromatic amines with CO<sub>2</sub> switchable ionic liquids aqueous two-phase systems", *Green Chem.* **2013**, *15*, 1941-1948.
- [48] P. J. Battye, E. M. Ihsan, R. B. Moodie, "Kinetics of hydrolysis and aminolysis of 1-methoxycarbonylpyridinium ions", *J. Chem. Soc. Perkin Trans. II* **1980**, 741-748.
- [49] C. H. Arrowsmith, H. X. Guo, A. J. Kresge, "Hydrogen Isotope Fractionation Factors for Benzylamine and Benzylammonium Ion. Comparison of Fractionation Factors for Neutral and Positively-Charged Nitrogen-Hydrogen Bonds", *J. Am. Chem. Soc.* **1994**, *116*, 8890-8894.
- [50] R. F. Jameson, G. Hunter, T. Kiss, "A <sup>1</sup>H nuclear magnetic resonance study of the deprotonation of L-dopa and adrenaline", *J. Chem. Soc. Perkin Trans. II* **1980**, 1105-1110.
- [51] C. Hansch, A. Leo, R. W. Taft, "A survey of Hammett substituent constants and resonance and field parameters", *Chem. Rev.* **1991**, *91*, 165-195.
- [52] T. A. Nigst, H. Mayr, "Comparison of the Electrophilic Reactivities of N-Acylpyridinium Ions and Other Acylating Agents", *Eur. J. Org. Chem.* **2013**, 2155-2163.
- [53] H. Mayr, "Reactivity scales for quantifying polar organic reactivity: the benzhydrylium methodology", *Tetrahedron* **2015**, *71*, 5095-5111.
- [54] G. Bringmann, T. Geuder, "The Directed Cleavage of Substituted 1-Phenylethylamines: A Novel Route to Enantiomerically Pure  $\beta$ -Amino Acid Esters and  $\beta$ -Lactams", *Synthesis* **1991**, 829-831.
- [55] R. A. Copeland, *Evaluation of Enzyme Inhibitors in Drug Discovery: A Guide for Medicinal Chemists and Pharmacologists*, 2nd Edition, Wiley, **2013**.
- [56] P. Imming, C. Sinning, A. Meyer, "Drugs, their targets and the nature and number of drug targets", *Nat. Rev. Drug. Discov.* **2006**, *5*, 821-834.
- [57] M. A. Azad, G. D. Wright, "Determining the mode of action of bioactive compounds", *Bioorg. Med. Chem.* **2012**, *20*, 1929-1939.
- [58] N. L. Anderson, N. G. Anderson, "Proteome and proteomics: New technologies, new concepts, and new words", *Electrophoresis* **1998**, *19*, 1853-1861.
- [59] W. P. Blackstock, M. P. Weir, "Proteomics: quantitative and physical mapping of cellular proteins", *Trends Biotechnol.* **1999**, *17*, 121-127.
- [60] S. A. Sieber, *Activity-Based Protein Profiling (Topics in Current Chemistry)*, vol. 324, Springer-Verlag, **2012**.
- [61] A. E. Speers, B. F. Cravatt, "Profiling Enzyme Activities In Vivo Using Click Chemistry Methods", *Chem. Biol.* **2004**, *11*, 535-546.



- [62] N. Li, H. S. Overkleeft, B. I. Florea, "Activity-based protein profiling: an enabling technology in chemical biology research", *Curr. Opin. Struct. Biol.* **2012**, *16*, 227-233.
- [63] B. F. Cravatt, A. T. Wright, J. W. Kozarich, "Activity-based protein profiling: from enzyme chemistry to proteomic chemistry", *Annu. Rev. Biochem.* **2008**, *77*, 383-414.
- [64] C. M. Kam, A. S. Abuelyaman, Z. Li, D. Hudig, J. C. Powers, "Biotinylated isocoumarins, new inhibitors and reagents for detection, localization, and isolation of serine proteases", *Biocon. Chem.* **1993**, *4*, 560-567.
- [65] A. S. Abuelyaman, D. Hudig, S. L. Woodard, J. C. Powers, "Fluorescent Derivatives of Diphenyl [1-(N-Peptidylamino)alkyl]phosphonate Esters: Synthesis and Use in the Inhibition and Cellular Localization of Serine Proteases", *Biocon. Chem.* **1994**, *5*, 400-405.
- [66] M. J. Evans, B. F. Cravatt, "Mechanism-Based Profiling of Enzyme Families", *Che. Rev.* **2006**, *106*, 3279-3301.
- [67] A. E. Speers, B. F. Cravatt, "Chemical Strategies for Activity-Based Proteomics", *Chem. Bio. Chem.* **2004**, *5*, 41-47.
- [68] A. E. Speers, G. C. Adam, B. F. Cravatt, "Activity-Based Protein Profiling in Vivo Using a Copper(I)-Catalyzed Azide-Alkyne [3 + 2] Cycloaddition", *J. Am. Chem. Soc.* **2003**, *125*, 4686-4687.
- [69] Y. Liu, M. P. Patricelli, B. F. Cravatt, "Activity-based protein profiling: The serine hydrolases", *Proc. Natl. Acad. Sci.* **1999**, *96*, 14694-14699.
- [70] M. Fonovic, M. Bogyo, "Activity Based Probes for Proteases: Applications to Biomarker Discovery, Molecular Imaging and Drug Screening", *Curr. Pharm. Dess.* **2007**, *13*, 253-261.
- [71] M. Fonović, M. Bogyo, "Activity-based probes as a tool for functional proteomic analysis of proteases", *Expert. Rev. Proteomic* **2008**, *5*, 721-730.
- [72] D. Greenbaum, K. F. Medzihradszky, A. Burlingame, M. Bogyo, "Epoxide electrophiles as activity-dependent cysteine protease profiling and discovery tools", *Chem. Biol.* **2000**, *7*, 569-581.
- [73] A. M. Sadaghiani, S. H. L. Verhelst, M. Bogyo, "Tagging and detection strategies for activity-based proteomics", *Curr. Opin. Chem. Biol.* **2007**, *11*, 20-28.
- [74] M. B. Nodwell, S. A. Sieber. ABPP Methodology: Introduction and Overview. *Activity-Based Protein Profiling*. Springer Berlin Heidelberg: Berlin, Heidelberg, **2012**, 1-41.
- [75] T. Böttcher, M. Pitscheider, S. A. Sieber, "Natural Products and Their Biological Targets: Proteomic and Metabolomic Labeling Strategies", *Angew. Chem. Int. Ed.* **2010**, *49*, 2680-2698.
- [76] S. A. Sieber, B. F. Cravatt, "Analytical platforms for activity-based protein profiling - exploiting the versatility of chemistry for functional proteomics", *Chem. Comm.* **2006**, 2311-2319.

- [77] R. Huisgen, *1,3 Dipolar Cycloaddition chemistry*, Wiley: New York, **1984**.
- [78] V. V. Rostovtsev, L. G. Green, V. V. Fokin, K. B. Sharpless, "A Stepwise Huisgen Cycloaddition Process: Copper(I)-Catalyzed Regioselective "Ligation" of Azides and Terminal Alkynes", *Angew. Chem. Int. Ed.* **2002**, *41*, 2596-2599.
- [79] C. W. Tornøe, C. Christensen, M. Meldal, "Peptidotriazoles on Solid Phase: [1,2,3]-Triazoles by Regiospecific Copper(I)-Catalyzed 1,3-Dipolar Cycloadditions of Terminal Alkynes to Azides", *J. Org. Chem.* **2002**, *67*, 3057-3064.
- [80] F. Marko, B. Matthew, "Activity Based Probes for Proteases: Applications to Biomarker Discovery, Molecular Imaging and Drug Screening", *Curr. Pharm. Des.* **2007**, *13*, 253-261.
- [81] P. J. Boersema, T. T. Aye, T. A. B. van Veen, A. J. R. Heck, S. Mohammed, "Triplex protein quantification based on stable isotope labeling by peptide dimethylation applied to cell and tissue lysates", *Proteomics* **2008**, *8*, 4624-4632.
- [82] P. J. Boersema, R. Raijmakers, S. Lemeer, S. Mohammed, A. J. R. Heck, "Multiplex peptide stable isotope dimethyl labeling for quantitative proteomics", *Nat. Protocols* **2009**, *4*, 484-494.
- [83] D. Kovanich, S. Cappadona, R. Raijmakers, S. Mohammed, A. Scholten, A. J. R. Heck, "Applications of stable isotope dimethyl labeling in quantitative proteomics", *Anal. Bioanal. Chem.* **2012**, *404*, 991-1009.
- [84] J. Marco-Contelles, M. T. Molina, S. Anjum, "Naturally Occurring Cyclohexane Epoxides: Sources, Biological Activities, and Synthesis", *Chem. Rev.* **2004**, *104*, 2857-2900.
- [85] I. Sattler, R. Thiericke, A. Zeeck, "The manumycin-group metabolites", *Nat. Prod. Rep.* **1998**, *15*, 221-240.
- [86] K.-I. Hayashi, M. Nakagawa, M. Nakayama, "Nisamycin, a new manumycin group antibiotic from *Streptomyces* sp. K106. I. Taxonomy, fermentation, isolation, physico-chemical and biological properties", *J. Antibiot.* **1994**, *47*, 1104-1109.
- [87] J. U. N. Kohno, M. Nishio, K. Kawano, N. Nakanishi, S.-I. Suzuki, T. Uchida, *et al.*, "TMC-1 A, B, C and D, New Antibiotics of the Manumycin Group Produced by *Streptomyces* sp. Taxonomy, Production, Isolation, Physico-chemical Properties, Structure Elucidation and Biological Properties", *J. Antibiot.* **1996**, *49*, 1212-1220.
- [88] C. R. Johnson, M. W. Miller, "Enzymic Resolution of a C<sub>2</sub> Symmetric Diol Derived from p-Benzoquinone: Synthesis of (+)- and (-)-Bromoxone", *J. Org. Chem.* **1995**, *60*, 6674-6675.
- [89] T. Fex, "A stereospecific synthesis of chalozone", *Tet. Lett.* **1981**, *22*, 2707-2708.
- [90] A. Ichihara, K. Moriyasu, S. Sakamura, "Syntheses of (±)-Epoformin (Desoxyepoxydon) and (±)-Epiepoformin (Desoxyepiepoxydon)", *Agric. Biol. Chem.* **1978**, *42*, 2421-2422.
- [91] A. Ichihara, R. Kimura, K. Oda, S. Sakamura, "Simple syntheses of dl-phyllostine, dl-epoxydon and dl-epiepoxydon", *Tet. Lett.* **1976**, *17*, 4741-4744.

- [92] Z. Kis, A. Closse, H. P. Sigg, L. Hruban, G. Snatzke, "Die Struktur von Panepoxydon und verwandten Pilzmetaboliten", *Helv. Chim. Acta.* **1970**, 53, 1577-1597.
- [93] M. W. Miller, C. R. Johnson, "Sonogashira Coupling of 2-Iodo-2-cycloalkenones: Synthesis of (+)- and (-)-Harveynone and (-)-Tricholomenyn A", *J. Org. Chem.* **1997**, 62, 1582-1583.
- [94] O. Block, Darstellung von Verbindungen vom Manumycin-Typ sowie von Zuckeranaloga aus unverzweigtem und verzweigtem p-Benzochinon, Dissertation **2000**.
- [95] Y. Fu, P. Wu, J. Xue, X. Wei, "Cytotoxic and Antibacterial Quinone Sesquiterpenes from a *Myrothecium* Fungus", *J. Nat. Prod.* **2014**, 77, 1791-1799.
- [96] C. Li, S. Bardhan, E. A. Pace, M.-C. Liang, T. D. Gilmore, J. A. Porco, "Angiogenesis Inhibitor Epoxyquinol A: Total Synthesis and Inhibition of Transcription Factor NF- $\kappa$ B", *Org. Lett.* **2002**, 4, 3267-3270.
- [97] J. B. Shotwell, B. Koh, H. W. Choi, J. L. Wood, C. M. Crews, "Inhibitors of NF- $\kappa$ B signaling: design and synthesis of a biotinylated isopanepoxydone affinity reagent", *Bioorg. Med. Chem. Lett.* **2002**, 12, 3463-3466.
- [98] G. Mehta, K. Islam, "Total Synthesis of the Novel NF- $\kappa$ B Inhibitor (-)-Cycloepoxydon", *Org. Lett.* **2004**, 6, 807-810.
- [99] M. Kara, S. Soga, K. Shono, J. U. N. Eishima, T. Mizukami, "UCF76 Compounds, New Inhibitors of Farnesyltransferase Produced by *Streptomyces*", *J. Antibiot.* **2001**, 54, 182-186.
- [100] V. Rukachaisirikul, C. Tansakul, S. Saithong, C. Pakawatchai, M. Isaka, R. Suvannakad, "Hirsutane Sesquiterpenes from the Fungus *Lentinus connatus* BCC 8996", *J. Nat. Prod.* **2005**, 68, 1674-1676.
- [101] M. G. Anderson, R. W. Rickards, E. Lacey, "Structures of Flagranones A, B and C, Cyclohexenoxide Antibiotics from the Nematode-trapping Fungus *Duddingtonia flagrans*", *J. Antibiot.* **1999**, 52, 1023-1028.
- [102] N. Matsumoto, T. Tsuchida, M. Umekita, N. Kinoshita, H. Iinuma, T. Sawa, *et al.*, "Epoxyquinomicins A, B, C and D, New Antibiotics from *Amycolatopsis*. I. Taxonomy, Fermentation, Isolation and Antimicrobial Activities", *J. Antibiot.* **1997**, 50, 900-905.
- [103] S. J. Box, M. L. Gilpin, M. Gwynn, G. Hanscomb, S. R. Spear, A. G. Brown, "MM14201, a new epoxyquinone derivative with antibacterial activity produced by a species of *Streptomyces*", *J. Antibiot.* **1983**, 36, 1631-1637.
- [104] O. Block, G. Klein, H.-J. Altenbach, D. J. Brauer, "New Stereoselective Route to the Epoxyquinol Core of Manumycin-Type Natural Products. Synthesis of Enantiopure (+)-Bromoxone, (-)-LL-C10037 $\alpha$ , and (+)-KT 8110", *J. Org. Chem.* **2000**, 65, 716-721.
- [105] H. Zaehner, "Metabolites of Microorganisms. 41. Manumycin", *Pharm. Acta. Helv.* **1963**, 871-874.
- [106] K. Schröder, A. Zeeck, "Manumycin", *Tet. Lett.* **1973**, 14, 4995-4998.

- [107] P. R. Shipley, C. C. Donnelly, A. D. Bernauer, A. Klegeris, "Antitumor activity of asukamycin, a secondary metabolite from the actinomycete bacterium *Streptomyces nodosus* subspecies *asukaensis*", *Int. J. Mol. Med.* **2009**, *24*, 711-715.
- [108] H. Kouchi, K. Nakamura, K. Fushimi, M. Sakaguchi, M. Miyazaki, T. Ohe, *et al.*, "Manumycin A, Inhibitor of ras Farnesyltransferase, Inhibits Proliferation and Migration of Rat Vascular Smooth Muscle Cells", *Biochem. Biophys. Res. Commun.* **1999**, *264*, 915-920.
- [109] Y. Shiono, T. Murayama, K. Takahashi, K. Okada, S. Katohda, M. Ikeda, "Three Oxygenated Cyclohexenone Derivatives Produced by an Endophytic Fungus", *Biosci. Biotechnol. Biochem.* **2005**, *69*, 287-292.
- [110] F. Li, R. P. Maskey, S. Qin, I. Sattler, H. H. Fiebig, A. Maier, *et al.*, "Chinikomycins A and B: Isolation, Structure Elucidation, and Biological Activity of Novel Antibiotics from a Marine *Streptomyces* sp. Isolate M045#1", *J. Nat. Prod.* **2005**, *68*, 349-353.
- [111] R. J. K. Taylor, L. Alcaraz, I. Kapfer-Eyer, G. Macdonald, X. Wei, N. Lewis, "The Synthesis of Alisamycin, Nisamycin, LL-C10037 $\alpha$  and Novel Epoxyquinol and Epoxyquinone Analogues of Manumycin A", *Synthesis* **1998**, *1998*, 775-790.
- [112] P. Wipf, P. D. G. Coish, "Total Synthesis of ( $\pm$ )-Nisamycin", *J. Org. Chem.* **1999**, *64*, 5053-5061.
- [113] N. Matsumoto, A. Ariga, S. To-e, H. Nakamura, N. Agata, S.-i. Hirano, *et al.*, "Synthesis of NF- $\kappa$ B activation inhibitors derived from epoxyquinomicin C", *Bioorg. Med. Chem. Lett.* **2000**, *10*, 865-869.
- [114] H. J. Altenbach, H. Stegelmeier, E. Vogel, "Einfache stereospezifische synthesen von anti-benzoldioxid und anti-benzoltrioxid", *Tet. Lett.* **1978**, *19*, 3333-3336.
- [115] T. Kamikubo, K. Ogasawara, "The enantiocontrolled synthesis of (-)-tricholomenyn A, a novel antimitotic enynylcyclohexenone from *Tricholoma acerbum*", *Chem. Comm.* **1996**, 1679-1680.
- [116] T. Kamikubo, K. Hiroya, K. Ogasawara, "Stereo- and enantio-controlled synthesis of two naturally occurring polyoxygenated cyclohexenemethanols, (+)-epiepoxydon and (-)-phyllostine, via catalytic asymmetrization of a meso substrate", *Tet. Lett.* **1996**, *37*, 499-502.
- [117] A. Ichihara, K. Oda, S. Sakamura, "Regiospecific syntheses of dl-phyllostine and dl-epoxydon (phyllosinol)", *Tet. Lett.* **1972**, *13*, 5105-5108.
- [118] P. Wipf, Y. Kim, "Synthesis of the Antitumor Antibiotic LL-C10037. $\alpha$ ", *J. Org. Chem.* **1994**, *59*, 3518-3519.
- [119] P. Wipf, Y. Kim, H. Jahn, "Synthesis of (-)-LL-C10037 $\alpha$  and Related Manumycin-Type Epoxyquinols", *Synthesis* **1995**, *1995*, 1549-1561.
- [120] L. Alcaraz, G. Macdonald, I. Kapfer, N. J. Lewis, R. J. K. Taylor, "The first total synthesis of a member of the manumycin family of antibiotics: Alisamycin", *Tet. Lett.* **1996**, *37*, 6619-6622.

- [121] I. Kapfer, N. J. Lewis, G. Macdonald, R. J. K. Taylor, "The synthesis of novel analogues of the manumycin family of antibiotics and the antitumour antibiotic LL-C10037 $\alpha$ ", *Tet. Lett.* **1996**, 37, 2101-2104.
- [122] L. Alcaraz, G. Macdonald, J. P. Ragot, N. Lewis, R. J. K. Taylor, "Manumycin A: Synthesis of the (+)-Enantiomer and Revision of Stereochemical Assignment", *J. Org. Chem.* **1998**, 63, 3526-3527.
- [123] G. Macdonald, L. Alcaraz, N. J. Lewis, R. J. K. Taylor, "Asymmetric synthesis of the mC7N core of the manumycin family: Preparation of (+)-MT 35214 and a formal total synthesis of (-)-alisamycin", *Tet. Lett.* **1998**, 39, 5433-5436.
- [124] L. Alcaraz, G. Macdonald, J. Ragot, N. J. Lewis, R. J. K. Taylor, "Synthetic approaches to the Manumycin A, B and C antibiotics: The first total synthesis of (+)-Manumycin A", *Tetrahedron* **1999**, 55, 3707-3716.
- [125] Y. Hu, C. R. Melville, S. J. Gould, H. G. Floss, "3-Amino-4-hydroxybenzoic Acid: the Precursor of the C7N Unit in Asukamycin and Manumycin", *J. Am. Chem. Soc.* **1997**, 119, 4301-4302.
- [126] C. Li, E. A. Pace, M.-C. Liang, E. Lobkovsky, T. D. Gilmore, J. A. Porco, "Total Synthesis of the NF- $\kappa$ B Inhibitor (-)-Cycloepoxydon: Utilization of Tartrate-Mediated Nucleophilic Epoxidation", *J. Am. Chem. Soc.* **2001**, 123, 11308-11309.
- [127] W. Adam, H. Kılç, C. R. Saha-Möller, "An Efficient Regioselective and Diastereoselective Synthesis of the Epoxy-quinol Functionality as Building Block for the Manumycin Antibiotics by the Sequence of Photooxygenation, Reduction and Weitz-Scheffer Epoxidation", *Synlett* **2002**, 510-512.
- [128] E. C. L. Gautier, N. J. Lewis, A. McKillop, R. J. K. Taylor, "Synthesis of bromoxone", *Tet. Lett.* **1994**, 35, 8759-8760.
- [129] M. G. Dolson, J. S. Swenton, "Anodic oxidation of mixed ethers of hydroquinones. A complementary route to benzoquinone monoketals", *J. Org. Chem.* **1981**, 46, 177-179.
- [130] R. K. Duke, R. W. Rickards, "Stereospecific total synthesis of the cyclohexene oxide antibiotic eupenoxide", *J. Org. Chem.* **1984**, 49, 1898-1904.
- [131] M. Shoji, J. Yamaguchi, H. Kakeya, H. Osada, Y. Hayashi, "Total Synthesis of (+)-Epoxyquinols A and B", *Angew. Chem. Int. Ed.* **2002**, 41, 3192-3194.
- [132] M. Shoji, S. Kishida, M. Takeda, H. Kakeya, H. Osada, Y. Hayashi, "A practical total synthesis of both enantiomers of epoxyquinols A and B", *Tet. Lett.* **2002**, 43, 9155-9158.
- [133] Y. Suzuki, C. Sugiyama, O. Ohno, K. Umezawa, "Preparation and biological activities of optically active dehydroxymethylepoxyquinomicin, a novel NF- $\kappa$ B inhibitor", *Tetrahedron* **2004**, 60, 7061-7066.
- [134] E. C. L. Gautier, A. E. Graham, A. McKillop, S. P. Standen, R. J. K. Taylor, "Acetal and ketal deprotection using montmorillonite K10: The first synthesis of syn-4,8-dioxatricyclo[5.1.0.0<sup>3,5</sup>]-2,6-octanedione", *Tet. Lett.* **1997**, 38, 1881-1884.

- [135] C. Chaicharoenpong, K. Kato, K. Umezawa, "Synthesis and Structure–Activity Relationship of Dehydroxymethylepoxyquinomicin Analogues as Inhibitors of NF- $\kappa$ B Functions", *Bioorg. Med. Chem.* **2002**, *10*, 3933-3939.
- [136] T. Tanaka, E. U. I. Tsukuda, Y. Uosaki, Y. Matsuda, "EI-1511-3, -5 and EI-1625-2, Novel Interleukin-1.BETA. Converting Enzyme Inhibitors Produced by Streptomyces sp. E-1511 and E-1625. III. Biochemical Properties of EI-1511-3, -5 and EI 1625-2", *J. Antibiot.* **1996**, *49*, 1085-1090.
- [137] K. Umezawa, "Inhibition of tumor growth by NF- $\kappa$ B inhibitors", *Cancer Sci.* **2006**, *97*, 990-995.
- [138] M. Bernier, Y.-K. Kwon, S. K. Pandey, T.-N. Zhu, R.-J. Zhao, A. Maciuk, *et al.*, "Binding of Manumycin A Inhibits I $\kappa$ B Kinase  $\beta$  Activity", *J. Biol. Chem.* **2006**, *281*, 2551-2561.
- [139] R. Thiericke, A. Zeeck, A. Nakagawa, S. Omura, R. E. Herrold, S. T. S. Wu, *et al.*, "Biosynthesis of the manumycin group antibiotics", *J. Am. Chem. Soc.* **1990**, *112*, 3979-3987.
- [140] A. V. Crain, J. B. Broderick, "Pyruvate Formate-lyase and Its Activation by Pyruvate Formate-lyase Activating Enzyme", *J. Biol. Chem.* **2014**, *289*, 5723-5729.
- [141] UniProt, <http://www.uniprot.org/uniprot/Q8Z808>.
- [142] J. M. Buis, J. B. Broderick, "Pyruvate formate-lyase activating enzyme: elucidation of a novel mechanism for glycyl radical formation", *Arch. Biochem. Biophys.* **2005**, *433*, 288-296.
- [143] UniProt, <http://www.uniprot.org/uniprot/Q8ZLR6>.
- [144] R. Ueshima, N. Fujita, A. Ishihama, "Identification of Escherichia coli proteins cross-reacting with antibodies against region 2.2 peptide of RNA polymerase sigma subunit", *Biochem. Biophys. Res. Commun.* **1992**, *184*, 634-639.
- [145] H. Hemmi, S.-i. Ohnuma, K. Nagaoka, T. Nishino, "Identification of Genes Affecting Lycopene Formation in *Escherichia coli* Transformed with Carotenoid Biosynthetic Genes: Candidates for Early Genes in Isoprenoid Biosynthesis", *J. Biochem.* **1998**, *123*, 1088-1096.
- [146] F. H. Niesen, H. Berglund, M. Vedadi, "The use of differential scanning fluorimetry to detect ligand interactions that promote protein stability", *Nat. Protoc.* **2007**, *2*, 2212-2221.
- [147] A. P. Demchenko, *Advanced Fluorescence Reporters in Chemistry and Biology III: Applications in Sensing and Imaging*, vol. Band 3 von Advanced Fluorescence Reporters in Chemistry and Biology, Springer, **2011**.
- [148] N. P. Blast, <https://blast.ncbi.nlm.nih.gov/Blast.cgi>.
- [149] J. Badger, J. M. Sauder, J. M. Adams, S. Antonysamy, K. Bain, M. G. Bergseid, *et al.*, "Structural analysis of a set of proteins resulting from a bacterial genomics project", *Protein Struct. Funct. Genet.* **2005**, *60*, 787-796.

- [150] Y. Wei, D. Ringe, M. A. Wilson, M. J. Ondrechen, "Identification of Functional Subclasses in the DJ-1 Superfamily Proteins", *PLoS Comput. Biol.* **2007**, *3*, e15.
- [151] A. V. Broek, P. Gysegom, O. Ona, N. Hendrickx, E. Prinsen, J. Van Impe, *et al.*, "Transcriptional Analysis of the *Azospirillum brasilense* Indole-3-Pyruvate Decarboxylase Gene and Identification of a cis-Acting Sequence Involved in Auxin Responsive Expression", *Mol. Plant Microbe Interact.* **2005**, *18*, 311-323.
- [152] H. J. Jung, S. Kim, Y. J. Kim, M.-K. Kim, S. G. Kang, J.-H. Lee, *et al.*, "Dissection of the Dimerization Modes in the DJ-1 Superfamily", *Mol. Cell* **2012**, *33*, 163-171.
- [153] M. M. Horvath, N. V. Grishin, "The C-terminal domain of HPIL catalase is a member of the type I glutamine amidotransferase superfamily", *Protein Struct. Funct. Genet.* **2001**, *42*, 230-236.
- [154] S.-J. Lee, S. J. Kim, I.-K. Kim, J. Ko, C.-S. Jeong, G.-H. Kim, *et al.*, "Crystal Structures of Human DJ-1 and *Escherichia coli* Hsp31, Which Share an Evolutionarily Conserved Domain", *J. Biol. Chem.* **2003**, *278*, 44552-44559.
- [155] J.-Y. Im, K.-W. Lee, J.-M. Woo, E. Junn, M. M. Mouradian, "DJ-1 induces thioredoxin 1 expression through the Nrf2 pathway", *Hum. Mol. Gen.* **2012**, *21*, 3013-3024.
- [156] M. Neumann, V. Müller, K. Görner, H. A. Kretschmar, C. Haass, P. J. Kahle, "Pathological properties of the Parkinson's disease-associated protein DJ-1 in  $\alpha$ -synucleinopathies and tauopathies: relevance for multiple system atrophy and Pick's disease", *Acta Neuropathologica* **2004**, *107*, 489-496.
- [157] X. Du, I.-G. Choi, R. Kim, W. Wang, J. Jancarik, H. Yokota, *et al.*, "Crystal structure of an intracellular protease from *Pyrococcus horikoshii* at 2-Å resolution", *Proc. Natl. Acad. Sci. USA* **2000**, *97*, 14079-14084.
- [158] D. L. Ollis, E. Cheah, M. Cygler, B. Dijkstra, F. Frolova, S. M. Franken, *et al.*, "The  $\alpha/\beta$  hydrolase fold", *Protein Eng.* **1992**, *5*, 197-211.
- [159] M. Di Berardino, A. Dijkstra, D. Stüber, W. Keck, M. Gubler, "The monofunctional glycosyltransferase of *Escherichia coli* is a member of a new class of peptidoglycan-synthesising enzymes: Overexpression and determination of the glycan-polymerising activity", *FEBS Lett.* **1996**, *392*, 184-188.
- [160] A. Derouaux, B. Wolf, C. Fraipont, E. Breukink, M. Nguyen-Distèche, M. Terrak, "The Monofunctional Glycosyltransferase of *Escherichia coli* Localizes to the Cell Division Site and Interacts with Penicillin-Binding Protein 3, FtsW, and FtsN", *J. Bacteriol.* **2008**, *190*, 1831-1834.
- [161] S. A. Carroll, T. Hain, U. Technow, A. Darji, P. Pashalidis, S. W. Joseph, *et al.*, "Identification and Characterization of a Peptidoglycan Hydrolase, MurA, of *Listeria monocytogenes*, a Muramidase Needed for Cell Separation", *J. Bacteriol.* **2003**, *185*, 6801-6808.
- [162] J. Vandooren, N. Geurts, E. Martens, P. E. Van den Steen, G. Opdenakker, "Zymography methods for visualizing hydrolytic enzymes", *Nat. Meth.* **2013**, *10*, 211-220.

- [163] D. a. L. Dufour, C. M., <http://www.bio-protocol.org/e855>Zymogram -Assay for the Detection of Peptidoglycan Hydrolases in Streptococcus mutans, protocol 3(16): e855, **2013**.
- [164] M. Willemoës, B. W. Sigurskjold, "Steady-state kinetics of the glutaminase reaction of CTP synthase from Lactococcus lactis", *Eur. J. Biochem.* **2002**, 269, 4772-4779.
- [165] C. W. Long, A. B. Pardee, "Cytidine Triphosphate Synthetase of Escherichia coli B : I. Purification and Kinetics", *J. Biol. Chem.* **1967**, 242, 4715-4721.
- [166] S. L. L. Wadskov-Hansen, M. Willemoës, J. Martinussen, K. Hammer, J. Neuhard, S. Larsen, "Cloning and Verification of the Lactococcus lactis pyrG Gene and Characterization of the Gene Product, CTP Synthase", *J. Biol. Chem.* **2001**, 276, 38002-38009.
- [167] B. labtech, <http://www.bmglabtech.com/en/applications/application-notes/185-enzyme-kinetic-measurements-performed-on-bmg-labtechs-fluostar-optima-obj-91-814.html>.
- [168] M. Levine, L. Lavis, R. Raines, "Trimethyl Lock: A Stable Chromogenic Substrate for Esterases", *Molecules* **2008**, 13, 204.
- [169] R. M. Canet-Avilés, M. A. Wilson, D. W. Miller, R. Ahmad, C. McLendon, S. Bandyopadhyay, *et al.*, "The Parkinson's disease protein DJ-1 is neuroprotective due to cysteine-sulfinic acid-driven mitochondrial localization", *Proc. Natl. Acad. Sci. USA* **2004**, 101, 9103-9108.
- [170] Y. J. Choi, C. B. Miguez, B. H. Lee, "Characterization and Heterologous Gene Expression of a Novel Esterase from Lactobacillus casei CL96", *Appl. Environ. Microbiol.* **2004**, 70, 3213-3221.
- [171] G. Liu, J. Zhou, Q. S. Fu, J. Wang, "The Escherichia coli Azoreductase AzoR Is Involved in Resistance to Thiol-Specific Stress Caused by Electrophilic Quinones", *J. Bacteriol.* **2009**, 191, 6394-6400.
- [172] G. C. Rudolf, M. F. Koch, F. A. M. Mandl, S. A. Sieber, "Subclass-Specific Labeling of Protein-Reactive Natural Products with Customized Nucleophilic Probes", *Chem. Eur. J.* **2015**, 21, 3701-3707.
- [173] R. Ortenberg, S. Gon, A. Porat, J. Beckwith, "Interactions of glutaredoxins, ribonucleotide reductase, and components of the DNA replication system of Escherichia coli", *Proc. Natl. Acad. Sci. USA* **2004**, 101, 7439-7444.
- [174] W. A. Prinz, F. Åslund, A. Holmgren, J. Beckwith, "The Role of the Thioredoxin and Glutaredoxin Pathways in Reducing Protein Disulfide Bonds in the Escherichia coli Cytoplasm", *J. Biol. Chem.* **1997**, 272, 15661-15667.
- [175] C. Scharf, S. Riethdorf, H. Ernst, S. Engelmann, U. Völker, M. Hecker, "Thioredoxin Is an Essential Protein Induced by Multiple Stresses in Bacillus subtilis", *J. Bacteriol.* **1998**, 180, 1869-1877.
- [176] E. Bjur, S. Eriksson-Ygberg, F. Åslund, M. Rhen, "Thioredoxin 1 Promotes Intracellular Replication and Virulence of Salmonella enterica Serovar Typhimurium", *Infect. Immun.* **2006**, 74, 5140-5151.



- [177] A. Negrea, E. Bjur, S. Puiac, S. E. Ygberg, F. Åslund, M. Rhen, "Thioredoxin 1 Participates in the Activity of the Salmonella enterica Serovar Typhimurium Pathogenicity Island 2 Type III Secretion System", *J. Bacteriol.* **2009**, *191*, 6918-6927.
- [178] R. Gosmini, V. L. Nguyen, J. Toum, C. Simon, J.-M. G. Brusq, G. Krysa, *et al.*, "The Discovery of I-BET726 (GSK1324726A), a Potent Tetrahydroquinoline ApoA1 Up-Regulator and Selective BET Bromodomain Inhibitor", *J. Med. Chem.* **2014**, *57*, 8111-8131.
- [179] J.-i. Sakaki, S. Kobayashi, M. Sato, C. Kaneko, "Synthesis of 1, 3-Dioxin-4-ones and Their Use in Synthesis. XVIII. : Synthesis of Azetidin-2-ones from 1, 3-Dioxin-4-ones via 3-Hydroxycarboxamides", *Chem. Pharm. Bull.* **1989**, *37*, 2952-2960.
- [180] R. P. Maskey, I. Kock, M. Shaaban, I. Grün-Wollny, E. Helmke, F. Mayer, *et al.*, "Low molecular weight oligo- $\beta$ -hydroxybutyric acids and 3-hydroxy-N-phenethyl-butylamide – new products from microorganisms", *Pol. Bull.* **2002**, *49*, 87-93.
- [181] D. S. Holmes, R. C. Bethell, N. Cammack, I. R. Clemens, J. Kitchin, P. McMeekin, *et al.*, "Synthesis and structure-activity relationships of a series of penicillin-derived HIV proteinase inhibitors containing a stereochemically unique peptide isostere", *J. Med. Chem.* **1993**, *36*, 3129-3136.
- [182] M. Hamada, Y. Niitsu, C. Hiraoka, I. Kozawa, T. Higashi, M. Shoji, *et al.*, "Chemoenzymatic synthesis of (2S,3S,4S)-form, the physiologically active stereoisomer of dehydroxymethylepoxyquinomicin (DHMEQ), a potent inhibitor on NF- $\kappa$ B", *Tetrahedron* **2010**, *66*, 7083-7087.
- [183] T. M. V. D. Pinho e Melo, D. M. Barbosa, P. J. R. S. Ramos, A. M. d'A. Rocha Gonsalves, T. L. Gilchrist, A. M. Beja, *et al.*, "Intramolecular dipolar cycloaddition reaction of 5H,7H-thiazolo[3,4-c]oxazol-4-ium-1-olates: synthesis of chiral 1H-pyrrolo[1,2-c]thiazole derivatives", *J. Chem. Soc., Perkin Trans. I* **1999**, 1219-1224.
- [184] S. Hiraoka, K. Hirata, M. Shionoya, "A Molecular Ball Bearing Mediated by Multiligand Exchange in Concert", *Angew. Chem. Int. Ed.* **2004**, *43*, 3814-3818.
- [185] T. Böttcher, S. A. Sieber, " $\beta$ -Lactones as Privileged Structures for the Active-Site Labeling of Versatile Bacterial Enzyme Classes", *Angew. Chem. Int. Ed.* **2008**, *47*, 4600-4603.
- [186] J. Eirich, R. Orth, S. A. Sieber, "Unraveling the Protein Targets of Vancomycin in Living *S. aureus* and *E. faecalis* Cells", *J. Am. Chem. Soc.* **2011**, *133*, 12144-12153.
- [187] O. A. Battenberg, Y. Yang, S. H. L. Verhelst, S. A. Sieber, "Target profiling of 4-hydroxyderricin in *S. aureus* reveals seryl-tRNA synthetase binding and inhibition by covalent modification", *Mol. Bio. System* **2013**, *9*, 343-351.
- [188] W. Kabsch, "Integration, scaling, space-group assignment and post-refinement", *Acta Crystallogr. Sect. D-Biol. Crystallogr.* **2010**, *66*, 133-144.
- [189] K. Diederichs, P. A. Karplus, "Better models by discarding data?", *Acta Crystallogr. Sect. D-Biol. Crystallogr.* **2013**, *69*, 1215-1222.

- [190] P. Evans, "Resolving Some Old Problems in Protein Crystallography", *Science* **2012**, 336, 986-987.
- [191] P. A. Karplus, K. Diederichs, "Linking Crystallographic Model and Data Quality", *Science* **2012**, 336, 1030-1033.
- [192] A. J. McCoy, R. W. Grosse-Kunstleve, P. D. Adams, M. D. Winn, L. C. Storoni, R. J. Read, "Phaser crystallographic software", *J. Appl. Crystallogr.* **2007**, 40, 658-674.
- [193] P. Emsley, B. Lohkamp, W. G. Scott, K. Cowtan, "Features and development of Coot", *Acta Crystallogr. Sect. D-Biol. Crystallogr.* **2010**, 66, 486-501.
- [194] J. Painter, E. A. Merritt, "TLSMDweb server for the generation of multi-group TLS models", *J. Appl. Crystallogr.* **2006**, 39, 109-111.
- [195] M. D. Winn, G. N. Murshudov, M. Z. Papiz. Macromolecular TLS Refinement in REFMAC at Moderate Resolutions. *Methods in Enzymology, Academic Press*, **2003**, 374, 300-321.



## VI – ABBREVIATIONS



3-HBA	3-Hydroxybutyric acid
ABC	Ammonium bicarbonate
ABPP	Activity-based protein profiling
AMP	Adenosine monophosphate
ATET	Anhydrotetracycline
BBL	<i>beta</i> -Butyrolactone
brine	saturated NaCl solution
C18	Octadecyl carbon chain bonded silica
calcd	calculated
cAMP	Cyclic adenosine monophosphate
cGMP	Cyclic guanosine monophosphate
CTP	Cytidine triphosphate
DHMEQ	Dehydroxymethylepoxyquinomicin
DIBAL	Diisobutylaluminiumhydrid
DIC	<i>N,N'</i> -Diisopropylcarbodiimide
DIPEA	Diisopropylethyl amine
DMAP	<i>N,N</i> -Dimethyl-4-aminopyridine
DMF	Dimethylformamide
DMSO	Dimethylsulfoxide
DTT	Dithiothreitol
ESBL	Extended spectrum <i>beta</i> -lactamase
ESI	Electrospray ionization
FDA	US food and drug administration
GAT	Glutamine amidotransferase
GMP	Guanosine monophosphate
GSH	Glutathione
HPLC	High-performance liquid chromatography
HRMS	High-resolution mass spectrometry
Hz	Hertz
IAA	2-Iodoacetamide
IPTG	Isopropyl- $\beta$ -D-1-thiogalactopyranoside
<i>J</i>	Coupling constant in Hz
LC	Liquid chromatography
LITQ-FTICR	Linear trap quadrupole - Fourier Transform - ion cyclotron resonance
<i>m/z</i>	Mass to charge ration
mCPBA	<i>meta</i> -Chloroperoxybenzoic acid
MeCN	Acetonitrile

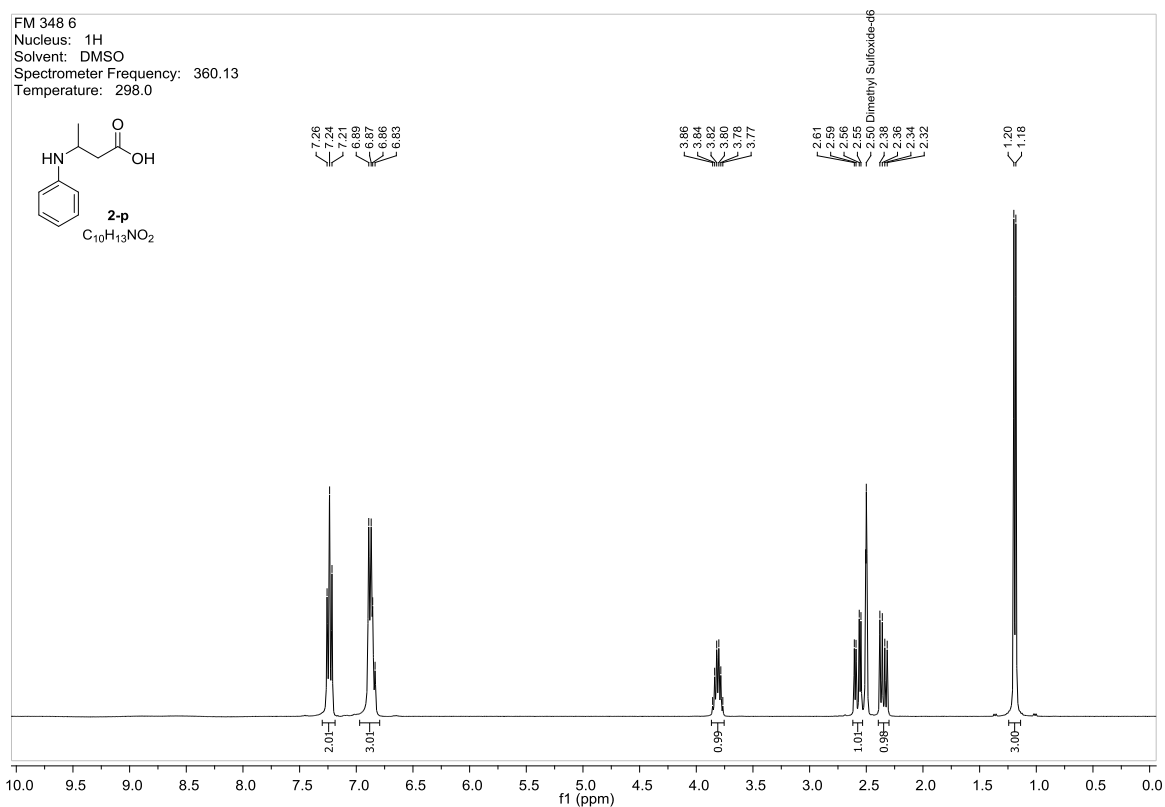
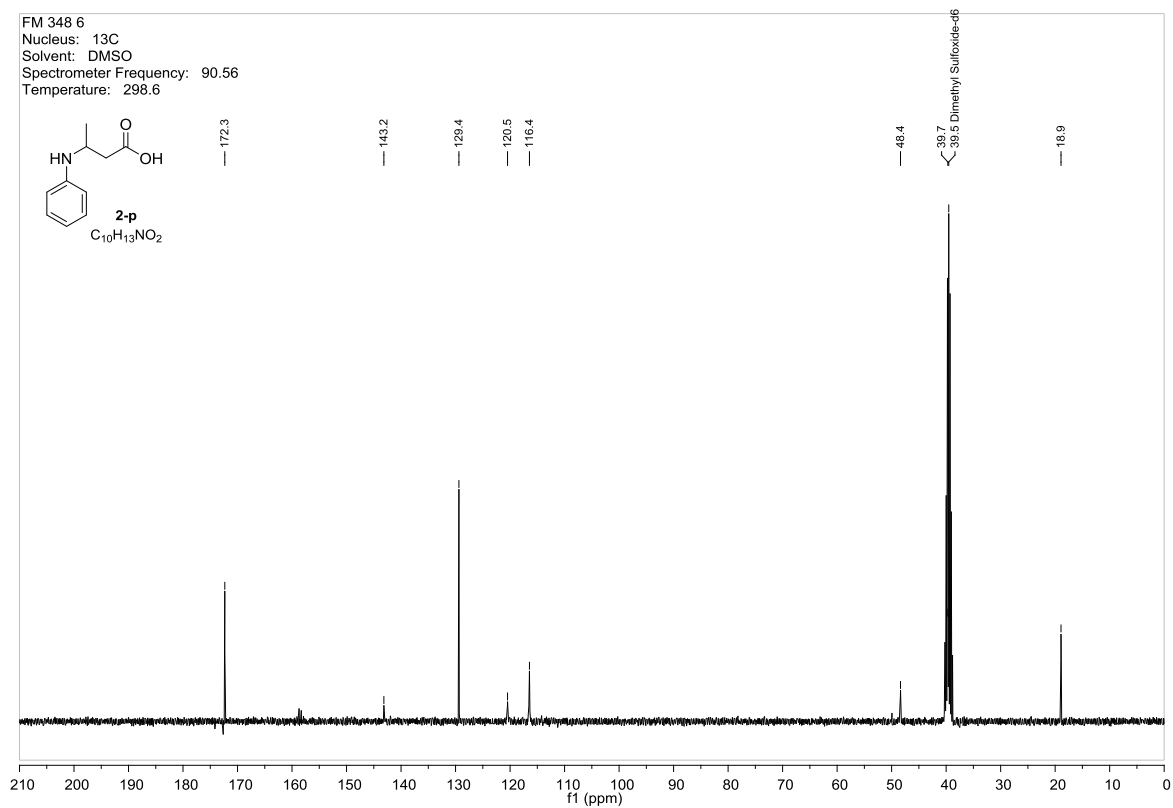
MIC	Minimal inhibitory concentration
MS	Mass spectrometry
MS/MS	Tandem mass spectrometry
MW	Molecular weight
NMR	Nuclear magnetic resonance
OD	Optical density
PBP	Penicillin-binding protein
PCC	Pyridinium chlorochromate
PCR	Polymerase chain reaction
PDC	Pyridinium dichromate
PEG	Polyethylene glycol
PenG	Penicillin G
pNP	<i>para</i> -Nitrophenol
pNPA	<i>para</i> -Nitrophenyl acetate
ppm	parts per million
QM/MM	Quantum mechanics/ molecular mechanics
RP	Reversed phase
rpm	Rotations per minute
RT	Room temperature
SCRP-27A	Sigma cross-reacting protein 27A
SDS-PAGE	Sodium dodecylsulfate polyacrylamide gel electrophoresis
ssp	Subspecies
TBTA	Tris(benzyltriazolylmethyl)amine
TCEP	Tris-(2-carboxyethyl)-phosphine
TEA	Triethanolamine
TEAB	Tetraethylammonium bromide
TEV	Tobacco etch virus
TFA	Trifluoroacetic acid
THF	Tetrahydrofuran
TLC	Thin layer chromatography
TMS	Trimethylsilyl
TRIS	Tris(hydroxymethyl)aminomethane
TPP	Tetraphenylporphyrin
UTP	Uridine triphosphate
WHO	World Health Organization
$\delta$	Chemical shift

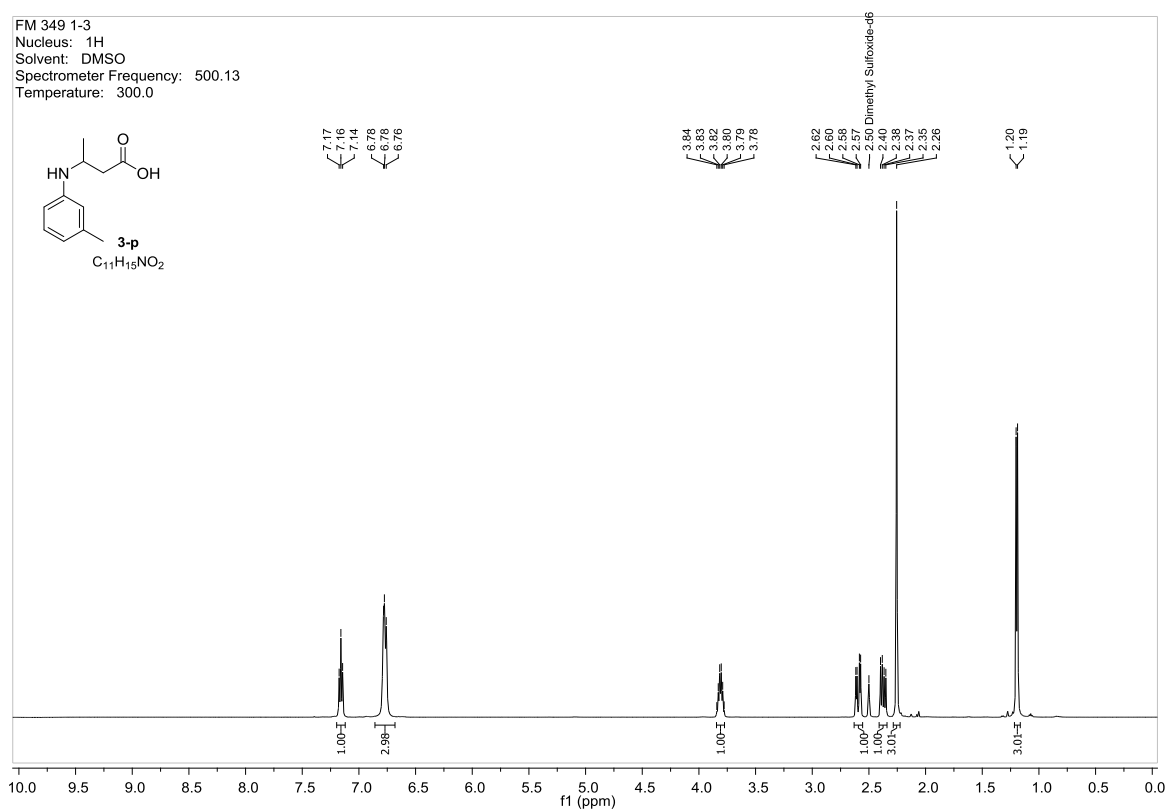
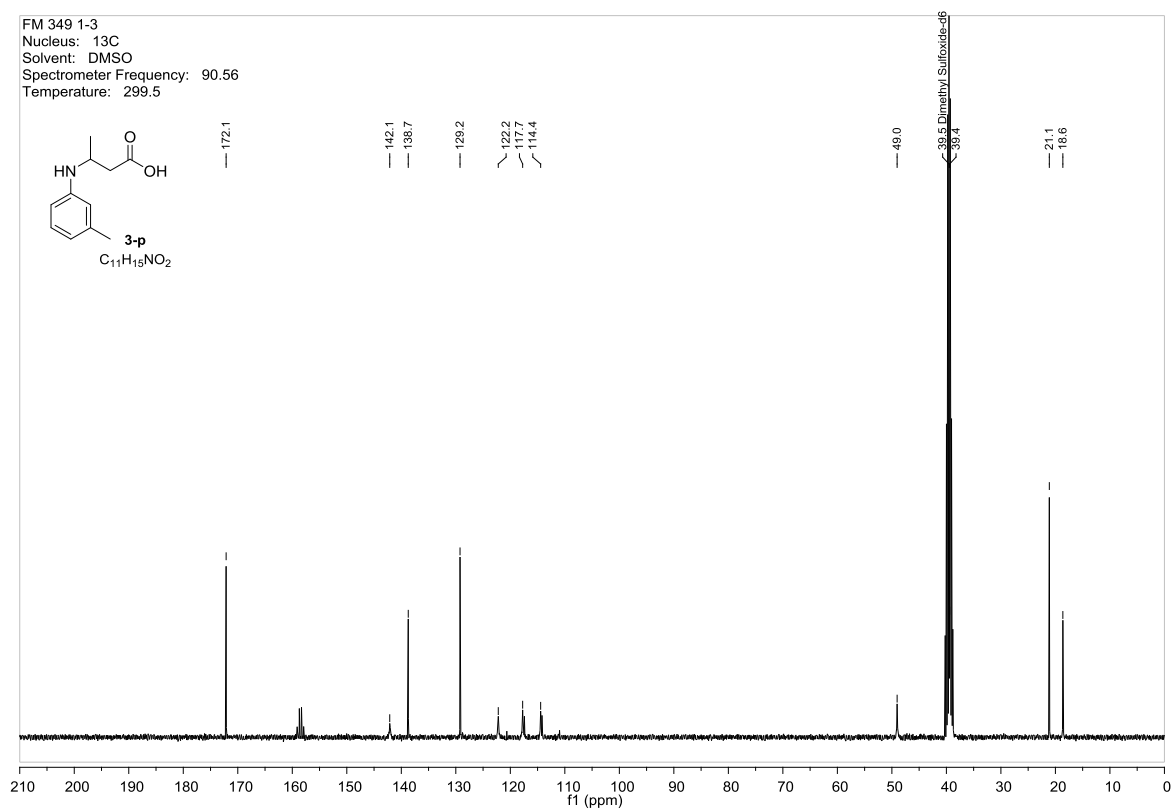
## VII – APPENDICES

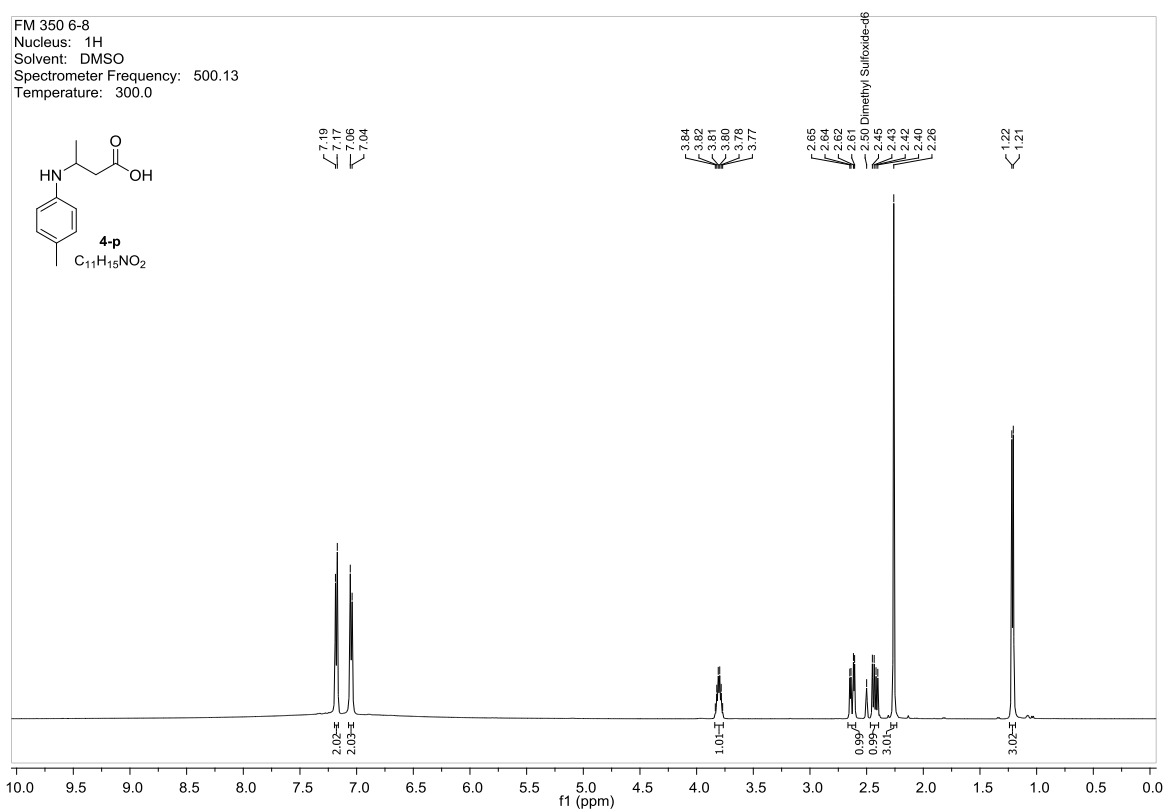
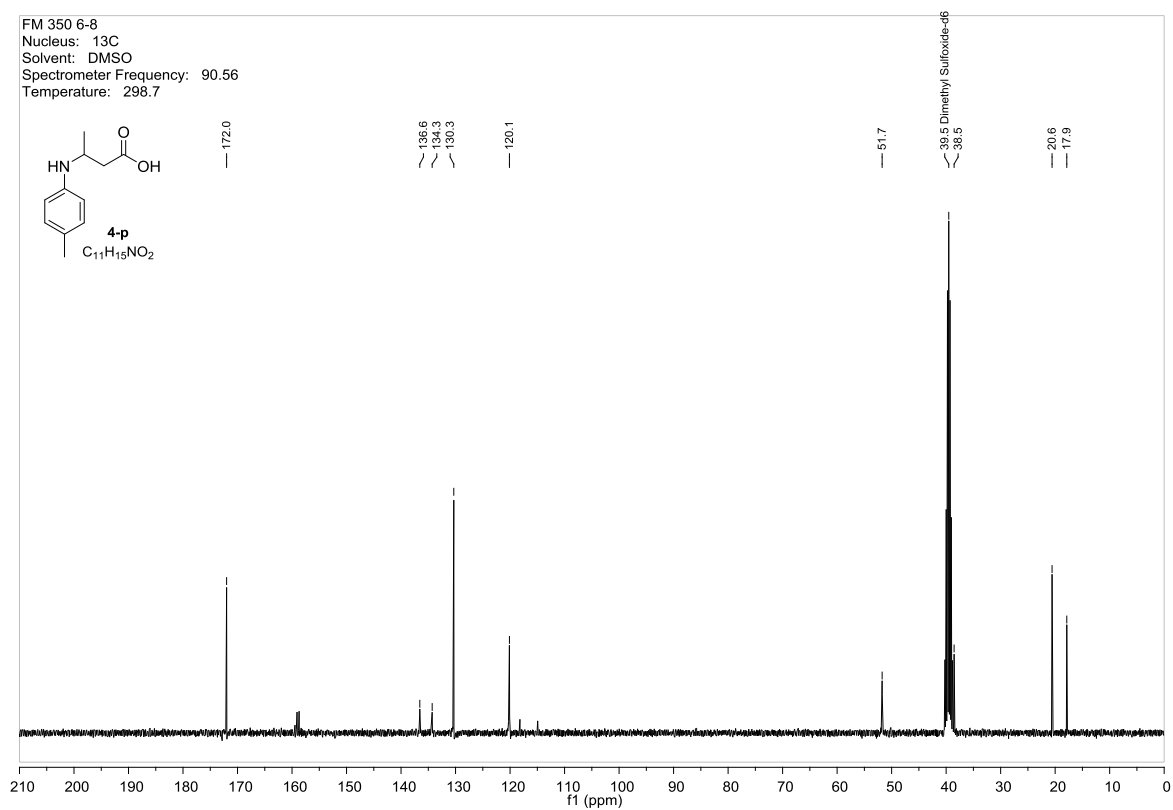


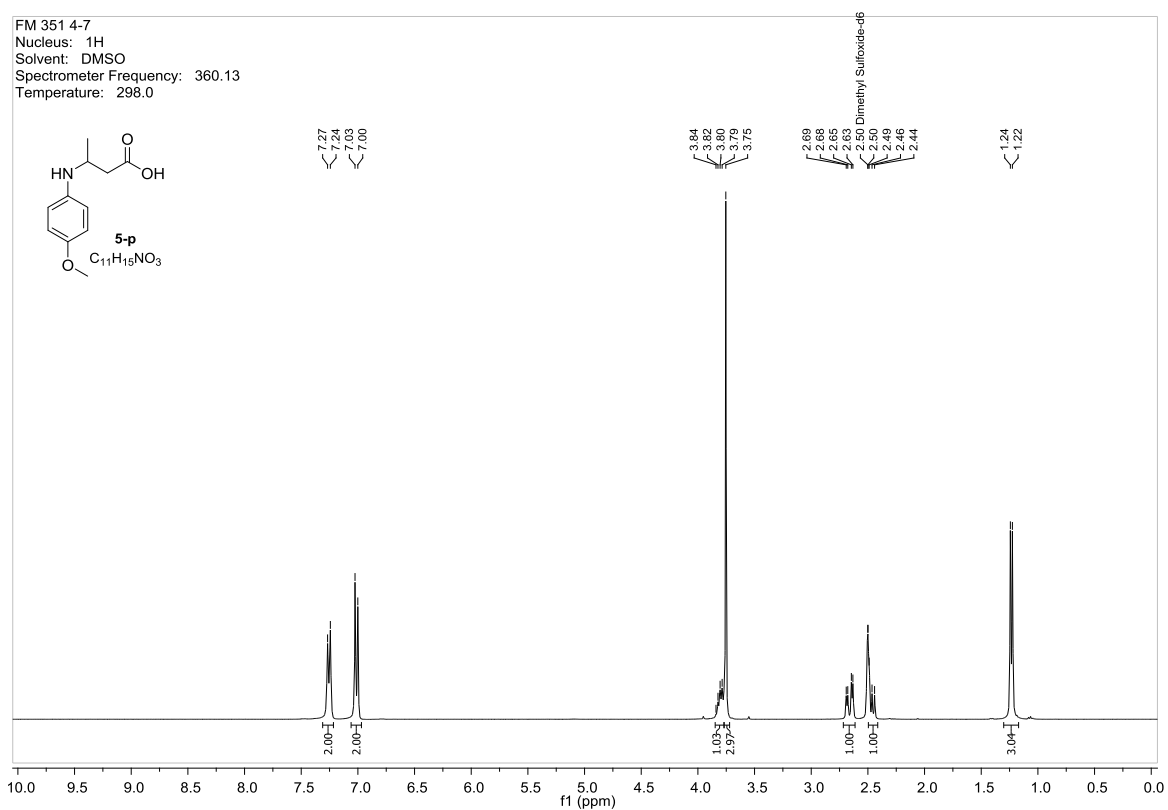
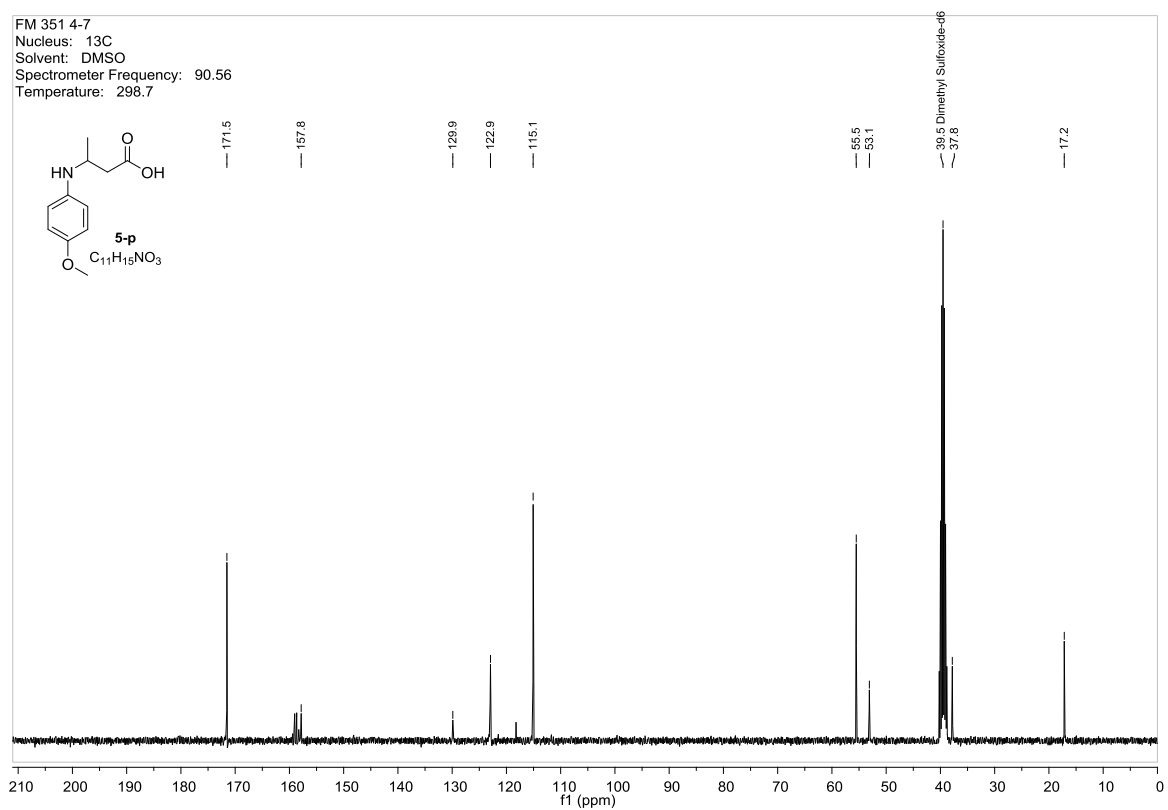


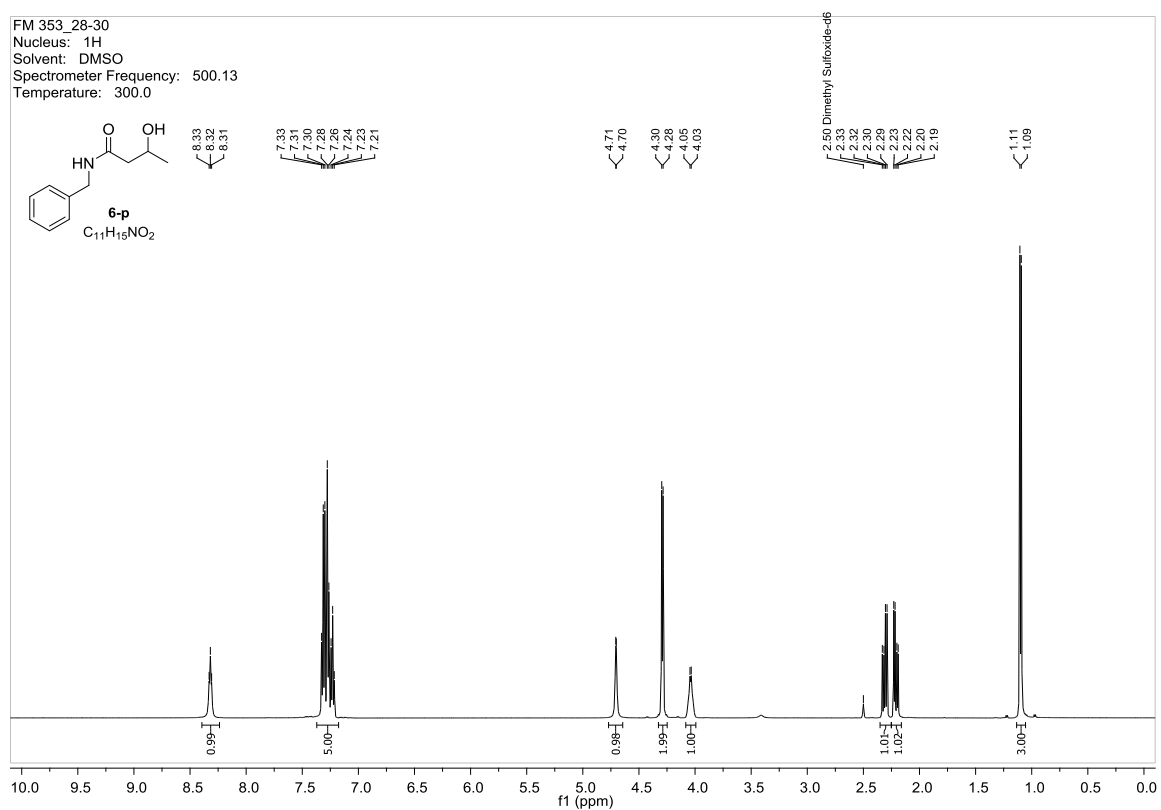
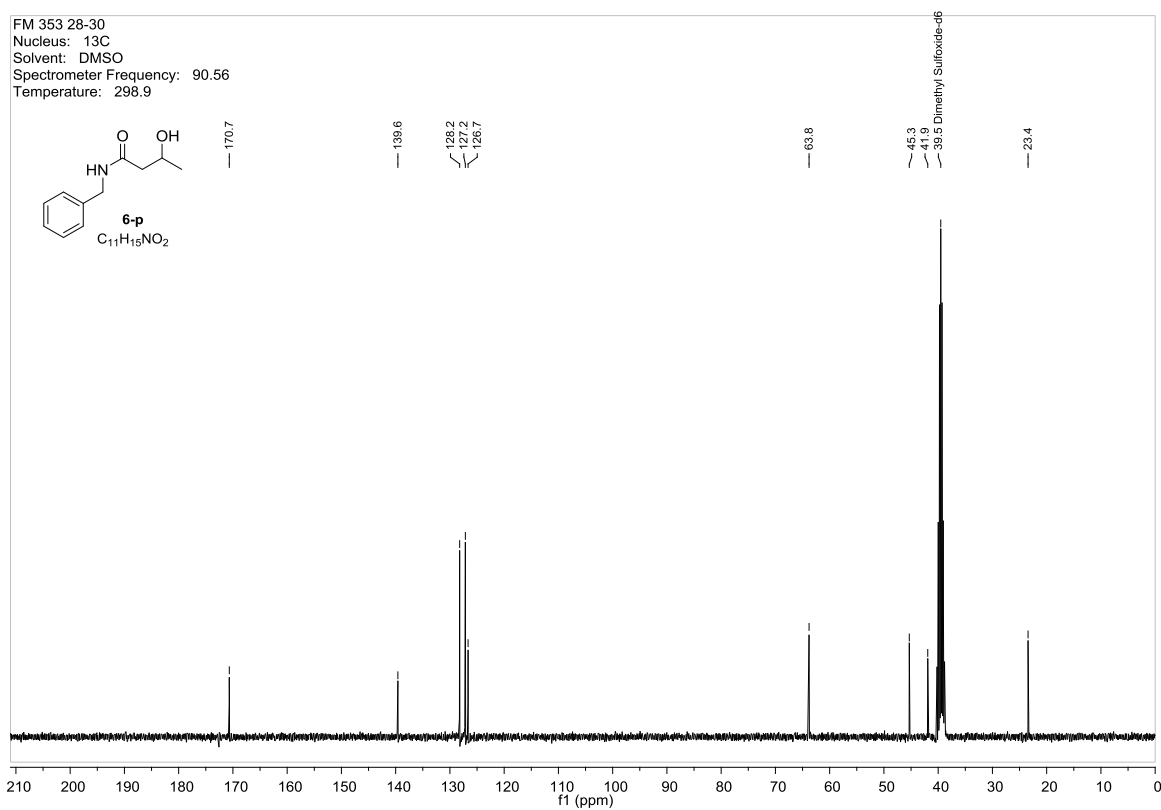
## II - KINETIC PRODUCTS

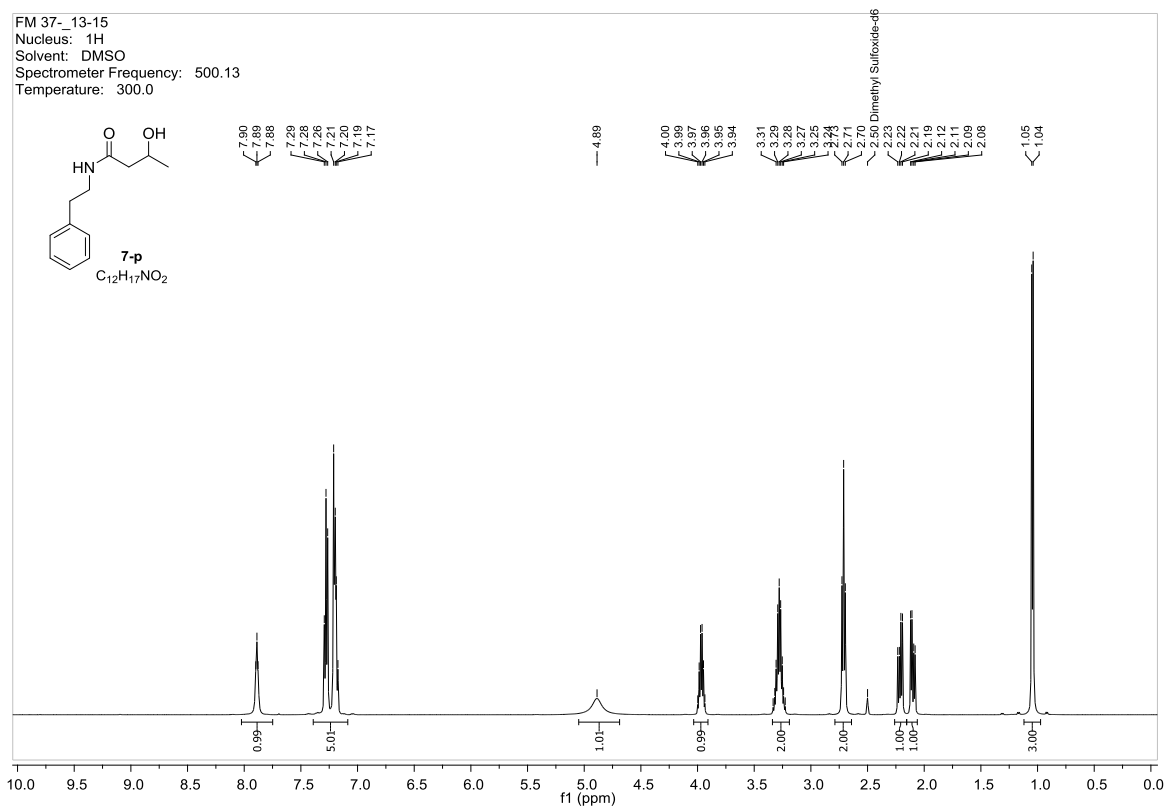
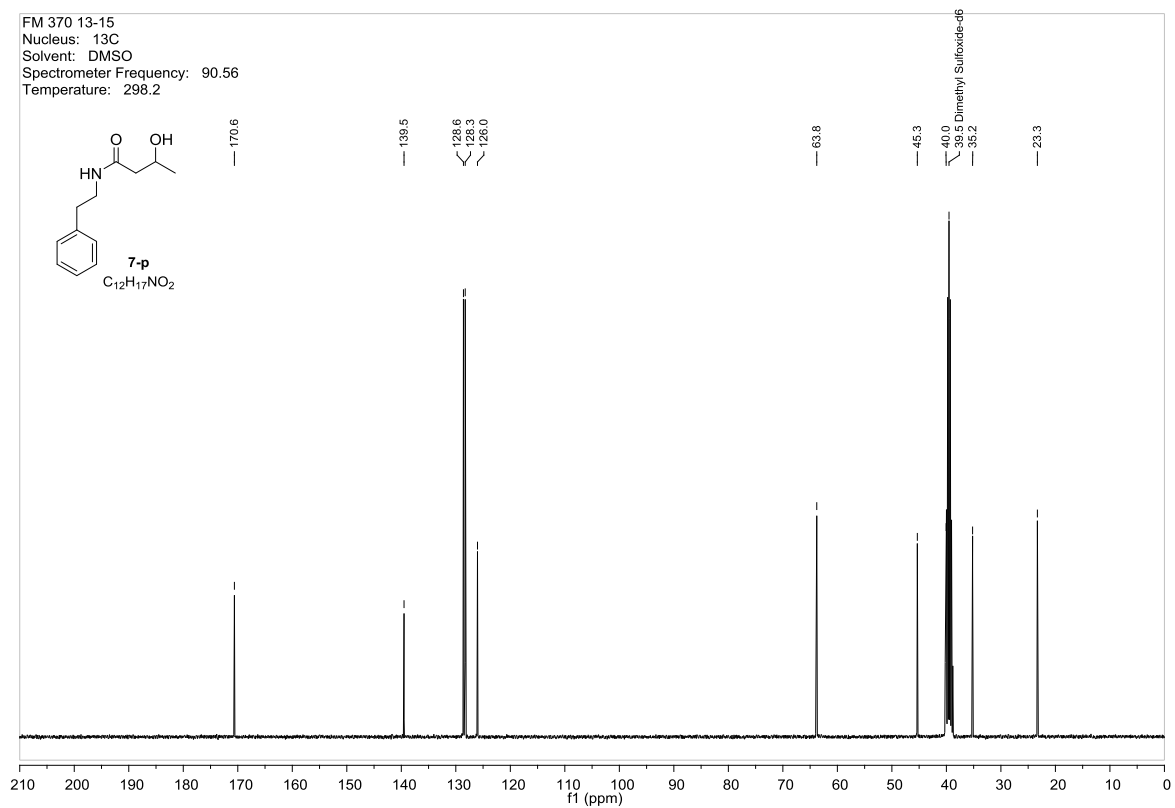
Figure 59:  $^1\text{H}$  NMR spectra of **2-p**.Figure 60:  $^{13}\text{C}$  NMR spectra of **2-p**.

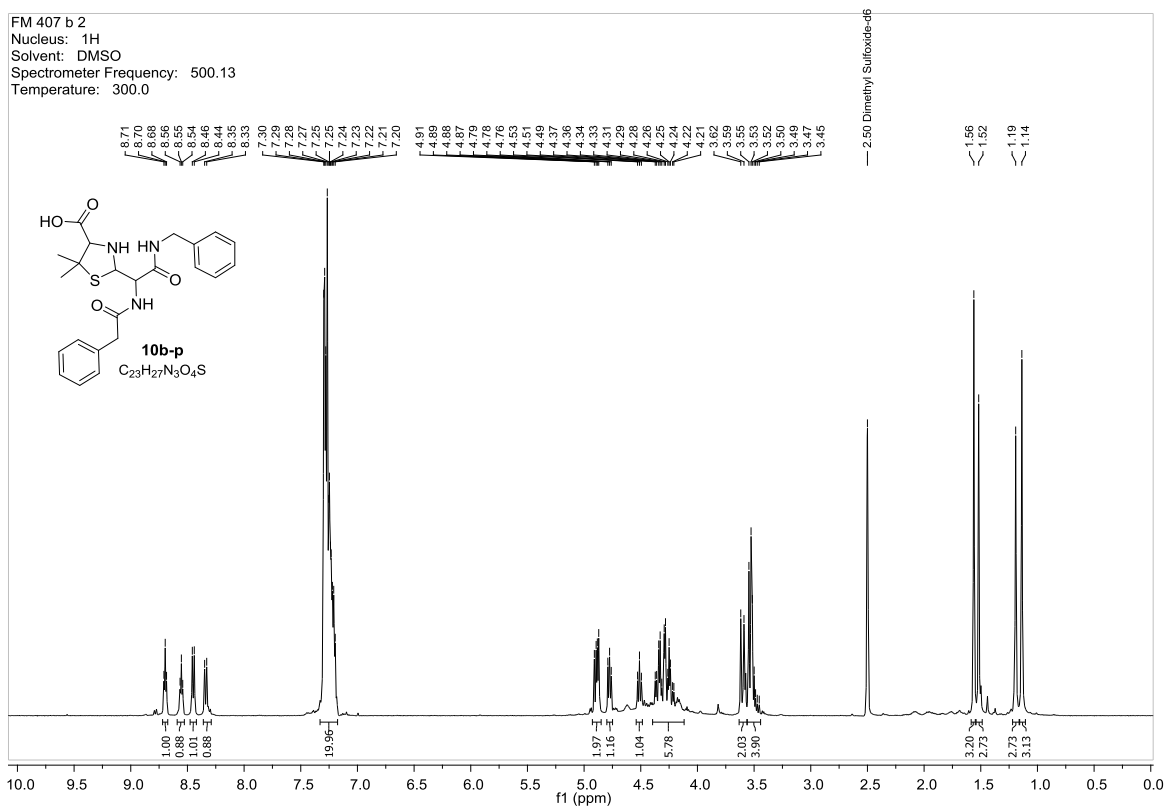
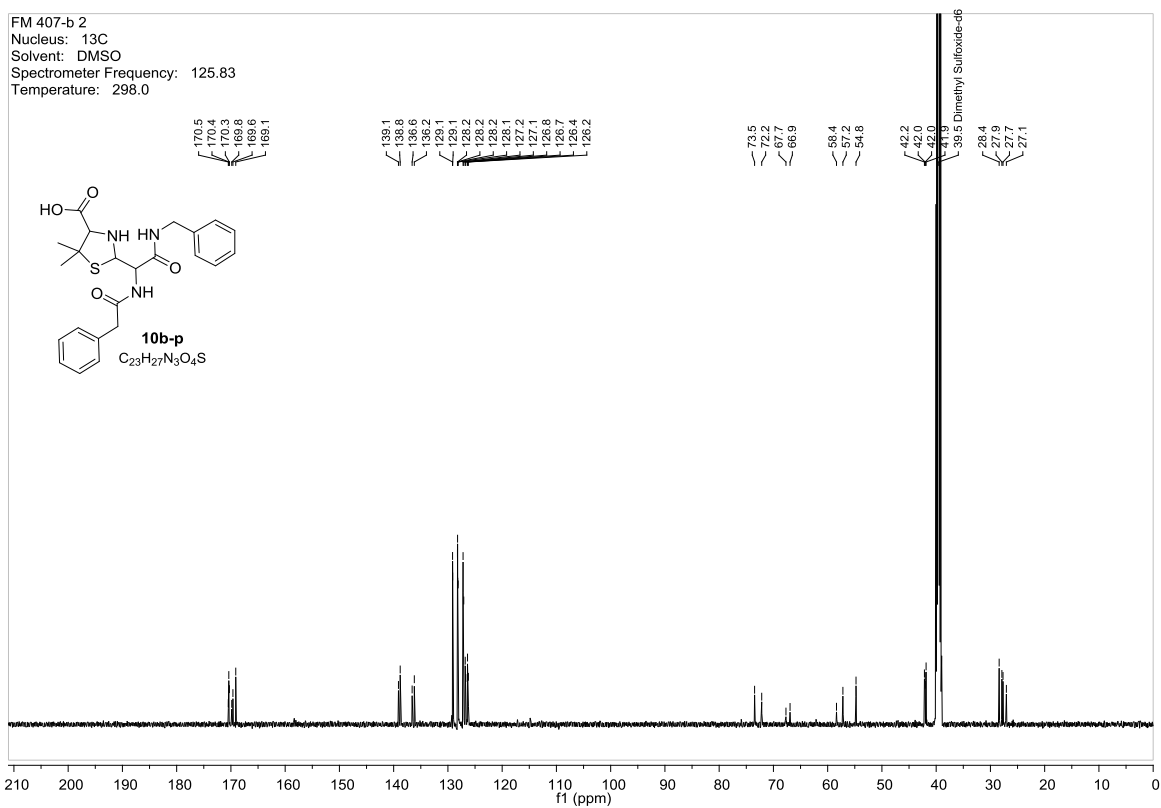
Figure 61:  $^1\text{H}$  NMR spectra of **3-p**.Figure 62:  $^{13}\text{C}$  NMR spectra of **3-p**.

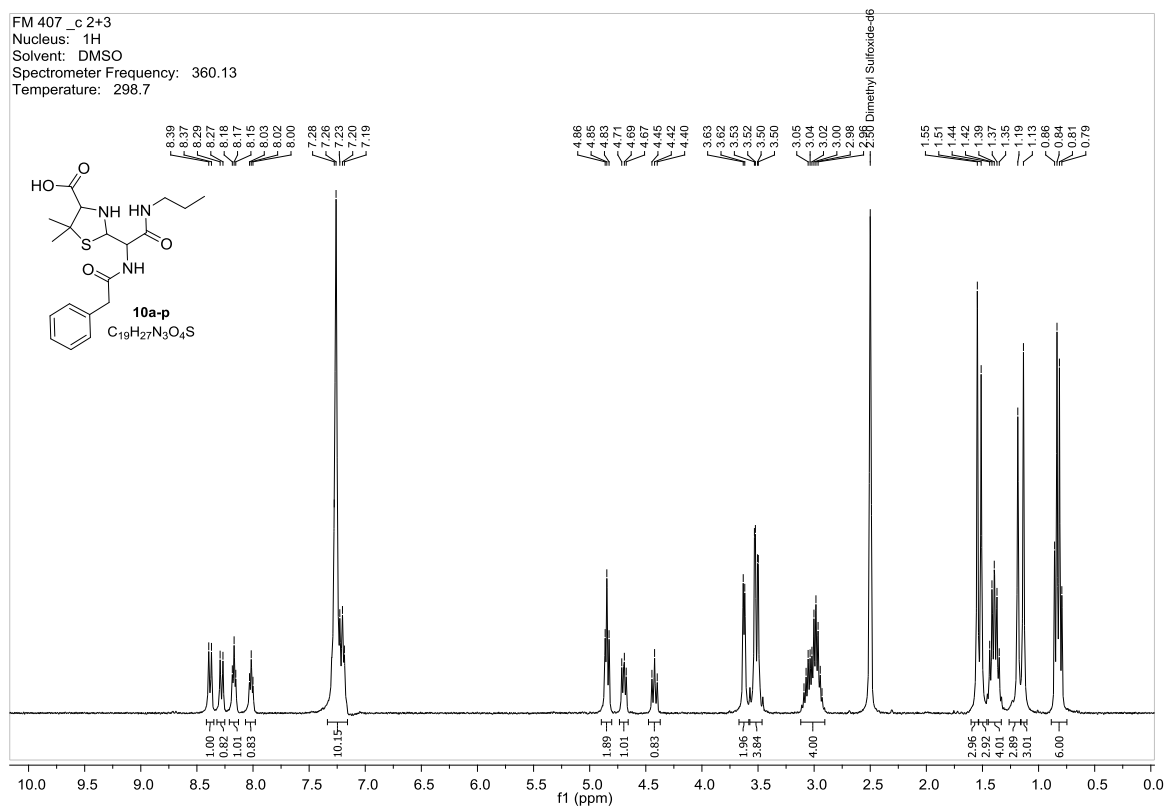
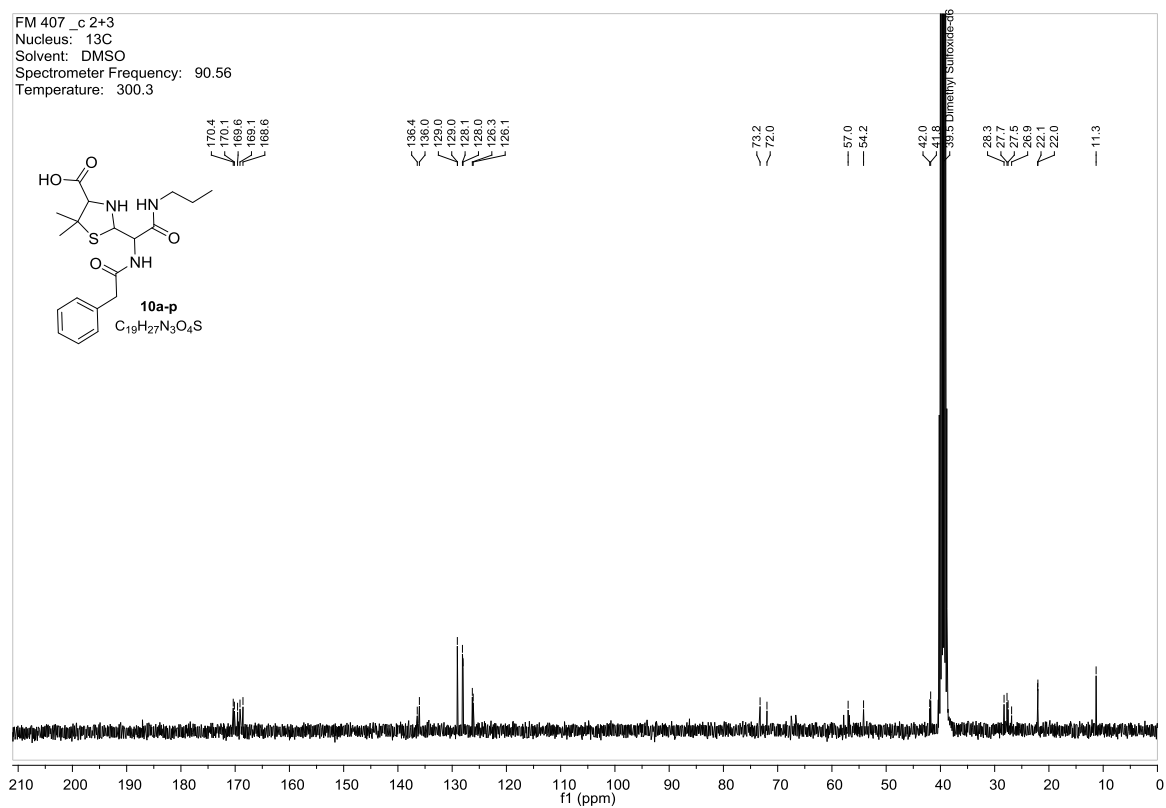
Figure 63:  $^1\text{H}$  NMR spectra of 4-p.Figure 64:  $^{13}\text{C}$  NMR spectra of 4-p.

Figure 65:  $^1\text{H}$  NMR spectra of **5-p**.Figure 66:  $^{13}\text{C}$  NMR spectra of **5-p**.

Figure 67:  $^1\text{H}$  NMR spectra of **6-p**.Figure 68:  $^{13}\text{C}$  NMR spectra of **6-p**.

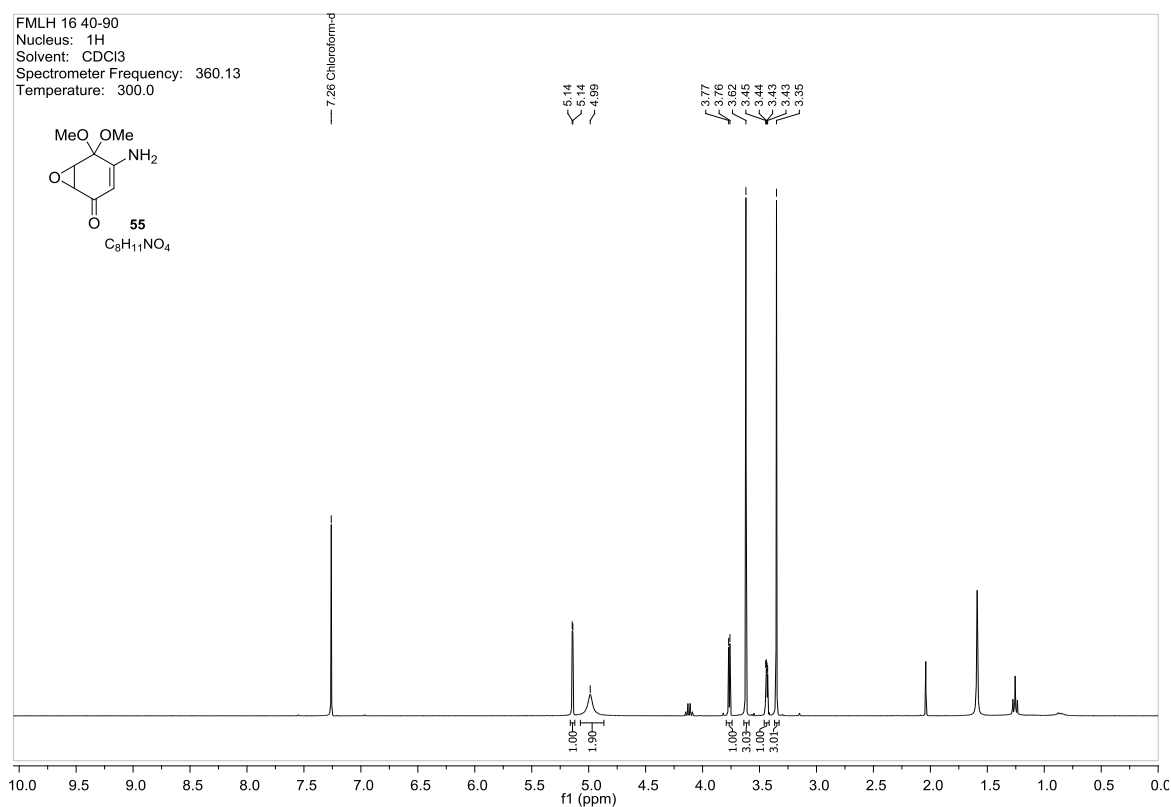
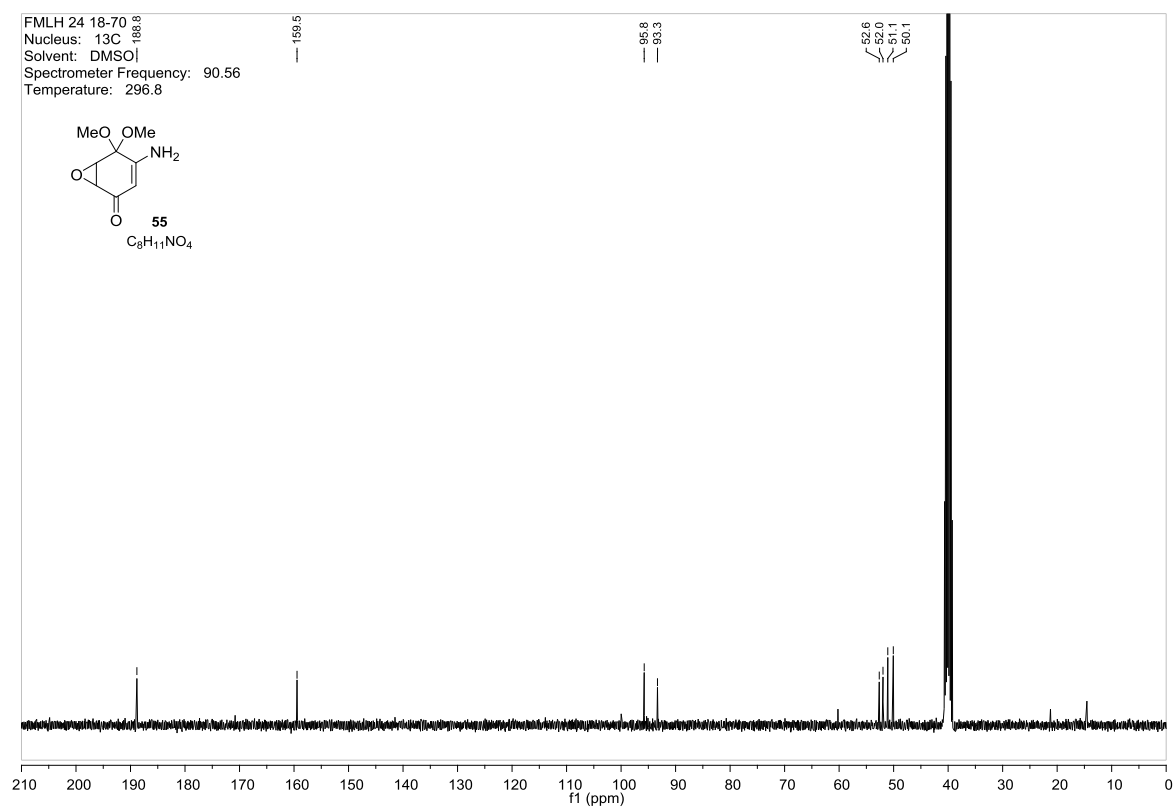
Figure 69:  $^1\text{H}$  NMR spectra of **7-p**.Figure 70:  $^{13}\text{C}$  NMR spectra of **7-p**.

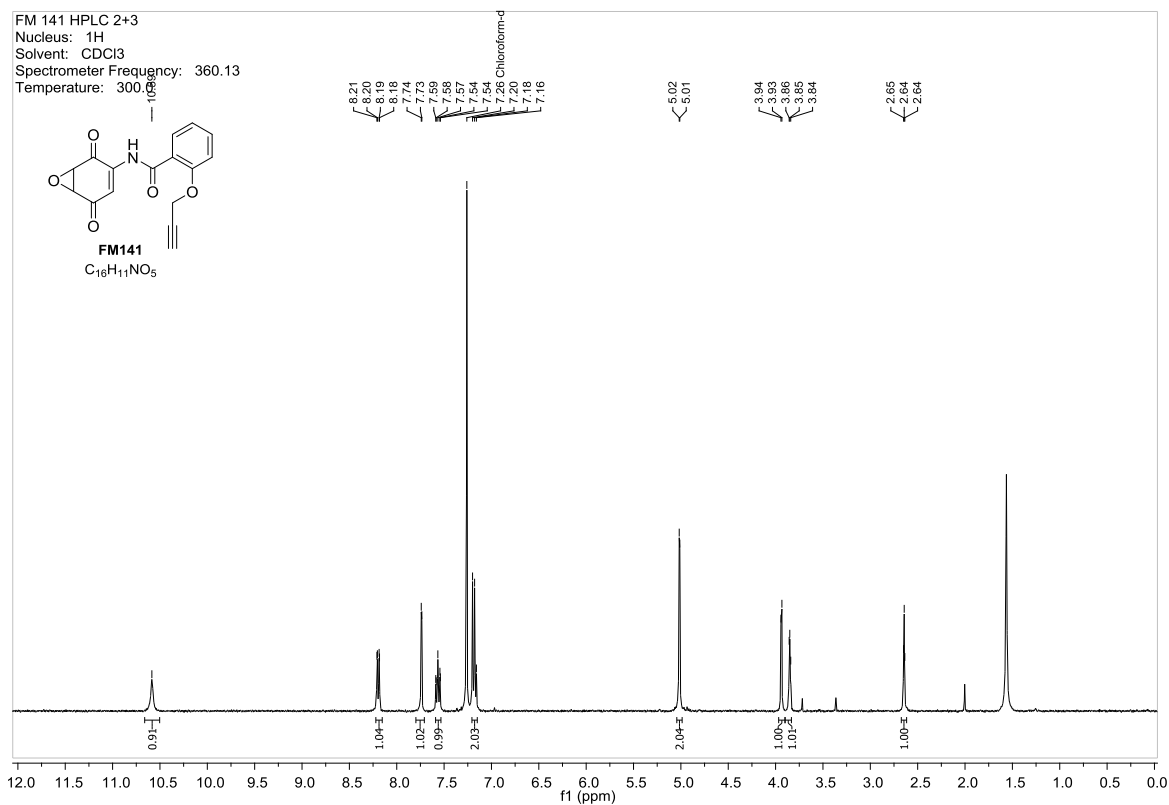
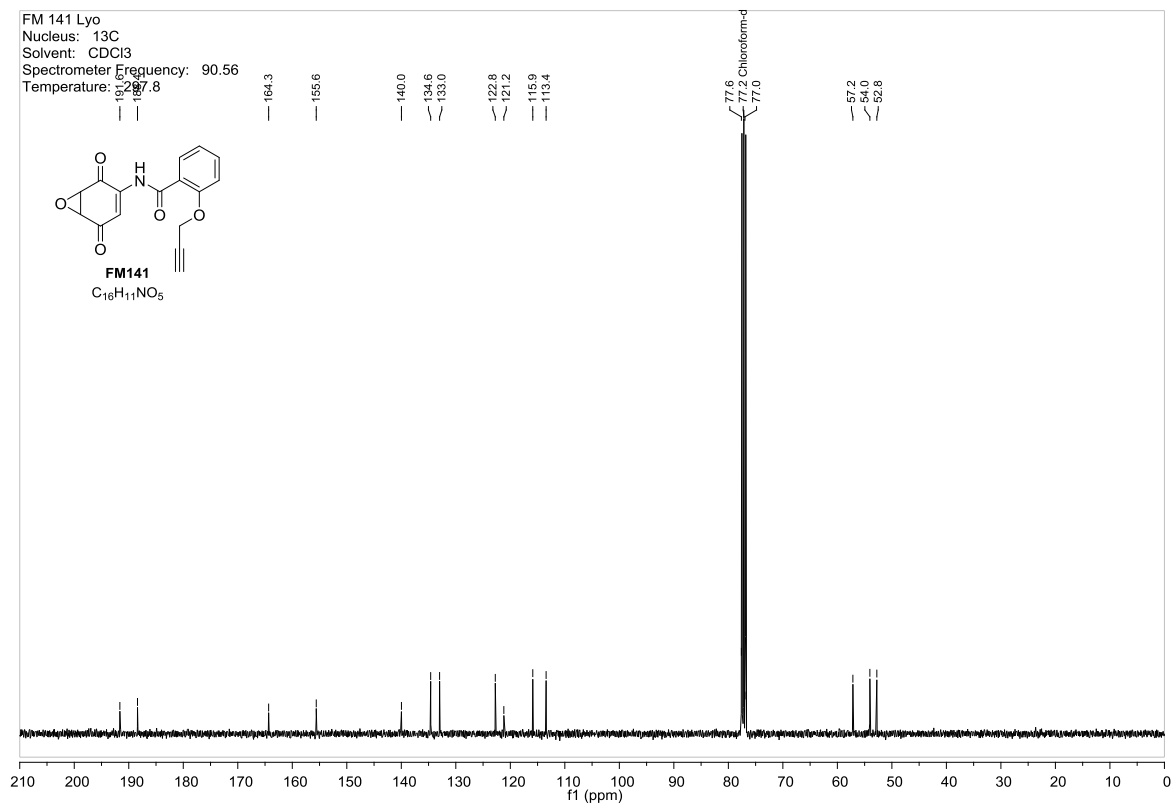
Figure 71:  $^1\text{H}$  NMR spectra of **10b-p**.Figure 72:  $^{13}\text{C}$  NMR spectra of **10b-p**.

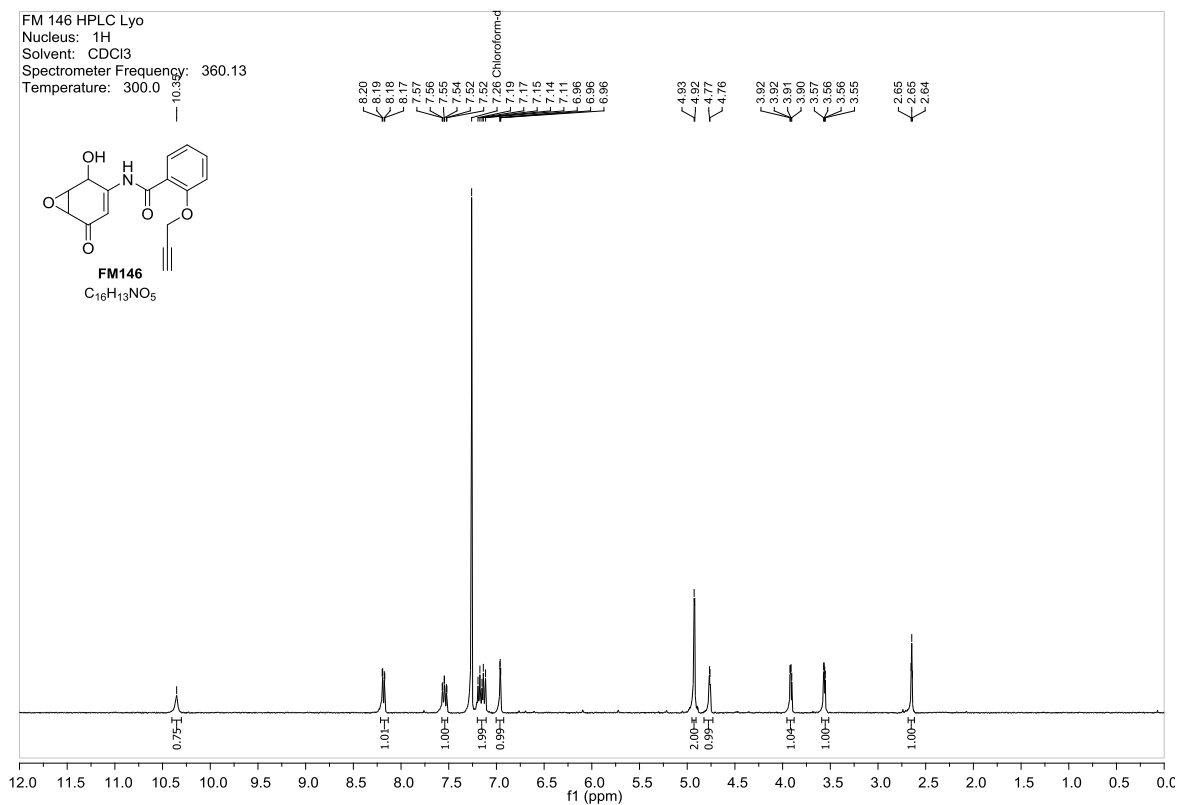
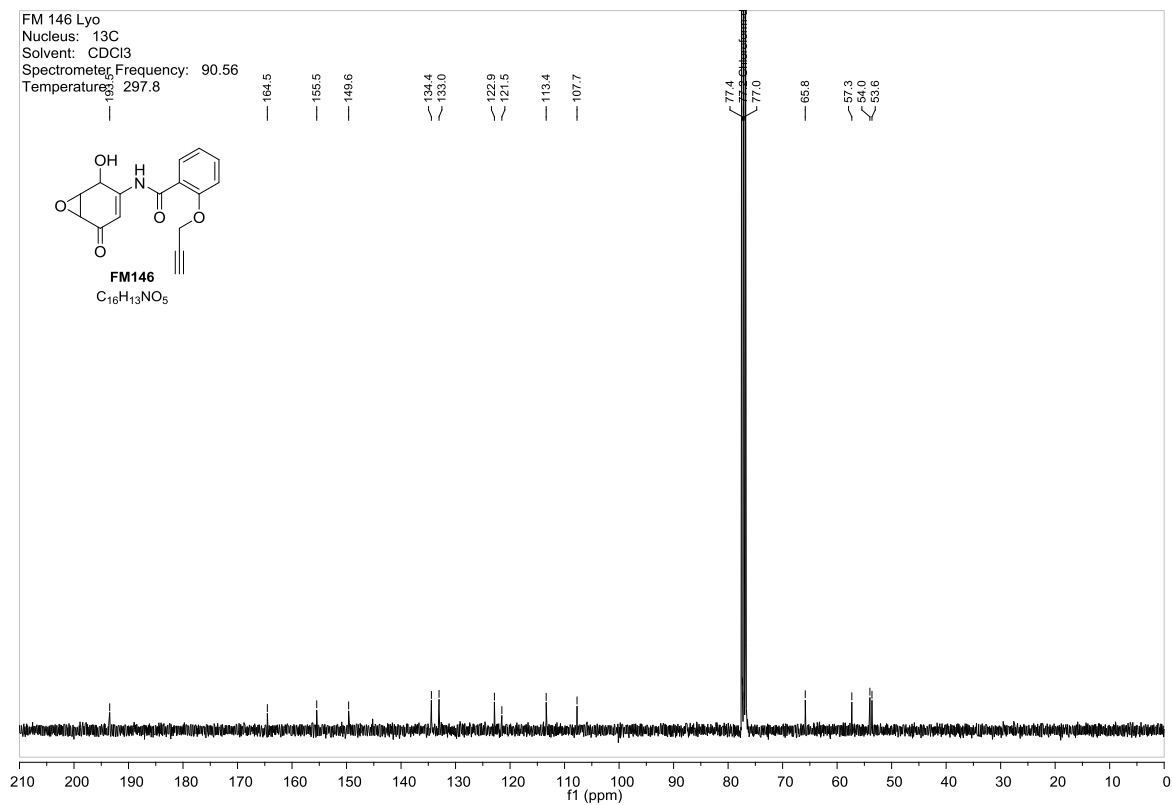
Figure 73:  $^1\text{H}$  NMR spectra of **10a-p**.Figure 74:  $^{13}\text{C}$  NMR spectra of **10a-p**.

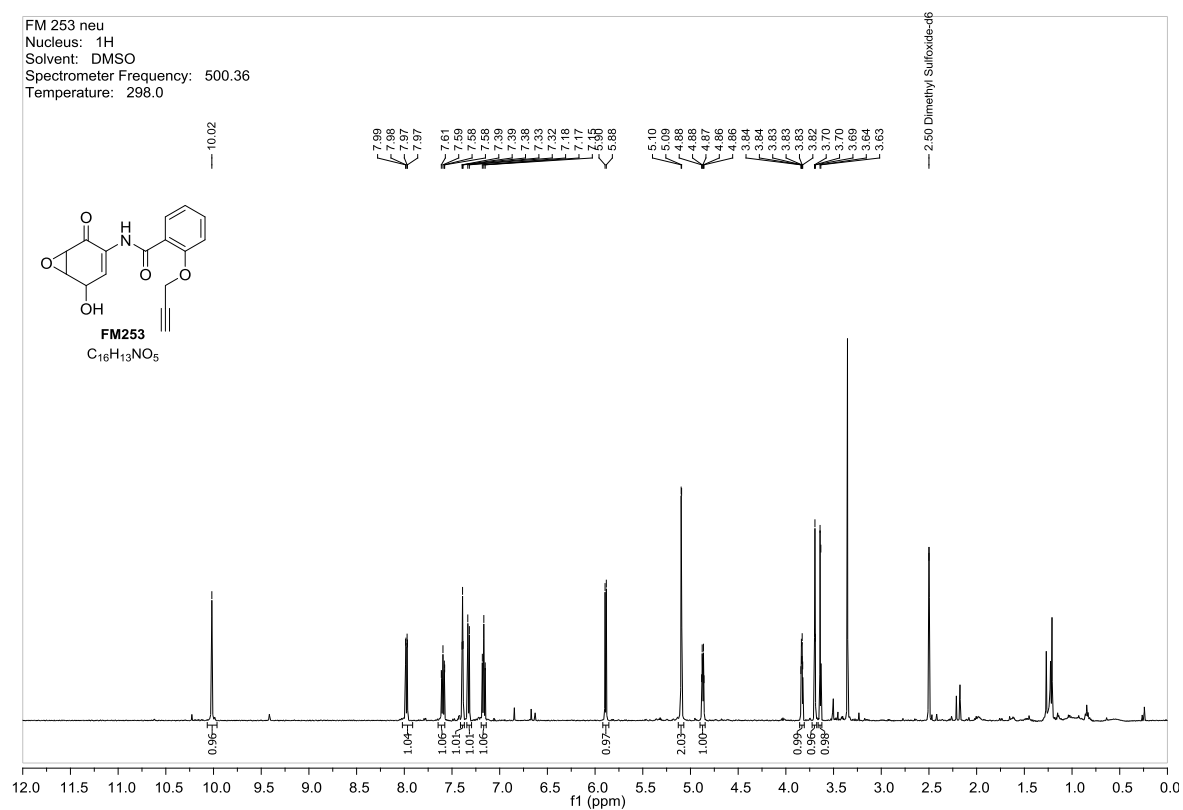
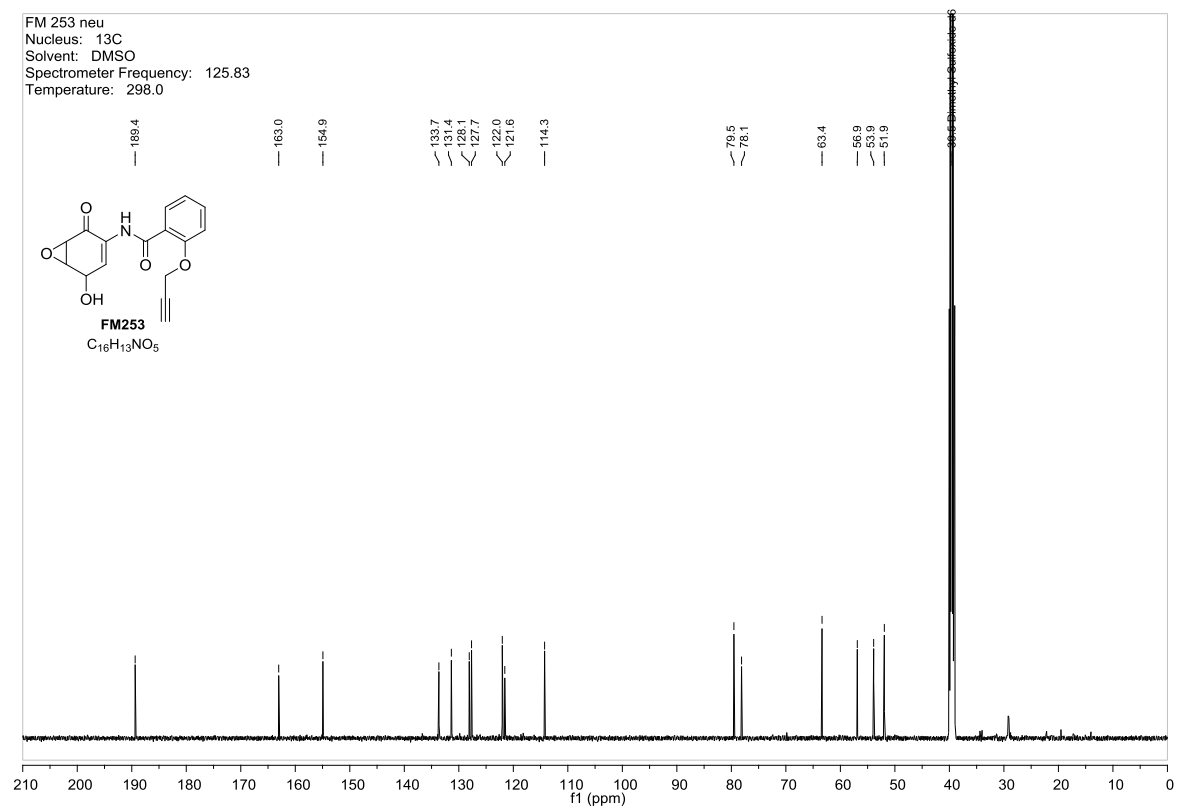


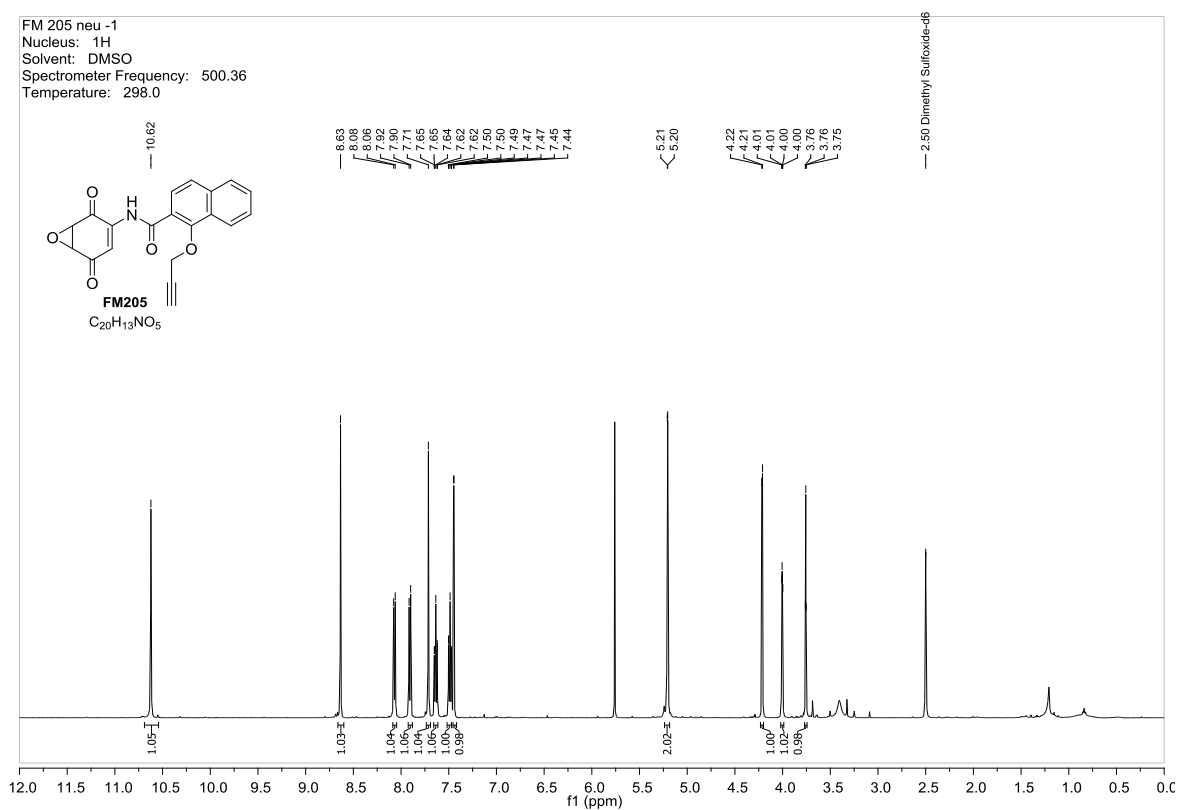
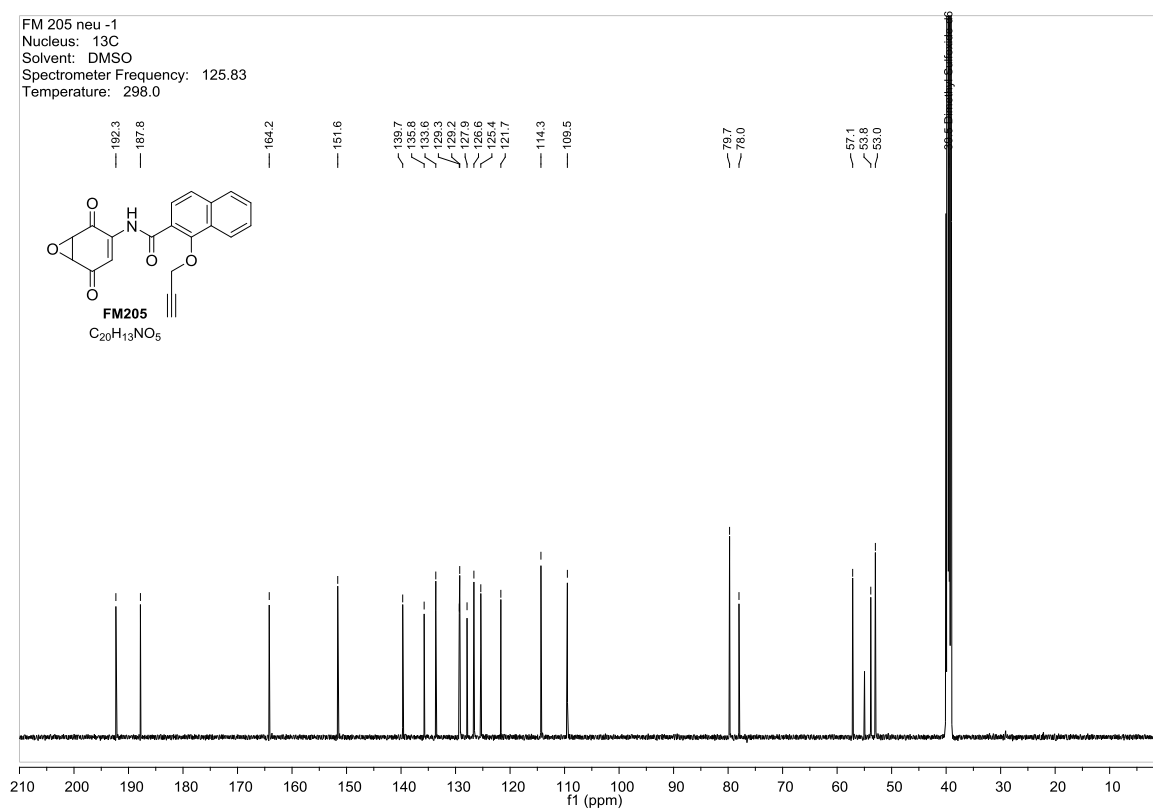
## III - ABPP PROBES

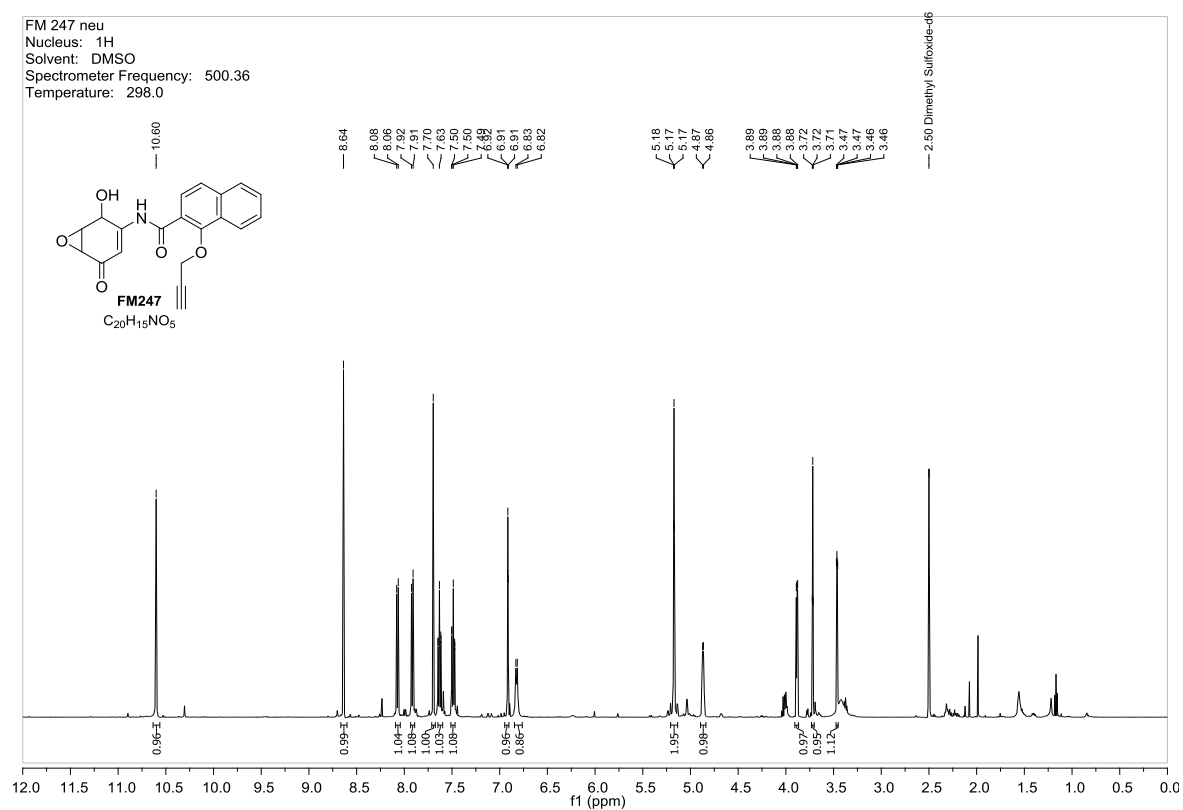
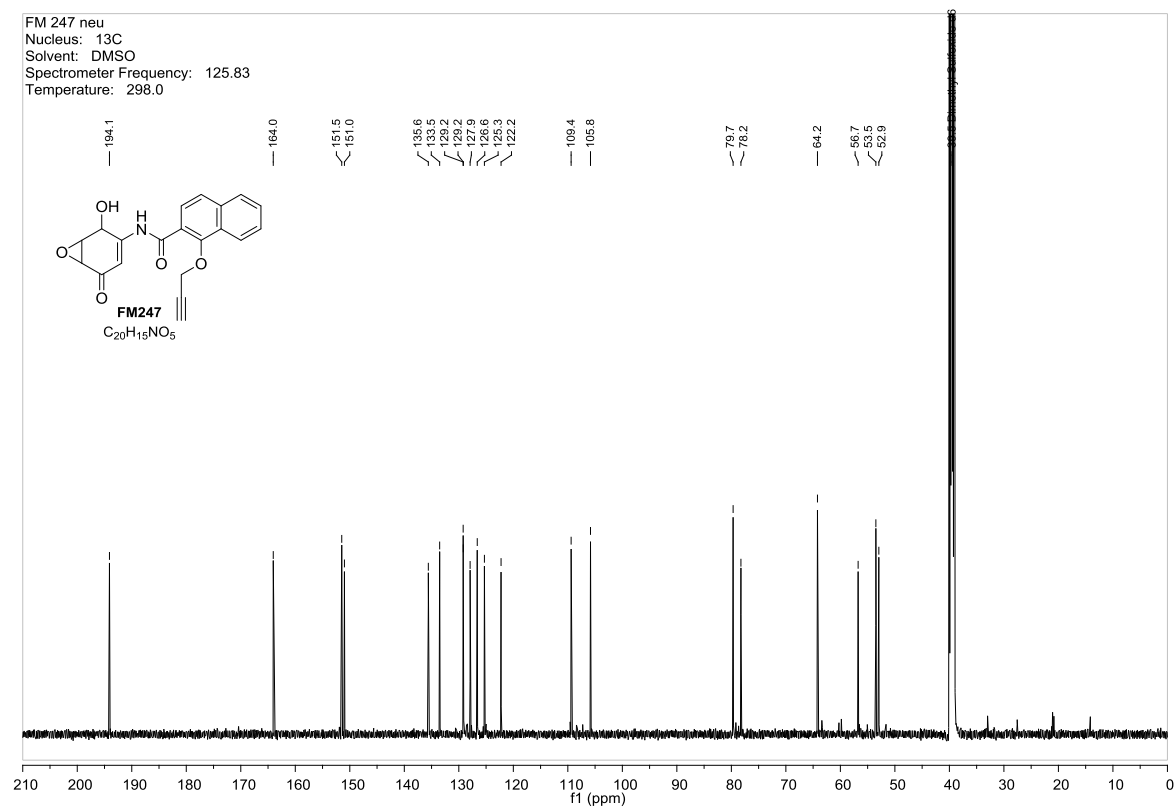
Figure 75:  $^1\text{H}$  NMR spectra of 55.Figure 76:  $^{13}\text{C}$  NMR spectra of 55.

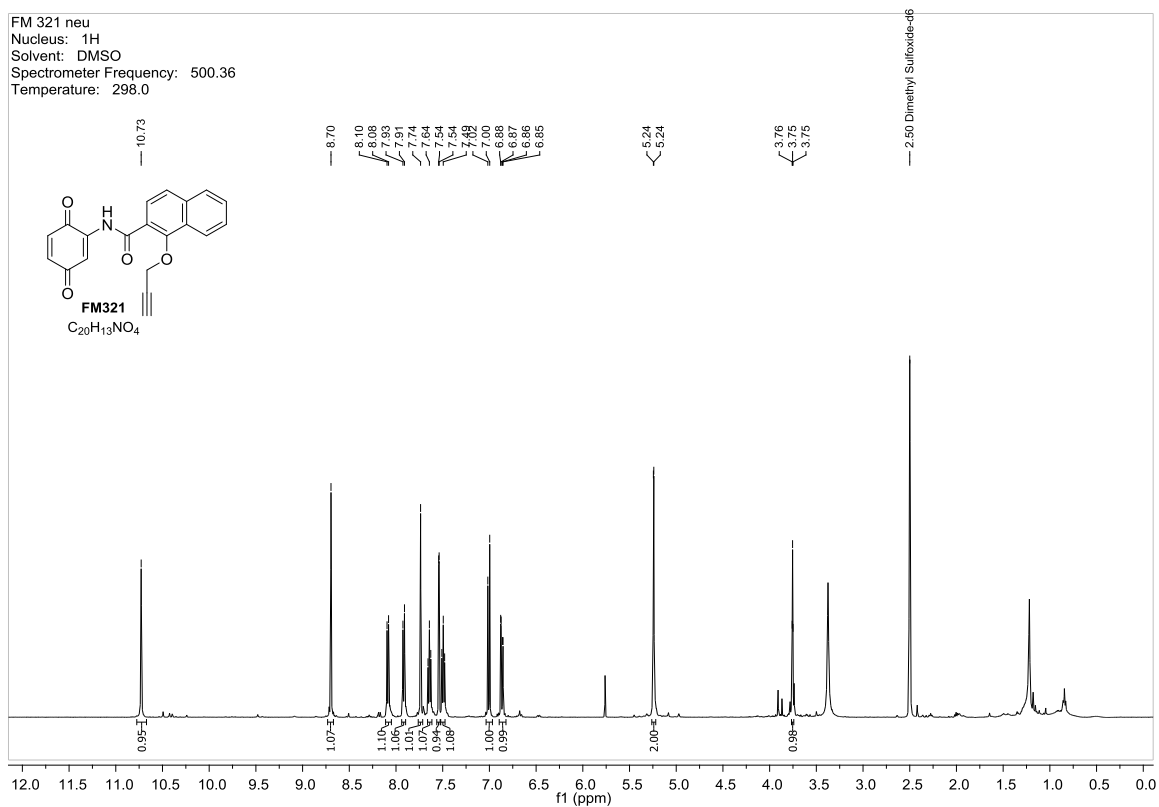
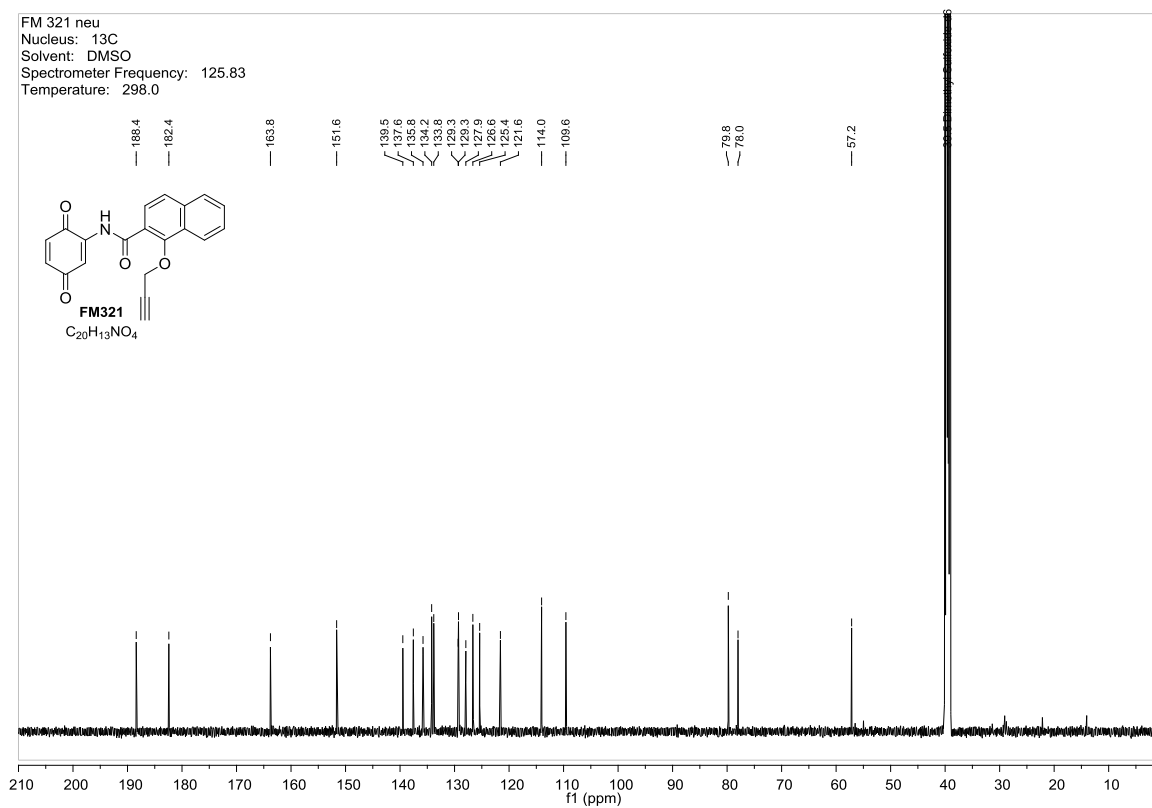
Figure 77:  $^1\text{H}$  NMR spectra of FM141.Figure 78:  $^{13}\text{C}$  NMR spectra of FM141.

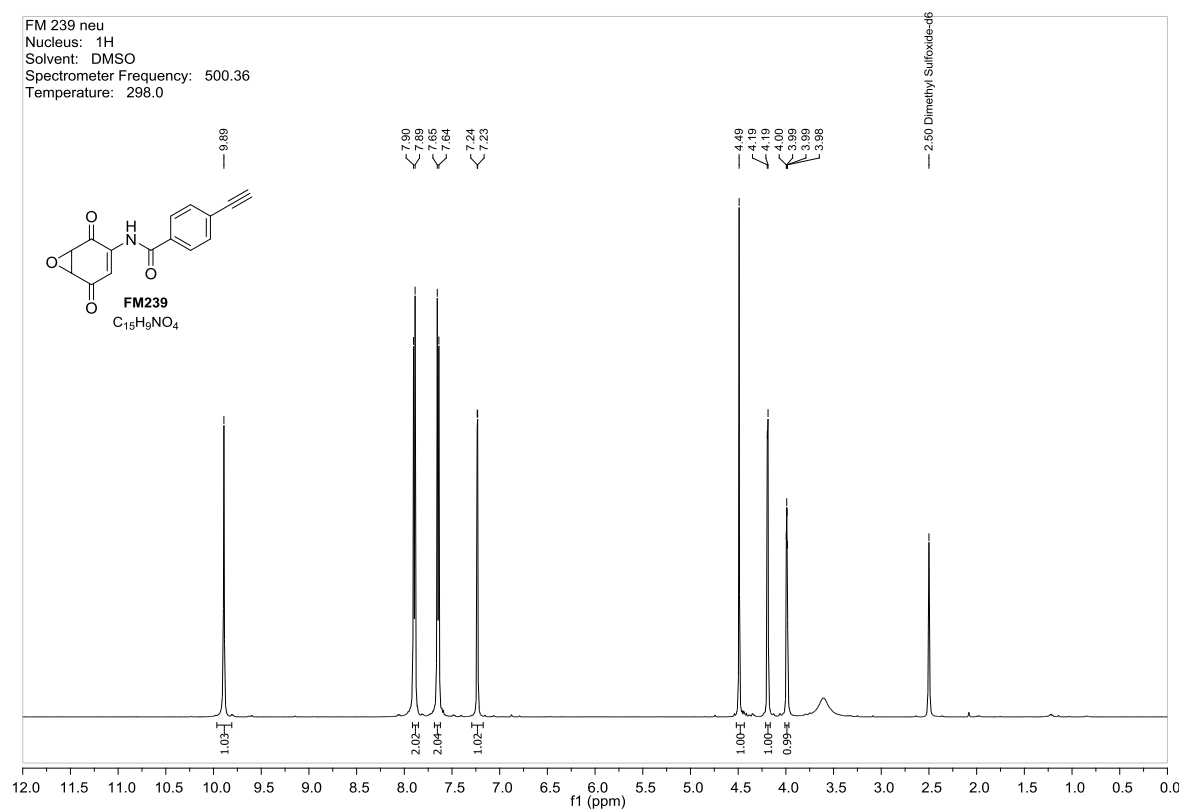
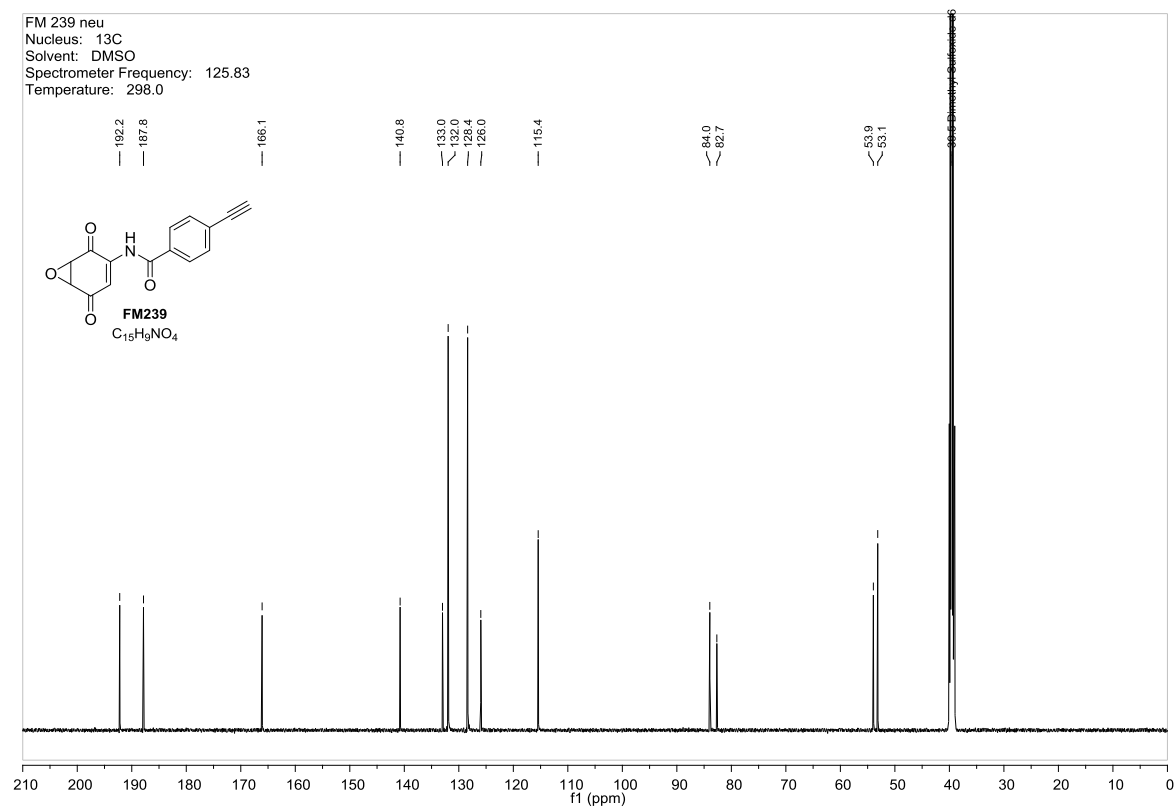
Figure 79:  $^1\text{H}$  NMR spectra of FM146.Figure 80:  $^{13}\text{C}$  NMR spectra of FM146.

Figure 81:  $^1\text{H}$  NMR spectra of FM253.Figure 82:  $^{13}\text{C}$  NMR spectra of FM253.

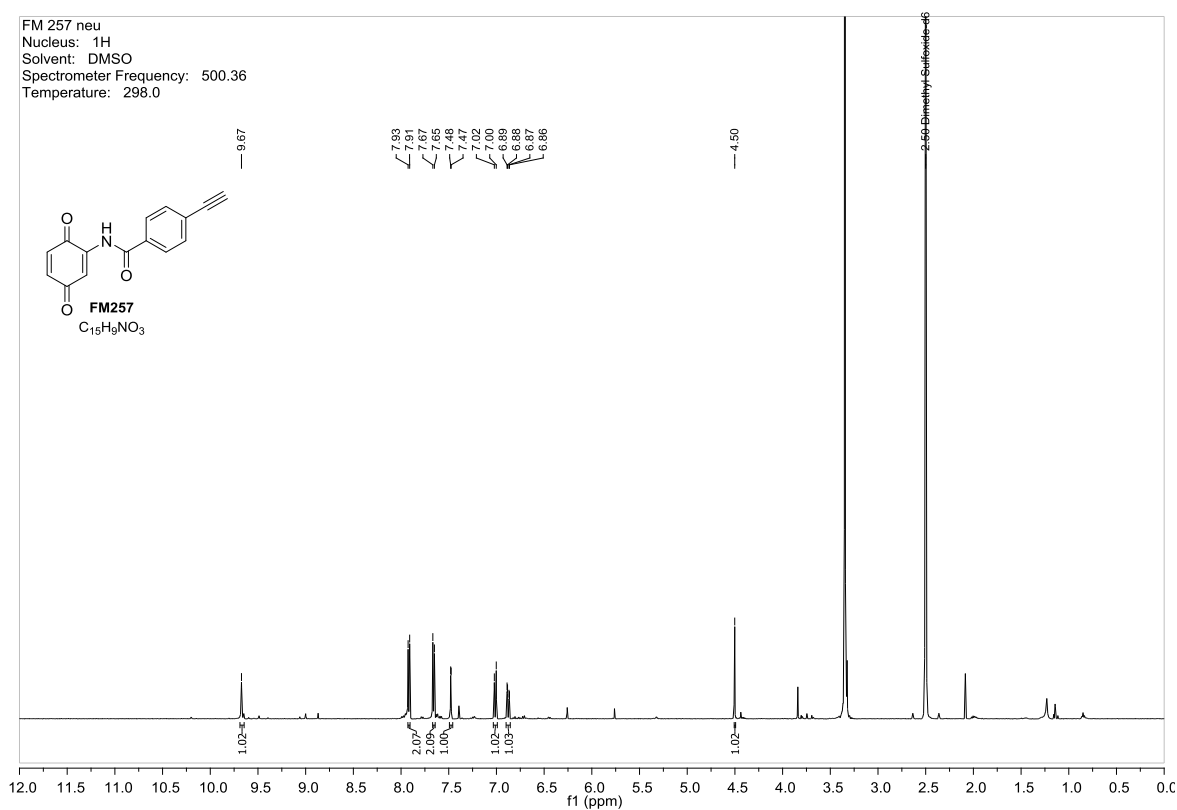
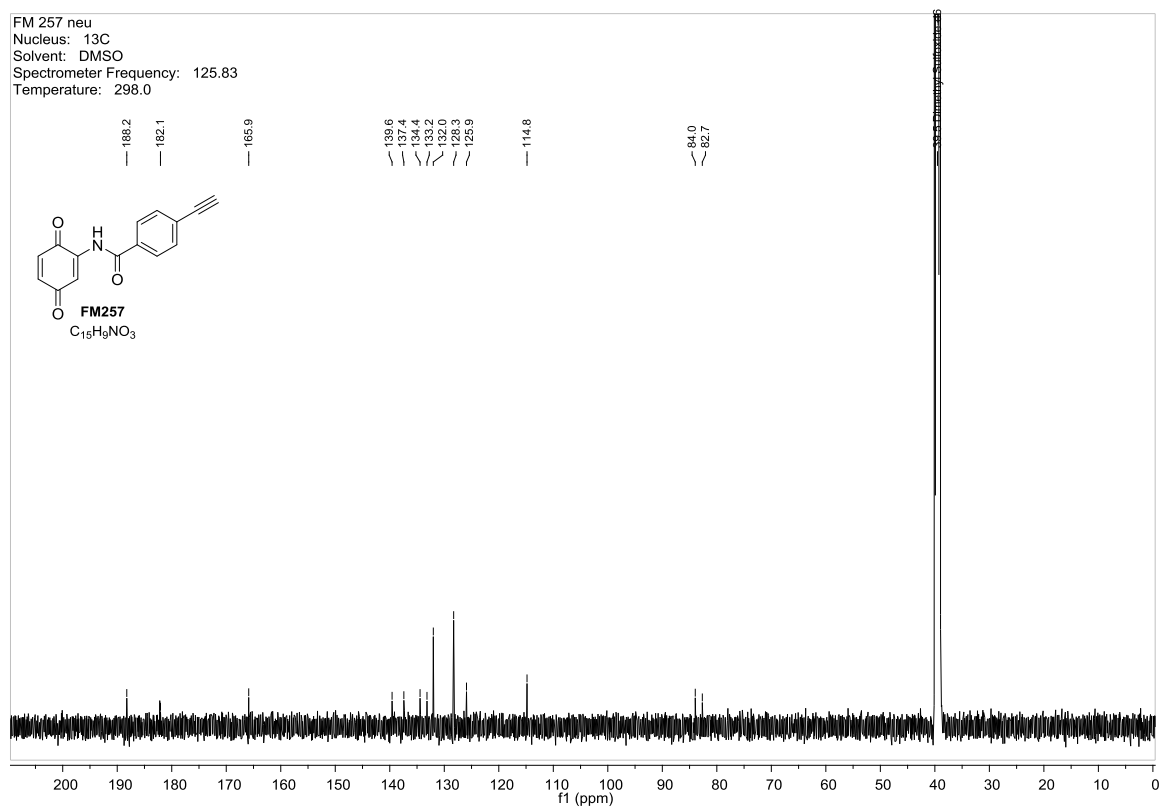
Figure 83:  $^1\text{H}$  NMR spectra of FM205.Figure 84:  $^{13}\text{C}$  NMR spectra of FM205.

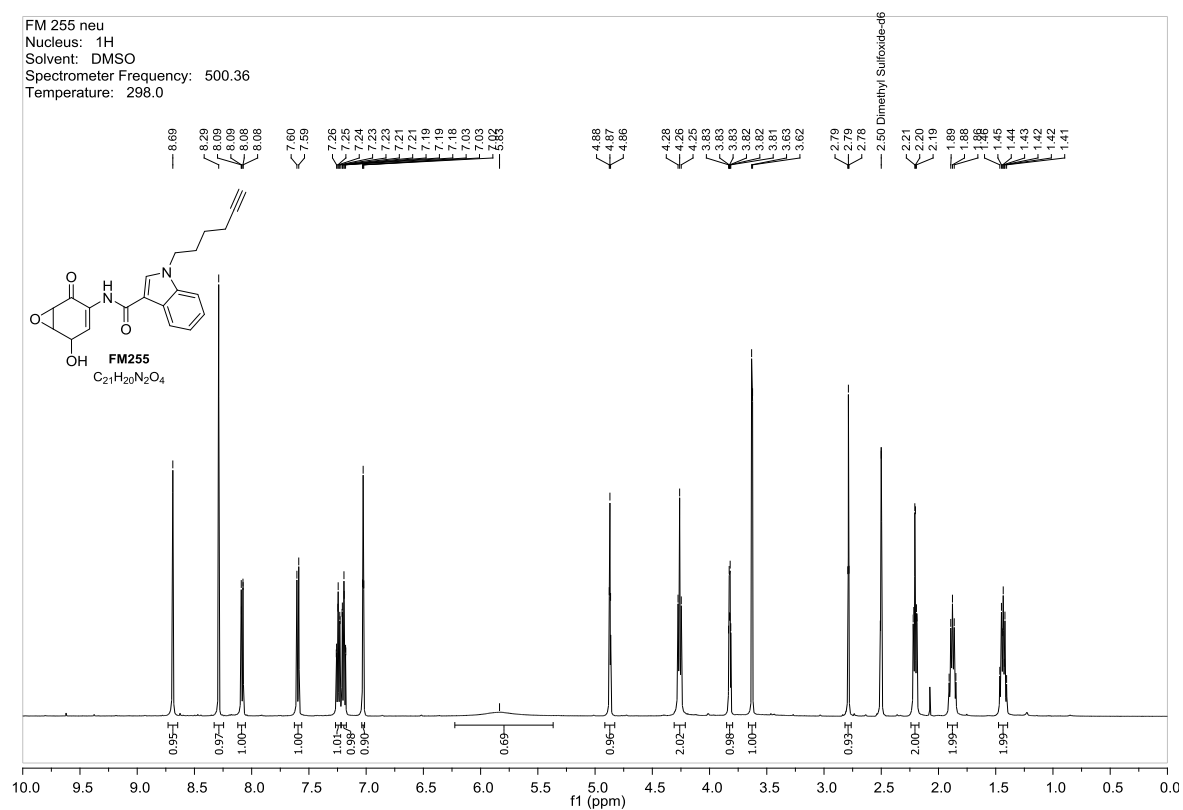
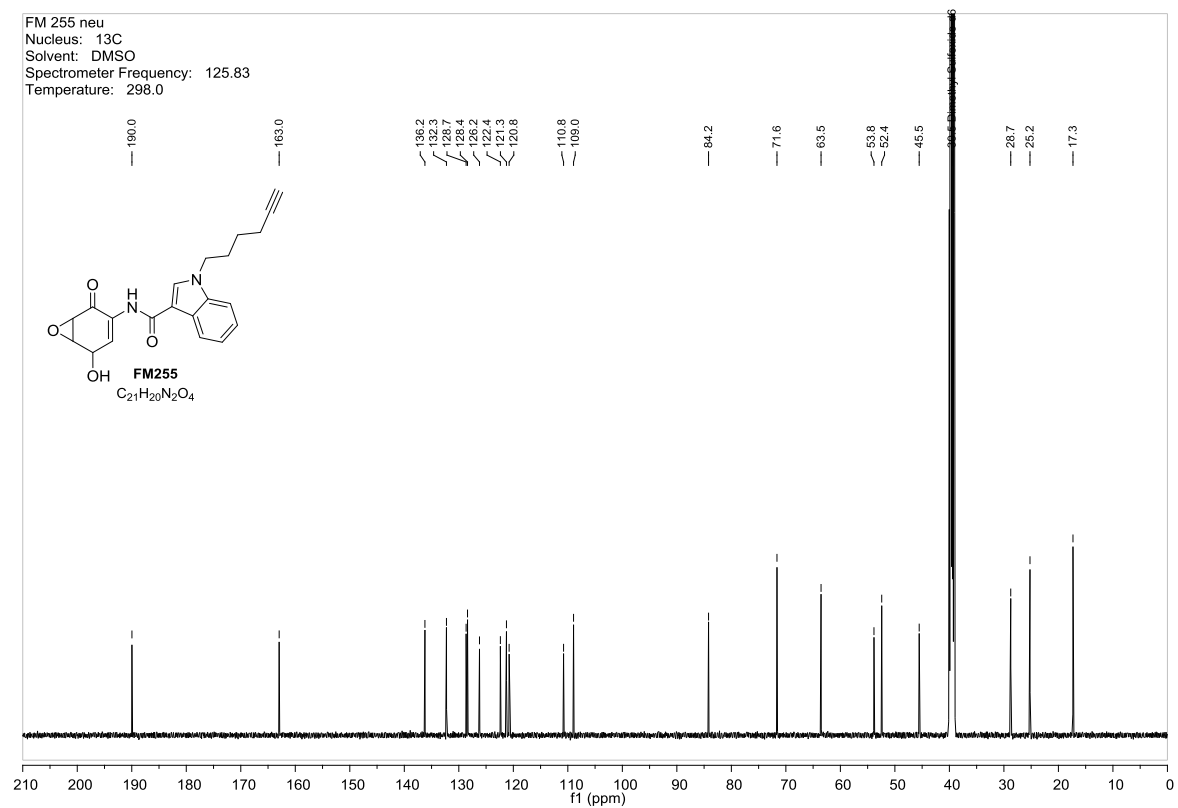
Figure 85:  $^1\text{H}$  NMR spectra of FM247.Figure 86:  $^{13}\text{C}$  NMR spectra of FM247.

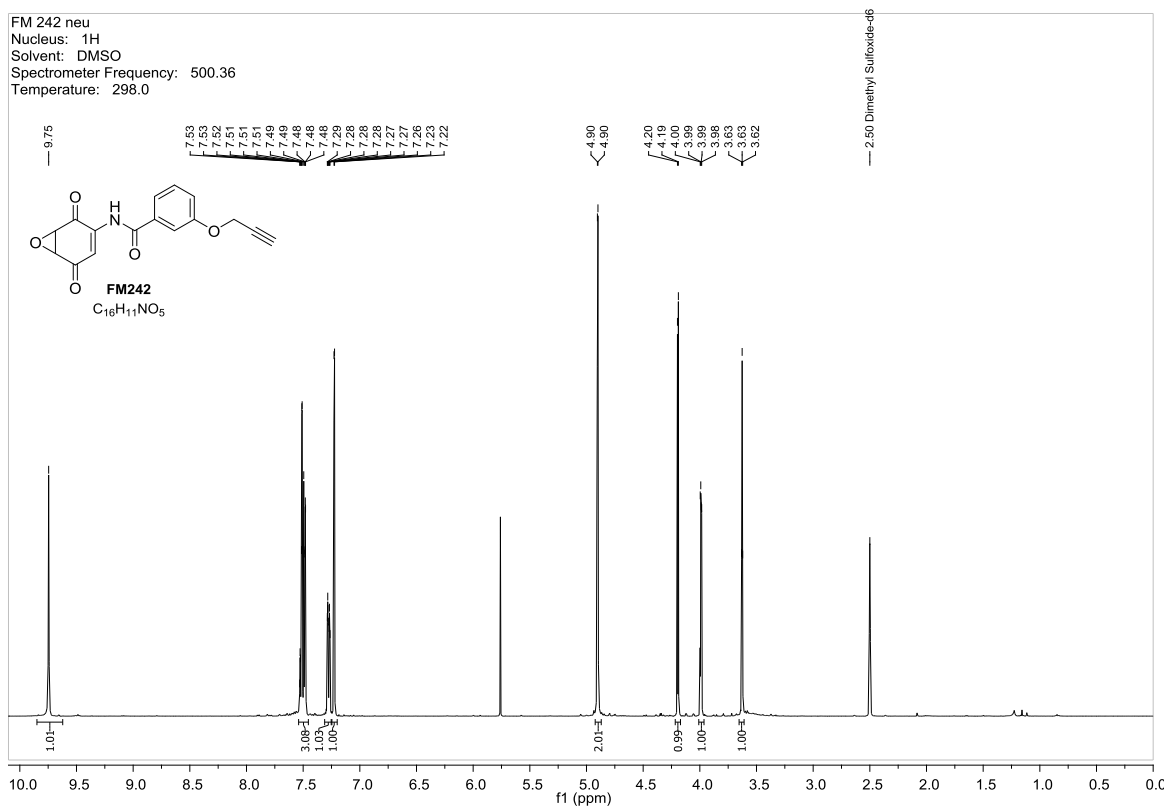
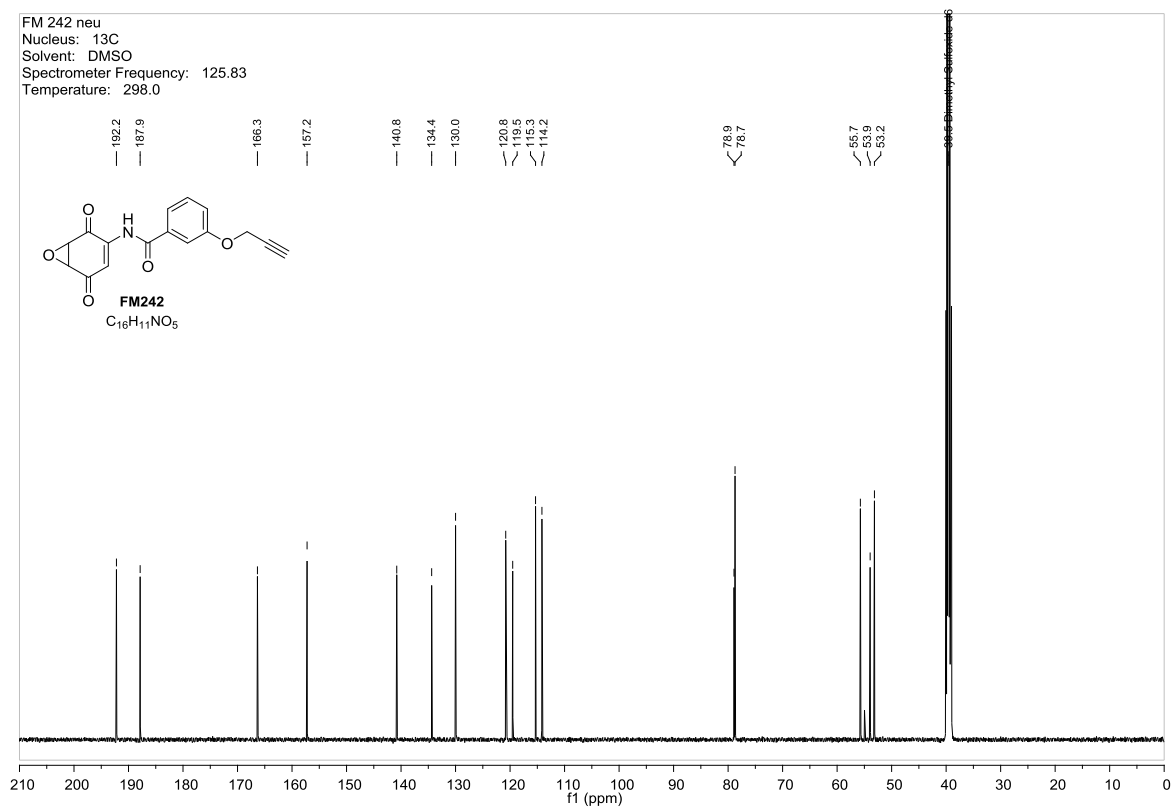
Figure 87:  $^1\text{H}$  NMR spectra of FM321.Figure 88:  $^{13}\text{C}$  NMR spectra of FM321.

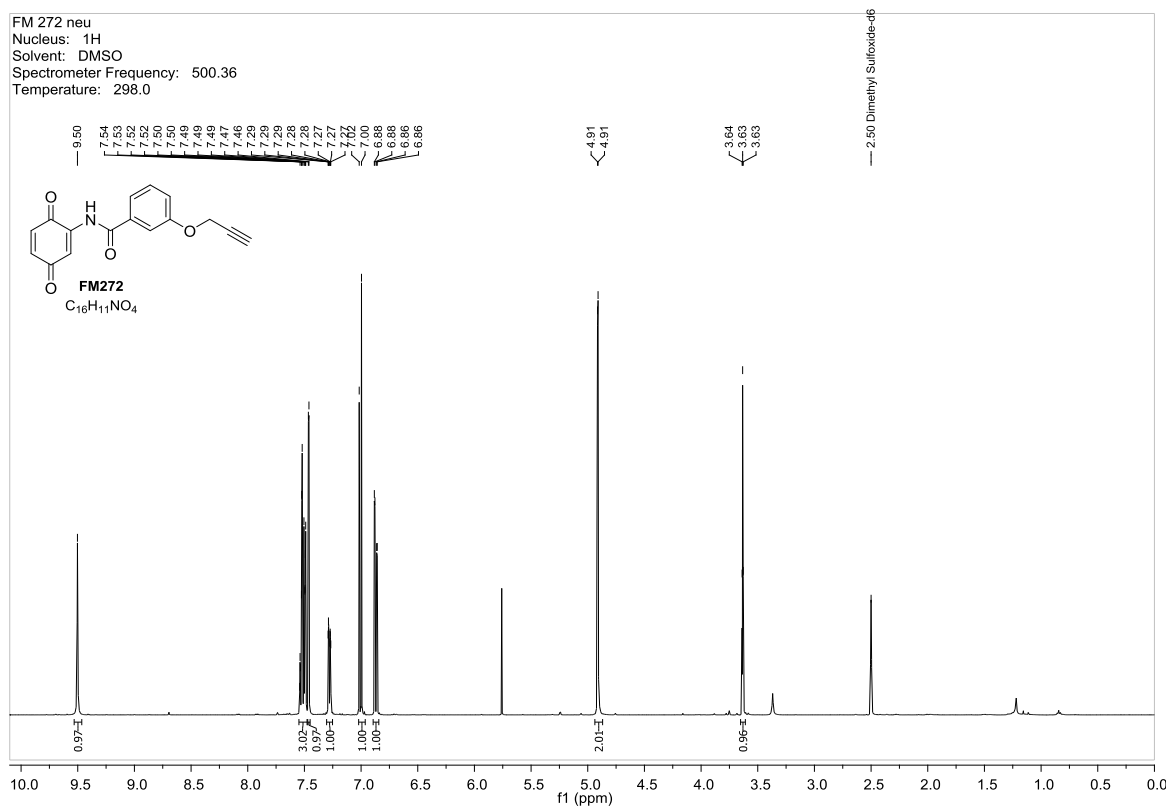
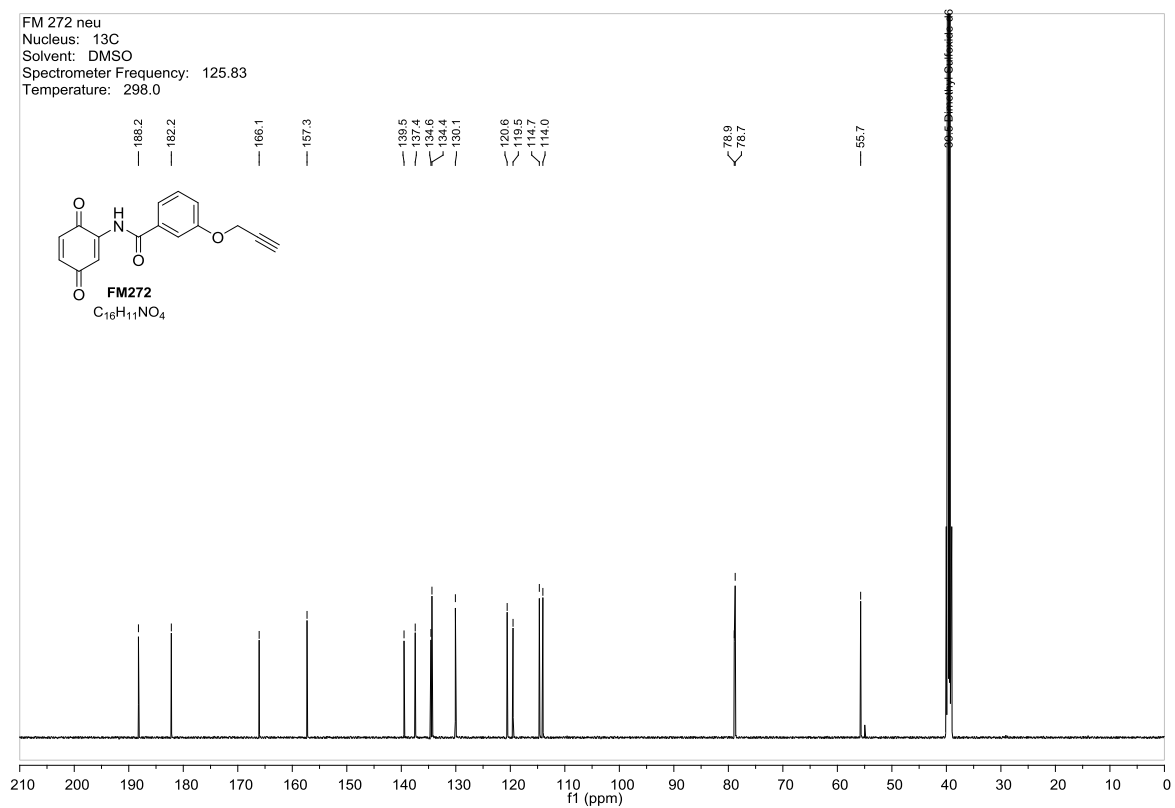
Figure 89:  $^1\text{H}$  NMR spectra of FM239.Figure 90:  $^{13}\text{C}$  NMR spectra of FM239.

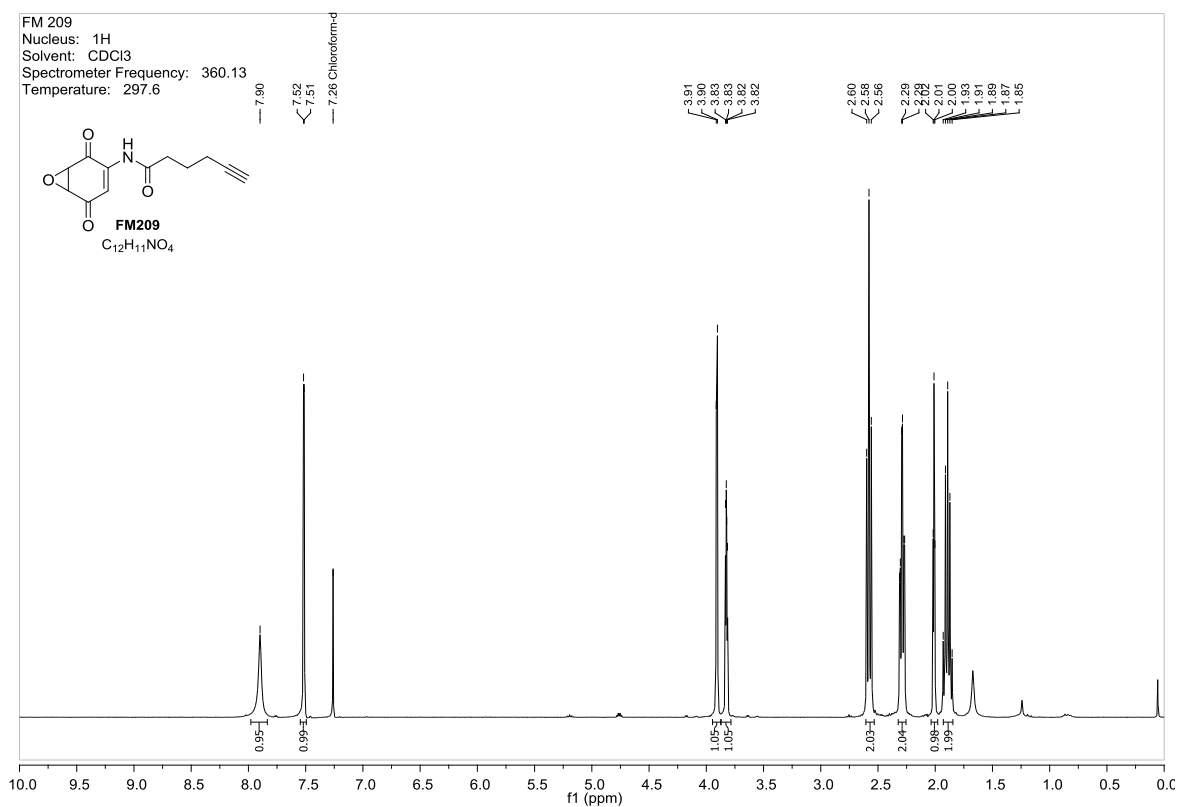
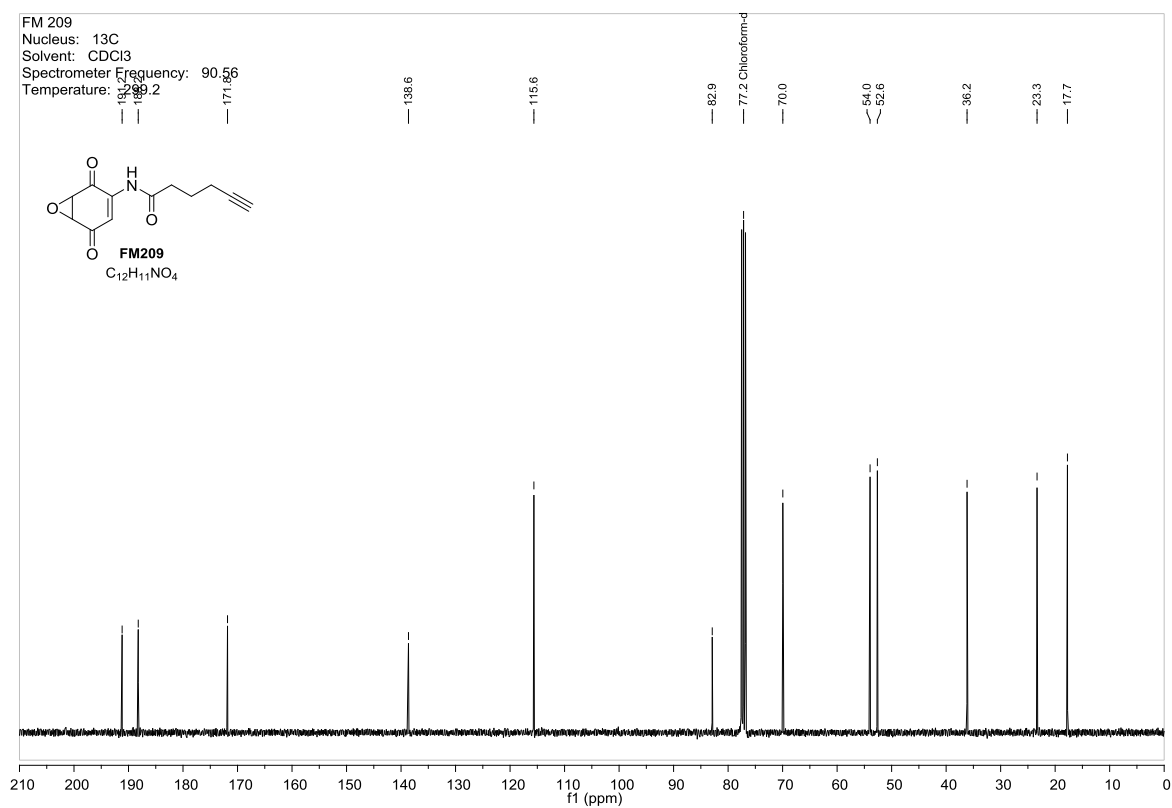


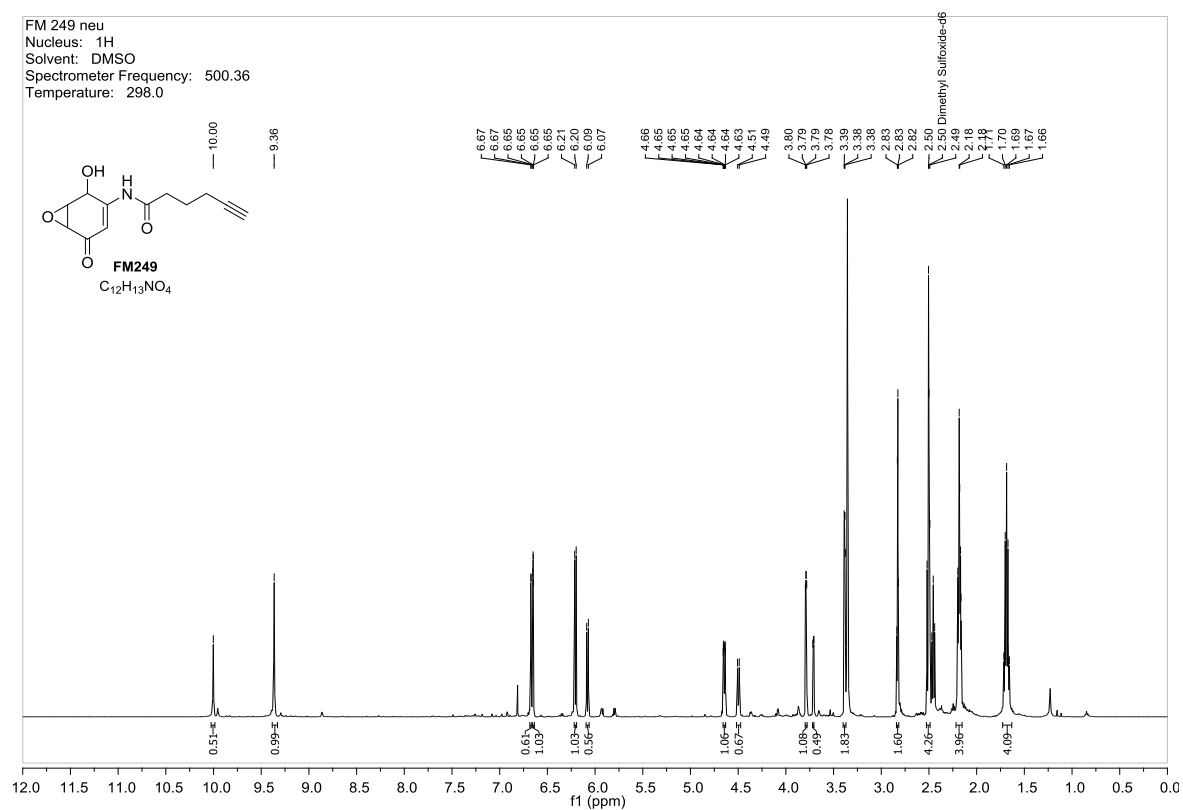
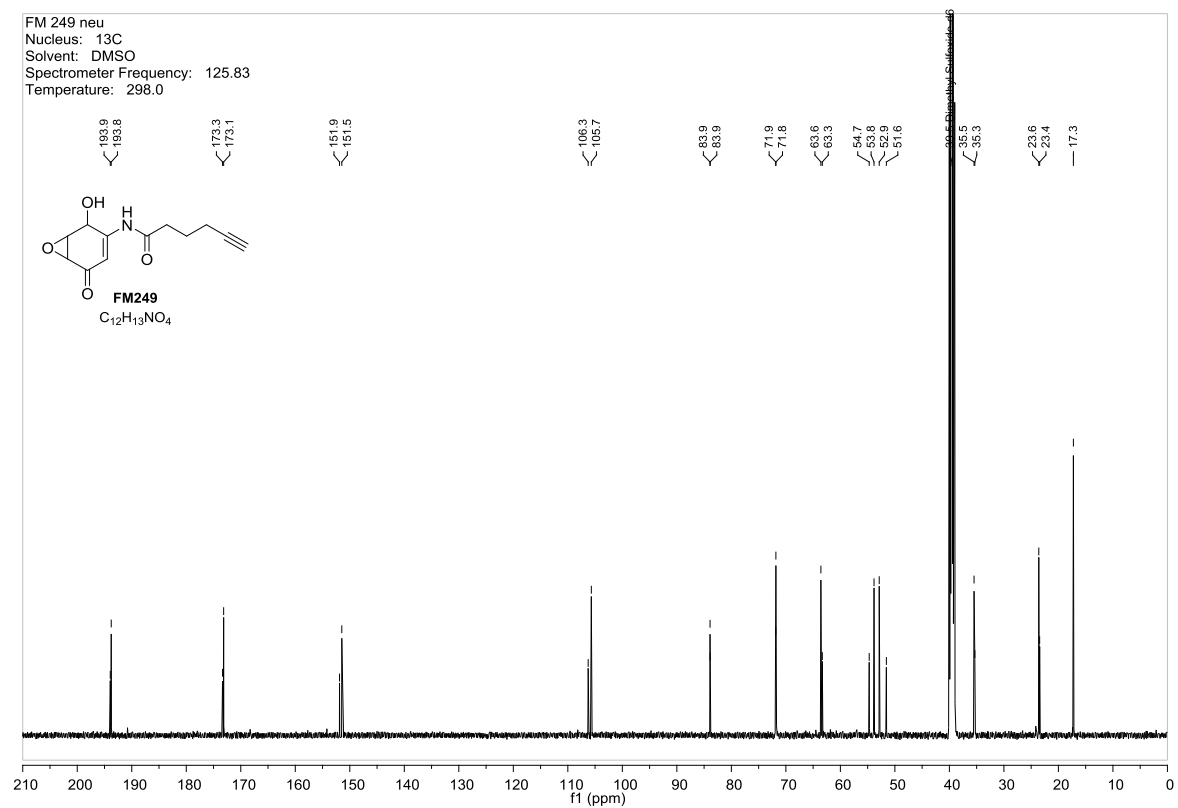
Figure 91:  $^1\text{H}$  NMR spectra of FM257.Figure 92:  $^{13}\text{C}$  NMR spectra of FM257.

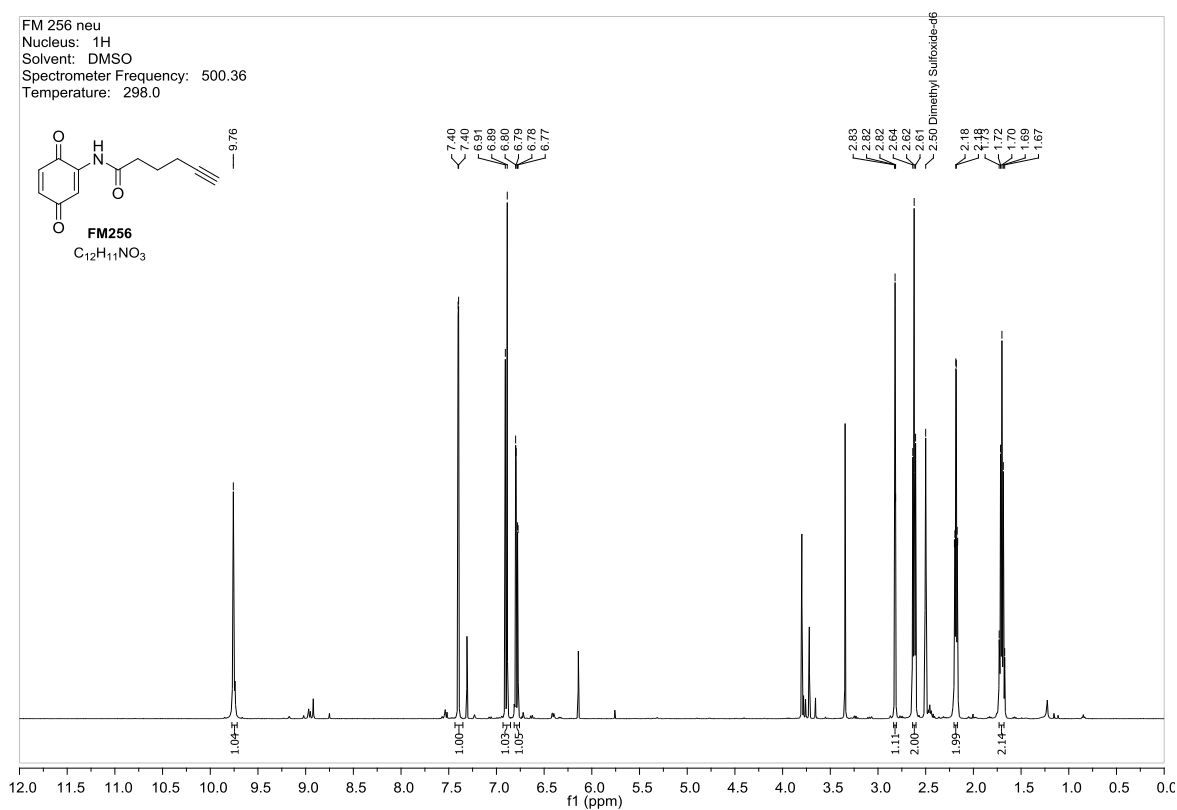
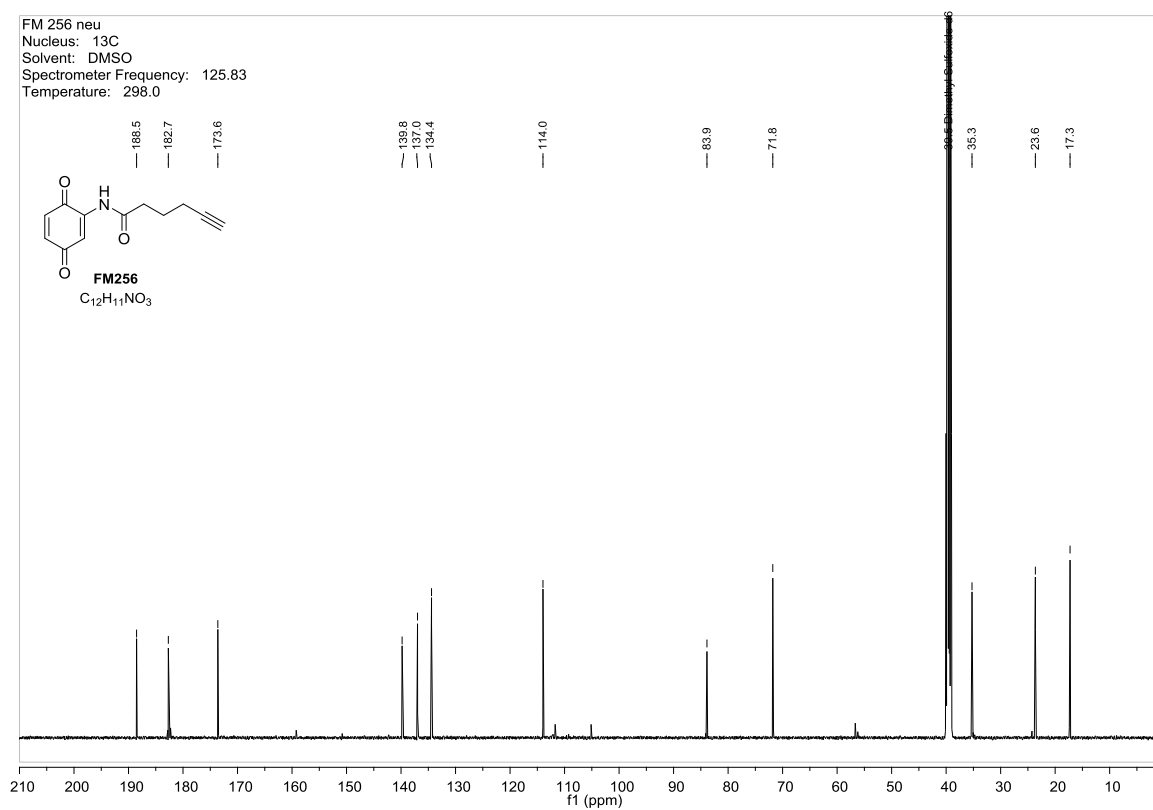
Figure 93:  $^1\text{H}$  NMR spectra of FM255.Figure 94:  $^{13}\text{C}$  NMR spectra of FM255.

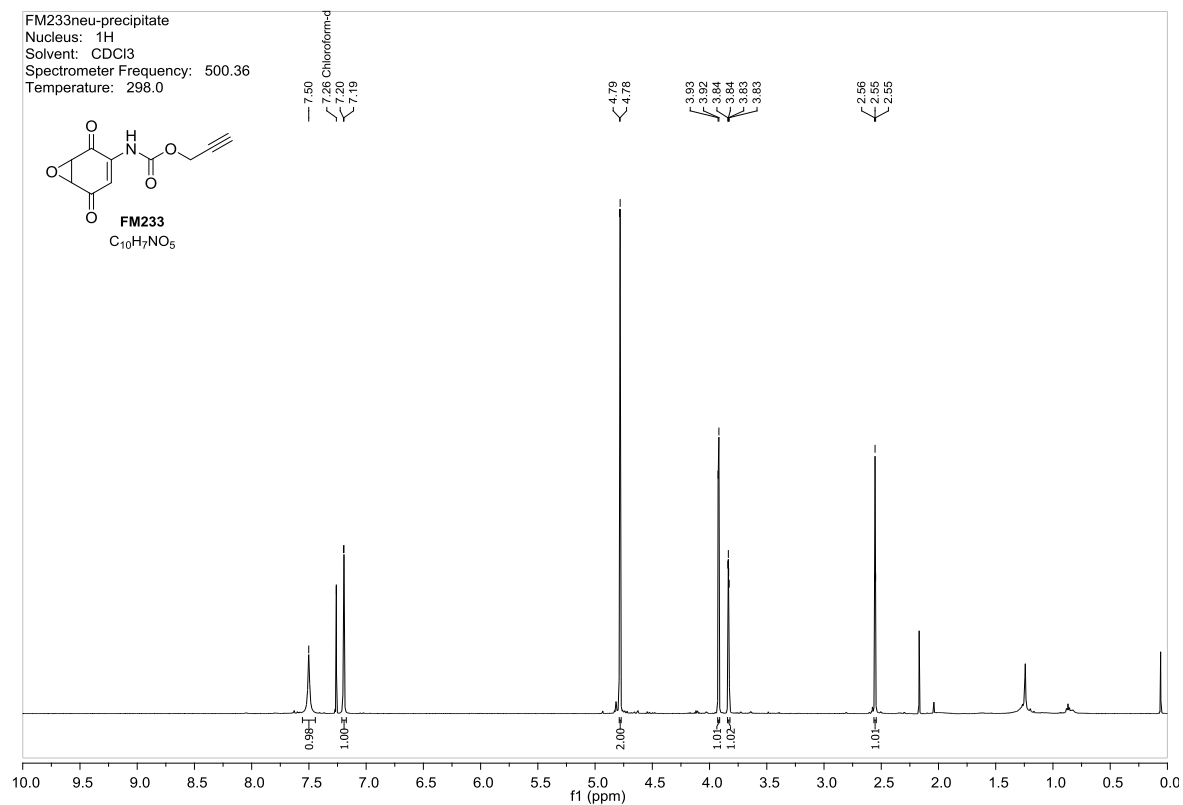
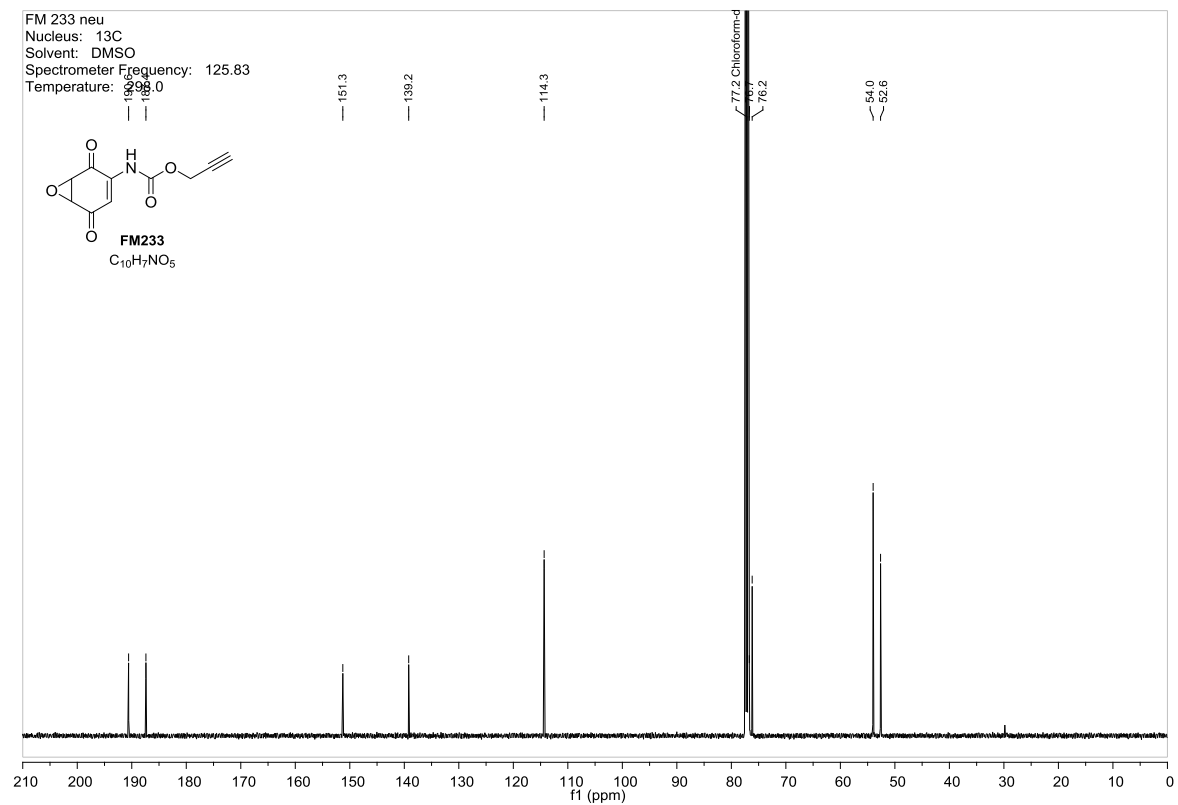
Figure 95:  $^1\text{H}$  NMR spectra of FM242.Figure 96:  $^{13}\text{C}$  NMR spectra of FM242.

Figure 97:  $^1\text{H}$  NMR spectra of FM272.Figure 98:  $^{13}\text{C}$  NMR spectra of FM272.

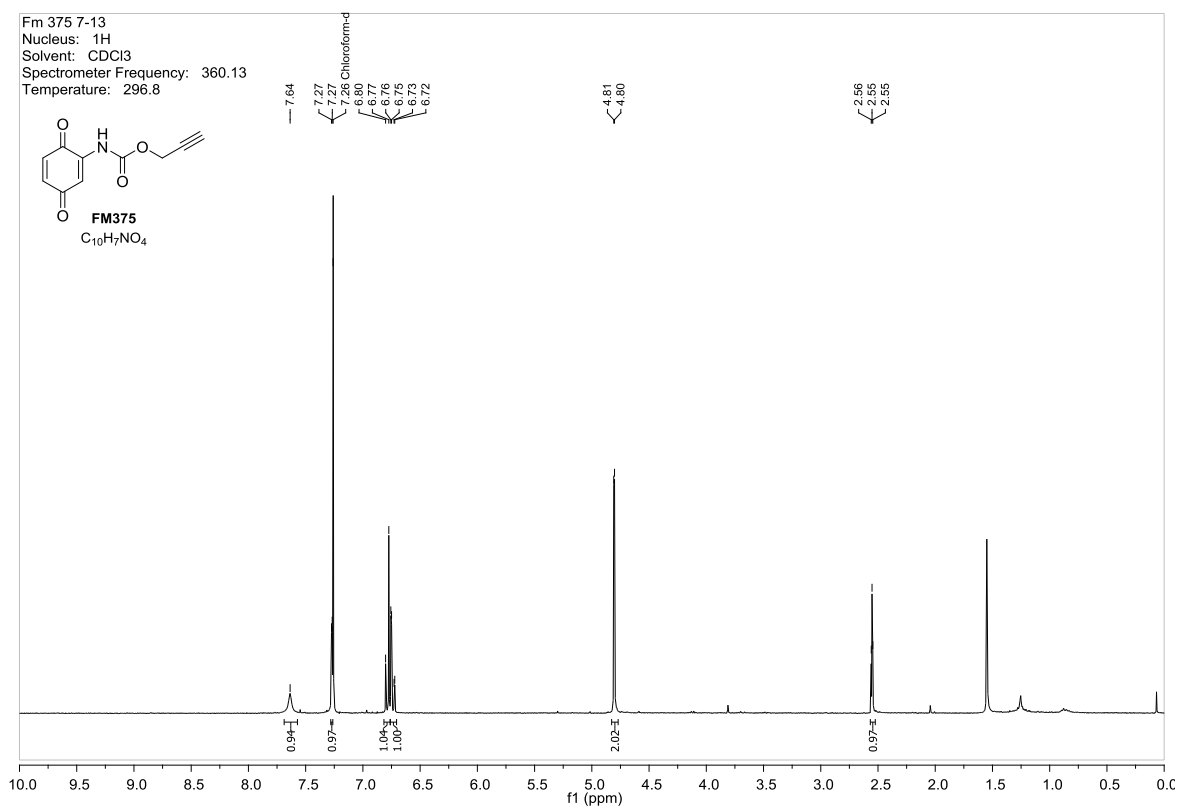
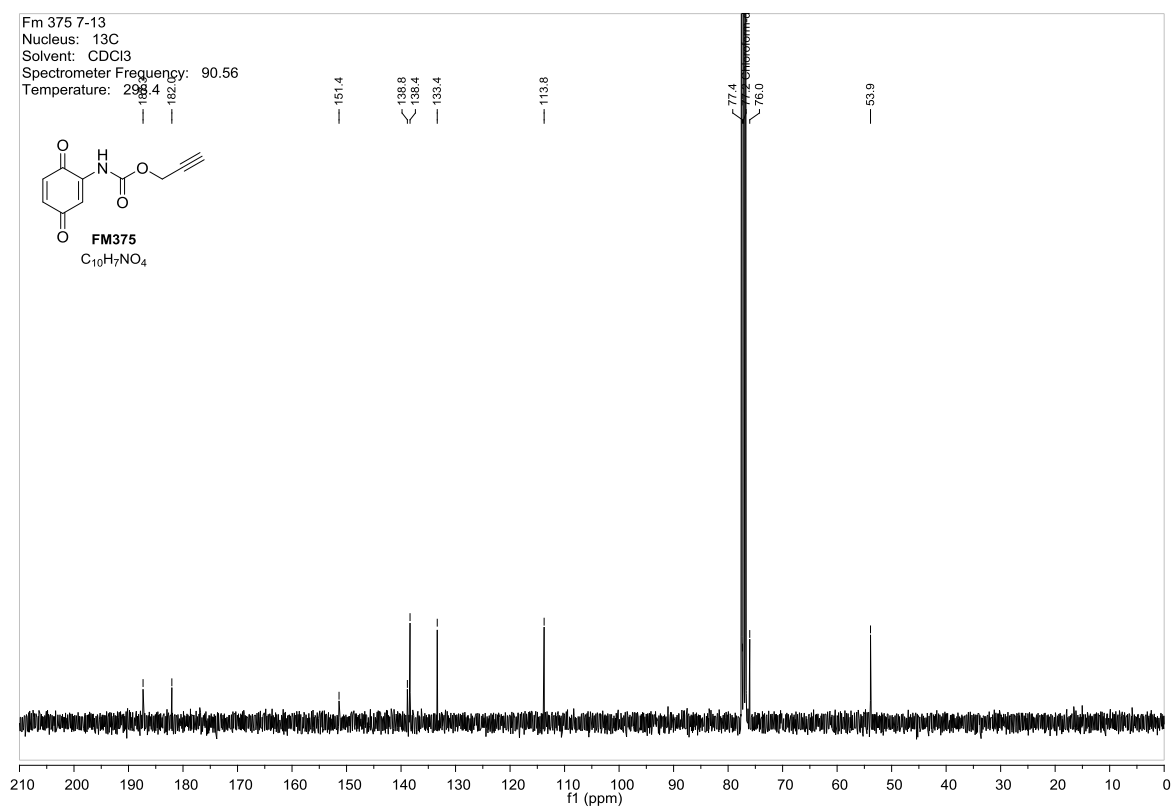
Figure 99:  $^1\text{H}$  NMR spectra of FM209.Figure 100:  $^{13}\text{C}$  NMR spectra of FM209.

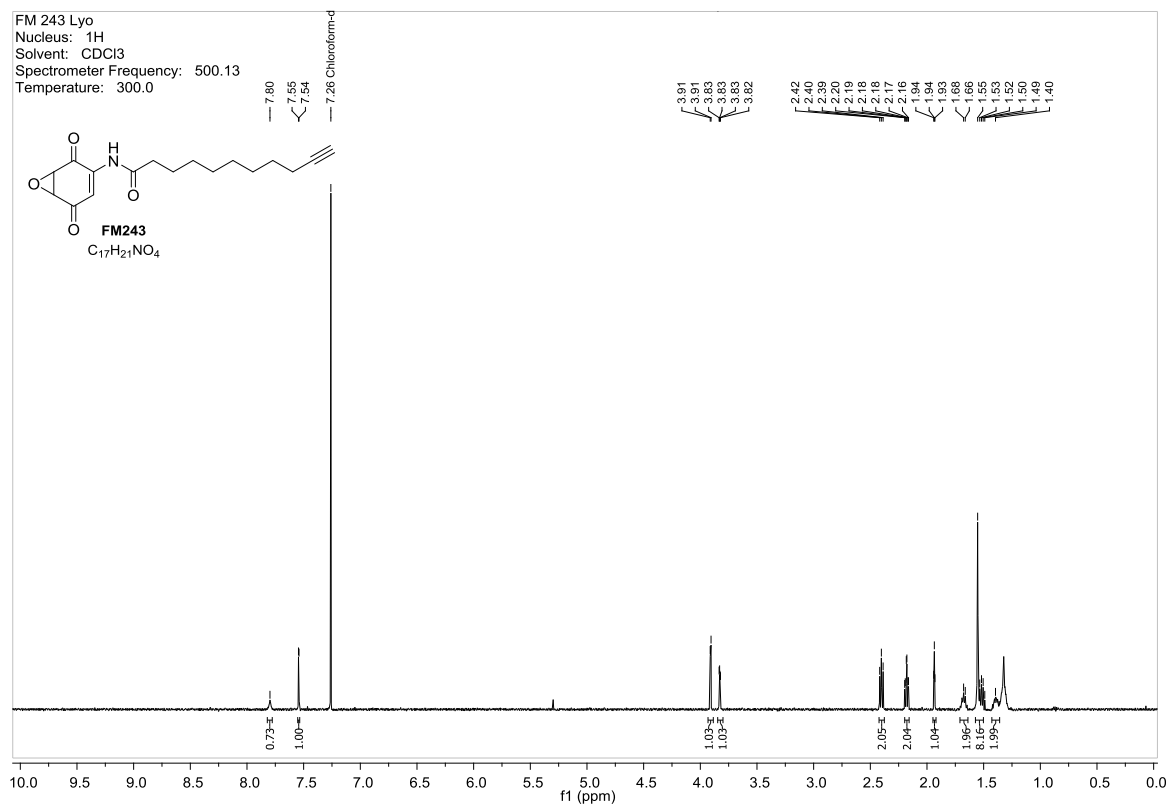
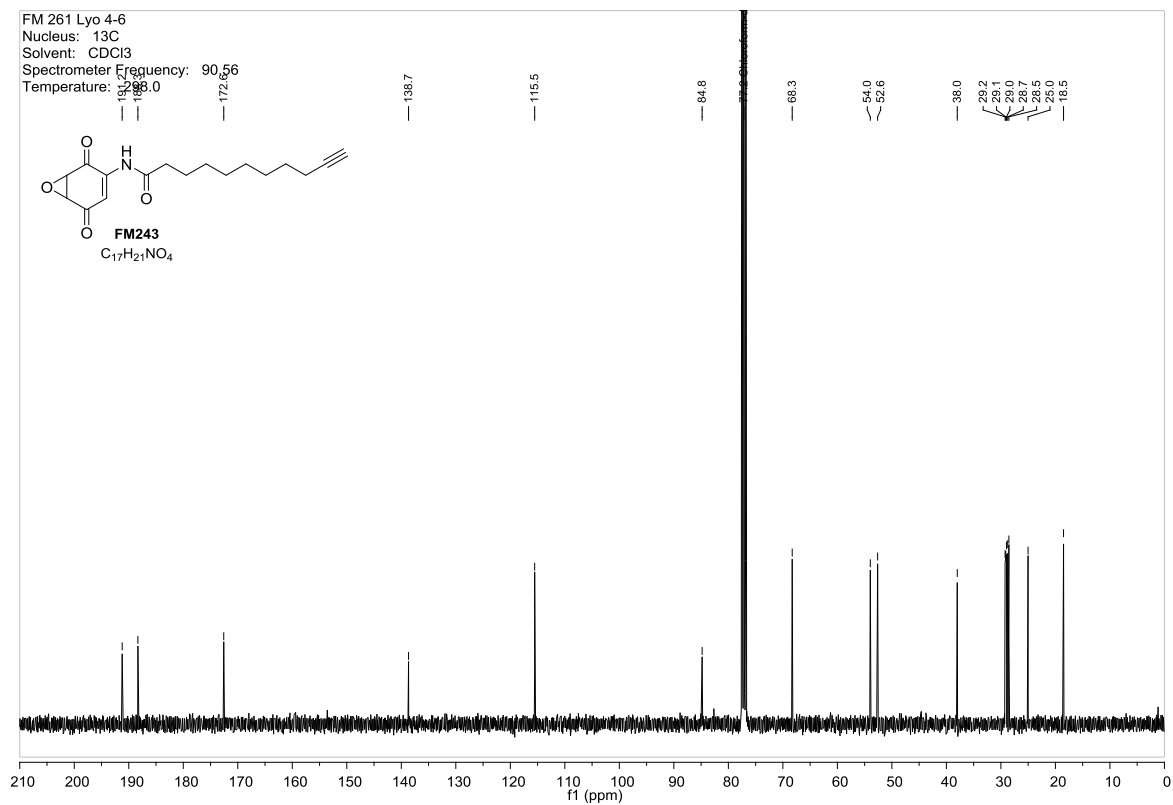
Figure 101:  $^1\text{H}$  NMR spectra of FM249.Figure 102:  $^{13}\text{C}$  NMR spectra of FM249.

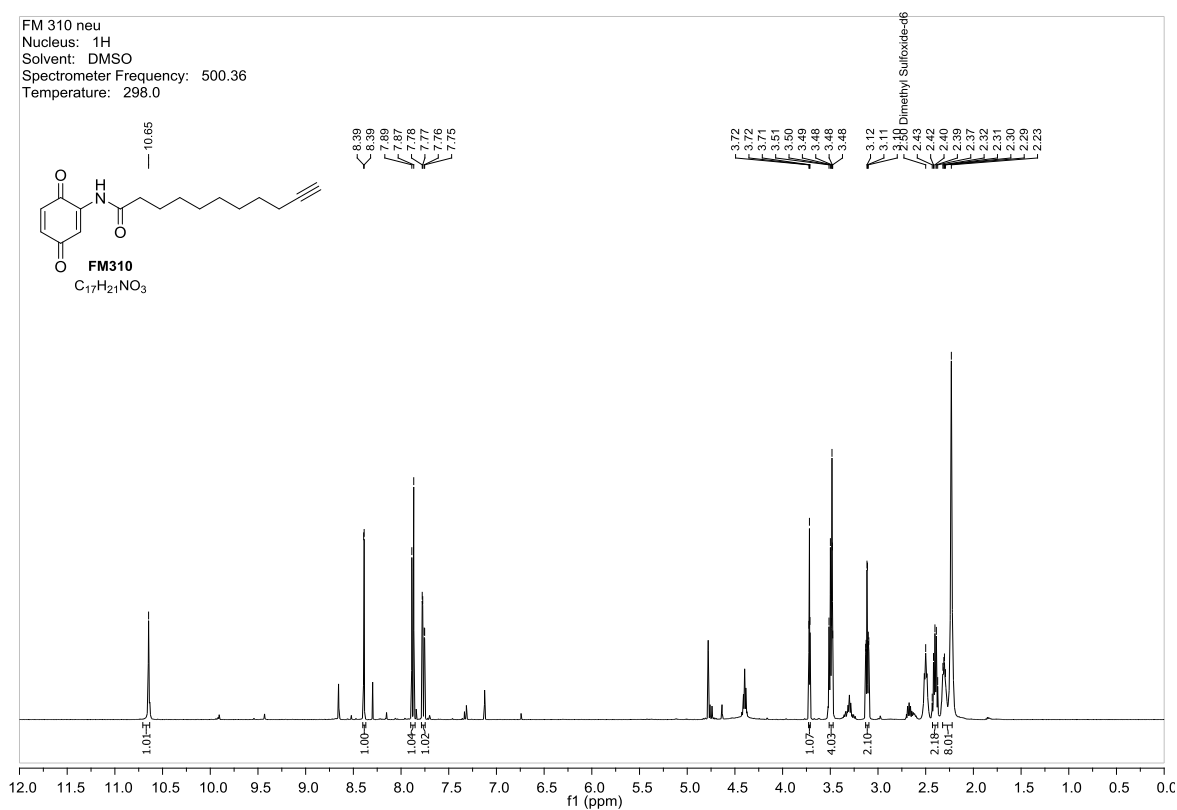
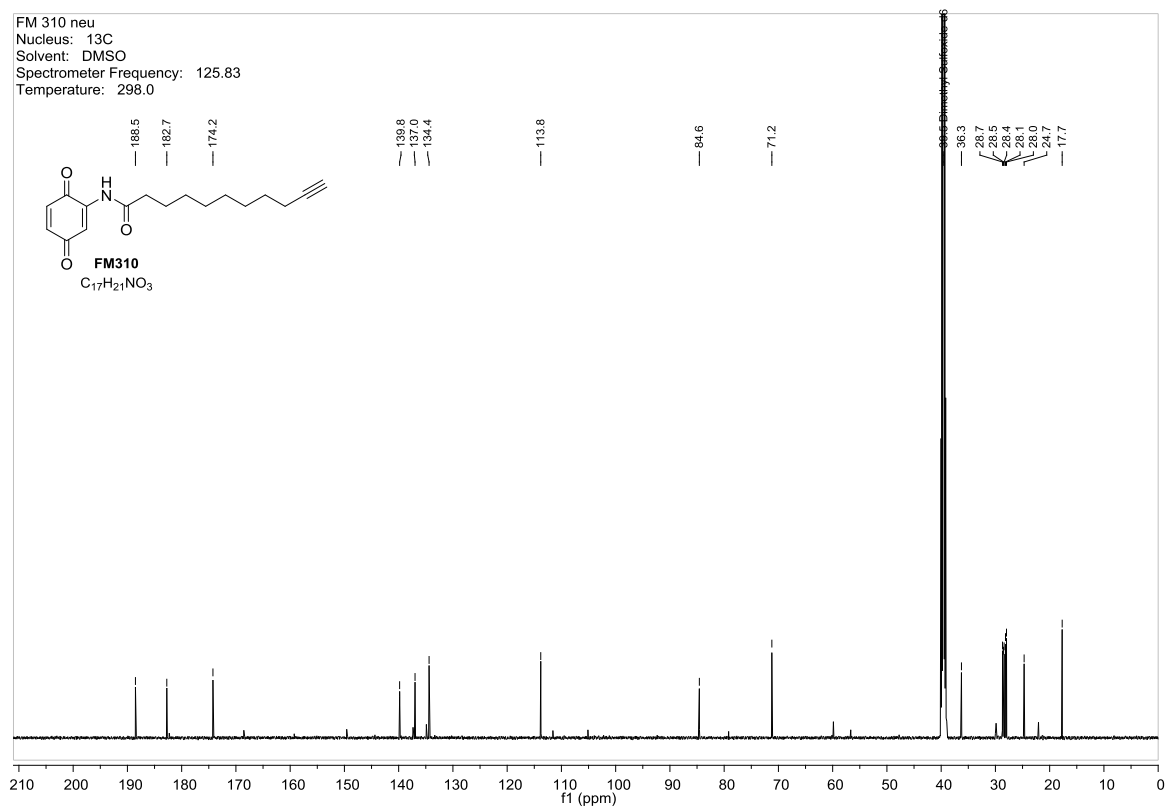
Figure 103:  $^1\text{H}$  NMR spectra of FM256.Figure 104:  $^{13}\text{C}$  NMR spectra of FM256.

Figure 105:  $^1\text{H}$  NMR spectra of FM233.Figure 106:  $^{13}\text{C}$  NMR spectra of FM233.



Figure 107:  $^1\text{H}$  NMR spectra of FM375.Figure 108:  $^{13}\text{C}$  NMR spectra of FM375.

Figure 109:  $^1\text{H}$  NMR spectra of FM243.Figure 110:  $^{13}\text{C}$  NMR spectra of FM243.

Figure 111:  $^1\text{H}$  NMR spectra of FM310.Figure 112:  $^{13}\text{C}$  NMR spectra of FM310.

## LICENSE CHEMPLUSCHEM

JOHN WILEY AND SONS LICENSE  
TERMS AND CONDITIONS

Jan 26, 2016

This Agreement between Franziska Mandl ("You") and John Wiley and Sons ("John Wiley and Sons") consists of your license details and the terms and conditions provided by John Wiley and Sons and Copyright Clearance Center.

License Number	3792540051051
License date	Jan 19, 2016
Licensed Content Publisher	John Wiley and Sons
Licensed Content Publication	CHEMPLUSCHEM
Licensed Content Title	Kinetic and Theoretical Studies of Beta-Lactone Reactivity—A Quantitative Scale for Biological Application
Licensed Content Author	Elija N. Wiedemann, Franziska A. Mandl, Iris D. Blank, Christian Ochsenfeld, Armin R. Ofial, Stephan A. Sieber
Licensed Content Date	Jul 16, 2015
Pages	7
Type of use	Dissertation/Thesis
Requestor type	Author of this Wiley article
Format	Print and electronic
Portion	Full article
Will you be translating?	No
Title of your thesis / dissertation	KINETIC AND THEORETICAL STUDIES OF BETA-LACTONE REACTIVITY and AMINO-EPOXYCYCLOHEXENONES AND THEIR PROTEIN TARGETS IN SALMONELLA TYPHIMURIUM
Expected completion date	Mar 2016
Expected size (number of pages)	230
Requestor Location	Franziska Mandl Lichtenbergstr. 4  Garching, Germany 85748 Attn: Franziska Mandl
Customer VAT ID	DE811193231

**Figure 113:** Permission for reproduction by ChemPlusChem, 19.01.2016, for DOI: 10.1002/cplu.201500246.



## VIII – CURRICULUM VITAE



Franziska Anna Maria Mandl, born 20<sup>th</sup> February 1987 in Munich, Germany

DOCTORAL  
STUDIES

03/2016

**Doctoral studies:**

Supervisor Prof. Dr. Stephan A. Sieber, Chair of Organic Chemistry II, Technische Universität München.

Projects:

(I) *Kinetic and theoretical studies of beta-lactone reactivity – a quantitative scale for biological application*

(II) *Epoxy-cyclohexenones and their protein targets in Salmonella typhimurium*

ACADEMIC  
EDUCATION

09/2009-10/2011

**Master of Science in chemistry**

Technische Universität München

Focus:

*Organic Chemistry and Analytical Chemistry*

**Master's Thesis**

Supervisor Prof. Dr. Stephan A. Sieber, Chair of Organic Chemistry II, Technische Universität München.

Project:

*Synthesis of manumycin A-based compounds for the application as ABPP-probes*

09/2006-09/2009

**Bachelor of Science in Chemistry**

Technische Universität München

**Bachelor's Thesis**

Supervisor Katrin Kloth, PhD student at the Institute of Hydrochemistry and Chair of Analytical Chemistry, Technische Universität München

Project:

*Optimization of the monitoring program for the detection of antibiotics on the MCR 3*

SCHOLAR EDUCATION	09/1997-06/2006	<b>Werner Heisenberg Gymnasium</b> , Garching Higher education entrance qualification (Abitur)
	09/1993-09/1997	<b>Grund- und Teilhauptschule Unterföhring</b> , Unterföhring
CONFERENCES	04/2014	SFB 749 project meeting with poster presentation, Venice
	03/2013	SFB 749 project meeting with poster presentation, Wildbad-Kreuth
	03/2012	SFB 749 project meeting with poster presentation, Wildbad-Kreuth
	10/2011	CIPSM-Fest of chemical biology, Munich
SEMINARS/ WORKSHOPS	02/2015	<i>Young chemists in European industries: Getting into a non-academic environment</i> , TUM Graduate School
	01/2013	<i>Project Management in Biotech Industries</i> , Technical University Munich
	11/2012	<i>Führung von Teams in Projekten</i> , TUM Graduate School
	06/2011	<i>Chemical Biology – Interactive Seminar</i> with Prof. Waldmann, <i>TUM Graduate School</i>



